Discrete Mechanics and Optimal Control

Der Fakultät für Elektrotechnik,
Informatik und Mathematik
der Universität Paderborn
zur Erlangung des akademischen Grades
Doktor der Naturwissenschaften

– Dr. rer. nat. –

vorgelegte Dissertation

von

Sina Ober-Blöbaum

Paderborn, 2008

THE FUNDAMENTAL VARIATIONAL PRINCIPLE

Namely, because the shape of the whole universe is the most perfect and, in fact, designed by the wisest creator, nothing in all the world will occur in which no maximum or minimum rule is somehow shining forth...

Leonhard Euler (1744)

Acknowledgements

To begin, I would like to thank my advisor Prof. Dr. Michael Dellnitz for his guidance, support, and motivation, and, in particular, for the great freedom he has given me during my PhD research.

I would also like to thank Prof. Dr. Oliver Junge from the *Technische Universität München* for his extensive supervision over the last years.

Professor Jerrold E. Marsden from the *California Institute of Technology* has provided valuable guidance during my studies. He introduced me to the area of discrete variational mechanics and provided interesting ideas for application. Mutual visits and discussions contributed to the progress of my research as well.

Special thanks goes to my co-workers Dr. Sigrid Leyendecker, Dr. Kathrin Padberg and Mirko Hessel-von Molo for many interesting and enlightening discussions, exciting joint work, and their constant support.

I gratefully acknowledge support under the DFG-sponsored research project *SFB 376* on *Massively Parallel Computation*.

My colleages in Paderborn participated in lengthy discusssions on scientific and unscientific topics and I appreciate their technical and administrative support, including Alessandro Dell'Aere, Olaf Bonorden, Tanja Bürger, Sebastian Hage-Packhäuser, Marianne Kalle, Stefan Klus, Anna-Lena Meyer, Marcus Post, Dr. Robert Preis, Marcel Schwalb, Stefan Sertl, Bianca Thiere, Julia Timmermann, and Katrin Witting.

I am very grateful to all my friends, primarly Oliver Krimmer and Farina Schneider for proof-reading the manuscript. Special thanks goes to Kay Klobedanz, who has been a great support and motivator over the last years. For support during the last months I would especially like to thank Helene Waßmann.

Most of all, I thank my family. In particular, the constant support and encouragement from my parents Ingetraud and Hartmut and my brother Mark has accompanied me through many years of studies.

Finally, I thank Andreas Kohlos - for a number of things.

Abstract

The optimal control of physical processes is of crucial importance in all modern technological sciences. In general, one is interested in prescribing the motion of a dynamical system in such a way that a certain optimality criterion is achieved. Typical challenges are the determination of a time-minimal path in vehicle dynamics, an energy-efficient trajectory in space mission design, or optimal motion sequences in robotics and biomechanics.

In order to solve optimal control problems for mechanical systems, this thesis links the theory of optimal control with concepts from variational mechanics. The application of discrete variational principles allows for the construction of an optimization algorithm that enables the discrete solution to inherit characteristic structural properties from the continuous problem.

The numerical performance of the developed method and its relationship to other existing optimal control methods are investigated. This is done by means of theoretical considerations as well as with the help of numerical examples arising in problems from trajectory planning and space mission design.

The development of efficient approaches for exploiting the mechanical system's structures reduce for example the computational effort. In addition, the optimal control framework is extended to mechanical systems with constraints in multibody dynamics and applied to robotical and biomechanical problems.

Zusammenfassung

Die optimale Steuerung physikalischer Prozesse ist in allen modernen technologischen Wissenschaften von wichtiger Bedeutung. Das Ziel ist es, die Bewegung eines dynamischen Systems so vorzuschreiben, dass ein bestimmtes Optimlitätskriterium erreicht wird. Typische Anwendungen sind die Bestimmung zeitoptimaler Wege in der Fahrzeugdynamik, energieeffizienter Trajektorien von Raumfahrtmissionen oder optimaler Bewegungsabläufe in der Robotik und der Biomechanik.

Diese Arbeit vereint die Theorie der optimalen Steuerung mit den Konzepten der Variationsmechanik, um Steuerungsprobleme mechanischer Systeme zu lösen. Die Anwendung diskreter Variationsprinzipien ermöglicht es, einen Optimierungsalgorithmus zu konstruieren, dessen Lösung charakteristische strukturelle Eigenschaften des kontinuierlichen Problems erbt.

Die numerische Effizienz der entwickelten Methode, sowie Vergleiche und Relationen zu existierenden optimalen Steuerungsmethoden, werden sowohl anhand theoretischer Betrachtungen als auch anhand numerischer Beispiele untersucht.

Die Entwicklung effizienter Ansätze zur Ausnutzung der speziellen Struktur des mechanischen Systems reduziert beispielsweise den rechnerischen Aufwand. Abschließend wird die vorgestellte Methode dahingehend erweitert, dass sie sich auf mechanische Systeme mit Zwangsbedingungen in der Mehrkörperdynamik anwenden lässt. Dabei werden Probleme aus der Robotik und der Biomechanik behandelt.

Contents

1 Introduction **1**

2 Optimal control **13**
2.1 Optimal control problem 13
2.1.1 Problem formulation 13
2.1.2 Necessary conditions for optimality 15
2.2 Solution methods for optimal control problems 16
2.2.1 Indirect methods 17
2.2.2 Direct methods 18
2.3 Solution methods for nonlinear constrained optimization problems 20
2.3.1 Local optimality conditions 20
2.3.2 Sequential Quadratic Programming (SQP) 21
2.4 Discussion of direct methods 23

3 Variational mechanics **25**
3.1 Lagrangian mechanics 26
3.1.1 Basic definitions and concepts 26
3.1.2 Discrete Lagrangian mechanics 29
3.2 Hamiltonian mechanics 32
3.2.1 Basic definitions and concepts 32
3.2.2 Discrete Hamiltonian mechanics 35
3.3 Forcing and control 37
3.3.1 Forced Lagrangian systems 37
3.3.2 Forced Hamiltonian systems 38
3.3.3 Legendre transform with forces 39
3.3.4 Noether's theorem with forcing 40
3.3.5 Discrete variational mechanics with control forces 40
3.3.6 Discrete Legendre transforms with forces 42
3.3.7 Discrete Noether's theorem with forcing 43

4 Discrete mechanics and optimal control (DMOC) 45
4.1 Optimal control of a mechanical system . . . 45
4.1.1 Lagrangian optimal control problem . . . 46
4.1.2 Hamiltonian optimal control problem . . . 47
4.1.3 Transformation to Mayer form . . . 48
4.2 Optimal control of a discrete mechanical system . . . 49
4.2.1 Discrete Optimal Control Problem . . . 51
4.2.2 Transformation to Mayer form . . . 52
4.2.3 Fixed boundary conditions . . . 53
4.3 Correspondence between discrete and continuous optimal control problem . . . 55
4.3.1 Exact discrete Lagrangian and forcing . . . 55
4.3.2 Order of consistency . . . 58
4.3.3 Discrete problem as direct solution method . . . 62
4.4 High-order discretization . . . 64
4.4.1 Quadrature approximation . . . 64
4.4.2 High-order discrete optimal control problem . . . 67
4.4.3 Correspondence to Runge-Kutta discretizations . . . 69
4.5 Adjoint system . . . 76
4.5.1 Continuous setting . . . 76
4.5.2 Discrete setting . . . 79
4.5.3 The transformed adjoint system . . . 82
4.6 Convergence . . . 85

5 Implementation, applications and extension 89
5.1 Implementation . . . 89
5.2 Comparison to existing methods . . . 91
5.2.1 Low thrust orbital transfer . . . 91
5.2.2 Two-link manipulator . . . 94
5.3 Application: Trajectory planning . . . 99
5.3.1 A group of hovercraft . . . 99
5.3.2 Perfect underwater glider . . . 102
5.4 Application: Optimal control of multi-body systems . . . 104
5.4.1 The falling cat . . . 104
5.4.2 A gymnast (three-link mechanism) . . . 109
5.5 Reconfiguration of formation flying spacecraft – a decentralized approach . . . 116

6 Optimal control of constrained mechanical systems in multi-body dynamics 127
6.1 Constrained dynamics and optimal control . . . 128

6.1.1 Optimization problem . . . 128
6.1.2 Constrained Lagrange-d'Alembert principle . . . 129
6.1.3 Null space method . . . 129
6.1.4 Reparametrization . . . 130
6.2 Constrained discrete dynamics and optimal control . . . 130
6.2.1 Discrete constrained Lagrange-d'Alembert principle . . . 130
6.2.2 Discrete null space method . . . 131
6.2.3 Nodal reparametrization . . . 132
6.2.4 Boundary conditions . . . 133
6.2.5 Discrete constrained optimization problem . . . 135
6.3 Optimal control for rigid body dynamics . . . 135
6.3.1 Constrained formulation of rigid body dynamics . . . 135
6.3.2 Actuation of the rigid body . . . 138
6.3.3 Kinematic pairs . . . 139
6.4 Applications . . . 143
6.4.1 Optimal control of a rigid body with rotors . . . 143
6.4.2 Biomechanics: The optimal pitch . . . 144

7 Conclusions and outlook **151**

A Definitions **157**

B Adjoint system **167**

C Convergence proof **171**

List of Figures

1.1 The calculus of variations in mechanics and optimal control theory 5
1.2 The discrete calculus of variations in discrete mechanics and optimization theory 8
1.3 Optimal control for mechanical systems: the order of variation and discretization for deriving the necessary optimality conditions . . 9

3.1 Left and right discrete forces 42
3.2 Correspondence between the forced discrete Lagrangian and the forced discrete Hamiltonian map 43

4.1 Correspondence between the exact discrete Lagrangian and forces and the continuous forced Hamiltonian flow 57
4.2 Comparison of solution strategies for optimal control problems: standard direct methods and DMOC 62
4.3 Correspondence of indirect and direct methods in optimal control theory 85

5.1 Low thrust orbital transfer: approximated cost 93
5.2 Low thrust orbital transfer: difference of force and change in angular momentum 95
5.3 Low thrust orbital transfer: accuracy of final point condition . . . 96
5.4 Two-link manipulator: model 96
5.5 Two-link manipulator: objective function value and momentum-force consistency 98
5.6 Two-link manipulator: convergence rates 99
5.7 Hovercraft: model 100
5.8 Hovercraft: optimal trajectories in phase space 102
5.9 Underwater glider: time and effort optimal 105
5.10 Underwater glider: energy, work and objective values 106
5.11 Falling cat: model 107
5.12 Falling cat: optimal solution 110
5.13 Falling cat: energy and angular momentum 111

5.14 Gymnast: modeled as three-link mechanism 111
5.15 Gymnast: optimal solution 114
5.16 Gymnast: snapshots of optimal motion sequence 115
5.17 Dynamical model for formation flying spacecraft: the circular restricted three body problem 117
5.18 Hierarchical formulation of the optimal control of formation flying spacecraft 120
5.19 Formation of six spacecraft 123
5.20 Formation of 30 spacecraft 124

6.1 Discrete redundant and generalized forces 133
6.2 Configuration of a rigid body with respect to an orthonormal frame $\{e_I\}$ fixed in space 136
6.3 Rigid body with three rotors: configuration 144
6.4 Rigid body with three rotors: torque 145
6.5 Rigid body with three rotors: energy and angular momentum . . 145
6.6 Rigid body with two rotors: configuration 146
6.7 Rigid body with two rotors: torque 146
6.8 Rigid body with two rotors: energy and angular momentum . . . 147
6.9 Model for a pitcher's arm 148
6.10 Pitcher: snapshots of the optimal motion sequence. 150

Nomenclature

In Chapters 2 to 5 we use a slighly different notation as in Chapter 6. This is due to the development of a uniform methodology consisting of two different existing methods with partly the same notation for different objects. Therefore, besides an overview of the used symbols in Chapters 2 to 5 we will give a list of symbols that are in additional or in different use in Chapter 6.

List of Acronyms

AD	Automatic Differentiation
CRTBP	Circular Restricted Three Body Problem
DMOC	Discrete Mechanics and Optimal Control
HOCP	Hamiltonian Optimal Control Problem
KKT	Karush-Kuhn-Tucker
LOCP	Lagrangian Optimal Control Problem
NLP	Nonlinear Programming
OCP	Optimal Control Problem
PMP	Pontryagin Maximum Principle
QP	Quadratic Programming
SQP	Sequential Quadratic Programming

List of Symbols

Q	real configuration manifold
TQ	tangent bundle
T^*Q	cotangent bundle
U	control manifold
$\ddot{Q}$	second order submanifold
$\ddot{Q}_d$	discrete second order submanifold
$\mathcal{C}$	path space
$\mathcal{C}_d$	discrete path space

$\mathcal{D}$	control path space
$\mathcal{D}_d$	discrete control path space
q	configuration vector
$\dot{q}$	velocity vector
p	momentum vector
u	control parameter (Chapters 2 to 5)
λ	Lagrange multiplier
L	Lagrangian of the mechanical system
L_d	discrete Lagrangian
L_d^E	exact discrete Lagrangian
H	Hamiltonian of the mechanical system
K	kinetic energy
V	potential energy
$\mathfrak{G}$	action map
$\mathfrak{G}_d$	discrete action map
X_L	Lagrangian vector field
X_{L_d}	discrete Lagrangian evolution operator
F_L	Lagrangian flow
F_{L_d}	discrete Lagrangian map
X_H	Hamiltonian vector field
F_H	Hamiltonian flow
$\tilde{F}_{L_d}$	discrete Hamiltonian map
Θ_L	Lagrangian one-form
$\Theta^{\pm}_{L_d}$	discrete Lagrangian one-form
Ω_L	Lagrangian symplectic form
Ω_{L_d}	discrete Lagrangian symplectic form
Θ	canonical one-form
Ω	canonical two-form
$\mathbf{J}$	momentum map
$\mathbf{J}_L$	Lagrangian momentum map
$\mathbf{J}_{L_d}$	discrete Lagrangian momentum map
$\mathbf{J}_H$	Hamiltonian momentum map
$\mathbb{F}L$	fiber derivative (Legendre transform)
$\mathbb{F}^{\pm}L_d$	discrete fiber derivatives (discrete Legendre transforms)
$\mathbb{F}H$	fiber derivative of the Hamiltonian
$D_{\mathrm{EL}}L$	Euler-Lagrange equations
$D_{\mathrm{DEL}}L$	discrete Euler-Lagrange equations

f_L	Lagrangian force
f_{LC}	Lagrangian control force
f_H	Hamiltonian force
f_{HC}	Hamiltonian control force
$f_d^{\pm}$	left and right discrete force
$f_{C_d}^{\pm}$	left and right discrete Lagrangian control force
$f_{C_d}^{E\pm}$	left and right exact discrete Lagrangian control force
J	objective functional
C	cost function of the objective functional (Chapters 2 to 5)
Φ	final condition of the objective functional (Mayer term)
$\mathcal{L}$	Lagrangian of the optimal control system
$\tilde{\mathcal{L}}$	Lagrangian of the constrained optimization problem
$\mathcal{H}$	Hamiltonian of the optimal control system
h	path constraint
r	final point constraint
∇	Jacobian
D_k	partial derivatives with respect to the k-th argument
$\mathbf{d}$	exterior derivative
$\mathbf{i}$	interior product
t	time
h	time step
T	final time
G	Lie group
$\mathfrak{g}$	Lie algebra
ϕ	action of a Lie group
τ_Q	natural projection
π_Q	canonical projection
C^k	set of k-times continuously differentiable functions
$\mathcal{F}(M)$	set of continuously differentiable real-valued functions on M
$L^p(\mathbb{R}^n)$	Lebesgue space of measurable functions $x : [0,T] \to \mathbb{R}^n$ with $\lvert x(\cdot)\rvert^p$ integrable
$W^{m,p}(\mathbb{R}^n)$	Sobolev space consisting of vector-valued measurable functions $x : [0,T] \to \mathbb{R}^n$ whith j-th derivative in L^p for all $0 \leq j \leq m$
$B_a(x)$	closed ball centered at x with radius a

Chapter 6

C	constraint manifold
W	space of generalized forces
φ	placement of center of mass
$\dot{\varphi}$	translational velocity of placement of center of mass
$\{d_I\}$	director triad
$\{\dot{d}_I\}$	director velocities
ω	angular velocity
ϱ	joint location with respect to body-fixed director triad
u_φ	incremental displacement of center of mass
θ	incremental rotation
f	redundant force
f_φ	force applied to the center of mass
f_I	force applied to director d_I
τ	generalized force
τ_φ	translational force
τ_θ	rotational torque
D	Jacobian
g	holonomic constraints
g_d	discrete holonomic constraints
G	constraint Jacobian
G_d	discrete constraint Jacobian
P	null space matrix
B	cost function of the objective functional

Chapter 1

Introduction

The optimization and control of physical processes is of crucial importance in all modern technological sciences. In particular, optimal control theory is a mathematical optimization method for deriving control policies such that a certain optimality criterion is achieved. Rather than describing its observed behavior, one is interested in prescribing the motion of a dynamical system. This means that the laws that govern the system's behavior must contain variables whose values can be changed by someone acting outside and independently of the system itself. Thus, in addition to state variables that define precisely what the system is doing at time t, we have control variables or parameters that can be used to modify the subsequent behavior of the system.

In mechanical engineering, one is often interested in steering or guiding a mechanical system from an initial to a final state under the influence of control forces such that a given quantity, for example control effort or maneuver time is minimal. Typical challenges arise in vehicle dynamics, space mission design, or robotics in determining the time-minimal path of a vehicle, an energy-efficient trajectory of a satellite in space, or in optimizing the motion of a robot.

Obviously, in contrast to machines, nature behaves in general in an optimal way. On the one hand, the theory and application of optimal control helps capturing and understanding certain biological processes, such as the motion of a falling cat that flips in an efficient way to land on its feet. On the other hand, it can be used to optimize the behavior of biomechanical models of, for example the human body. In this way, the simulation of optimal control processes may support the development of prostheses and implants in modern medical surgery. Another area of growing interest is the optimization of movement in sports. The knowledge gained from optimal control simulations may help to improve individual techniques or even suggest the development of new techniques (as has been observed during the last decades, for example for high and ski jumping).

In economies, the determination of optimal financing and investment strate-

gies (for example, finding an optimal capital structure or optimal mix of funds, or optimal portfolio choice) for corporations and the economy is important for an efficient allocation of resources.

Having mentioned just a few fields of application, one can see that optimal control theory obviously has a high relevance to modern developments in science, industry and commerce.

As a consequence of nonlinearities present in even the simplest models of interest, an analytical solution to the optimal control system is rarely feasible. This necessitates numerical methods that approximate the solution of the mathematical model. For the numerical treatment, discretization techniques are required. A variety of solution strategies exist differing in manner and point in time of the discretization, which results in different approximation behaviors and properties. Naturally, one seeks realistic approximations that share the relevant properties of the analytical solution.

For the simulation of mechanical systems in particular it is desirable to preserve certain qualitative properties and structures such as energy, momentum, and symplecticity, or, in the case of forced systems, the change in energy and momentum due to the actuation by control forces. Time-stepping schemes which inherit the (conservation) properties of the continuous mechanical system are referred to as *mechanical integrators*. In addition to the benefit of good energy behavior, the conversation of momentum maps or the symplectic form along the discrete solution enhances its veritableness since its qualitative and structural characteristics are transferred to the discrete solution. Energy-momentum conserving schemes relying on a direct discretization of the ODEs, have been widely investigated; see for example [9, 34, 83, 82, 133, 141, 142, 143, 145]. Based on concepts from discrete variational mechanics, namely the discretization of the variational formulation behind the ODEs, symplectic-momentum integrators have been derived for example by [56, 73, 91, 93, 113, 132]; see [140, 144] for a discussion on energy-momentum and symplectic schemes.

In order to solve optimal control problems for mechanical systems, this thesis links two important areas of research:

optimal control and variational mechanics.

The motivation for combining these fields of investigation is twofold. Besides the aim of preserving certain properties of the mechanical system for the approximated optimal solution, optimal control theory and variational mechanics have their common origin in the *calculus of variations* - the theory of the optimization of integrals. In mechanics, the concept of calculus of variations is the *principle of stationary action* which, when applied to the action of a mechanical system can be used to obtain the equations of motion for that system. This principle led to the development of the Lagrangian and Hamiltonian formulations of classical mechanics. In optimal control theory the concept of calculus of variations

bears fundamental results in order to derive optimality conditions for the control system under consideration.

In addition to the importance in continuous mechanics and control theory, *discrete calculus of variations* and the corresponding discrete variational principles play an important role in constructing efficient numerical methodologies for the simulation of mechanical systems and for optimizing dynamical systems.

Due to their common origin in theory as well as in computational approaches, the combination of these two fields of research provides interesting insight into theoretical and computational issues and provides profitable approaches to specific problems.

Optimal control and variational mechanics The theory of optimal control is an area developed since the 1950s in response to American and Russian efforts to explore the solar system. The mathematical problems of space navigation include optimization problems. One wishes to construct trajectories along which a space vehicle, controlled by a small rocket motor, will reach its destination in minimum time or using the minimum amount of fuel. These new problems were not solvable by the methods available at that time and the theory had to be extended to meet new challenges.

In contrast to the theory of optimal control, classical mechanics is one of the oldest and largest subjects in science and technology. It deals with the dynamics of particles, rigid bodies, continuous media (fluid, plasma, and solid mechanics), as well as other fields of physics (such as electromagnetism, gravity, etc.). The problem of computing the dynamics of general mechanical systems arose already in the work of Galilei (published 1638). Newton's *Principia* (1687, [122]) allowed reducing the analysis of the motion of free mass points (the mass points being planets such as Mars or Jupiter) to the solution of differential equations. However, many important ideas in mechanics are based on variational principles and are accredited to Euler, Lagrange and Hamilton. The notion that the laws of nature act in such a way as to extremize some function facilitates the description of motions of more complicated systems such as rigid bodies or bodies attached to each other by rods or springs. We consider the variational problem of extremizing the *action integral*

$$\int_0^T L(q(t), \dot{q}(t))\,\mathrm{d}t$$

among all curves $q(t)$ that connect two given points $q(0) = q^0$ and $q(T) = q^T$. Here, the *Lagrangian* L consists of the difference between kinetic energy $K = K(q, \dot{q})$ (which is often of the form $\frac{1}{2}\dot{q}^T M(q)\dot{q}$ where $M(q)$ is symmetric and positive definite) and potential energy $V = V(q)$. In fact, assuming $q(t)$ to be

extremal and considering a variation $q(t) + \varepsilon\delta q(t)$ with the same endpoints, that is with $\delta q(0) = \delta q(T) = 0$ and using partial integration yields

$$0 = \int_0^T \left(\frac{\partial L}{\partial q}\delta q + \frac{\partial L}{\partial \dot{q}}\delta\dot{q} \right) \mathrm{d}t = \int_0^T \left(\frac{\partial L}{\partial q} - \frac{d}{dt}\frac{\partial L}{\partial \dot{q}} \right) \delta q \, \mathrm{d}t.$$

This leads to the differential equations

$$\frac{d}{dt}\left(\frac{\partial L}{\partial \dot{q}}\right) = \frac{\partial L}{\partial q}, \tag{1.1}$$

which constitute the *Lagrangian equations* or *Euler-Lagrange equations* of the system. The (numerical or analytical) integration of these equations allows one to predict the motion of any such system from given initial values.

Lagrange (1736-1813, [84, 85]) himself did not recognize the equations of motion as being equivalent to a variational principle. This was observed only a few decades later by Hamilton (1805-1865) and is therefore known as *Hamilton's principle*.

A special property of the solutions of the equations of motion in Lagrangian or Hamiltonian dynamics is the conservation of first integrals. Under certain suppositions, the energy, the momentum maps related to the system's symmetries and the symplectic form remain unchanged along these solutions. This is for example stated within Noether's theorem (see Section 3).

If one wishes to talk about control theory for mechanical systems then the natural "inputs" for these systems are forces. We may think of the Euler-Lagrange equations for a Lagrangian L as representing the"natural" motion of the system, that is the motion of the system in the absence of external interaction. A force, on the other hand is an external interaction. The *Lagrange-d'Alembert principle* states how a force f should appear in the Euler-Lagrange equations. Given a Lagrangian L and a force field f, the Lagrange-d'Alembert principle for a curve $q(t)$ in Q is

$$\delta \int_0^T L(q(t), \dot{q}(t)) \, \mathrm{d}t + \int_0^T f(q(t), \dot{q}(t)) \cdot \delta q(t) \, \mathrm{d}t = 0,$$

for a given variation δq (vanishing at the end points). Thus, the condition for a stationary curve takes the form of the standard Euler-Lagrange equations with forces:

$$\frac{d}{dt}\left(\frac{\partial L}{\partial \dot{q}}\right) - \frac{\partial L}{\partial q} = f(q, \dot{q}). \tag{1.2}$$

These are a generalization of Lagrange's equations for mechanical systems with forcing. For forced systems, the forced version of Noether's theorem (see Section 3) still gives a relation between the evolution of first integrals over time and the amount of the applied forces changing the quantities that have been conserved in the unforced case.

From a purely mathematical point of view, optimal control problems are also variants of a class of problems of the calculus of variations. As in Hamilton's principle, the problem is to minimize an integral (the objective functional) which is now subject to constraints describing the dynamical behavior of the underlying system. These constraints also determine the set of admissible variations and are typically differential equations or, for mechanical systems, given by the Lagrange-d'Alembert principle. The constraints on these system's dynamics can be adjoined to the objective functional by introducing a time-varying *Lagrange multiplier* vector λ, whose elements are called the *costates* (or *adjoints*) of the system. The optimal control law that minimizes the augmented objective functional can be derived using the *Pontryagin maximum principle (PMP)* (a necessary condition). This condition - as a generalization of the Euler-Lagrange equation - forms the fundamental theorem of optimal control theory (see Chapter 2). The resulting boundary value system is also known as state-costate(adjoint) system.

In Figure 1.1 the analogy of the role of the calculus of variations in both mechanics and optimal control theory is depicted.

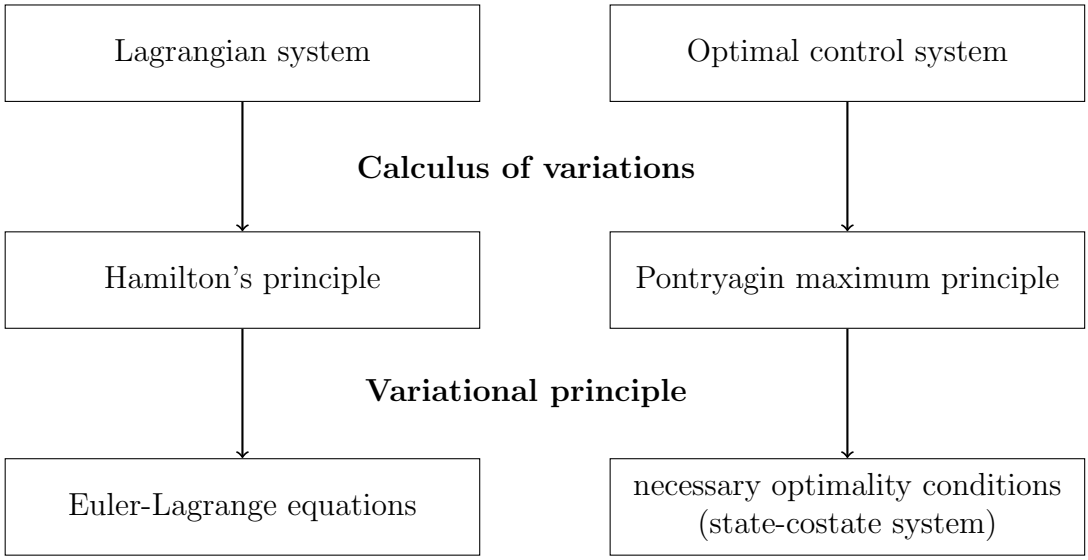

Figure 1.1: The calculus of variations in mechanics and optimal control theory.

Discrete optimal control and discrete variational mechanics The theory of discrete variational mechanics has its roots in the optimal control literature of the 1960s, see for example [29, 61, 65]. In [29] Cadzow developed a discrete calculus of variations theory in the following way: A function is introduced whose values depend on a sequence of numbers. This sequence can be thought of as a discrete time sequence of numbers which evolve with discrete time. The problem of finding the discrete time sequence minimizing this function requests that the optimal sequence must satisfy a second-order difference equation. This set of necessary conditions is called the *discrete Euler equation* because of its similarity to the Euler equation of classical calculus of variations.

Equivalent to the application of variational techniques in the optimization of continuous dynamical systems to derive necessary optimality conditions (Pontryagin maximum principle), discrete variational techniques provide necessary optimality conditions for discrete control systems. This procedure has been referred to as the *discrete maximum principle* ([61]).

The numerical application of discrete calculus of variations to optimal control problems is known as *direct solution method*. *Direct* and *indirect* methods for the numerical solution of optimal control problems exist (see Section 2.2 for an overview and references). The indirect methods are based on the explicit expression of the necessary optimality conditions that are derived via the Pontryagin maximum principle. In contrast, direct methods transform the optimal control problem into a finite dimensional nonlinear optimization problem by a finite dimensional parametrization of the controls only or of both, states and controls (see Section 2.2.2). For example, one uses discrete time-stepping schemes to derive a discrete description of the dynamical system under consideration. The discrete equations then serve as equality constraints for the optimization problem. A solution of the necessary conditions for the resulting constrained optimization problem known as *Karush-Kuhn-Tucker equations* is in accordance with a critical point of the discrete variational principle applied to the discrete objective function augmented by adjoining the discrete dynamical equations as constraints. Due to new generations of computers with rapidly growing capacities and the development of new and efficient techniques for the solution of large constrained optimization problems, the direct methods have become more popular since the 1970s.

The theory of discrete variational mechanics describes a variational approach to discrete mechanics and mechanical integrators. The simple but important idea in discrete mechanics is the following: Consider a mechanical system with configuration manifold Q. The velocity phase space is then TQ and the Lagrangian is a map $L : TQ \to \mathbb{R}$. In discrete mechanics, the starting point is to replace TQ with $Q \times Q$ and we intuitively regard two nearby points q_0 and q_1 as being the discrete analogue of a velocity vector. Now consider a discrete Lagrangian

$L_d(q_0, q_1)$, which we think of as approximating the action integral along the curve segment between q_0 and q_1. For a discrete curve of points $\{q_k\}_{k=0}^N$ we calculate the discrete action along this sequence by summing the discrete Lagrangian on each adjacent pair. Computing variations of this action with the fixed boundary points q_0 and q_N gives a discrete version of Hamilton's principle and results in the *discrete Euler-Lagrange equations*.

Analogous to the continuous case, conservation of discrete energy, discrete momentum maps related to the discrete system's symmetries and the discrete symplectic form can be shown. This is due to the discretization of the variational structure of the mechanical system directly. Early work on discrete mechanics was often independently done by [30, 89, 90, 100, 103, 104, 105]. In this work, the point of the discrete action sum, the discrete Euler-Lagrange equations and the discrete Noether's theorem were clearly understood. The variational view of discrete mechanics and its numerical implementation is further developed in [158, 159] and then extended in [18, 19, 72, 73, 109, 110].

In considering a discrete Lagrangian system as an approximation of a given continuous system, the discrete system is an integrator for the continuous system. Since discrete Lagrangian maps preserve the symplectic structure, they are, regarded as integrators, necessarily symplectic. This route of a variational approach to symplectic-momentum integrators has been taken by Suris [147], MacKay [102] and in a series of papers by Marsden and coauthors, see the review by Marsden and West [113] and references therein. In [113] a detailed derivation and investigation of these *variational integrators* for conservative as well as for forced and constrained systems is given.

In Figure 1.2 the analogy of applying the discrete calculus of variations to mechanical and optimal control systems is depicted.

Combining optimal control and variational mechanics This thesis concerns the optimal control of dynamical systems whose behavior can be described by the Lagrange-d'Alembert principle. To numerically solve this kind of problem, we make use of discrete calculus of variations only, that means we apply the discrete variational principle on two layers. On the one hand we use it for the description of the mechanical system under consideration, and on the other hand for the derivation of necessary optimality conditions for the optimal control problem.

In Figure 1.3 the different possibilities arranging discretization and variations for deriving necessary optimality conditions are illustrated. The left branch is based on variations on the continuous level only (*variation, variation, discretization*), and corresponds to the application of an indirect solution method. The middle branch consisting of a mixture of variations on the continuous and the dis-

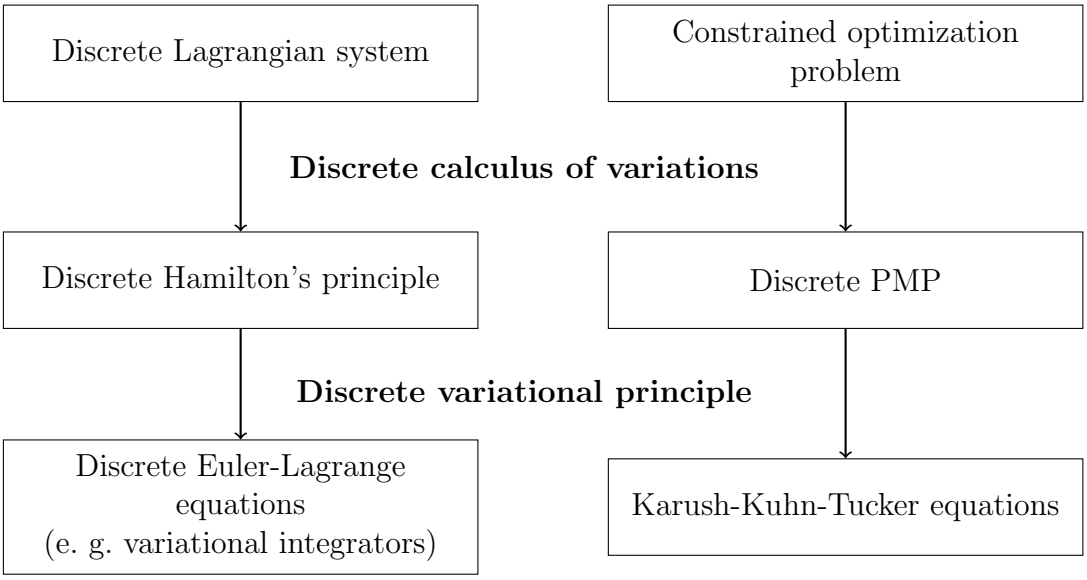

Figure 1.2: The discrete calculus of variations in discrete mechanics and optimization theory.

crete stage (*variation, discretization, discrete variation*) denotes the strategy of a direct solution method. The approach depicted in the right branch (*discretization, discrete variation, discrete variation*), as presented in this thesis comprises the calculus of variations on the discrete level only. This method is denoted by *DMOC*, standing for *Discrete Mechanics and Optimal Control*.

The application of discrete variational principles already on the dynamical level (namely the discretization of the Lagrange-d'Alembert principle) leads to structure-preserving time-stepping equations which serve as equality constraints for the resulting finite dimensional nonlinear optimization problem. The benefits of variational integrators are handed down to the optimal control context. For example, in the presence of symmetry groups in the continuous dynamical system, also along the discrete trajectory the change in momentum maps is consistent with the control forces. Choosing the objective function to represent the control effort, which has to be minimized is only meaningful if the system responds exactly according to the control forces.

Related work A survey of different methods for the optimal control of dynamical systems described by ordinary differential equations is given in Section 2.2. However, to our knowledge, DMOC is the first approach to solutions of optimal control problems involving the concept of discrete mechanics to derive

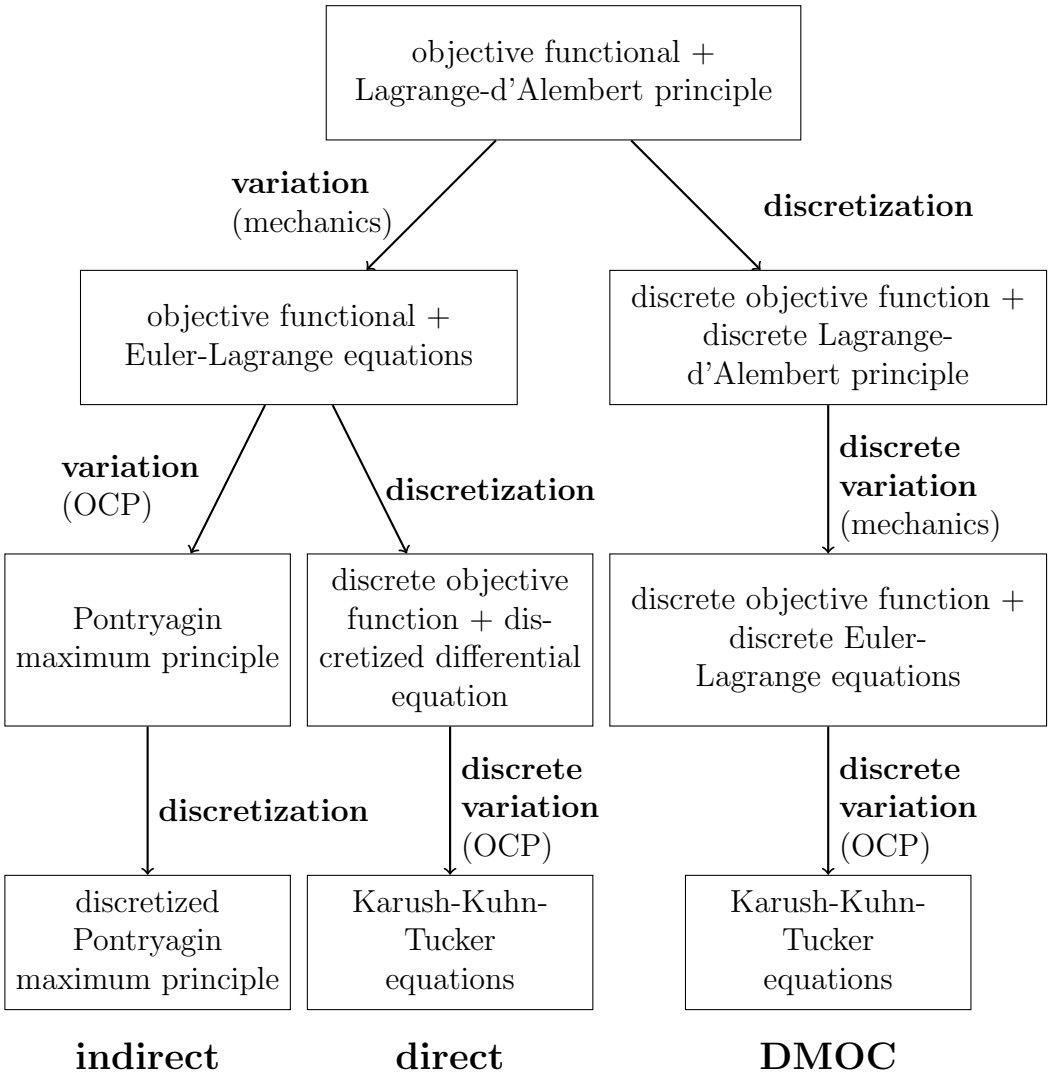

Figure 1.3: Optimal control for mechanical systems: the order of variation and discretization for deriving the necessary optimality conditions.

structure-preserving schemes for the resulting optimization algorithm.

Since our first formulations and applications to space mission design and formation flying ([67, 69, 68]), DMOC has been applied for example to problems from robotics and biomechanics ([74, 78, 79, 114, 124, 134]) and to image analysis ([116]). From the theoretical point of view, considering the development of variational integrators, extensions of DMOC to mechanical systems with nonholonomic constraints or to systems with symmetries are quite natural and have already been analyzed in [78, 79]. Further extensions are currently under investigation, for example DMOC for hybrid systems [124] and for constrained multi-body dynamics (see Chapter 6 and [98, 99]).

DMOC related approaches are presented in [87, 88]. The authors discretize the dynamics by a Lie group variational integrator. Rather than solving the resulting optimization problem numerically, they construct the discrete necessary optimality conditions via the discrete variational principle and solve the resulting discrete boundary value problem (the discrete state and adjoint system). The method is applied to the optimal control of a rigid body and to the computation of attitude maneuvers of a rigid spacecraft.

Main issues and outline of this work

The primary objective of this work is the development of a unified variational framework for the optimal control of mechanical systems in a continuous and a discrete setting. Based on discrete variational principles on all levels, the discrete optimal control problem yields a strategy for the efficient solution of these kind of problems.

In addition to the theoretical and numerical investigation of this method, we (i) give a focused survey of optimal control theory and existing methods and on discrete variational mechanics, (ii) present numerical results of a variety of different problems arising in different areas of application, (iii) develop efficient computational approaches for exploiting system structures to reduce for example the computational effort, (iv) extend the optimal control framework to mechanical systems with constraints in multi-body dynamics.

Moreover, the numerical performance of the developed method and its relationship to other existing optimal control methods are investigated both through theoretical considerations as well as with the help of numerical examples.

The outline of this thesis is as follows:

Chapter 2 and Chapter 3 comprise the basic principles of the two areas of research linked within this work. In Chapter 2 we review the relevant concepts from classical optimal control theory, ranging from the problem formulation

to a discussion of different solution methodologies to optimal control problems. We introduce the Pontryagin maximum principle and the Karush-Kuhn-Tucker equations providing the necessary conditions of optimality for optimal control problems and for constrained optimization problems, respectively. Both kinds of problems are linked via the application of direct solution methods transforming the optimal control problem into a constrained optimization problem. We give a brief overview of numerical solution strategies and refer to corresponding software packages.

In Chapter 3 we introduce the relevant concepts from classical variational mechanics and discrete variational mechanics. Following the work of [113], we give basic definitions and concepts for both Lagrangian mechanics as well as for Hamiltonian mechanics. In this context, we introduce Hamilton's principle, Noether's theorem concerning preservation properties, and the Legendre transform linking Lagrangian and Hamiltonian mechanics. We transfer these concepts to the discrete mechanics framework. In the second part of Chapter 3, we focus on the Lagrangian and Hamiltonian description of control forces for the established framework of variational mechanics. Definitions and concepts of the variational principle, the Legendre transform, and Noether's theorem are readopted for the forced case in both the continuous as well as the discrete setting.

The main part of this work - the description of our optimal control method DMOC - is presented in Chapter 4 linking optimal control theory and variational mechanics to set up a variational formulation for a special class of problems: optimal control problems for mechanical systems. Again, we develop a continuous and a discrete framework for Lagrangian and Hamiltonian optimal control problems. We link both frameworks viewing the discrete problem as an approximation of the continuous one. The application of discrete variational principles for a discrete description of the dynamical system leads to structure-preserving time-stepping equations. Here, the special benefits of variational integrators are handed down to the optimal control context. These time-stepping equations serve as equality constraints for the resulting finite dimensional nonlinear optimization problem, therefore the described procedure can be categorized as a direct solution method as introduced in Chapter 2.

Based on quadrature approximation we construct optimal control problem approximations of higher order and show how to compute the order of consistency with the help of a comparison of continuous and discrete Lagrangians and forces. In arranging our formulation in the context of existing concepts and methodologies for optimal control problems, we show the equivalence of the discrete Lagrangian optimal control problems to those resulting from Runge-Kutta discretizations of the corresponding Hamiltonian system. This equivalence allows us to construct and compare the adjoint systems of the continuous and the discrete Lagrangian optimal control problem. In this way, one of our main results

is related to the order of approximation of the adjoint system of the discrete optimal control problem to that of the continuous one. With the help of this approximation result, we show that the solution of the discrete Lagrangian optimal control system converges to the continuous solution of the original optimal control problem. The proof strategy is based on existing convergence results of optimal control problems discretized via Runge-Kutta methods ([41, 53]).

Chapter 5 gives a detailed description of implementation issues of DMOC as well as a short overview of existing routines for the optimization and differentiation of the resulting problem. Furthermore, a variety of numerical examples and results demonstrating the capability of DMOC to solve optimal control problems are presented. Applications range from trajectory planning problems of single and multiple vehicles in formation to the optimal control of multi-body dynamics. Here, a variety of different formulations for objective functionals, boundary conditions and path constraints are used. We numerically verify the preservation and convergence properties of DMOC and the benefits of using DMOC compared to other standard methods to the solution of optimal control problems. Finally, we develop and investigate a spatial decentralized approach to a problem in space mission design: the efficient reconfiguration of formation flying spacecraft.

In Chapter 6 we extend the developed framework for the optimal control of mechanical systems to constrained mechanical systems in multi-body dynamics. In this context, the multi-body system is formulated as a constrained system, that is each body is viewed as a constrained continuum, described in terms of redundant coordinates subject to holonomic constraints. The couplings between the bodies are characterized via external holonomic constraints describing the kinematic conditions arising from the specific joint connections. Within the variational framework of Lagrangian mechanics the configuration constraints are enforced adjoining them to the Lagrangian with Lagrange multipliers. With the help of the null space method (see [7]), we reduce the number of unknowns (configurations and torques at the time nodes) and the dynamic constraints to the minimal possible number. The combination with DMOC leads to an optimization algorithm that inherits both the conservation properties from the constrained scheme as well as the benefit of exact constraint fulfillment, correct computation of the change in momentum maps and good energy behavior. We apply the developed methodology to the optimal control of two multi-body systems arising in robotics and biomechanics.

The thesis concludes with a summary of the results and a discussion of open problems and possible future directions.

The Appendix provides a collection of definitions and relevant notions. Moreover, it contains details concerning the derivation of the transformed adjoint system introduced in Section 4.5 and a detailed proof of the convergence result stated in Section 4.6 based on the proof in [41, 53].

Chapter 2

Optimal control

In this chapter we give an introduction into optimal control theory beginning with the general problem formulation and the necessary optimality conditions derived by the *Pontryagin maximum principle*. We give an overview of existing solution methods for optimal control problems falling into two kinds of approaches - *indirect* and *direct* methods - where the focus will be on the latter one. The solution methods are thoroughly compared and their advantages and disadvantages are discussed. Here, we mainly follow the work of [17].

2.1 Optimal control problem

The aim of optimal control is to guide or steer certain processes, arising in nature and engineering, such that a given quantity, for example control effort or maneuver time is minimal. To be more precise, a given *objective functional* has to be optimized by taking into account the dynamics of the process described by a *dynamical system*. In this section we give a mathematical formulation of optimal control problems and introduce necessary optimality conditions for this kind of problems.

2.1.1 Problem formulation

Assume that on the time interval $I = [0, T]$, a dynamical system is given by a differential equation of the form

$$\dot{x}(t) = f(x(t), u(t)) \tag{2.1}$$

with the state function $x : I \to \mathbb{R}^{n_x}$, the control function $u : I \to \mathbb{R}^{n_u}$ and $f : \mathbb{R}^{n_x} \times \mathbb{R}^{n_u} \to \mathbb{R}^{n_x}$ continuously differentiable. Assume that the system has to

be steered within the time interval I from an initial to a final state given by the *final point constraint* $r : \mathbb{R}^{n_x} \to \mathbb{R}^{n_r}$, $0 \leq n_r \leq n_x$,

$$r(x(T)) = 0, \tag{2.2}$$

and the trajectories $x(t)$ and $u(t)$ are bounded by the *path constraint* defined by $h : \mathbb{R}^{n_x} \times \mathbb{R}^{n_u} \to \mathbb{R}^{n_h}$,

$$h(x(t), u(t)) \geq 0. \tag{2.3}$$

At the same time, a given *objective functional*

$$J(x, u) = \int_0^T C(x(t), u(t))\,\mathrm{d}t \tag{2.4}$$

with $C : \mathbb{R}^{n_x} \times \mathbb{R}^{n_u} \to \mathbb{R}$ continuously differentiable and a final condition defined by $\Phi : \mathbb{R}^{n_x} \to \mathbb{R}$,

$$\Phi(x(T)), \tag{2.5}$$

the *Mayer term* of the objective, have to be minimized. The sum of (2.4) and (2.5) is called the *Bolza type objective functional*. An optimal control problem can now be formulated as

Problem 2.1.1 (Optimal Control Problem (OCP))

$$\min_{x(\cdot),u(\cdot),(T)} J(x, u) = \int_0^T C(x(t), u(t))\,\mathrm{d}t + \Phi(x(T)) \tag{2.6a}$$

subject to

$$\dot{x}(t) = f(x(t), u(t)), \tag{2.6b}$$
$$x(0) = x_0, \tag{2.6c}$$
$$0 \leq h(x(t), u(t)), \tag{2.6d}$$
$$0 = r(x(T)). \tag{2.6e}$$

The interval length T may either be fixed, or appear as a degree of freedom in the optimization problem.

Remark 2.1.2 More general, additional algebraic constraints can be included as well. Then we obtain a differential algebraic system instead of the ordinary differential equation (2.6b). As the optimal control of differential algebraic systems is not the main focus in this thesis we restrict ourselves to the problem formulation above. In Chapter 6 optimal control problems with additional algebraic constraints arising from constrained multi-body dynamics are considered.

Definition 2.1.3 A pair $(x(\cdot), u(\cdot))$ is *admissible* (or *feasible*), if the constraints (2.6b)-(2.6e) are fulfilled. The set consisting of all admissible (feasible) pairs is the *admissible (feasible) set* of Problem 2.1.1. An admissible (feasible) pair (x^*, u^*) is an *optimal solution* of Problem 2.1.1, if

$$J(x^*, u^*) \leq J(x, u)$$

for all admissible (feasible) pairs (x, u). The admissible (feasible) pair (x^*, u^*) is a *local optimal solution*, if there exists a neighborhood $B_\delta((x^*, u^*)), \delta > 0$, such that

$$J(x^*, u^*) \leq J(x, u)$$

for all admissible (feasible) pairs $(x, u) \in B_\delta((x^*, u^*))$. The function $x^*(t)$ is called *(locally) optimal trajectory*, and the function $u^*(t)$ is the *(locally) optimal control*.

2.1.2 Necessary conditions for optimality

In this section, we introduce necessary conditions for the optimality of a solution $(x^*(t), u^*(t))$ to Problem 2.1.1. We restrict ourselves to the case of optimal control problems with the controls constrained to the (nonempty) *pointwise control constraint set* $U = \{u(t) \in \mathbb{R}^{n_u} \,|\, h(u(t)) \geq 0\}$ (also called the *set of pointwise admissible controls*) and fixed final time T. Therefore, (2.6) reduces to

$$\min_{x(\cdot), u(\cdot)} J(x, u) = \int_0^T C(x(t), u(t))\,\mathrm{d}t + \Phi(x(T)) \tag{2.7a}$$

subject to

$$\dot{x}(t) = f(x(t), u(t)), \tag{2.7b}$$
$$x(0) = x_0, \tag{2.7c}$$
$$0 = r(x(T)), \tag{2.7d}$$
$$u(t) \in U. \tag{2.7e}$$

Necessary conditions for optimality of solution trajectories $\eta(t) = (x^*(t), u^*(t))$, $t \in I$ can be derived based on variations of an augmented cost function, the *Lagrangian* of the control system.

Definition 2.1.4 The *Lagrangian* of the optimal control system (2.7) is a function $\mathcal{L} : \mathbb{R}^{n_x} \times \mathbb{R}^{n_u} \times \mathbb{R}^{n_x}$ defined by

$$\mathcal{L}(\eta, \lambda) = \int_0^T C(x(t), u(t)) + \lambda^T(t) \cdot (\dot{x} - f(x(t), u(t)))\,\mathrm{d}t + \Phi(x(T)), \tag{2.8}$$

where the variables λ_i, $i = 1, \ldots, n_x$, are the *adjoint variables* or the *costates*. A point $(\eta^*(t), \lambda^*(t))$ is a *saddle point* of (2.8), if for all $\eta(t)$ and $\lambda(t)$ it holds

$$\mathcal{L}(\eta(t), \lambda^*(t)) \leq \mathcal{L}(\eta^*(t), \lambda^*(t)) \leq \mathcal{L}(\eta^*(t), \lambda(t)).$$

The function $\mathcal{H} : \mathbb{R}^{n_x} \times \mathbb{R}^{n_u} \times \mathbb{R}^{n_x} \to \mathbb{R}$ defined by

$$\mathcal{H}(x, u, \lambda) := -C(x, u) + \lambda^T \cdot f(x, u), \tag{2.9}$$

is called the *Hamiltonian* of the optimal control problem.

To motivate Theorem 2.1.5, we associate a local solution of (2.7) with a saddle point of the Lagrangian $\mathcal{L}$. Thus, by setting variations of $\mathcal{L}$ with respect to η and λ to zero, the resulting *Euler-Lagrange equations* (see Chapter 3) provide necessary optimality condition for the optimal control problem (2.7). This result is stated in the following Theorem.

Theorem 2.1.5 (Pontryagin Maximum Principle) *Let (x^*, u^*) be an optimal solution of (2.7). Then, there exists a piecewise continuous differentiable function $\lambda : [0, T] \to \mathbb{R}^{n_x}$ and a vector $\alpha \in \mathbb{R}^{n_r}$ such that*

$$\mathcal{H}(x^*(t), u^*(t), \lambda(t)) = \max_{u(t) \in U} \mathcal{H}(x(t), u(t), \lambda(t)) \text{ for all } t \in [0, T], \tag{2.10a}$$

$$\dot{x}^*(t) = \nabla_\lambda \mathcal{H}(x^*(t), u^*(t), \lambda(t)), \quad x^*(0) = x_0, \tag{2.10b}$$

$$\dot{\lambda}(t) = -\nabla_x \mathcal{H}(x^*(t), u^*(t), \lambda(t)), \tag{2.10c}$$

$$\lambda(T) = \nabla_x \Phi(x^*(T)) - \nabla_x r(x^*(T))\, \alpha. \tag{2.10d}$$

Proof: A general proof requires more technical details as the intuitive derivation via the calculus of variations and can be found, for example in [127]. □

Early developments of the maximum principle have been carried out by Pontryagin et al. [127], Isaacs [63], and Hestenes [59]. The approach has been extended to handle general constraints (2.6d) on the control and state variables (for an overview see, for example Hartl, Sethi, and Vickson [58]). The Pontryagin maximum principle plays an important role in the construction of solution methods (see Section 2.2.1) and to analyze their convergence properties (see Section 4.6).

2.2 Solution methods for optimal control problems

In this section, solution methods for optimal control problems of the form of Problem 2.1.1 are introduced and discussed (an overview of existing solution

methods and a more detailed description can be found, for example in [17]). The numerical treatment of optimal control problems can be mainly divided into two branches: the *indirect* and the *direct* methods.

Indirect methods use the explicit expression of the necessary conditions for the optimal control problem, derived via the Pontryagin maximum principle. Instead, direct methods transform the problem into a finite dimensional nonlinear optimization problem by a finite dimensional parametrization of the controls only or of both, states and controls.

2.2.1 Indirect methods

The necessary conditions for optimality of solution trajectories $x^*(t)$ and $u^*(t),\ t \in I$ given by the Pontryagin maximum principle can be formulated as a boundary value problem

$$\begin{aligned} x^*(0) &= x_0, \\ 0 &= r(x^*(T)), \\ \lambda^*(T) &= \nabla_x \Phi(x^*(T)) - \nabla_x r(x^*(T))\,\alpha, \\ \dot{x}^*(t) &= \nabla_\lambda \mathcal{H}(x^*(t), u^*(t), \lambda^*(t)), \\ \dot{\lambda}^*(t) &= -\nabla_x \mathcal{H}(x^*(t), u^*(t), \lambda^*(t)), \end{aligned} \tag{2.11}$$

with $\alpha \in \mathbb{R}^{n_r}$ being the Lagrange multipliers for the end point constraints. The optimal controls are obtained by a pointwise maximization of the Hamiltonian:

$$u^*(t) = \arg\max_{u(t)\in U} \mathcal{H}(x^*(t), u^*(t), \lambda^*(t)). \tag{2.12}$$

Gradient methods can now be used to iteratively improve an approximation of the optimal control by maximizing the Hamiltonian subject to the boundary value problem (2.11) (Cauchy [31]; Kelley [77]; Tolle [152]; Bryson and Ho [27]; Miele [117]; Chernousko and Luybushin [33]). In each iteration step, the differential equation (2.6b) is numerically integrated forward in time while the adjoint differential equations are integrated backwards in time.

On the other hand *multiple shooting* and *collocation* can be used to solve the resulting multipoint boundary value problem (MPBVP) derived from the necessary conditions of optimality. Numerical multiple shooting methods have been developed by Fox [47], Keller [76], Bulirsch [28], Deuflhard [36], Bock [20], and Hiltmann [60], collocation methods by for example Dickmanns and Well [37], Bär [5] and Ascher et al. [2]. For an introduction into multiple shooting we refer to Ascher et al. [3] or Stoer and Bulirsch [146].

For the practical use of indirect methods significant knowledge and experience in the theory and the problem under consideration is required. Proper formulations of the necessary conditions in a numerically suitable way must be derived. In addition, changes in the problem formulation (for example by a modification of the model equations) are difficult to include in the solution procedure. Furthermore, indirect methods are sensitive with respect to initial guesses for the adjoints and controls. Therefore, carefully chosen suitable initial guesses of the state and adjoint trajectories must be provided.

These practical drawbacks of indirect methods motivate the introduction of a second class of numerical techniques finding solutions to optimal control problems, the class of *direct methods*.

2.2.2 Direct methods

The basic idea of direct methods for the solution of optimal control problems is to transcribe the original infinite dimensional problem (2.6) into a finite dimensional Nonlinear Programming (NLP) problem (Kraft [80]; Bock and Plitt [21]; Biegler [16]; Betts [11, 12]; Polak [126]; von Stryk and Bulirsch [156]). This approach has been pushed by the progress in nonlinear optimization (Han [57]; Powell [128]; Barclay, Gill, and Rosen [6]; Betts [11]). Two basically different solution strategies for the reformulated problem exist (see Pytlak, [129], for a survey):

(i) Sequential simulation and optimization: In every iteration step of the optimization method, the model equations are solved "exactly" by a numerical integration method for the current guess of control parameters.

(ii) Simultaneous simulation and optimization: The discretized differential equations enter the transcribed optimization method as nonlinear constraints that can be violated during the optimization procedure. At the solution, however, they have to be satisfied.

In the following, we briefly sketch three different strategies of direct methods: *single shooting* (a pure sequential approach), *collocation methods* (a pure simultaneous approach) and *multiple shooting* (a mixture of sequential and simultaneous approach).

Direct single shooting In the direct single shooting method (for example Kraft [80]) the control function is approximated by a finite dimensional parametrization. In each iteration step, the initial value problem (2.6b), (2.6c) determined by a guess for the control parameter vector, can be solved for the solution trajectory $x(t)$ depending on the control parameters only. By substituting this trajectory into the objective functional one obtains a cost function depending

on the control parameters only. This has to be minimized subject to path constraints, which have been discretized on a given time grid and subject to the final point constraint. Here, all equations are formulated depending on the control parameters only.

Direct multiple shooting The direct multiple shooting method (Bock and Plitt [21]) is based on the same idea as the single shooting approach, but additionally, the time interval I is divided into subintervals. On each subinterval a corresponding initial value problem has to be solved. To guarantee continuity of the solution trajectories over the interval boundaries, the states at the boundaries of each interval are introduced as extra variables (*node values*). For these nodes we enforce, that the solution trajectory of the previous interval matches the initial value of the following. This strategy results in an optimization problem that depends on the control parameters and the node values only. The problem is restricted by the discretized path constraints and the matching conditions between the intervals as inequality and equality constraints, respectively.

Direct collocation In the direct collocation method (for example von Stryk [153]), both state and control variables are approximated by piecewise defined functions on a given time grid. Within each collocation interval these functions are chosen as parameter dependent polynomials. The polynomials' coefficients are determined by enforcing continuity or higher order differentiability of the approximating functions at the boundaries of the subintervals. In order to formulate a nonlinear optimization problem, the model equations and the continuous constraints are explicitly discretized. For example the model equations are only to be satisfied at the *collocation points* within each subinterval and the inequality constraints on a second grid within the time interval I. Substituting the approximating functions into the objective functional leads to the formulation of an optimization problem that is restricted by discrete path constraints and discrete model equations.

Other discrete approximation techniques are based for example on the use of Runge-Kutta discretizations ([53]), finite differences ([106]), or Galerkin methods ([43]).

Remark 2.2.1 In Section 2.4 we give a short comparison of the direct methods introduced above as well as a classification of the optimal control method DMOC within these concepts.

2.3 Solution methods for nonlinear constrained optimization problems

In this section, methods for the solution of nonlinear optimization problems are presented. These problems arise from the discretization of optimal control problems by direct transcription methods as described in Section 2.2.2.

Let ξ be the set of parameters introduced by the discretization of an infinite dimensional optimal control problem. Then, the nonlinear programming problem to be solved is

$$\begin{aligned} &\min_{\xi} \varphi(\xi) \\ &\text{subject to} \quad a(\xi) = 0,\ b(\xi) \geq 0, \end{aligned} \tag{2.13}$$

where $\varphi : \mathbb{R}^n \to \mathbb{R}$, $a : \mathbb{R}^n \to \mathbb{R}^m$, and $b : \mathbb{R}^n \to \mathbb{R}^p$ are continuously differentiable.

2.3.1 Local optimality conditions

First of all, we review some conditions, which allow to decide whether a point ξ^* is a (local) solution of an optimization problem.

A *feasible point* is a point $\xi \in \mathbb{R}^n$ that satisfies $a(\xi) = 0$ and $b(\xi) \geq 0$. A *local minimum* of (2.13) is a feasible point ξ^* which has the property that $\varphi(\xi^*) \leq \varphi(\xi)$ for all feasible points ξ in a neighborhood of ξ^*. A *strict local minimum* satisfies $\varphi(\xi^*) < \varphi(\xi)$ for all neighboring feasible points $\xi \neq \xi^*$.

Active inequality constraints $b^{\text{act}}(\xi)$ at a feasible point ξ are those components $b_j(\xi)$ of $b(\xi)$ with $b_j(\xi) = 0$. We subsume the equality constraints and the active inequalities at a point ξ (known as *active set*) in a combined vector function of *active constraints* as

$$\tilde{a}(\xi) := \begin{pmatrix} a(\xi) \\ b^{\text{act}}(\xi) \end{pmatrix}.$$

Note that the active set may be different at different feasible points.

Regular points are feasible points ξ that satisfy the condition that the Jacobian of the active constraints, $\nabla\tilde{a}(\xi)^T$, has full rank, that means that all rows of $\nabla\tilde{a}(\xi)^T$ are linearly independent.

To investigate local optimality in the presence of constraints, we introduce the *Lagrangian multiplier* vectors $\lambda \in \mathbb{R}^m$ and $\mu \in \mathbb{R}^p$, that are also called *adjoint variables*, and we define the *Lagrangian function* $\tilde{\mathcal{L}}$ by

$$\tilde{\mathcal{L}}(\xi, \lambda, \mu) := \varphi(\xi) - \lambda^T a(\xi) - \mu^T b(\xi). \tag{2.14}$$

We now state a variant of the *Karush-Kuhn-Tucker* necessary conditions for local optimality of a point ξ^*. These conditions have been derived first by Karush in

1939 ([75]) and independently by Kuhn and Tucker in 1951 ([81]). For brevity, we restrict our attention to regular points only.

Theorem 2.3.1 (Karush-Kuhn-Tucker conditions (KKT)) *If a regular point $\xi^* \in \mathbb{R}^n$ is a local optimum of the NLP problem (2.13), then there exist unique Lagrange multiplier vectors $\lambda^* \in \mathbb{R}^m$ and $\mu^* \in \mathbb{R}^p$ such that the triple $(\xi^*, \lambda^*, \mu^*)$ satisfies the following necessary conditions:*

$$\begin{aligned} \nabla_\xi \tilde{\mathcal{L}}(\xi^*, \lambda^*, \mu^*) &= 0, \\ a(\xi^*) &= 0, \\ b(\xi^*) &\geq 0, \\ \mu^* &\geq 0, \\ \mu^* b_j(\xi^*) &= 0, \quad j = 1, \ldots, p. \end{aligned}$$

Proof: See for example [64]. □

A triple $(\xi^*, \lambda^*, \mu^*)$ that satisfies the Karush-Kuhn-Tucker conditions is called a *Karush-Kuhn-Tucker point (KKT point)*.

2.3.2 Sequential Quadratic Programming (SQP)

Sequential quadratic programming (SQP) (Han [57]; Powell [128]) is a very efficient iterative method to find a KKT point $(\xi^*, \lambda^*, \mu^*)$ of the NLP problem (2.13). The basic idea of SQP is to model (2.13) at a given approximate solution ξ^k, by a quadratic programming (QP) subproblem derived from a quadratic approximation of the Lagrangian of the NLP problem subject to the linearized constraints. Then the solution of this subproblem is used to construct a better approximation ξ^{k+1}, where the QP problem is assumed to reflect in some way the local properties of the original problem (for a detailed description see for example Barclay, Gill, and Rosen [6]; Gill, Murray, and Saunders [48]; Boggs and Tolle [22]). This process is iterated to create a sequence of approximations that will converge to a solution ξ^*.

To establish global convergence for constrained optimization algorithms, a way of measuring progress towards a solution is needed. For SQP this is done by constructing a *merit function*, a reduction in which implies that an acceptable step has been taken.

For the class of SQP methods considered, the vector of optimization variables $\xi_k \in \mathbb{R}^n$ itself and the vector of multipliers $v_k := (\lambda, \mu)_k \in \mathbb{R}^{m+p}$ are changed from (the major SQP) iteration number k to iteration number $k+1$ by

$$\begin{pmatrix} \xi_{k+1} \\ v_{k+1} \end{pmatrix} = \begin{pmatrix} \xi_k \\ v_k \end{pmatrix} + \alpha_k \begin{pmatrix} d_k \\ u_k - v_k \end{pmatrix}, \quad k = 0, 1, 2, \ldots,$$

where the *search direction* (d_k, u_k) is obtained as a solution of a nearly constrained quadratic problem resulting from a quadratic approximation of the Lagrangian

$$\tilde{\mathcal{L}}(\xi, \lambda, \mu) = \varphi(\xi) - \sum_{i=1}^{m} \lambda_i a_i(\xi) - \sum_{j=1}^{p} \mu_j b_j(\xi), \quad \lambda \in \mathbb{R}^m, \quad \mu \in \mathbb{R}^p :$$

$$\begin{aligned} & \min_d \tfrac{1}{2} d^T A_k d^T + \nabla\varphi(\xi_k)^T d \\ \text{subject to} \quad & \nabla a_i(\xi_k)^T d + a_i(\xi_k) = 0, \ i = 1, \ldots, m, \\ & \nabla b_j(\xi_k)^T d + b_j(\xi_k) \geq 0, \ j = 1, \ldots, p. \end{aligned} \tag{2.15}$$

Usually, A_k is a positive definite approximation of the Hessian H_k of the Lagrangian $\tilde{\mathcal{L}}(\xi_k, \lambda_k, \mu_k)$. The search direction d_k is the solution of the QP problem (2.15) and u_k is the corresponding multiplier. The quadratic (sub-)problem (2.15) itself is solved by an iterative method (usually, an active set strategy or an interior point method is employed). The success of SQP depends on the existence of a rapid and accurate algorithm for solving quadratic programs.

The *step size* $\alpha_k \in \mathbb{R}$ is obtained by an (approximate) one-dimensional minimization of a merit function (*line search*)

$$\psi_r \left(\begin{pmatrix} \xi \\ v \end{pmatrix} + \alpha \begin{pmatrix} d \\ u - v \end{pmatrix} \right)$$

with respect to α. A suitable merit function is, for example the Lagrangian augmented by penalty terms.

Existing SQP methods differ mainly by the choice of the step length α_k, and the choice of the approximation of the Hessian matrix A_k. The iterates (ξ_k, v_k) form a sequence that is expected to converge towards a KKT point (ξ^*, v^*) of the NLP problem. In practice, the iterations are stopped when a prespecified convergence criterion is fulfilled.

Remark 2.3.2 SQP methods are only guaranteed to find a local solution of the NLP problem. Algorithms for finding the global solution are of an entirely different flavor.

A widely used and robust general-purpose line search based SQP method is NPSOL (Gill, Murray, Saunders, and Wright [49]), which is suitable for small to medium sized problems. The treatment of optimal control problems via direct transcription methods usually results in large scale problems with sparsity properties, that is the Jacobians of objective and constraint function are sparse matrices. This structure can be exploited to solve large quadratic programming problems more efficiently. For example, the sparse SQP method SNOPT is a successor of NPSOL and an efficient and robust, general-purpose SQP method for large-scale problems (Gill, Murray, and Saunders [48]).

2.4 Discussion of direct methods

In this section we briefly compare different direct methods. Some advantages and disadvantages of their application are discussed. After an overview of corresponding software tools, this chapter concludes with a brief classification of the optimal control method DMOC developed within this thesis.

Comparison For direct single shooting in each major SQP iteration an initial value problem is numerically solved with high solution accuracy. Consequently, the resulting NLP problem remains small and the dynamic model is fulfilled during all SQP iterations, such that in time critical cases, a premature stop yields a physical trajectory, which however may still violate state and endpoint constraints. Similarly, in the direct multiple shooting method, the underlying initial value problems are numerically solved within prescribed accuracy in each SQP iteration. However, the continuity of the system trajectory is only fulfilled after successful termination of the SQP solution procedure. Although the resulting NLP problem is larger than for single shooting, its structure can be exploited to yield even faster convergence.

The direct collocation method leads to potentially faster computations compared to shooting techniques, as the ODE simulation and the control optimization problems are solved simultaneously. For efficient computations, the sparsity of the problem can be exploited at all levels.

For highly unstable systems (that is, initial value problems with a strong dependence on the initial values) the direct shooting optimization algorithm inherits the ill-conditioning of the initial value problem, even if the optimization problem itself is well-conditioned. In contrast, multiple shooting and collocation are able to optimize such systems much better.

Additionally, the use of collocation methods enables a reliable estimation of the adjoint variables on the entire state variable discretization grid [153].

Software The single shooting algorithm can, for example be found in software packages gOPT (Process Systems Enterprise, [101]), DYNOPT (Abel et al. [1]), OPTISIM (Engl et al. [42]). An implementation of the multiple shooting method is found, for example within the optimal control package MUSCOD-II (Leineweber, [92]), or in Petzold et al. [125]). Collocation algorithms have been implemented by Betts and Huffmann [15] (SOCS), Cervantes and Biegler [32], Schulz [136] (OCPRSQP), and von Stryk [155] (DIRCOL).[1]

[1]OCPRSQP uses a partially reduced SQP method. DIRCOL employs SNOPT (Gill et al. [48]). SNOPT approximates the Hessian of the NLP Lagrangian by limited-memory quasi-Newton updates and uses a reduced Hessian algorithm for solving the QP subproblems. The

DMOC Arranging the optimal control method DMOC within the context of the presented methodologies, it mostly resembles a direct transcription method and would therefore be classified within the category of simultaneous methods. However, the derivation is of a different flavor as we will present in Chapter 4. Differences and similarities to existing simultaneous methods will be discussed in Sections 4.3.3 and 4.4.3 and numerically compared in Section 5.2. .

null-space matrix of the working set in each iteration is obtained from a sparse LU factorization. In the code SOCS of Betts and Frank [14] a Schur-complement QP method is implemented instead of a reduced-Hessian QP method.

Chapter 3

Variational mechanics

During the progress of classical mechanics two main branches developed: Lagrangian and Hamiltonian mechanics. The Lagrangian formulation of mechanics can be based on the observation that there are variational principles behind the fundamental laws of force balance as given by Newton's law $F = ma$. That means that the laws of nature act in such a way as to extremize some functional known as action. The Hamiltonian formalism focuses on the observation of energy and can be embedded into a certain geometrical structure. The Lagrangian formalism relies on the coordinate's position and velocity in the phase space TQ. The Hamiltonian formalism instead considers the position and the momentum as independent coordinates in the phase space T^*Q, which is the cotangent bundle to the configuration manifold Q. Fortunately, in many cases these formulations are equivalent, as we shall see within this chapter. However, since the Hamiltonian perspective is advantageous over the Lagrangian in some situations and disadvantageous in others, we introduce the main concepts of variational mechanics from both, the Lagrangian and the Hamiltonian point of view. Starting with the continuous formulation, we present the corresponding discrete formulation for each geometric structure. For both, the continuous and the discrete framework, we introduce the most important properties that are relevant for the focus of this work.

Our formulations are mainly based on the work of Marsden and West in [113]. They used the concept of discrete variational mechanics to derive variational integrators simulating initial value problems in dynamical mechanics. This thesis aims a description of optimal control systems. Therefore, the last section in this chapter gives an extensive formulation of control forces that are included to the existing concepts of variational mechanics with dissipative forces.

For a detailed description of discrete variational mechanics for Lagrangian and Hamiltonian systems we refer to [73, 86, 94, 95, 113, 158]. In [113] an overview of references and the history concerning variational mechanics and variational

integrators is given. In addition, we refer to Marsden and Ratiu [111] for historical remarks and background on geometric mechanics.

3.1 Lagrangian mechanics

3.1.1 Basic definitions and concepts

Consider an n-dimensional *configuration manifold* Q (see A.1) with local coordinates $q = (q^1, \ldots, q^n)$, with associated *state space* given by the *tangent bundle* TQ (see A.3), and a *Lagrangian* $L : TQ \to \mathbb{R}$. Given a time interval $[0, T]$, we define the *path space* to be

$$\mathcal{C}(Q) = \mathcal{C}([0,T], Q) = \{q : [0,T] \to Q \,|\, q \text{ is a } C^2 \text{ curve}\}$$

and the *action map* $\mathfrak{G} : \mathcal{C} \to \mathbb{R}$ to be

$$\mathfrak{G}(q) = \int_0^T L(q(t), \dot{q}(t))\, \mathrm{d}t. \tag{3.1}$$

The tangent space $T_q\mathcal{C}(Q)$ to $\mathcal{C}(Q)$ at the point q (see A.3) is the set of C^2 maps $v_q : [0,T] \to TQ$ such that $\tau_Q \circ v_q = q$, where $\tau_Q : TQ \to Q$ is the natural projection (see A.4). We define the *second order submanifold* of $T(TQ)$ (see A.2) to be

$$\ddot{Q} = \{w \in T(TQ) \,|\, T\tau_Q(w) = \tau_{TQ}(w)\} \subset T(TQ)$$

where $\tau_{TQ} : T(TQ) \to TQ$ and $\tau_Q : TQ \to Q$ are the natural projections. $\ddot{Q}$ is the set of second order derivatives $\mathrm{d}^2q/\mathrm{d}t^2(0)$ of curves $q : \mathbb{R} \to Q$, which are elements of the form $((q, \dot{q}), (\dot{q}, \ddot{q})) \in T(TQ)$.

To describe the dynamics of a mechanical system given by a Lagrangian L on the tangent bundle TQ, we have the following theorem.

Theorem 3.1.1 (Hamilton's principle) *Given a C^k Lagrangian L, $k \geq 2$, there exists a unique C^{k-2} mapping $D_{EL}L : \ddot{Q} \to T^*Q$ and a unique C^{k-1} one-form Θ_L on TQ (see A.8), such that, for all variations $\delta q \in T_q\mathcal{C}(Q)$ of $q(t)$ (see A.27), we have*

$$\mathbf{d}\mathfrak{G}(q) \cdot \delta q = \int_0^T D_{EL}L(\ddot{q}) \cdot \delta q \, \mathrm{d}t + \Theta_L(\dot{q}) \cdot \hat{\delta q}\Big|_0^T, \tag{3.2}$$

with $\mathbf{d}\mathfrak{G}$ the differential *of $\mathfrak{G}$ (see A.7), and where*

$$\hat{\delta q} = \left(\left(q(t), \frac{\partial q}{\partial t}(t) \right), \left(\delta q(t), \frac{\partial \delta q}{\partial t}(t) \right) \right).$$

The mapping $D_{EL}L$ is called the Euler-Lagrange map *and has the coordinate expression*

$$(D_{EL}L)_i = \frac{\partial L}{\partial q^i} - \frac{\mathrm{d}}{\mathrm{d}t}\frac{\partial L}{\partial \dot{q}^i}.$$

The one-form Θ_L is called the Lagrangian one-form *and in coordinates is given by*

$$\Theta_L = \frac{\partial L}{\partial \dot{q}^i}\mathbf{d}q^i. \tag{3.3}$$

Proof: Computing the variations of the action map gives

$$\begin{aligned}\mathbf{d}\mathfrak{G}(q)\cdot\delta q &= \int_0^T \left[\frac{\partial L}{\partial q^i}\delta q^i + \frac{\partial L}{\partial \dot{q}^i}\frac{\mathrm{d}}{\mathrm{d}t}\delta q^i\right]\mathrm{d}t \\ &= \int_0^T \left[\frac{\partial L}{\partial q^i} - \frac{\mathrm{d}}{\mathrm{d}t}\frac{\partial L}{\partial \dot{q}^i}\right]\delta q^i\,\mathrm{d}t + \left[\frac{\partial L}{\partial \dot{q}^i}\delta q^i\right]_0^T,\end{aligned}$$

using integration by parts. The terms of this expression can be identified as the Euler-Lagrange map and the Lagrangian one-form. □

Lagrangian vector fields and flows

The *Lagrangian vector field* $X_L : TQ \to T(TQ)$ is a second order vector field on TQ (see A.6) satisfying

$$D_{\mathrm{EL}}L \circ X_L = 0 \tag{3.4}$$

and the *Lagrangian flow* $F_L : TQ \times \mathbb{R} \to TQ$ is the flow of X_L (see A.6). For the map F_L at some fixed time t we shall write $F_L^t : TQ \to TQ$.[1]

A curve $q \in \mathcal{C}(Q)$ is said to be a *solution of the Euler-Lagrange equations* if the first term on the right-hand side of (3.2) vanishes for all variations $\delta q \in T_q\mathcal{C}(Q)$. This is equivalent to $(q, \dot{q})$ being an integral curve of X_L (see A.6), and means that q must satisfy the *Euler-Lagrange equations*

$$\frac{\partial L}{\partial q^i}(q,\dot{q}) - \frac{\mathrm{d}}{\mathrm{d}t}\left(\frac{\partial L}{\partial \dot{q}^i}(q,\dot{q})\right) = 0 \tag{3.5}$$

for all $t \in (0, T)$.

[1] For a regular (see Section 3.2.1) Lagrangian L, these objects exist and are unique.

Properties of Lagrangian flows In the following we summarize some well known properties of Lagrangian flows, which play an important role in the discrete formulation as well.

First of all, Lagrangian flows are symplectic, that is the *Lagrangian symplectic form* $\Omega_L = \mathbf{d}\Theta_L$, given in coordinates by

$$\Omega_L(q,\dot{q}) = \frac{\partial^2 L}{\partial q^i \partial \dot{q}^j}\mathbf{d}q^i \wedge \mathbf{d}q^j + \frac{\partial^2 L}{\partial \dot{q}^i \partial \dot{q}^j}\mathbf{d}\dot{q}^i \wedge \mathbf{d}q^j$$

is preserved under the Lagrangian flow, as

$$(F_L^T)^*(\Omega_L) = \Omega_L,$$

where $(F_L^T)^*(\Omega_L)$ is the pullback of the Lagrangian symplectic form Ω_L by the map F_L^T (see A.9).

Another key property of Lagrangian flows is its behavior with respect to group actions. Assume a Lie group G (see A.14) with Lie algebra $\mathfrak{g}$ (see A.16) acts on Q by the (left or right) action $\phi : G \times Q \to Q$ (see A.18). Consider the tangent lift (see A.5) of this action to $\phi^{TQ} : G \times TQ$ given by $\phi_g^{TQ}(v_q) = T(\phi_g) \cdot v_q$, which is

$$\phi^{TQ}(g,(q,\dot{q})) = \left(\phi^i(g,q), \frac{\partial \phi^i}{\partial q^j}(g,q)\dot{q}^j\right).$$

For $\xi \in \mathfrak{g}$ the *infinitesimal generators* (see A.19) $\xi_Q : Q \to TQ$ and $\xi_{TQ} : TQ \to T(TQ)$ are defined by

$$\xi_Q(q) = \frac{\mathrm{d}}{\mathrm{d}g}\left(\phi_g(q)\right) \cdot \xi, \quad \xi_{TQ}(v_q) = \frac{\mathrm{d}}{\mathrm{d}g}\left(\phi_g^{TQ}(v_q)\right) \cdot \xi,$$

and the *Lagrangian momentum map* $\mathbf{J}_L : TQ \to \mathfrak{g}^*$ (see A.24) is defined to be

$$\mathbf{J}_L(v_q) \cdot \xi = \Theta_L \cdot \xi_{TQ}(v_q).$$

If the Lagrangian is *invariant* under the lift of the action, that is we have $L \circ \phi_g^{TQ} = L$ for all $g \in G$ (we also say, the group action is a *symmetry* of the Lagrangian), the Lagrangian momentum map is preserved of the Lagrangian flow. More formally it holds

Theorem 3.1.2 (Noether's theorem) *Consider a Lagrangian system $L : TQ \to \mathbb{R}$ which is invariant under the lift of the (left or right) action $\phi : G \times Q \to Q$, that is $L \circ \phi_g^{TQ} = L$ for all $g \in G$. Then the corresponding Lagrangian momentum map $\boldsymbol{J}_L : TQ \to \mathfrak{g}^*$ is a conserved quantity of the flow, such that $\boldsymbol{J}_L \circ F_L^t = \boldsymbol{J}_L$ for all times t.*

Proofs for the symplecticity and the preservation of the momentum map of Lagrangian flows can be found for example in [113].

Examples 3.1.3 (Momentum maps) (i) Let $Q = \mathbb{R}^n$ and let $G = \mathbb{R}^n$ operate on Q by translation, that is $\phi : G \times Q \to Q$ is given by $\phi(g, q) = g + q$. Then the momentum map (see A.22) can be calculated as $J(\xi)(q_j, p^j) = \sum_{j=1}^{N} p^j \cdot \xi$, that is $\mathbf{J}(q_j, p^j) = \sum_{j=1}^{N} p^j$ is the total linear momentum.

(ii) For the Lie group of proper rotations $G = SO(3)$ acting on the configuration space $Q = \mathbb{R}^3$ via $\phi(A, q) = A \cdot q$, the momentum map is the angular momentum $\mathbf{J}(q, p) = q \times p$.

3.1.2 Discrete Lagrangian mechanics

Again we consider a configuration manifold Q, but now we define the *discrete state space* to be $Q \times Q$. That means that rather than taking a position q and velocity $\dot{q}$, we now consider two positions q_0 and q_1 and a *time step* $h \in \mathbb{R}$. These positions should be thought of as being two points on a curve at time h apart, such that $q_0 \approx q(0)$ and $q_1 \approx q(h)$. $Q \times Q$ contains the same amount of information as (is locally isomorphic to) TQ. A *discrete Lagrangian* is a function $L_d : Q \times Q \times \mathbb{R} \to \mathbb{R}$, which we think of as approximating the action integral along the curve segment between q_0 and q_1. In the following chapters we neglect the h dependence except where it is important and consider the discrete Lagrangian as a function $L_d : Q \times Q \to \mathbb{R}$.

We construct the increasing sequence of times $\{t_k = kh \,|\, k = 0, \ldots, N\} \subset \mathbb{R}$ from the time step h, and define the *discrete path space* to be

$$\mathcal{C}_d(Q) = \mathcal{C}_d(\{t_k\}_{k=0}^N, Q) = \{q_d : \{t_k\}_{k=0}^N \to Q\}.$$

We will identify a discrete trajectory $q_d \in \mathcal{C}_d(Q)$ with its image $q_d = \{q_k\}_{k=0}^N$, where $q_k = q_d(t_k)$. The *discrete action map* $\mathfrak{G}_d : \mathcal{C}_d(Q) \to \mathbb{R}$ along this sequence is calculated by summing the discrete Lagrangian on each adjacent pair and defined by

$$\mathfrak{G}_d(q_d) = \sum_{k=0}^{N-1} L_d(q_k, q_{k+1}).$$

As the discrete path space $\mathcal{C}_d$ is isomorphic to $Q \times \cdots \times Q$ ($N + 1$ copies), it can be given a smooth product manifold structure. The discrete action $\mathfrak{G}_d$ inherits the smoothness of the discrete Lagrangian L_d.

The tangent space $T_{q_d}\mathcal{C}_d(Q)$ to $\mathcal{C}_d(Q)$ at q_d is the set of maps $v_{q_d} : \{t_k\}_{k=0}^N \to TQ$ such that $\tau_q \circ v_{q_d} = q_d$, which we will denote by $v_{q_d} = \{(q_k, v_k)\}_{k=0}^N$.

The discrete object corresponding to $T(TQ)$ is the set $(Q \times Q) \times (Q \times Q)$. With the *projection operator* π and the *translation operator* σ defined as

$$\pi : ((q_0, q_1), (q_0', q_1')) \mapsto (q_0, q_1)$$
$$\sigma : ((q_0, q_1), (q_0', q_1')) \mapsto (q_0', q_1'),$$

the *discrete second order submanifold* of $(Q \times Q) \times (Q \times Q)$ is defined to be

$$\ddot{Q}_d = \{w_d \in (Q \times Q) \times (Q \times Q) | \pi_1 \circ \sigma(w_d) = \pi_2 \circ \pi(w_d)\},$$

which has the same information content as (is locally isomorphic to) $\ddot{Q}$. Concretely, the discrete second order submanifold is the set of pairs of the form $((q_0, q_1), (q_1, q_2))$.

Now, analogously to the continuous setting, the discrete version of Hamilton's principle describes the dynamics of the discrete mechanical system determined by a discrete Lagrangian L_d on $Q \times Q$.

Theorem 3.1.4 (Discrete Hamilton's principle) *Given a C^k discrete Lagrangian L_d, $k \geq 1$, there exists a unique C^{k-1} mapping $D_{DEL}L_d : \ddot{Q}_d \to T^*Q$ and unique C^{k-1} one-forms $\Theta^+_{L_d}$ and $\Theta^-_{L_d}$ on $Q \times Q$, such that, for all variations $\delta q_d \in T_{q_d}\mathcal{C}(Q)$ of q_d, we have*

$$\begin{aligned}\mathbf{d}\mathfrak{G}_d(q_d) \cdot \delta q_d = &\sum_{k=1}^{N-1} D_{DEL}L_d((q_{k-1}, q_k), (q_k, q_{k+1})) \cdot \delta q_k \\ &+\Theta^+_{L_d}(q_{N-1}, q_N) \cdot (\delta q_{N-1}, \delta q_N) - \Theta^-_{L_d}(q_0, q_1) \cdot (\delta q_0, \delta q_1). \end{aligned} \tag{3.6}$$

The mapping $D_{DEL}L_d$ is called the discrete Euler-Lagrange map *and has coordinate expression*

$$D_{DEL}L_d((q_{k-1}, q_k), (q_k, q_{k+1})) = D_2L_d(q_{k-1}, q_k) + D_1L_d(q_k, q_{k+1}).$$

The one-forms are $\Theta^+_{L_d}$ and $\Theta^-_{L_d}$ are called the discrete Lagrangian one-forms *and in coordinates are*

$$\Theta^+_{L_d}(q_0, q_1) = D_2L_d(q_0, q_1)\mathbf{d}q_1 = \frac{\partial L_d}{\partial q_1^i} dq_1^i, \tag{3.7a}$$

$$\Theta^-_{L_d}(q_0, q_1) = -D_1L_d(q_0, q_1)\mathbf{d}q_0 = -\frac{\partial L_d}{\partial q_0^i} dq_0^i. \tag{3.7b}$$

Proof: Computing the derivative of the discrete action map gives

$$\begin{aligned}\mathbf{d}\mathfrak{G}_d(q_d) \cdot \delta q_d &= \sum_{k=0}^{N-1} [D_1L_d(q_k, q_{k+1}) \cdot \delta q_k + D_2L_d(q_k, q_{k+1}) \cdot \delta q_{k+1}] \\ &= \sum_{k=1}^{N-1} [D_1L_d(q_k, q_{k+1}) + D_2L_d(q_{k-1}, q_k)] \cdot \delta q_k \\ &\quad + D_1L_d(q_0, q_1) \cdot \delta q_0 + D_2L_d(q_{N-1}, q_N) \cdot \delta q_N\end{aligned}$$

using a discrete integration by parts (rearrangement of the summation). Identifying the terms with the discrete Euler-Lagrange map and the discrete Lagrangian one-forms now gives the desired result. □

Note that unlike the continuous case, in the discrete case there are two one-forms that arise from the boundary terms. Observe, however, that $\mathbf{d}L_d = \Theta^+_{L_d} - \Theta^-_{L_d}$ and so using $\mathbf{d}^2 = 0$ (see A.11) shows that

$$\mathbf{d}\Theta^+_{L_d} = \mathbf{d}\Theta^-_{L_d}.$$

Thus, as the continuous situation, there is only a single discrete two-form, which is important for symplecticity as reflected below.

Discrete Lagrangian evolution operator and mappings

The *discrete Lagrangian evolution operator* X_{L_d} plays the same role as the continuous Lagrangian vector field, and is defined to be the map $X_{L_d} : Q \times Q \to (Q \times Q) \times (Q \times Q)$ satisfying $\pi \circ X = id$ and

$$D_{\mathrm{DEL}} L_d \circ X_{L_d} = 0.$$

The discrete object corresponding to the Lagrangian flow is the *discrete Lagrangian map* $F_{L_d} : Q \times Q \to Q \times Q$ defined by $F_{L_d} = \sigma \circ X_{L_d}$. Since X_{L_d} is of second order which corresponds to the requirement that $X(Q \times Q) \subset \ddot{Q}_d$, it has the form $X_{L_d} : (q_0, q_1) \mapsto (q_0, q_1, q_1, q_2)$, and so the corresponding Lagrangian map will be $F_{L_d} : (q_0, q_1) \mapsto (q_1, q_2)$.[2]

A discrete path $q_d \in \mathcal{C}_d(Q)$ is said to be a *solution of the discrete Euler-Lagrange equations* if the first term on the right-hand side of (3.6) vanishes for all variations $\delta q_d \in T_{q_d}\mathcal{C}_d(Q)$. This means that the points $\{q_k\}$ satisfy $F_{L_d}(q_{k-1}, q_k) = (q_k, q_{k+1})$ or, equivalently, that they satisfy the *discrete Euler-Lagrange equations*

$$D_2 L_d(q_{k-1}, q_k) + D_1 L_d(q_k, q_{k+1}) = 0, \quad \text{for all } k = 1, \ldots, N-1. \tag{3.8}$$

Properties of discrete Lagrangian maps One can show that discrete Lagrangian maps inherit the properties we summarized for continuous Lagrangian flows. That means the *discrete Lagrangian symplectic form* $\Omega_{L_d} = \mathbf{d}\Theta^+_{L_d} = \mathbf{d}\Theta^-_{L_d}$, with coordinate expression

$$\Omega_{L_d}(q_0, q_1) = \frac{\partial^2 L_d}{\partial q_0^i \partial q_1^j} \mathbf{d}q_0^i \wedge \mathbf{d}q_1^j$$

[2]For a regular discrete Lagrangian L_d (see Section 3.2.2), these objects are well-defined and the discrete Lagrangian map is invertible.

is preserved under the discrete Lagrangian map as

$$(F_{L_d})^*(\Omega_{L_d}) = \Omega_{L_d}.$$

We say that F_{L_d} is *discretely symplectic*.

There exists a discrete analogue of Noether's theorem which states, that momentum maps of symmetries are constants of the motion. To see this, we introduce the action lift to $Q \times Q$ by the product $\phi_g^{Q\times Q}(q_0, q_1) = (\phi_g(q_0), \phi_g(q_1))$, which has an infinitesimal generator $\xi_{Q\times Q} : Q \times Q \to T(Q \times Q)$ given by

$$\xi_{Q\times Q}(q_0, q_1) = (\xi_Q(q_0), \xi_Q(q_1)),$$

where $\xi_Q : Q \to TQ$ is the infinitesimal generator of the action. The two *discrete Lagrangian momentum maps* are

$$\begin{aligned}\mathbf{J}^+_{L_d}(q_0, q_1) \cdot \xi &= \Theta^+_{L_d} \cdot \xi_{Q\times Q}(q_0, q_1),\\ \mathbf{J}^-_{L_d}(q_0, q_1) \cdot \xi &= \Theta^-_{L_d} \cdot \xi_{Q\times Q}(q_0, q_1),\end{aligned}$$

or alternatively written as

$$\begin{aligned}\mathbf{J}^+_{L_d}(q_0, q_1) \cdot \xi &= \langle D_2 L_d(q_0, q_1), \xi_Q(q_1)\rangle\,,\\ \mathbf{J}^-_{L_d}(q_0, q_1) \cdot \xi &= \langle -D_1 L_d(q_0, q_1), \xi_Q(q_0)\rangle\,.\end{aligned}$$

$\mathbf{J}^+_{L_d}$ and $\mathbf{J}^-_{L_d}$ are equal in the case of a discrete Lagrangian that is invariant under the lifted action, that is $L_d \circ \phi_g^{Q\times Q} = L_d$ holds for all $g \in G$. Then, $\mathbf{J}_{L_d} : Q \times Q \to \mathfrak{g}^*$ is the unique single *discrete Lagrangian momentum map*.

Theorem 3.1.5 (Discrete Noether's theorem) *Consider a given discrete Lagrangian system $L_d : Q \times Q \to \mathbb{R}$ which is invariant under the lift of the (left or right) action $\phi : G \times Q \to Q$. Then the corresponding discrete Lagrangian momentum map $\boldsymbol{J}_{L_d} : Q \times Q \to \mathfrak{g}^*$ is a conserved quantity of the discrete Lagrangian map $F_{L_d} : Q \times Q \to Q \times Q$, such that $\boldsymbol{J}_{L_d} \circ F_{L_d} = \boldsymbol{J}_{L_d}$.*

In [113] proofs for the discrete symplecticity and the preservation of discrete momentum maps by discrete Lagrangian maps are presented.

3.2 Hamiltonian mechanics

3.2.1 Basic definitions and concepts

Consider an n-dimensional configuration manifold Q, and define the phase space to be the cotangent bundle T^*Q (see A.7). The *Hamiltonian* is a function H :

$T^*Q \to \mathbb{R}$. We will take local coordinates on T^*Q to be (q, p) with $q = (q^1, \ldots, q^n)$ and $p = (p_1, \ldots, p_n)$.

Define the *canonical one-form* Θ on T^*Q by

$$\Theta(p_q) \cdot u_{p_q} = \langle p_q, T_{\pi_Q} \cdot u_{p_q} \rangle, \tag{3.9}$$

where $p_q \in T^*Q$, $u_{p_q} \in T_{p_q}(T^*Q)$, $\pi_Q : T^*Q \to Q$ is the canonical projection, $T_{\pi_Q} : T(T^*Q) \to TQ$ is the tangent map of π_Q and $\langle \cdot, \cdot \rangle$ denotes the natural pairing between vectors and covectors. In coordinates, we have $\Theta(q, p) = p_i \mathbf{d}q^i$. The *canonical two-form* Ω on T^*Q is defined to be

$$\Omega = -\mathbf{d}\Theta,$$

which has the coordinate expression $\Omega(q, p) = \mathbf{d}q^i \wedge \mathbf{d}p_i$.

Given now a Hamiltonian H, define the corresponding *Hamiltonian vector field* X_H to be the unique vector field on T^*Q satisfying

$$\mathbf{i}_{X_H}\Omega = \mathbf{d}H, \tag{3.10}$$

where $\mathbf{i}$ denotes the *interior product* (see A.10). Writing $X_H = (X_q, X_p)$ in coordinates, we see that the above expression is

$$-X_{p_i}\mathbf{d}q^i + X_{q^i}\mathbf{d}p_i = \frac{\partial H}{\partial q^i}\mathbf{d}q^i + \frac{\partial H}{\partial p_i}\mathbf{d}p_i,$$

which gives the familiar *Hamilton's equations* for the components of X_H, namely

$$X_{q^i}(q, p) = \frac{\partial H}{\partial p_i}(q, p), \tag{3.11a}$$

$$X_{p_i}(q, p) = -\frac{\partial H}{\partial q^i}(q, p). \tag{3.11b}$$

The *Hamiltonian flow* $F_H : T^*Q \times \mathbb{R} \to T^*Q$ is the flow of the Hamiltonian vector field X_H. Note that, unlike the Lagrangian situation, the Hamiltonian vector field X_H and the flow map F_H are always well-defined for any Hamiltonian.

For any fixed $t \in \mathbb{R}$, the flow map $F_H^t : T^*Q \to T^*Q$ is symplectic, that is $(F_H^t)^*\Omega = \Omega$ holds.

Legendre transform

To relate Lagrangian mechanics to Hamiltonian mechanics we define the *Legendre transform* or *fiber derivative* $\mathbb{F}L : TQ \to T^*Q$ by

$$\mathbb{F}L(v_q) \cdot w_q = \left.\frac{\mathrm{d}}{\mathrm{d}\epsilon}\right|_{\epsilon=0} L(v_q + \epsilon w_q),$$

where $v_q, w_q \in T_qQ$, and which has coordinate form

$$\mathbb{F}L : (q, \dot{q}) \mapsto (q, p) = \left(q, \frac{\partial L}{\partial \dot{q}}(q, \dot{q}) \right).$$

If the fiber derivative of L is a local isomorphism then we say that L is *regular*, and if it is a global isomorphism then L is said to be *hyperregular*. We will generally assume that we are working with hyperregular Lagrangians.

The fiber derivative of a Hamiltonian is the map $\mathbb{F}H : T^*Q \to TQ$ defined by

$$\alpha_q \cdot \mathbb{F}H(\beta_q) = \left. \frac{\mathrm{d}}{\mathrm{d}\epsilon} \right|_{\epsilon=0} H(\beta_q + \epsilon \alpha_q),$$

where $\alpha_q, \beta_q \in T_q^*Q$, and which in coordinates is

$$\mathbb{F}H : (q, p) \mapsto (q, \dot{q}) = \left(q, \frac{\partial H}{\partial p}(q, p) \right).$$

Similarly to the situation for Lagrangians, we say that H is *regular* if $\mathbb{F}H$ is a local isomorphism, and that H is *hyperregular* if $\mathbb{F}H$ is a global isomorphism.

The canonical one- and two-forms and the Hamiltonian momentum maps (see A.23) are related to the Lagrangian one- and two-forms and the Lagrangian momentum maps by pullback under the fiber derivative, such that

$$\Theta_L = (\mathbb{F}L)^* \Theta, \quad \Omega_L = (\mathbb{F}L)^* \Omega, \quad \text{and} \quad \mathbf{J}_L = (\mathbb{F}L)^* \mathbf{J}_H.$$

If we additionally relate the Hamiltonian to the Lagrangian by

$$H(q, p) = \mathbb{F}L(q, \dot{q}) \cdot \dot{q} - L(q, \dot{q}), \tag{3.12}$$

where (q, p) and $(q, \dot{q})$ are related by the Legendre transform, then the Hamiltonian and Lagrangian vector fields and their associated flow maps will also be related by pullback

$$X_L = (\mathbb{F}L)^* X_H; \quad F_L^t = (\mathbb{F}L)^{-1} \circ F_H^t \circ \mathbb{F}L.$$

In coordinates this means that Hamilton's equations (3.11) are equivalent to the Euler-Lagrange equations (3.5). To see this, we compute the derivatives of (3.12)

to give

$$\begin{aligned}
\frac{\partial H}{\partial q}(q,p) &= p \cdot \frac{\partial \dot{q}}{\partial q} - \frac{\partial L}{\partial q}(q,\dot{q}) - \frac{\partial L}{\partial \dot{q}}(q,\dot{q})\frac{\partial \dot{q}}{\partial q} \\
&= -\frac{\partial L}{\partial q}(q,\dot{q}) \\
&= -\frac{\mathrm{d}}{\mathrm{d}t}\left(\frac{\partial L}{\partial \dot{q}}(q,\dot{q})\right) \\
&= -\dot{p}, \\
\frac{\partial H}{\partial p}(q,p) &= \dot{q} + p \cdot \frac{\partial \dot{q}}{\partial p} - \frac{\partial L}{\partial \dot{q}}(q,\dot{q})\frac{\partial \dot{q}}{\partial p} \\
&= \dot{q},
\end{aligned}$$

where $p = \mathbb{F}L(q,\dot{q})$ defines $\dot{q}$ as a function of (q,p).

A calculation similar to the above also shows that if L is hyperregular and H is defined by (3.12), then H is also hyperregular and the fiber derivatives satisfy $\mathbb{F}H = (\mathbb{F}L)^{-1}$. The converse statement also holds (see [111] for more details).

3.2.2 Discrete Hamiltonian mechanics

Discrete Legendre transforms

Just as the standard Legendre transform maps the Lagrangian state space TQ to the Hamiltonian phase space T^*Q, we can define *discrete Legendre transforms* or *discrete fiber derivatives* $\mathbb{F}^+L_d, \mathbb{F}^-L_d : Q \times Q \to T^*Q$, which map the discrete state space $Q \times Q$ to T^*Q. These are given by

$$\begin{aligned}
\mathbb{F}^+L_d(q_0,q_1) \cdot \delta q_1 &= D_2L_d(q_0,q_1) \cdot \delta q_1, \\
\mathbb{F}^-L_d(q_0,q_1) \cdot \delta q_0 &= -D_1L_d(q_0,q_1) \cdot \delta q_0,
\end{aligned}$$

which can be written as

$$\begin{aligned}
\mathbb{F}^+L_d : (q_0,q_1) &\mapsto (q_1,p_1) = (q_1, D_2L_d(q_0,q_1)), \\
\mathbb{F}^-L_d : (q_0,q_1) &\mapsto (q_0,p_0) = (q_0, -D_1L_d(q_0,q_1)).
\end{aligned}$$

We say that L_d is regular if both discrete fiber derivatives are local isomorphisms (for nearby q_0 and q_1). In general we assume working with regular discrete Lagrangians. If both discrete fiber derivatives are global isomorphisms we say that L_d is hyperregular.

The canonical one- and two-forms and Hamiltonian momentum maps are related to the discrete Lagrangian forms and discrete momentum maps by pullback by the discrete fiber derivatives, such that

$$\Theta^{\pm}_{L_d} = (\mathbb{F}^{\pm}L_d)^*\Theta, \quad \Omega_{L_d} = (\mathbb{F}^{\pm}L_d)^*\Omega, \quad \text{and} \quad J^{\pm}_{L_d} = (\mathbb{F}^{\pm}L_d)^*J_H.$$

Momentum matching

By introducing the notation

$$p^+_{k,k+1} = p^+(q_k, q_{k+1}) = \mathbb{F}^+ L_d(q_k, q_{k+1}),$$
$$p^-_{k,k+1} = p^-(q_k, q_{k+1}) = \mathbb{F}^- L_d(q_k, q_{k+1}),$$

for the momentum at the two endpoints of each interval $[k, k+1]$ the discrete fiber derivatives permit a new interpretation of the discrete Euler-Lagrange equations

$$D_2 L_d(q_{k-1}, q_k) = -D_1 L_d(q_k, q_{k+1}),$$

which can be written as

$$\mathbb{F}^+ L_d(q_{k-1}, q_{k+1}) = \mathbb{F}^- L_d(q_k, q_{k+1}), \tag{3.13}$$

or simply

$$p^+_{k-1,k} = p^-_{k,k+1}.$$

That is, the discrete Euler-Lagrange equations are enforcing the condition that the momentum at time k should be the same when being evaluated from the lower interval $[k-1, k]$ or the upper interval $[k, k+1]$. This means that along a solution curve there is a unique momentum at each time k, which is denoted by

$$p_k = p^+_{k-1,k} = p^-_{k,k+1}.$$

A discrete trajectory $\{q_k\}_{k=0}^N$ in Q can thus also be regarded as either a trajectory $\{(q_k, q_{k+1})\}_{k=0}^{N-1}$ in $Q \times Q$ or, equivalently, as a trajectory $\{(q_k, p_k)\}_{k=0}^N$ in T^*Q.

Note that (3.13) can be written as

$$\mathbb{F}^+ L_d = \mathbb{F}^- L_d \circ F_{L_d}. \tag{3.14}$$

Discrete Hamiltonian maps

Using the discrete fiber derivatives also enables us to push the discrete Lagrangian map $F_{L_d} : Q \times Q \to Q \times Q$ forward to T^*Q. We define the *discrete Hamiltonian map* $\tilde{F}_{L_d} : T^*Q \to T^*Q$ by $\tilde{F}_{L_d} = \mathbb{F}^\pm L_d \circ F_{L_d} \circ (\mathbb{F}^\pm L_d)^{-1}$ with coordinate expression $\tilde{F}_{L_d} : (q_0, p_0) \mapsto (q_1, p_1)$, where

$$p_0 = -D_1 L_d(q_0, q_1), \tag{3.15a}$$
$$p_1 = D_2 L_d(q_0, q_1). \tag{3.15b}$$

As the discrete Lagrangian map preserves the discrete symplectic form and discrete momentum maps on $Q \times Q$, the discrete Hamiltonian map will preserve the pushforwards of these structures. As we saw above, however, these are simply the canonical symplectic form and canonical momentum maps on T^*Q, and so the discrete Hamiltonian map is symplectic and momentum-preserving.

3.3 Forcing and control

Our aim is to optimally control Lagrangian and Hamiltonian systems. Thus, in this section we extend the discrete variational framework to include external forcing resulting from dissipation and friction or control forces and loading on mechanical systems.

In contrast to [73] and [113], we consider forces depending on control parameters from the beginning. Therefore, we extend the definitions for Lagrangian forces in [113] to Lagrangian control forces.

3.3.1 Forced Lagrangian systems

As defined in [113], a *Lagrangian force* is a fiber-preserving map $f_L : TQ \to T^*Q$ over the identity id_Q (see A.25), which we write in coordinates as

$$f_L : (q, \dot{q}) \mapsto (q, f_L(q, \dot{q})).$$

This kind of forces results for example from dissipation and friction or from configuration- and velocity-dependent but time-independent loading on mechanical systems. To define time-dependent control forces for Lagrangian systems, we introduce a *control manifold* $U \subset \mathbb{R}^m$ and for a given interval $I = [0, T]$ we define the *control path space* to be

$$\mathcal{D}(U) = \mathcal{D}([0, T], U) = \{u : [0, T] \to U \,|\, u \in L^\infty\},$$

with $u(t) \in U$ also called the *control parameter*. $L^p(\mathbb{R}^m)$ denotes the usual Lebesgue space of measurable functions $x : [0, T] \to \mathbb{R}^m$ with $|x(\cdot)|^p$ integrable, equipped with its standard norm

$$\|x\|_{L^p} = \left(\int_0^T |x(t)|^p \, \mathrm{d}t \right)^{\frac{1}{p}},$$

where $|\cdot|$ is the Euclidean norm. $p = \infty$ corresponds to the space of essentially bounded, measurable functions equipped with the essential supremum norm. With this notation we define a *Lagrangian control force* as a map $f_{LC} : TQ \times U \to T^*Q$, which is given in coordinates as

$$f_{LC} : (q, \dot{q}, u) \mapsto (q, f_{LC}(q, \dot{q}, u)).$$

We interpret a Lagrangian control force as a parameter-dependent Lagrangian force, that is a parameter-dependent fiber-preserving map $f_L(u) : TQ \to T^*Q$ over the identity id_Q, which we write in coordinates as

$$f_L(u) : (q, \dot{q}) \mapsto (q, f_L(u)(q, \dot{q})).$$

Here and in the sequel, whenever we denote $f_{LC}(q, \dot{q}, u)$ as one-form on TQ, we mean the parameter-dependent horizontal one-form $f_L(u)(q, \dot{q})$ on TQ induced by the parameter-dependent fiber-preserving map $f_L(u)$ (see A.26 and A.1).

Remark 3.3.1 Note that the definition of a Lagrangian control force also includes forces that are independent on the control parameter. Thus in the following we restrict ourselves to a formulation with control forces which gives us the opportunity to include friction or dissipative forces as well.

Given a control force, we modify Hamilton's principle, seeking stationary points of the action, to the *Lagrange-d'Alembert principle*, which seeks curves $q \in \mathcal{C}(Q)$ satisfying

$$\delta \int_0^T L(q(t), \dot{q}(t))\,\mathrm{d}t + \int_0^T f_{LC}(q(t), \dot{q}(t), u(t)) \cdot \delta q(t)\,\mathrm{d}t = 0, \tag{3.16}$$

where δ represents variations vanishing at the endpoints. The second integral in (3.16) is the *virtual work* acting on the mechanical system via the force f_{LC}. Using integration by parts shows that this is equivalent to the *forced Euler-Lagrange equations*, which have the coordinate expression

$$\frac{\partial L}{\partial q}(q, \dot{q}) - \frac{\mathrm{d}}{\mathrm{d}t}\left(\frac{\partial L}{\partial \dot{q}}(q, \dot{q})\right) + f_{LC}(q, \dot{q}, u) = 0. \tag{3.17}$$

Note that these are the same as the standard Euler-Lagrange equations (3.5) with the forcing term added and implicitly define the *forced Lagrangian flow* $F_L(u) : TQ \times \mathbb{R} \to TQ$.

3.3.2 Forced Hamiltonian systems

A Hamiltonian control force is a map $f_{HC} : T^*Q \times U \to T^*Q$ identified by a parameter-dependent fiber preserving map $f_H(u) : T^*Q \to T^*Q$ over the identity. Given such a control force, we define the corresponding horizontal one-form (see A.26 and A.1) $f'_H(u)$ on T^*Q by

$$f'_H(u)(p_q) \cdot w_{p_q} = \langle f_H(u)(p_q), T_{\pi_Q} \cdot w_{p_q} \rangle,$$

where $\pi_Q : T^*Q \to Q$ is the projection. This expression is reminiscent of definition (3.9) of the canonical one-form Θ on T^*Q, and in coordinates it reads $f'_H(u)(q, p) \cdot (\delta q, \delta p) = f_{HC}(q, p, u) \cdot \delta q$, thus the one-form is clearly horizontal.

The *forced Hamiltonian vector field* X_H is now defined by the equation

$$\mathbf{i}_{X_H}\Omega = \mathbf{d}H - f'_H(u)$$

and in coordinates this gives the well-known *forced Hamilton's equations*

$$X_q(q,p) = \frac{\partial H}{\partial p}(q,p), \tag{3.18a}$$

$$X_p(q,p,u) = -\frac{\partial H}{\partial q}(q,p) + f_{HC}(q,p,u), \tag{3.18b}$$

which are the same as the standard Hamilton's equations (3.11) in coordinates with the forcing term added to the momentum equation. This defines the *forced Hamiltonian flow* $F_H(u) : T^*Q \times \mathbb{R} \to T^*Q$ of the *forced Hamiltonian vector field* $X_H = (X_q, X_p)$.

3.3.3 Legendre transform with forces

Given a Lagrangian L, we can take the standard Legendre transform $\mathbb{F}L : TQ \to T^*Q$ and relate Hamiltonian and Langrangian control forces by

$$f_L(u) = f_H(u) \circ \mathbb{F}L.$$

If we also have a Hamiltonian H related to L by the Legendre transform according to (3.12), then the forced Euler-Lagrange equations and the forced Hamilton's equations are equivalent. That is, if X_L and X_H are the forced Lagrangian and Hamiltonian vector fields, respectively, then $(\mathbb{F}L)^*(X_H) = X_L$. To see this, we compute

$$\begin{aligned}
\frac{\partial H}{\partial q}(q,p) &= p \cdot \frac{\partial \dot{q}}{\partial q} - \frac{\partial L}{\partial q}(q,\dot{q}) - \frac{\partial L}{\partial \dot{q}}(q,\dot{q})\frac{\partial \dot{q}}{\partial q} \\
&= -\frac{\partial L}{\partial q}(q,\dot{q}) \\
&= -\frac{\mathrm{d}}{\mathrm{d}t}\left(\frac{\partial L}{\partial \dot{q}}(q,\dot{q})\right) + f_{LC}(q,\dot{q},u) \\
&= -\dot{p} + f_H(u) \circ \mathbb{F}L(q,\dot{q}), \\
&= -\dot{p} + f_{HC}(p,q,u), \\
\frac{\partial H}{\partial p}(q,p) &= \dot{q} + p \cdot \frac{\partial \dot{q}}{\partial p} - \frac{\partial L}{\partial \dot{q}}(q,\dot{q})\frac{\partial \dot{q}}{\partial p} \\
&= \dot{q},
\end{aligned}$$

where $p = \mathbb{F}L(q,\dot{q})$ defines $\dot{q}$ as a function of (q,p).

3.3.4 Noether's theorem with forcing

We now consider the effect of forcing on the evolution of momentum maps that arise from symmetries of the Lagrangian. In [113] it is shown that the evolution of the momentum map from time 0 to time T is given by the relation

$$\left[(\mathbf{J}_L \circ F_L^T(u))(q(0),\dot{q}(0)) - \mathbf{J}_L(q(0),\dot{q}(0))\right]\cdot\xi = \int_0^T f_{LC}(q(t),\dot{q}(t),u(t))\cdot\xi_Q(q(t))\,\mathrm{d}t, \tag{3.19}$$

where $\xi \in \mathfrak{g}$ and $\xi_Q : Q \to TQ$ is the *infinitesimal generator* (see A.19). Equation (3.19) shows, that forcing will generally alter the momentum map. However, in the special case that the forcing is orthogonal to the group action, the above relation shows that Noether's theorem will still hold.

Theorem 3.3.2 (Forced Noether's theorem) *Consider a Lagrangian system $L : TQ \to \mathbb{R}$ with control forcing $f_{LC} : TQ \times U \to T^*Q$ and a symmetry action $\phi : G \times Q \to Q$ such that $\langle f_{LC}(q,\dot{q},u), \xi_Q(q)\rangle = 0$ for all $(q,\dot{q}) \in TQ$, $u \in U$ and all $\xi \in \mathfrak{g}$. Then the Lagrangian momentum map $\boldsymbol{J}_L : TQ \to \mathfrak{g}^*$ will be preserved by the flow, such that $\boldsymbol{J}_L \circ F_L^t(u) = \boldsymbol{J}_L$ for all t.*

3.3.5 Discrete variational mechanics with control forces

To complete the discrete setting for forced mechanical systems, in this section we present a discrete formulation of the control forces introduced in the previous section. Since the control parameter function $u : I \to U$ has no geometric interpretation, we have to find an appropriate discrete formulation to identify a discrete structure for the Lagrangian control force.

Discrete Lagrangian control forces

In Section 3.1.2 we replaced the path space by a discrete path space defined on the time grid $\{t_k\}_{k=0}^N$ as $q_d(t_k) = q_k$. For the replacement of the control path space by a discrete one we introduce a new time grid $\Delta\tilde{t}$. This time grid is generated via an increasing sequence of intermediate control points $c = \{c_l \,|\, 0 \le c_l \le 1, l = 1,\dots,s\}$ as $\Delta\tilde{t} = \{t_{kl} \,|\, k \in \{0,\dots,N-1\}, l \in \{1,\dots,s\}\}$, where $t_{kl} = t_k + c_l h$. With this notation the *discrete control path space* is defined to be

$$\mathcal{D}_d(U) = \mathcal{D}_d(\Delta\tilde{t}, U) = \{u_d : \Delta\tilde{t} \to U\}.$$

We define the *intermediate control samples* u_k on $[t_k, t_{k+1}]$ as $u_k = (u_{k1},\dots,u_{ks}) \in U^s$ to be the values of the control parameters guiding the system from $q_k = q_d(t_k)$ to $q_{k+1} = q_d(t_{k+1})$, where $u_{kl} = u_d(t_{kl})$ for $l \in \{1,\dots,s\}$.

The set of the discrete controls U^s can be viewed as a finite dimensional subspace of the control path space $\mathcal{D}([0,h],U)$.

Examples 3.3.3 a) For $s=1$ and $c=0.5$ we obtain just one intermediate control parameter per interval that approximates the control parameter on $[t_k,t_{k+1}]$ as $u_k = u_d(t_k+h/2) \in U$.

b) For $s=2$ and $c=\{0,1\}$ the control parameter is approximated via two discrete control parameters at the left and right boundary of each interval, respectively, as $u_k = (u_d(t_k), u_d(t_{k+1})) \in U \times U$.

With this interpretation of the discrete control path space, we take two *discrete Lagrangian control forces* $f^+_{C_d}, f^-_{C_d} : Q \times Q \times U^s \to T^*Q$, given in coordinates as

$$f^+_{C_d}(q_k,q_{k+1},u_k) = (q_{k+1}, f^+_{C_d}(q_k,q_{k+1},u_k)), \tag{3.20}$$
$$f^-_{C_d}(q_k,q_{k+1},u_k) = (q_k, f^-_{C_d}(q_k,q_{k+1},u_k)), \tag{3.21}$$

also called *left and right discrete forces.*[3] Analogously to the continuous case, we interpret the two discrete Lagrangian control forces as two parameter-dependent discrete fiber-preserving Lagrangian forces $f^\pm_d(u_k) : Q \times Q \to T^*Q$ in the sense that $\pi_Q \circ f^\pm_d = \pi^\pm_Q$ with $f^\pm_d(u_k)(q_k,q_{k+1}) = f^\pm_{C_d}(q_k,q_{k+1},u_k)$ and with the projection operators $\pi^+_Q : Q \times Q \to Q, (q_k,q_{k+1}) \mapsto q_{k+1}$ and $\pi^-_Q : Q \times Q \to Q, (q_k,q_{k+1}) \mapsto q_k$. We combine the two discrete control forces to give a single one-form $f_d(u_k) : Q \times Q \to T^*(Q \times Q)$ defined by

$$f_d(u_k)(q_k,q_{k+1}) \cdot (\delta q_k, \delta q_{k+1}) = f^+_d(u_k)(q_k,q_{k+1}) \cdot \delta q_{k+1} + f^-_d(u_k)(q_k,q_{k+1}) \cdot \delta q_k, \tag{3.22}$$

and we define

$$f_{C_d}(q_k,q_{k+1},u_k) = f_d(u_k)(q_k,q_{k+1}).$$

Remark 3.3.4 To simplify the notation we denote the left and right discrete forces by $f^\pm_k := f^\pm_{C_d}(q_k,q_{k+1},u_k)$, respectively, and the combination of both by $f_k := f_{C_d}(q_k,q_{k+1},u_k)$.

Corresponding to Figure 3.1 we interpret the left discrete force f^+_{k-1} as the force resulting from the continuous control force acting during the time span $[t_{k-1},t_k]$ on the configuration node q_k. The right discrete force f^-_k is the force acting on q_k resulting from the continuous control force during the time span $[t_k,t_{k+1}]$.

[3] Observe, that the discrete control force is now dependent on the discrete control path.

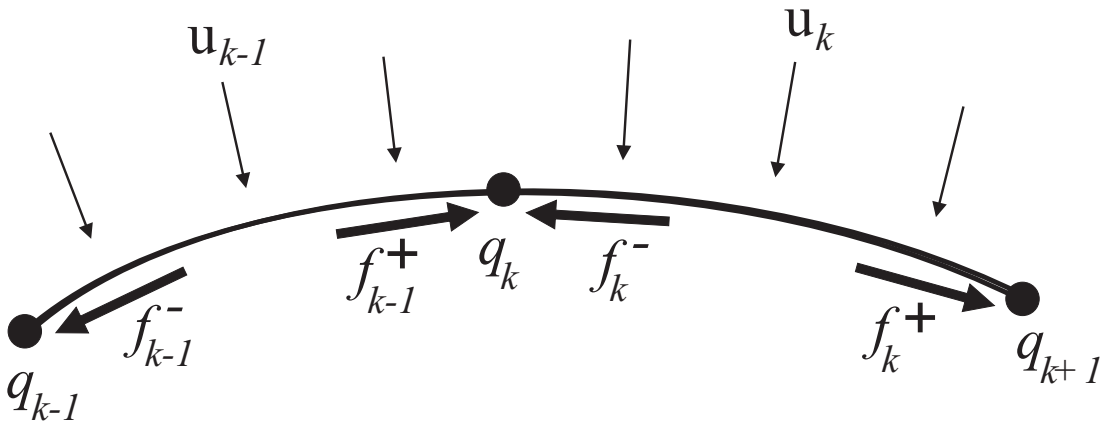

Figure 3.1: Left and right discrete forces.

Discrete Lagrange-d'Alembert principle

As with discrete Lagrangians, the discrete control forces also depend on the time step h, which is important when relating discrete and continuous mechanics. Given such forces, we modify the discrete Hamilton's principle, following [73], to the *discrete Lagrange-d'Alembert principle*, which seeks discrete curves $\{q_k\}_{k=0}^N$ that satisfy

$$\delta \sum_{k=0}^{N-1} L_d(q_k, q_{k+1}) + \sum_{k=0}^{N-1} \left[f_{C_d}^-(q_k, q_{k+1}, u_k) \cdot \delta q_k + f_{C_d}^+(q_k, q_{k+1}, u_k) \cdot \delta q_{k+1} \right] = 0 \tag{3.23}$$

for all variations $\{\delta q_k\}_{k=0}^N$ vanishing at the endpoints. This is equivalent to the *forced discrete Euler-Lagrange equations*

$$D_2 L_d(q_{k-1}, q_k) + D_1 L_d(q_k, q_{k+1}) + f_{C_d}^+(q_{k-1}, q_k, u_{k-1}) + f_{C_d}^-(q_k, q_{k+1}, u_k) = 0, \tag{3.24}$$

which are the same as the standard discrete Euler-Lagrange equations (3.8) with the discrete forces added. These implicitly define the *forced discrete Lagrangian map* $F_{L_d}(u_{k-1}, u_k) : Q \times Q \to Q \times Q$.

3.3.6 Discrete Legendre transforms with forces

Although in the continuous case we used the standard Legendre transform for systems with forcing, in the discrete case it is necessary to take the *forced discrete Legendre transforms* to be

$$\mathbb{F}^{f+} L_d(u_0) : (q_0, q_1) \mapsto (q_1, p_1) = (q_1, D_2 L_d(q_0, q_1) + f_{C_d}^+(q_0, q_1, u_0)), \tag{3.25a}$$

$$\mathbb{F}^{f-} L_d(u_0) : (q_0, q_1) \mapsto (q_0, p_0) = (q_0, -D_1 L_d(q_0, q_1) - f_{C_d}^-(q_0, q_1, u_0)). \tag{3.25b}$$

Using these definitions and the forced discrete Euler-Lagrange equations (3.24), we can see that the corresponding *forced discrete Hamiltonian map* $\tilde{F}_{L_d}(u_0) = \mathbb{F}^{f\pm}L_d(u_1) \circ F_{L_d}(u_0, u_1) \circ (\mathbb{F}^{f\pm}L_d)^{-1}(u_0)$ is given by the map $\tilde{F}_{L_d}(u_0) : (q_0, p_0) \mapsto (q_1, p_1)$, where

$$p_0 = -D_1 L_d(q_0, q_1) - f^-_{C_d}(q_0, q_1, u_0), \tag{3.26a}$$
$$p_1 = D_2 L_d(q_0, q_1) + f^+_{C_d}(q_0, q_1, u_0), \tag{3.26b}$$

which is the same as the standard discrete Hamiltonian map (3.15) with the discrete forces added.

Figure 3.2 shows that the following two definitions of the forced discrete Hamiltonian map

$$\tilde{F}_{L_d}(u_0) = \mathbb{F}^{f\pm}L_d(u_1) \circ F_{L_d}(u_0, u_1) \circ (\mathbb{F}^{f\pm}L_d)^{-1}(u_0), \tag{3.27a}$$
$$\tilde{F}_{L_d}(u_0) = \mathbb{F}^{f+}L_d(u_0) \circ (\mathbb{F}^{f-}L_d)^{-1}(u_0), \tag{3.27b}$$

are equivalent with coordinate expression (3.26). Thus from expression (3.27b) and Figure 3.2, it becomes clear, that the forced discrete Hamiltonian map that maps (q_0, p_0) to (q_1, p_1), just depends on u_0.

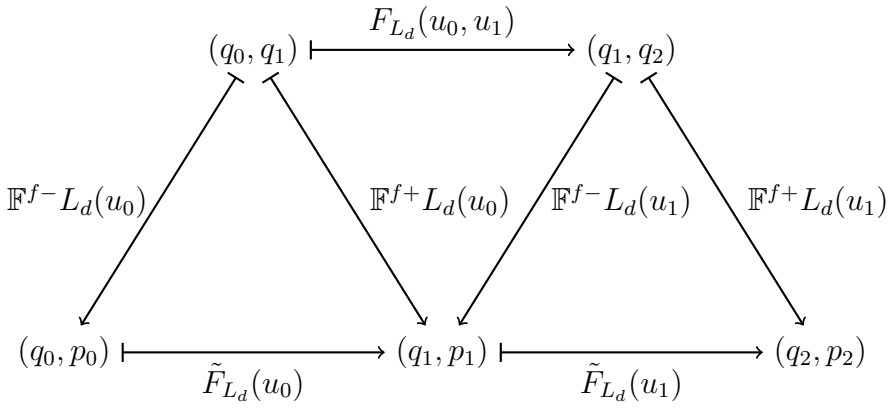

Figure 3.2: Correspondence between the forced discrete Lagrangian and the forced discrete Hamiltonian map.

3.3.7 Discrete Noether's theorem with forcing

As for the unforced case, we can formulate a discrete version of the forced Noether's theorem (for the derivation see for example [113]). Therefor, the dis-

crete momentum map in presence of forcing is defined as

$$\mathbf{J}_{L_d}^{f+}(q_0,q_1)\cdot\xi = \langle \mathbb{F}^{f+}L_d(u_0)(q_0,q_1), \xi_Q(q_1)\rangle,$$
$$\mathbf{J}_{L_d}^{f-}(q_0,q_1)\cdot\xi = \langle \mathbb{F}^{f-}L_d(u_0)(q_0,q_1), \xi_Q(q_0).$$

The evolution of the discrete momentum map is described by

$$\left[\mathbf{J}_{L_d}^{f+}\circ F_{L_d}^{N-1}(u_d) - \mathbf{J}_{L_d}^{f-}\right](q_0,q_1)\cdot\xi = \sum_{k=0}^{N-1} f_{C_d}(q_k,q_{k+1},u_k)\cdot\xi_{Q\times Q}(q_k,q_{k+1}). \quad (3.28)$$

Again, in the case that the forcing is orthogonal to the group action we have the unique momentum map $\mathbf{J}_{L_d}^{f} : Q\times Q\to\mathfrak{g}^*$ and it holds:

Theorem 3.3.5 (Forced discrete Noether's theorem) *Consider a discrete Lagrangian system $L_d : Q\times Q\to\mathbb{R}$ with discrete control forces $f_{C_d}^+, f_{C_d}^- : Q\times Q\times U^s\to T^*Q$ and a symmetry action $\phi : G\times Q\to Q$ such that $\langle f_{C_d}, \xi_{Q\times Q}\rangle = 0$ for all $\xi\in\mathfrak{g}$. Then the discrete Lagrangian momentum map $\boldsymbol{J}_{L_d}^{f} : Q\times Q\to\mathfrak{g}^*$ will be preserved by the discrete Lagrangian evolution map, such that $\boldsymbol{J}_{L_d}^{f}\circ F_{L_d} = \boldsymbol{J}_{L_d}^{f}$.*

Chapter 4

Discrete mechanics and optimal control (DMOC)

This chapter comprises the main part of this work: Having introduced the basics of optimal control and variational mechanics in Chapters 2 and 3, we combine both concepts to build up a setting for the optimal control of a continuous and a discrete mechanical system in Sections 4.1 and 4.2, respectively. Furthermore, in Section 4.3, we compare both problems and show that the discrete formulation results in a direct solution method as it has been introduced in Chapter 2. The remainder of this chapter aims at showing the convergence of the discrete optimal solution of the discrete optimal control system to the continuous solution of the original optimal control problem. To this end, in Section 4.4, we first give an appropriate formulation for the optimal control of high-order discretized mechanical systems. We show the equivalence of these problems to those resulting from Runge-Kutta discretizations of the corresponding Hamiltonian system. This equivalence allows us to construct and compare the adjoint systems of the continuous and the discrete optimal control problem in Section 4.5. In this context, one of our main results is stated that concerns the order of approximation of the adjoint system of the discrete to the continuous optimal control problem. Together with existing convergence results of optimal control problems discretized via Runge-Kutta methods (see for example [41, 53]) this leads directly to the convergence formulation of DMOC in Section 4.6.

4.1 Optimal control of a mechanical system

On the configuration space Q we consider a mechanical system described by a regular Lagrangian $L : TQ \to \mathbb{R}$. Additionally, there acts a Lagrangian control force on the system defined by the map $f_{LC} : TQ \times U \to T^*Q$ with $f_{LC} :$

$(q, \dot{q}, u) \mapsto (q, f_{LC}(q, \dot{q}, u))$ and $u : I \to U, t \mapsto u(t)$ the time-dependent control parameter. Note, that the Lagrangian control force can imply both, dissipative forces within the mechanical system and external control forces resulting from actuators steering the system.

4.1.1 Lagrangian optimal control problem

Consider now the following optimal control problem: During a time interval $I = [0, T]$ the mechanical system described by the Lagrangian L is to be moved on a curve $q(t) \in Q$ from an initial state $(q(0), \dot{q}(0)) = (q^0, \dot{q}^0) \in TQ$ to a final state. The motion is influenced via a Lagrangian control force f_{LC} with chosen control parameter $u(t)$ such that a given *objective functional*

$$J(q, \dot{q}, u) = \int_0^T C(q(t), \dot{q}(t), u(t)) \, \mathrm{d}t + \Phi(q(T), \dot{q}(T)) \tag{4.1}$$

is minimized with $J : TQ \times U \to \mathbb{R}$, the cost function $C : TQ \times U \to \mathbb{R}$ and the final condition (Mayer term) $\Phi : TQ \to \mathbb{R}$ continuously differentiable. In this way, the final state is given by the final time constraint $r(q(T), \dot{q}(T), q^T, \dot{q}^T) = 0$ with $r : TQ \times TQ \to \mathbb{R}^{n_r}$, where $(q^T, \dot{q}^T) \in TQ$ is a fixed value for the desired final state.

At the same time, the motion $q(t)$ of the system is to satisfy the Lagrange-d'Alembert principle, which requires that

$$\delta \int_0^T L(q(t), \dot{q}(t)) \, \mathrm{d}t + \int_0^T f_{LC}(q(t), \dot{q}(t), u(t)) \cdot \delta q(t) \, \mathrm{d}t = 0 \tag{4.2}$$

for all variations δq with $\delta q(0) = \delta q(T) = 0$. Additionally, there are constraints on states and control parameters to be fulfilled given by the path constraints $h : TQ \times U \to \mathbb{R}^{n_h}, h(q(t), \dot{q}(t), u(t)) \geq 0$.

The optimal control problem for a Lagrangian system can now be formulated as follows

Problem 4.1.1 (Lagrangian optimal control problem (LOCP))

$$\min_{q(\cdot), \dot{q}(\cdot), u(\cdot), (T)} J(q, \dot{q}, u) = \int_0^T C(q(t), \dot{q}(t), u(t)) \, \mathrm{d}t + \Phi(q(T), \dot{q}(T)) \tag{4.3a}$$

subject to

$$\delta \int_0^T L(q(t), \dot{q}(t)) \, \mathrm{d}t + \int_0^T f_{LC}(q(t), \dot{q}(t), u(t)) \cdot \delta q(t) \, \mathrm{d}t = 0, \tag{4.3b}$$

$$q(0) = q^0,\ \dot{q}(0) = \dot{q}^0, \tag{4.3c}$$

$$h(q(t), \dot{q}(t), u(t)) \geq 0, \tag{4.3d}$$

$$r(q(T), \dot{q}(T), q^T, \dot{q}^T) = 0. \tag{4.3e}$$

As in Chapter 2 the final time T may either be fixed, or appear as degree of freedom in the optimization problem.

Definition 4.1.2 A triple $(q(\cdot), \dot{q}(\cdot), u(\cdot))$ is *admissible* (or *feasible*), if the constraints (4.3b)-(4.3e) are fulfilled. The set consisting of all admissible (feasible) triples is the *admissible (feasible) set* of Problem 2.1.1. An admissible (feasible) triple $(q^*, \dot{q}^*, u^*)$ is an *optimal solution* of Problem 4.1.1, if

$$J(q^*, \dot{q}^*, u^*) \leq J(q, \dot{q}, u)$$

for all admissible (feasible) triples $(q, \dot{q}, u)$. The admissible (feasible) triple $(q^*, \dot{q}^*, u^*)$ is a *local optimal solution*, if there exists a neighborhood $B_\delta((q^*, \dot{q}^*, u^*))$, $\delta > 0$, such that

$$J(q^*, \dot{q}^*, u^*) \leq J(q, \dot{q}, u)$$

for all admissible (feasible) triples $(q, \dot{q}, u) \in B_\delta((q^*, \dot{q}^*, u^*))$. The function $q^*(t)$ is called *(locally) optimal trajectory*, and the function $u^*(t)$ is the *(locally) optimal control*.

4.1.2 Hamiltonian optimal control problem

For describing the optimal control problem within the Hamiltonian framework we use the Hamiltonian formulation for the system dynamics. This is equivalent to the Lagrangian formulation as we have seen in Section 3.2.

In addition, we need equivalent formulations for the objective functional, the boundary conditions and the path constraints. Altogether, these conditions determine the admissible set for configuration and velocity in the tangent space. To this end we are searching for constraints on the configuration and the momentum level that determine the corresponding admissible set in the cotangent space.

Assume, the feasible set determined via a constraint $g : TQ \to \mathbb{R}^{n_g}$ on TQ is given by

$$\mathcal{R} = \{(q, \dot{q}) \in TQ \mid g(q, \dot{q}) \geq 0\}.$$

By defining

$$\tilde{g} : T^*Q \to \mathbb{R}^{n_g}, (q, p) \mapsto g \circ (\mathbb{F}L)^{-1}(q, p)$$

using the standard Legendre transform $\mathbb{F}L : TQ \to T^*Q$

$$\mathbb{F}L : (q, \dot{q}) \mapsto (q, p) = (q, D_2L(q, \dot{q})),$$

we correspondingly get the feasible set in the cotangent space as

$$\tilde{\mathcal{R}} = \{(q,p) \in T^*Q \mid \tilde{g}(q,p) \geq 0\}.$$

We apply the Legendre transform to the final condition Φ, the initial velocity constraint, the boundary conditions, and the path constraints. Then, the optimal control problem in the Hamiltonian formulation reads as follows:

Problem 4.1.3 (Hamiltonian optimal control problem (HOCP))

$$\min_{q(\cdot),p(\cdot),u(\cdot),(T)} J(q,p,u) = \int_0^T \tilde{C}(q(t),p(t),u(t))\,\mathrm{d}t + \tilde{\Phi}(q(T),p(T)) \tag{4.4a}$$

subject to

$$\begin{aligned}
\dot{q}(t) &= \nabla_p H(q(t),p(t)), \quad q(0) = q^0, && \text{(4.4b)}\\
\dot{p}(t) &= -\nabla_q H(q(t),p(t)) + f_{HC}(q(t),p(t),u(t)), \quad p(0) = p^0, && \text{(4.4c)}\\
0 &\leq \tilde{h}(q(t),p(t),u(t)), && \text{(4.4d)}\\
0 &= \tilde{r}(q(T),p(T),q^T,p^T). && \text{(4.4e)}
\end{aligned}$$

with $\tilde{C} = C \circ ((\mathbb{F}L)^{-1}(q,p),u)$, $\tilde{\Phi} = \Phi \circ (\mathbb{F}L)^{-1}(q,p)$, $\tilde{h} = h \circ ((\mathbb{F}L)^{-1}(q,p),u)$, $\tilde{r} = r \circ \big((\mathbb{F}L)^{-1}(q,p),(\mathbb{F}L)^{-1}(q^T,p^T)\big)$ with $(q^T,p^T) = \mathbb{F}L(q^T,\dot{q}^T)$ and $p(0) = D_2L(q(0),\dot{q}(0))$, $p^0 = D_2L(q^0,\dot{q}^0)$.

Remark 4.1.4 By defining $x(t) = (q(t),p(t))$, this optimal control formulation is equivalent to the formulation in (2.6) introduced in Section 2.1.1.

4.1.3 Transformation to Mayer form

Within the previous sections we introduced optimal control problems in the Bolza form, where the objective functional consists of the final point constraint and a cost functional of integral form. For error analysis (see Section 4.5), it is useful to transform the optimal control problem into the *Mayer form*, that means the objective functional consists of the final point constraint only, thus, reduces to an objective function.

To construct an optimal control problem of Mayer type we define for the Lagrangian optimal control problem a new state variable as

$$z(t) := \int_0^t C(q(t),\dot{q}(t),u(t))\,\mathrm{d}t, \quad 0 \leq t \leq T.$$

Analogously, we define

$$y(t) := \int_0^t \tilde{C}(q(t),p(t),u(t))\,\mathrm{d}t, \quad 0 \leq t \leq T,$$

for the Hamiltonian optimal control problem. By extension of the state space from TQ to $TQ \times \mathbb{R}$, and from T^*Q to $T^*Q \times \mathbb{R}$, respectively, the new objective function of Mayer type reads as

$$J(q, \dot{q}, z) = z(T) + \Phi(q(T), \dot{q}(T))$$

and

$$J(q, p, y) = y(T) + \tilde{\Phi}(q(T), p(T)),$$

respectively. Additionally, we obtain an extended set of equations describing the extended dynamical system, namely an ordinary differential equation with an initial value describing the evolution of the new variable as

$$\dot{z}(t) = C(q(t), \dot{q}(t), u(t)), \quad z(0) = 0, \tag{4.5a}$$

and

$$\dot{y}(t) = \tilde{C}(q(t), p(t), u(t)), \quad y(0) = 0, \tag{4.5b}$$

respectively.

4.2 Optimal control of a discrete mechanical system

For the numerical solution we need a discretized version of Problem 4.1.1. To this end we formulate an optimal control problem for the discrete mechanical system described by discrete variational mechanics introduced in Chapter 3. In Section 4.3 we show how the optimal control problem for the continuous and the discrete mechanical system are related.

To obtain a discrete formulation, we replace each expression in (4.3) by its discrete counterpart in terms of discrete variational mechanics. As described in Chapter 3, we replace the state space TQ of the system by $Q \times Q$ and a path $q : [0, T] \to Q$ by a discrete path $q_d : \{0, h, 2h, \ldots, Nh = T\} \to Q$, $N \in \mathbb{N}$, with $q_k = q_d(kh)$. Analogously, the continuous control path $u : [0, T] \to U$ is replaced by a discrete control path $u_d : \Delta\tilde{t} \to U$ (writing $u_k = \{u_d(kh + c_l h)\}_{l=1}^s \in U^s$ for $c_l \in [0, 1]$, $l = 1, \ldots, s$).

Discrete Lagrange-d'Alembert principle Based on this discretization, the action integral in (4.2) is approximated on a time slice $[kh, (k+1)h]$ by the *discrete Lagrangian* $L_d : Q \times Q \to \mathbb{R}$ defined in Section 3.1.2,

$$L_d(q_k, q_{k+1}) \approx \int_{kh}^{(k+1)h} L(q(t), \dot{q}(t))\, \mathrm{d}t,$$

and likewise the virtual work by the left and right discrete forces, defined in Section 3.3.5, as

$$f_k^- \cdot \delta q_k + f_k^+ \cdot \delta q_{k+1} \approx \int_{kh}^{(k+1)h} f_{LC}(q(t), \dot{q}(t), u(t)) \cdot \delta q(t) \, \mathrm{d}t,$$

where $f_k^-, f_k^+ \in T^*Q$.

As introduced in Section 3.1.2 the discrete version of the Lagrange-d'Alembert principle (4.2) requires one to find discrete paths $\{q_k\}_{k=0}^N$ such that for all variations $\{\delta q_k\}_{k=0}^N$ with $\delta q_0 = \delta q_N = 0$, one has

$$\delta \sum_{k=0}^{N-1} L_d(q_k, q_{k+1}) + \sum_{k=0}^{N-1} \left[f_k^- \cdot \delta q_k + f_k^+ \cdot \delta q_{k+1} \right] = 0. \tag{4.6}$$

or, equivalently, the forced discrete Euler-Lagrange equations

$$D_2 L_d(q_{k-1}, q_k) + D_1 L_d(q_k, q_{k+1}) + f_{k-1}^+ + f_k^- = 0, \tag{4.7}$$

where $k = 1, \ldots, N-1$.

Boundary conditions In the next step, we need to incorporate the boundary conditions $q(0) = q^0, \dot{q}(0) = \dot{q}^0$ and $r(q(T), \dot{q}(T), q^T, \dot{q}^T) = 0$ into the discrete description. Those on the configuration level can be used as constraints in a straightforward way as $q_0 = q^0$. However, since in the present formulation velocities are approximated in a time interval $[t_k, t_{k+1}]$ (as opposed to an approximation at the time nodes), the velocity conditions have to be transformed to conditions on the conjugate momenta. These are defined at each and every time node using the discrete Legendre transform. The presence of forces at the time nodes has to be incorporated into that transformation leading to the forced discrete Legendre transforms $\mathbb{F}^{f^-} L_d$ and $\mathbb{F}^{f+} L_d$ defined in (3.25). Using the standard Legendre transform $\mathbb{F}L : TQ \to T^*Q, (q, \dot{q}) \mapsto (q, p) = (q, D_2 L(q, \dot{q}))$ leads to the discrete initial constraint on the conjugate momentum

$$D_2 L(q^0, \dot{q}^0) + D_1 L_d(q_0, q_1) + f_{C_d}^-(q_0, q_1, u_0) = 0.$$

As shown in the previous section, we can transform the boundary condition from a formulation with configuration and velocity to a formulation with configuration and conjugate momentum. Thus, instead of considering a discrete version of the final time constraint r on TQ we use a discrete version of the final time constraint $\tilde{r}$ on T^*Q. We define the *discrete boundary condition* on the configuration level to be

$$r_d : Q \times Q \times U^s \times TQ \to \mathbb{R}^{n_r},$$

$$r_d(q_{N-1}, q_N, u_{N-1}, q^T, \dot{q}^T) = \tilde{r}\left(\mathbb{F}^{f+}L_d(q_{N-1}, q_N, u_{N-1}), \mathbb{F}L(q^T, \dot{q}^T)\right),$$

with $(q_N, p_N) = \mathbb{F}^{f+}L_d(q_{N-1}, q_N, u_{N-1})$ and $(q^T, p^T) = \mathbb{F}L(q^T, \dot{q}^T)$, that is $p_N = D_2L_d(q_{N-1}, q_N) + f_{C_d}^+(q_{N-1}, q_N, u_{N-1})$ and $p^T = D_2L(q^T, \dot{q}^T)$.

Remark 4.2.1 For the simple final velocity constraint $r(q(T), \dot{q}(T), q^T, \dot{q}^T) = \dot{q}(T) - \dot{q}^T$, we obtain for the transformed condition on the momentum level $\tilde{r}(q(T), p(T), q^T, p^T) = p(T) - p^T$ the discrete constraint

$$-D_2L(q^T, \dot{q}^T) + D_2L_d(q_{N-1}, q_N) + f_{C_d}^+(q_{N-1}, q_N, u_{N-1}) = 0.$$

Discrete path constraints Opposed to the final time constraint we approximate the path constraint in (4.3d) on each time interval $[t_k, t_{k+1}]$ rather than at each time node. Thus, we maintain the formulation on the velocity level and replace the continuous path constraint via a *discrete path constraint* defined by

$$h_d : Q \times Q \times U^s \to \mathbb{R}^{sn_h}, (q_k, q_{k+1}, u_k) \mapsto h_d(q_k, q_{k+1}, u_k), \quad k = 0, \dots, N-1,$$

where $h_d(q_k, q_{k+1}, u_k) \geq 0 \in \mathbb{R}^{sn_h}$, $k = 0, \dots, N-1$, replaces $h(q(t), \dot{q}(t), u(t)) \geq 0$ on s nodes within the interval $[t_k, t_{k+1}]$.

Discrete objective function Similar to the Lagrangian we approximate the objective functional in (4.1) on the time slice $[kh, (k+1)h]$ by

$$C_d(q_k, q_{k+1}, u_k) \approx \int_{kh}^{(k+1)h} C(q(t), \dot{q}(t), u(t))\,\mathrm{d}t.$$

Analogously to the final time constraint, we approximate the final condition via a discrete version $\Phi_d : Q \times Q \times U^s \to \mathbb{R}$ yielding the *discrete objective function*

$$J_d(q_d, u_d) = \sum_{k=0}^{N-1} C_d(q_k, q_{k+1}, u_k) + \Phi_d(q_{N-1}, q_N, u_{N-1}).$$

4.2.1 Discrete Optimal Control Problem

To summarize, after performing the above discretization steps, one is faced with the following discrete optimal control problem.

Problem 4.2.2 (Discrete Lagrangian optimal control problem)

$$\min_{q_d, u_d, (h)} J_d(q_d, u_d) = \sum_{k=0}^{N-1} C_d(q_k, q_{k+1}, u_k) + \Phi_d(q_{N-1}, q_N, u_{N-1}) \tag{4.8a}$$

subject to

$$\delta \sum_{k=0}^{N-1} L_d(q_k, q_{k+1}) + \sum_{k=0}^{N-1} \left[f_k^- \cdot \delta q_k + f_k^+ \cdot \delta q_{k+1} \right] = 0, \tag{4.8b}$$

$$q_0 = q^0, \; D_2 L(q^0, \dot{q}^0) + D_1 L_d(q_0, q_1) + f_0^- = 0, \tag{4.8c}$$

$$h_d(q_k, q_{k+1}, u_k) \geq 0 \quad k = 0, \ldots, N-1, \tag{4.8d}$$

$$r_d(q_{N-1}, q_N, u_{N-1}, q^T, \dot{q}^T) = 0. \tag{4.8e}$$

This problem is equivalent to

$$\min_{q_d, u_d, (h)} J_d(q_d, u_d) = \sum_{k=0}^{N-1} C_d(q_k, q_{k+1}, u_k) + \Phi_d(q_{N-1}, q_N, u_{N-1}) \tag{4.9a}$$

subject to

$$q_0 = q^0, \tag{4.9b}$$

$$D_2 L(q^0, \dot{q}^0) + D_1 L_d(q_0, q_1) + f_0^- = 0, \tag{4.9c}$$

$$D_2 L_d(q_{k-1}, q_k) + D_1 L_d(q_k, q_{k+1}) + f_{k-1}^+ + f_k^- = 0, \quad k = 1, \ldots, N-1, \tag{4.9d}$$

$$h_d(q_k, q_{k+1}, u_k) \geq 0, \quad k = 0, \ldots, N-1, \tag{4.9e}$$

$$r_d(q_{N-1}, q_N, u_{N-1}, q^T, \dot{q}^T) = 0. \tag{4.9f}$$

Recall that the $f_k^{\pm}$ are dependent on $u_k \in U^s$. To incorporate a free final time T as in the continuous setting, the step size h appears as a degree of freedom within the optimization problem. However, in the following formulations and considerations we restrict ourselves to the case of fixed final time T and thus fixed step size h.

4.2.2 Transformation to Mayer form

As in the continuous setting the discrete optimal control problem (4.9) can be transformed into a problem in Mayer form, that is the objective function consists of a final condition only. The transformation is performed on the discrete level to keep the Lagrangian structure of the original problem.

We introduce extra variables $z_d = \{z_l\}_{l=0}^N$ such that

$$\begin{aligned} z_0 &= 0, \\ z_l &= \sum_{k=0}^{l-1} C_d(q_k, q_{k+1}, u_k), \quad l = 1, \ldots, N, \end{aligned}$$

and reformulate the discrete optimal control problem (4.9) into a problem of Mayer type as

$$\min_{q_d,u_d,z_d} \tilde{\Phi}_d(q_d,u_d,z_N) = z_N + \Phi_d(q_{N-1},q_N,u_{N-1}) \tag{4.10a}$$

subject to

$$q_0 = q^0, \tag{4.10b}$$
$$z_0 = 0, \tag{4.10c}$$
$$D_2L(q^0,\dot{q}^0) + D_1L_d(q_0,q_1) + f_0^- = 0, \tag{4.10d}$$
$$D_2L_d(q_{k-1},q_k) + D_1L_d(q_k,q_{k+1}) + f_{k-1}^+ + f_k^- = 0, \quad k = 1,\dots,N-1, \tag{4.10e}$$
$$h_d(q_k,q_{k+1},u_k) \geq 0, \quad k = 0,\dots,N-1, \tag{4.10f}$$
$$r_d(q_{N-1},q_N,u_{N-1},q^T,\dot{q}^T) = 0, \tag{4.10g}$$
$$z_{k+1} - z_k - C_d(q_k,q_{k+1},u_k) = 0, \quad k = 0,\dots,N-1. \tag{4.10h}$$

Thus equations (4.10c) and (4.10h) provide the corresponding discretization for the additional equation of motion (4.5a) resulting from the Mayer transformation of the Lagrangian optimal control problem on the continuous level.

4.2.3 Fixed boundary conditions

Consider the special case of an optimal control problem with fixed initial and final configuration and velocities and without path constraints as

$$\min_{q(\cdot),\dot{q}(\cdot),u(\cdot)} J(q,\dot{q},u) = \int_0^T C(q(t),\dot{q}(t),u(t))\,\mathrm{d}t \tag{4.11a}$$

subject to

$$\delta \int_0^T L(q(t),\dot{q}(t))\,\mathrm{d}t + \int_0^T f_{LC}(q(t),\dot{q}(t),u(t)) \cdot \delta q(t)\,\mathrm{d}t = 0, \tag{4.11b}$$
$$q(0) = q^0,\ \dot{q}(0) = \dot{q}^0,\ q(T) = q^T,\ \dot{q}(T) = \dot{q}^T. \tag{4.11c}$$

A straightforward way to derive initial and final constraints for the conjugate momenta rather than for the velocities from the variational principle directly is stated in the following proposition:

Proposition 4.2.3 *With $(q^0,p^0) = \mathbb{F}L(q^0,\dot{q}^0)$ and $(q^T,p^T) = \mathbb{F}L(q^N,\dot{q}^N)$ equations (4.11b) and (4.11c) are equivalent to the following principle with free initial and final variation and with augmented Lagrangian*

$$\begin{aligned} 0 \;=\; & \delta\left(\int_0^T L(q(t),\dot{q}(t))\,\mathrm{d}t + p^0(q(0)-q^0) - p^T(q(T)-q^T)\right) \\ & + \int_0^T f_{LC}(q(t),\dot{q}(t),u(t)) \cdot \delta q(t)\,\mathrm{d}t = 0. \end{aligned} \tag{4.12}$$

Proof: Variations of (4.11b) with respect to q and zero initial and final variation $\delta q(0) = \delta q(T) = 0$ together with (4.11c) yield

$$\frac{\mathrm{d}}{\mathrm{d}t}\frac{\partial}{\partial \dot{q}}L(q(t),\dot{q}(t)) - \frac{\partial}{\partial q}L(q(t),\dot{q}(t)) = f_{LC}(q(t),\dot{q}(t),u(t)), \tag{4.13a}$$

$$q(0) = q^0,\ \dot{q}(0) = \dot{q}^0,\ q(T) = q^T,\ \dot{q}(T) = \dot{q}^T. \tag{4.13b}$$

On the other hand variations of (4.12) with respect to q and $\lambda = (p^0, p^T)$ with free initial and final variation lead to

$$\frac{\mathrm{d}}{\mathrm{d}t}\frac{\partial}{\partial \dot{q}}L(q(t),\dot{q}(t)) - \frac{\partial}{\partial q}L(q(t),\dot{q}(t)) = f_{LC}(q(t),\dot{q}(t),u(t)), \tag{4.14a}$$

$$\frac{\partial}{\partial \dot{q}}L(q(t),\dot{q}(t))\bigg|_{t=0} = p^T, \tag{4.14b}$$

$$\frac{\partial}{\partial \dot{q}}L(q(t),\dot{q}(t))\bigg|_{t=T} = p^0, \tag{4.14c}$$

$$q(0) = q^0,\ q(T) = q^T. \tag{4.14d}$$

The Legendre transform applied to the velocity boundary equations in (4.13b) gives the corresponding momenta boundary equations (4.14b) and (4.14c) . □

On the discrete level we derive the optimal control problem for fixed initial and final configurations and velocities in an equivalent way. Thus, we consider the discrete principle with discrete augmented Lagrangian

$$\delta\left(\sum_{k=0}^{N-1} L_d(q_k,q_{k+1}) + p^0(q_0 - q^0) - p^T(q_N - q^T)\right) + \sum_{k=0}^{N-1}\left[f_k^- \cdot \delta q_k + f_k^+ \cdot \delta q_{k+1}\right] = 0, \tag{4.15}$$

which, with free initial and final variation δq_0 and δq_N, respectively, is equivalent to

$$\delta\sum_{k=0}^{N-1} L_d(q_k,q_{k+1}) + \sum_{k=0}^{N-1}\left[f_k^- \cdot \delta q_k + f_k^+ \cdot \delta q_{k+1}\right] = 0, \tag{4.16a}$$

$$q_0 = q^0,\ p^0 + D_1L_d(q_0,q_1) + f_0^- = 0, \tag{4.16b}$$

$$q_N = q^T,\ -p^T + D_2L_d(q_{N-1},q_N) + f_{N-1}^+ = 0, \tag{4.16c}$$

where the second equations in (4.16b) and (4.16c) are exactly the discrete initial and final velocity constraints derived in Remark 4.2.1 with $p^0 = D_2L(q^0,\dot{q}^0)$ and $p^T = D_2L(q^T,\dot{q}^T)$.

Remark 4.2.4 This derivation of the discrete initial and final conditions directly gives the same formulation that we found before by first transforming the boundary condition on the momentum level T^*Q and then formulating the corresponding discrete constraints on $Q \times Q \times U^s$.

4.3 Correspondence between discrete and continuous optimal control problem

In this section, we relate the continuous and the discrete optimal control problem to specify certain properties that the discrete problem inherits from the continuous one.

First, along the lines of [113], we define expressions for the discrete mechanical objects that exactly reflect the continuous mechanical objects. Based on the exact discrete expressions, we determine the order of consistency concerning the difference between the continuous and the discrete mechanical system. Finally, we give an interpretation of the discrete optimal control problem as an approximation of the continuous optimal control problem. We classify the discrete problem as a standard solution strategy for Lagrangian optimal control problems as it is presented in Chapter 2.

4.3.1 Exact discrete Lagrangian and forcing

Along the lines of [113] we define a particular choice of discrete Lagrangian and discrete forces which give an exact correspondence between discrete and continuous systems.

Given a regular Lagrangian $L : TQ \to \mathbb{R}$ and a Lagrangian control force $f_{LC} : TQ \times U \to T^*Q$, we define the *exact discrete Lagrangian* $L_d^E : Q \times Q \times \mathbb{R} \to \mathbb{R}$ and the *exact discrete control forces* $f_{C_d}^{E+}, f_{C_d}^{E-} : Q \times Q \times \mathcal{D}([0,h], U) \times \mathbb{R} \to T^*Q$ to be

$$L_d^E(q_0, q_1, h) = \int_0^h L(q(t), \dot{q}(t))\, \mathrm{d}t, \tag{4.17}$$

$$f_{C_d}^{E+}(q_0, q_1, u|_{[0,h]}, h) = \int_0^h f_{LC}(q(t), \dot{q}(t), u(t)) \cdot \frac{\partial q(t)}{\partial q_1}\, \mathrm{d}t, \tag{4.18}$$

$$f_{C_d}^{E-}(q_0, q_1, u|_{[0,h]}, h) = \int_0^h f_{LC}(q(t), \dot{q}(t), u(t)) \cdot \frac{\partial q(t)}{\partial q_0}\, \mathrm{d}t, \tag{4.19}$$

where $q : [0,h] \to Q$ is the solution of the forced Euler-Lagrange equations (3.17) with control function $u : [0,h] \to U$ for L and f_{LC} satisfying the boundary conditions $q(0) = q_0$ and $q(h) = q_1$. Observe, that the exact discrete control forces now depend on the control path space, rather than on the control parameter as for the continuous control forces. Consequently, the *exact forced discrete Legendre transforms* are given by

$$\begin{aligned}
\mathbb{F}^{f+}L_d^E(q_0,q_1,u|_{[0,h]},h) &= (q_1, D_2L_d^E(q_0,q_1,h) + f_{C_d}^{E+}(q_0,q_1,u|_{[0,h]},h)),\\
\mathbb{F}^{f-}L_d^E(q_0,q_1,u|_{[0,h]},h) &= (q_0, -D_1L_d^E(q_0,q_1,h) - f_{C_d}^{E-}(q_0,q_1,u|_{[0,h]},h)).
\end{aligned}$$

The next lemma is based on a result in [113] (Lemma 1.6.2) extended to the presence of control forces and establishes a special relationship between the Legendre transforms of a regular Lagrangian and its corresponding exact discrete Lagrangian. This also proves that exact discrete Lagrangians are automatically regular.

Lemma 4.3.1 *A regular Lagrangian L and the corresponding exact discrete Lagrangian L_d^E have Legendre transforms related by*

$$\begin{aligned}
\mathbb{F}^{f+}L_d^E(q_0,q_1,u|_{[0,h]},h) &= \mathbb{F}L(q_{0,1}(h),\dot{q}_{0,1}(h)),\\
\mathbb{F}^{f-}L_d^E(q_0,q_1,u|_{[0,h]},h) &= \mathbb{F}L(q_{0,1}(0),\dot{q}_{0,1}(0)),
\end{aligned}$$

for sufficiently small h and close $q_0, q_1 \in Q$.

Proof: Analogous to the proof in [113] (Lemma 1.6.2) for the unforced case we begin with $\mathbb{F}^{f-}L_d^E$ and compute

$$\begin{aligned}
\mathbb{F}^{f-}L_d^E(q_0,q_1,u|_{[0,h]},h) &= -\int_0^h \left[\frac{\partial L}{\partial q}\cdot\frac{\partial q_{0,1}}{\partial q_0} + \frac{\partial L}{\partial \dot{q}}\cdot\frac{\partial \dot{q}_{0,1}}{\partial q_0}\right]\mathrm{d}t - \int_0^h f_{LC}\cdot\frac{\partial q_{0,1}}{\partial q_0}\,\mathrm{d}t\\
&= -\int_0^h \left[\frac{\partial L}{\partial q} - \frac{\mathrm{d}}{\mathrm{d}t}\frac{\partial L}{\partial \dot{q}} - f_{LC}\right]\cdot\frac{\partial q_{0,1}}{\partial q_0}\,\mathrm{d}t - \left[\frac{\partial L}{\partial \dot{q}}\cdot\frac{\partial q_{0,1}}{\partial q_0}\right]_0^h,
\end{aligned}$$

using integration by parts. Since $q_{0,1}(t)$ is a solution of the forced Euler-Lagrange equations the first term is zero. With $q_{0,1}(0) = q_0$ and $q_{0,1}(h) = q_1$ for the second term we get

$$\frac{\partial q_{0,1}}{\partial q_0}(0) = \mathrm{id} \quad \text{and} \quad \frac{\partial q_{0,1}}{\partial q_0}(h) = 0.$$

Substituting these into the above expression for $\mathbb{F}^{f-}L_d^E$ now gives

$$\mathbb{F}^{f-}L_d^E(q_0,q_1,u|_{[0,h]},h) = \frac{\partial L}{\partial \dot{q}}(q_{0,1}(0),\dot{q}_{0,1}(0)),$$

which is simply the definition of $\mathbb{F}L(q_{0,1}(0), \dot{q}_{0,1}(0))$.

The result for $\mathbb{F}^{f+}L_d^E$ can be established by a similar computation. □

Combining this result with the diagram in Figure 3.2 gives the commutative diagram shown in Figure 4.1 for the exact discrete Lagrangian and forces. The diagram also clarifies the following observation, that was already proved in [113] (Theorem 1.6.3) for unforced systems and can now be established for the forced case as well: Consider the pushforward of both, the continuous Lagrangian and forces and their exact discrete Lagrangian and discrete forces to T^*Q, yielding a forced Hamiltonian system with Hamiltonian H and a forced discrete Hamiltonian map $\tilde{F}_{L_d^E}(u_k)$, respectively. Then, for a sufficiently small time step $h \in \mathbb{R}$, the forced Hamiltonian flow map equals the pushforward discrete Lagrangian map: $F_H^h(u|_{[0,h]}) = \tilde{F}_{L_d^E}(u|_{[0,h]})$.

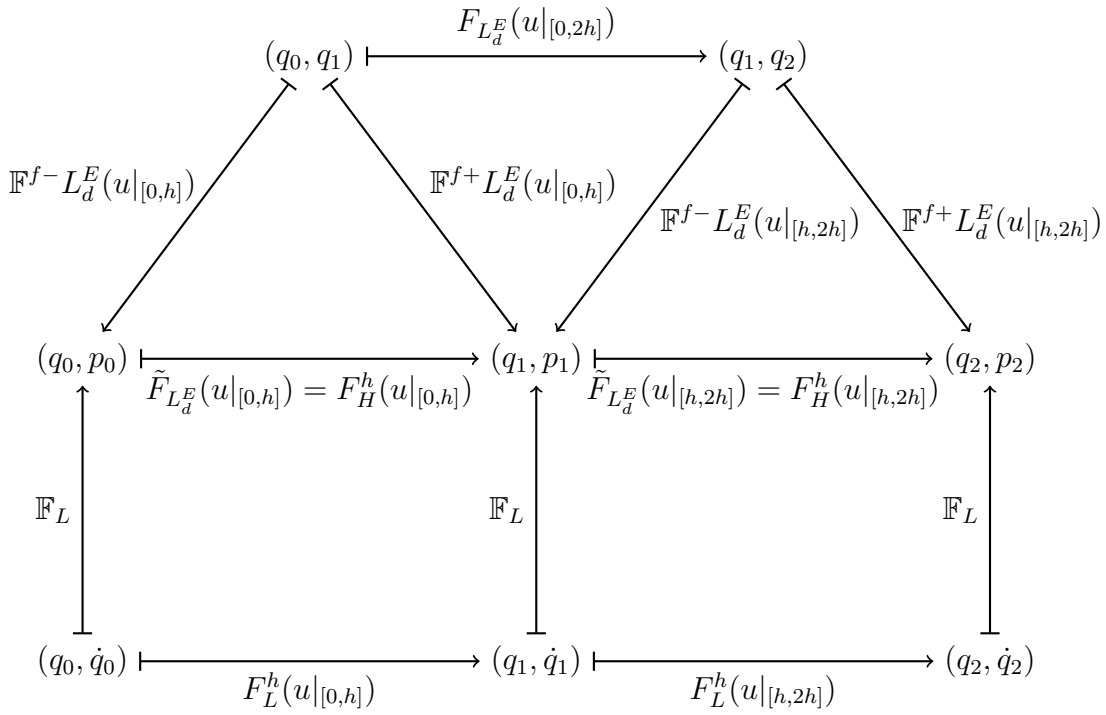

Figure 4.1: Correspondence between the exact discrete Lagrangian and forces and the continuous forced Hamiltonian flow.

4.3.2 Order of consistency

In the previous section we observed that the exact discrete Lagrangian and forces generate a forced discrete Hamiltonian map that exactly equals the forced Hamiltonian flow of the continuous system. Since we are interested in using discrete mechanics to reformulate optimal control problems, we generally do not assume that L_d and L or H are related by (4.17). Moreover, the exact discrete Lagrangian and exact discrete forces are generally not computable. In this section we determine the error we obtain by using discrete approximations for the Lagrangian and the control forces.

Forward error analysis is concerned with the difference between an exact trajectory given by the Hamiltonian flow $F_H : T^*Q \times \mathbb{R} \to T^*Q$ of a given Hamiltonian vector field X_H and a discrete trajectory determined by a numerical method $F : T^*Q \times \mathbb{R} \to T^*Q$ which approximates the Hamiltonian flow. The *consistency* of the numerical method F is described by its deviation from the flow F_H: An integrator F of X_H is said to be *(consistent) of order* r if there exist an open set $V \subset T^*Q$ and constants $C_l > 0$ and $h_l > 0$ such that

$$\|F(q,p,h) - F_H(q,p,h)\| \leq C_l h^{r+1}$$

for all $(q,p) \in V$ and $h \leq h_l$. The expression on the left-hand side of this inequality is known as the *local error*, and if a method is at least of order 1 then it is said to be *consistent*. The integrator F of X_H is said to be *convergent of order* r if there exist an open set $V \subset T^*Q$ and constants $C_g > 0, h_g > 0$ and $T_g > 0$ such that

$$\|(F)^N(q,p,h) - F_H(q,p,T)\| \leq C_g h^r,$$

where $h = T/N$, for all $(q,p) \in V$, $h \leq h_g$ and $T \leq T_g$. The expression on the left-hand side is the *global error* and indicates the total effect of all local errors "propagated" by the flow. For one-step methods used as integrators for a mechanical system, convergence follows from a local error bound on the method and a Lipschitz bound on X_H. The convergence of solution trajectories of a discrete optimal control problem to solution trajectories of the continuous optimal control problem needs some more analysis and is treated in Sections 4.5 and 4.6.

Rather than considering how closely the trajectory of F matches the exact trajectory given by F_H, we use the concepts variational error analysis as introduced in [113]. In this context we consider how closely a discrete Lagrangian matches the exact discrete Lagrangian given by the action. For forced systems, we additionally take into account how closely the discrete forces match the exact discrete forces. As was stated in the last section, if the discrete Lagrangian is equal to the action and the discrete forces are given by (4.18) and (4.19), then the corresponding forced discrete Hamiltonian map $\tilde{F}_{L_d}(u_k)$ will exactly equal the

forced flow $F_H(u)$. Usually, this is just an approximation, therefore we define the local variational error as follows (see [113]).

Definition 4.3.2 (Order of consistency) A given discrete Lagrangian L_d is *of order* r, if there exist an open subset $V_v \subset TQ$ with compact closure and constants $C_v > 0$ and $h_v > 0$ such that

$$\|L_d(q(0), q(h), h) - L_d^E(q(0), q(h), h)\| \leq C_v h^{r+1} \tag{4.20}$$

for all solutions $(q(t), u(t))$ of the forced Euler-Lagrange equations with initial condition $(q^0, \dot{q}^0) \in V_v$ and for all $h \leq h_v$. Analogously, a given discrete force $f_{C_d}^{\pm}$ is *of order* r, if there exist an open subset $V_w \subset TQ$ with compact closure and constants $C_w > 0$ and $h_w > 0$ such that

$$\|f_{C_d}^{\pm}(q(0), q(h), \{u(c_i h)\}_{i=1}^s, h) - f_{C_d}^{E\pm}(q(0), q(h), u|_{[0,h]}, h)\| \leq C_w h^{r+1} \tag{4.21}$$

for all solutions $(q(t), u(t))$ of the forced Euler-Lagrange equations with initial condition $(q^0, \dot{q}^0) \in V_w$ for all $h \leq h_w$. The discrete Legendre transforms $\mathbb{F}^+ L_d$ and $\mathbb{F}^- L_d$ of a discrete Lagrangian L_d are *of order* r if there exist an open subset $V_f \subset TQ$ with compact closure and constants $C_f > 0$ and $h_f > 0$ such that

$$\|\mathbb{F}^{\pm} L_d(q(0), q(h), \{u(c_i h)\}_{i=1}^s, h) - \mathbb{F}^{\pm} L_d^E(q(0), q(h), u|_{[0,h]}, h)\| \leq C_f h^{r+1} \tag{4.22}$$

for all solutions $(q(t), u(t))$ of the forced Euler-Lagrange equations with initial condition $(q^0, \dot{q}^0) \in V_f$ and for all $h \leq h_f$.

To give a relationship between the orders of a discrete Lagrangian, discrete forces, the forced discrete Legendre transforms, and their forced discrete Hamiltonian maps, we first have to introduce what we mean by *equivalence* of discrete Lagrangians: L_d^1 is *equivalent* to L_d^2 if their discrete Hamiltonian maps are equal. For the forced case, we say analogously, that the discrete pair $(L_d^1, f_{C_d}^1)$ is equivalent to the discrete pair $(L_d^2, f_{C_d}^2)$ if their forced discrete Hamiltonian maps are equal, such that $\tilde{F}_{L_d^1} = \tilde{F}_{L_d^2}$. With $\tilde{F}_{L_d^1} = \mathbb{F}^{f+} L_d^1 \circ (\mathbb{F}^{f-} L_d^1)^{-1}$, it follows that if $(L_d^1, f_{C_d}^1)$ and $(L_d^2, f_{C_d}^2)$ are equivalent, then their forced discrete Legendre transforms are equal. Thus, equivalent pairs of discrete Lagrangians and control forces generate the same integrators.

The following theorem is an extended version of the unforced case stated in [113] (Theorem 2.3.1).

Theorem 4.3.3 *Given a regular Lagrangian L, a Lagrangian control force f_{LC} and a corresponding Hamiltonian H with Hamiltonian control force f_{HC}, the following statements are equivalent for a discrete Lagrangian L_d and the discrete forces $f_{C_d}^{\pm}$:*

(i) *the forced discrete Hamiltonian map for* $(L_d, f_{C_d}^{\pm})$ *is of order* r,

(ii) *the forced discrete Legendre transforms of* $(L_d, f_{C_d}^{\pm})$ *are of order* r,

(iii) $(L_d, f_{C_d}^{\pm})$ *is equivalent to a pair of discrete Lagrangian and discrete forces, both of order* r.

Proof: Considering the proof of the unforced version in [113] (Theorem 2.3.1), this proof is straightforward by taking into account the discrete Lagrangian control forces.

Variational order calculation

Given a discrete Lagrangian and discrete forces, their order can be calculated by expanding the expressions for $L_d(q(0), q(h), h)$ and $f_{C_d}^{\pm}$ in a Taylor series in h and comparing these to the same expansions for the exact Lagrangian and the exact forces, respectively. If the series agree up to r terms, then the discrete Lagrangian is of order r. Analogously, the discrete forces are of order r, if for both expansions the first r terms are identical.

The first few terms of the expansion of the exact discrete Lagrangian are given by

$$L_d^E(q(0), q(h), h) = hL(q^0, \dot{q}^0) + \frac{1}{2}h^2 \left(\frac{\partial L}{\partial q}(q^0, \dot{q}^0) \cdot \dot{q}^0 + \frac{\partial L}{\partial \dot{q}}(q^0, \dot{q}^0) \cdot \ddot{q}^0 \right) + \mathcal{O}(h^3), \tag{4.23}$$

where $q^0 = q(0), \dot{q}^0 = \dot{q}(0)$ and so forth. Higher derivatives of $q(t)$ are determined by the Euler-Lagrange equations. In the same way we evaluate the first few terms of the expansion of the exact discrete control forces and obtain

$$\begin{aligned} f_{C_d}^{E-}(q(0), q(h), u|_{[0,h]}, h) = hf_{LC}(q^0, \dot{q}^0, u^0) + \frac{1}{2}h^2 \Bigg(& f_{LC}(q^0, \dot{q}^0, u^0) \cdot \frac{\partial \dot{q}^0}{\partial q} \\ & + \frac{\partial f_{LC}}{\partial q}(q^0, \dot{q}^0, u^0) \cdot \dot{q}^0 + \frac{\partial f_{LC}}{\partial \dot{q}}(q^0, \dot{q}^0, u^0) \cdot \ddot{q}^0 + \frac{\partial f_{LC}}{\partial u}(q^0, \dot{q}^0, u^0) \cdot \dot{u}^0 \Bigg) \\ & + \mathcal{O}(h^3), \end{aligned} \tag{4.24}$$

with $q^0 = q(0), u^0 = u(0), \dot{q}^0 = \dot{q}(0), \dot{u}^0 = \dot{u}(0)$ and so forth and analogously,

$$\begin{aligned} f_{C_d}^{E+}(q(0), q(h), u|_{[0,h]}, h) = hf_{LC}(q^h, \dot{q}^h, u^h) - \frac{1}{2}h^2 \Bigg(& f_{LC}(q^h, \dot{q}^h, u^h) \cdot \frac{\partial \dot{q}^h}{\partial q} \\ & + \frac{\partial f_{LC}}{\partial q}(q^h, \dot{q}^h, u^h) \cdot \dot{q}^h + \frac{\partial f_{LC}}{\partial \dot{q}}(q^h, \dot{q}^h, u^h) \cdot \ddot{q}^h + \frac{\partial f_{LC}}{\partial u}(q^h, \dot{q}^h, u^h) \cdot \dot{u}^h \Bigg) \\ & + \mathcal{O}(h^3), \end{aligned} \tag{4.25}$$

with $q^h = q(h), u^h = u(h), \dot{q}^h = \dot{q}(h), \dot{u}^h = \dot{u}(h)$ and so forth.

Example 4.3.4 Given a discrete Lagrangian

$$L_d^\alpha(q_0, q_1, h) = hL\left((1-\alpha)q_0 + \alpha q_1, \frac{q_1 - q_0}{h}\right)$$

and discrete control forces

$$\begin{aligned}
&f_{C_d}^{\alpha-}(q_0, q_1, u_0, h) = \\
&\quad hf_{LC}\left((1-\alpha)q_0 + \alpha q_1, \frac{q_1 - q_0}{h}, u((1-\alpha)t_0 + \alpha t_1)\right) \cdot \frac{\partial\left((1-\alpha)q_0 + \alpha q_1\right)}{\partial q_0} = \\
&\quad (1-\alpha)hf_{LC}\left((1-\alpha)q_0 + \alpha q_1, \frac{q_1 - q_0}{h}, u((1-\alpha)t_0 + \alpha t_1)\right) \\
&f_{C_d}^{\alpha+}(q_0, q_1, u_0, h) = \\
&\quad hf_{LC}\left((1-\alpha)q_0 + \alpha q_1, \frac{q_1 - q_0}{h}, u((1-\alpha)t_0 + \alpha t_1)\right) \cdot \frac{\partial\left((1-\alpha)q_0 + \alpha q_1\right)}{\partial q_1} = \\
&\quad \alpha hf_{LC}\left((1-\alpha)q_0 + \alpha q_1, \frac{q_1 - q_0}{h}, u((1-\alpha)t_0 + \alpha t_1)\right)
\end{aligned}$$

for some parameter $\alpha \in [0, 1]$ and calculating the expansions in h gives

$$L_d^\alpha(q(0), q(h), h) = hL(q, \dot{q}) + \frac{1}{2}h^2\left(2\alpha\frac{\partial L}{\partial q}(q, \dot{q}) \cdot \dot{q} + \frac{\partial L}{\partial \dot{q}}(q, \dot{q}) \cdot \ddot{q}\right) + \mathcal{O}(h^3),$$

and

$$\begin{aligned}
f_{C_d}^{\alpha-}(q(0), q(h), \{u(c_i h)\}_{i=1}^s, h) &= hf_{LC}(q, \dot{q}, u) + \frac{1}{2}h^2\left(2\alpha f_{LC}(q, \dot{q}, u) \cdot \frac{\partial \dot{q}}{\partial q}\right. \\
&\quad \left. + 2\alpha\frac{\partial f_{LC}}{\partial q}(q, \dot{q}, u) \cdot \dot{q} + \frac{\partial f_{LC}}{\partial \dot{q}}(q, \dot{q}, u) \cdot \ddot{q} + 2\alpha\frac{\partial f_{LC}}{\partial u}(q, \dot{q}, u) \cdot \dot{u}\right) \\
&\quad + \mathcal{O}(h^3), \\
f_{C_d}^{\alpha+}(q(0), q(h), \{u(c_i h)\}_{i=1}^s, h) &= hf_{LC}(q, \dot{q}, u) - \frac{1}{2}h^2\left(2(1-\alpha)f_{LC}(q, \dot{q}, u) \cdot \frac{\partial \dot{q}}{\partial q}\right. \\
&\quad \left. + 2(1-\alpha)\frac{\partial f_{LC}}{\partial q}(q, \dot{q}, u) \cdot \dot{q} + \frac{\partial f_{LC}}{\partial \dot{q}}(q, \dot{q}, u) \cdot \ddot{q} + 2(1-\alpha)\frac{\partial f_{LC}}{\partial u}(q, \dot{q}, u) \cdot \dot{u}\right) \\
&\quad + \mathcal{O}(h^3).
\end{aligned}$$

Comparing these to the expansions (4.23), (4.24) and (4.25) for the exact discrete Lagrangian and the exact discrete control forces shows that the method is second order if and only if $\alpha = 1/2$.

4.3.3 Discrete problem as direct solution method

Within the discrete context, all relevant objects are approximated by discrete expressions. Therefore, we obtain a finite dimensional optimization problem restricted by the forced discrete Euler-Lagrange equations, the boundary conditions, and the path constraints. Thus, by understanding the discrete optimal control problem as a discrete approximation of the continuous Lagrangian optimal control problem 4.1.1, a direct solution method is provided as described in Chapter 2. The main difference here is, that rather than discretizing the differential equations arising from the Lagrange-d'Alembert principle, we discretize one step earlier. Namely, we derive the discrete equations for the optimization problem by considering the discrete Lagrange-d'Alembert principle directly. In Figure 4.2 we present schematically the different strategies of standard direct methods and DMOC.

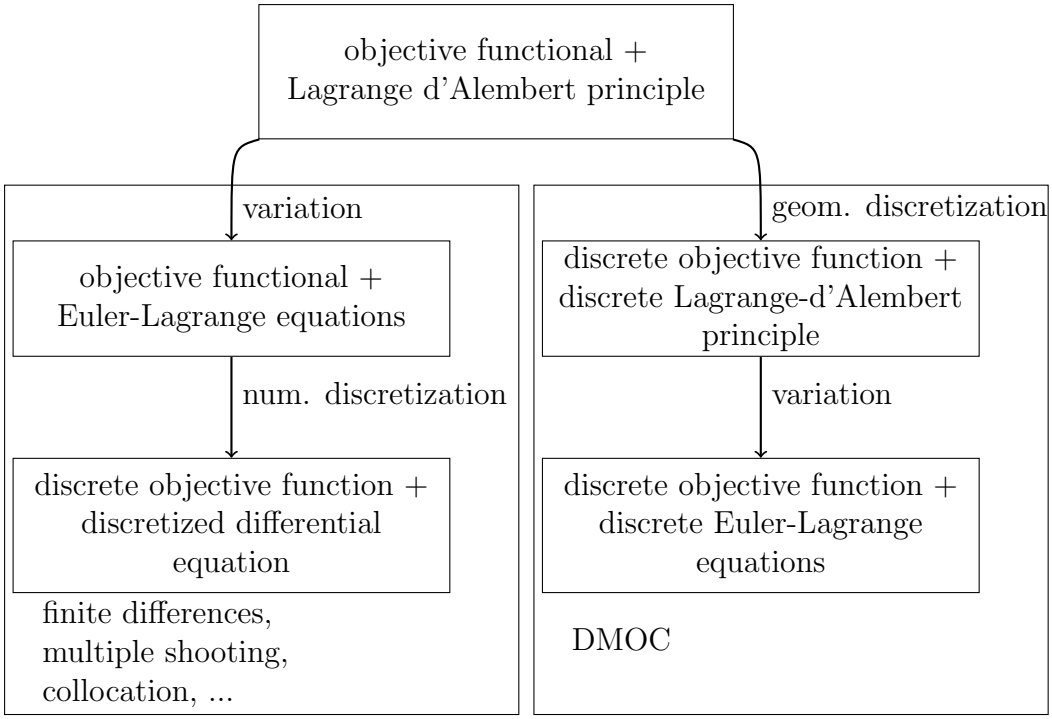

Figure 4.2: Comparison of solution strategies for optimal control problems: standard direct methods and DMOC.

Our approach derived via the concept of discrete mechanics leads to a special discretization of the system equations based on variational integrators, which are dealt with in detail in [113]. Thus, the discrete optimal control problem inherits

special properties exhibited by variational integrators. In the following, we specify particular important properties and phenomena of variational integrators and try to translate their meaning into the optimal control context.

Preservation of momentum maps If the discrete system, obtained by applying variational integration to a mechanical system, inherits the same symmetry groups as the continuous system, the corresponding discrete momentum maps are preserved (see Theorem 3.1.5). For the forced case the same statement holds, if the forcing is orthogonal to the group action (see Theorem 3.3.5).

On the one hand, this means for the optimal control problem, that if the control force is orthogonal to the group action, our discretization leads to a discrete system, for which the corresponding momentum map is preserved. An example is given in Section 5.4.1. On the other hand, in the case of the forcing not being orthogonal to the group action, the forced discrete Noether's theorem provides an exact coherence between the change in angular momentum and the applied control force via

$$[\mathbf{J}_{L_d}^{f+} \circ F_{L_d}^{N-1}(u_d) - \mathbf{J}_{L_d}^{f-}](q_0, q_1) \cdot \xi = \sum_{k=0}^{N-1} f_{C_d}(q_k, q_{k+1}, u_k) \cdot \xi_{Q\times Q}(q_k, q_{k+1}),$$

(see Section 5.2 for examples).

Conservation of modified energy As shown in Section 3.1.2 variational integrators are symplectic, which implies that a certain modified energy is conserved (see for example [55]). This is an important property if the long time behavior of dynamical systems is considered. For the case of the optimal control of systems with long maneuver time such as low thrust space missions, it would therefore be interesting to investigate the relation between a modified energy and the virtual work. However, this has not been considered within this thesis.

Implementation Rather than using a configuration-momentum implementation of variational integrators as proposed in [113], we stay on $Q \times Q$. That means we just determine the optimal trajectory for the configuration and the control forces and reconstruct the corresponding momenta and velocities via the forced discrete Legendre transforms. This yields computational savings. A more detailed description of the computational savings compared to standard discretizations for optimal control problems is given in Remark 4.4.4.

4.4 High-order discretization

As shown in the previous section, we have to construct discrete Lagrangians and discrete forces which accurately approximate the action integral and the virtual work to design high-order discretizations.

In this section, we first show how to create such discretizations in practice. An appropriate way is to use polynomial approximations to the trajectories and numerical quadrature to approximate the integrals. We formulate the corresponding discrete optimal control problem and show the equivalence to the optimization problem resulting by a special form of Runge-Kutta discretization for Hamiltonian dynamics.

This equivalence is important for following sections concerning error analysis and convergence, since much is known about optimal control problems discretized by Runge-Kutta methods (for example Hager et al. [39, 40, 41, 53, 54]).

4.4.1 Quadrature approximation

We approximate the space of trajectories $\mathcal{C}([0,h],Q) = \{q : [0,h] \to Q \mid q(0) = q_0, q(h) = q_1\}$ by a finite-dimensional approximation $\mathcal{C}^s([0,h],Q) \subset \mathcal{C}([0,h],Q)$ of the trajectory space given by

$$\mathcal{C}^s([0,h],Q) = \{q \in \mathcal{C}([0,h],Q) \mid q \in \Pi^s\},$$

with Π^s the space of polynomials of degree s. Analogously, we approximate the control trajectory by a polynomial of degree m and define the corresponding control space as

$$\mathcal{D}^m([0,h],U) = \{u \in \mathcal{D}([0,h],U) \mid u \in \Pi^m\},$$

with $\mathcal{D}([0,h],U) = \{u : [0,h] \to U\}$ the original control space. Given control times $0 = d_0 < d_1 < \cdots < d_{s-1} < d_s = 1$ and control points $q_0^0 = q_0, q_0^1, q_0^2, \ldots, q_0^{s-1}, q_0^s = q_1$ the degree s polynomial $q_d(t; q_0^\nu, h)$ which passes through each q_0^ν at time $d_\nu h$, that is, $q_d(d_\nu h) = q_0^\nu$ for $\nu = 0, \ldots, s$, is uniquely defined. Analogously, we choose a set of interior points $u_0^0, \ldots, u_0^m$ that represents a parametrization of the space of polynomials of degree m mapping $[0,h]$ to U.

Now we approximate the action integral with numerical quadrature to give an approximate action $\mathfrak{G}^s : \mathcal{C}([0,h],Q) \to \mathbb{R}$ by

$$\mathfrak{G}^s(q_d(t; q_0^\nu, h)) = h \sum_{i=1}^{s} b_i L\left(q_d(c_i h), \dot{q}_d(c_i h)\right), \tag{4.26}$$

where $c_i \in [0,1],\ i = 1, \ldots, s$ are a set of quadrature points and b_i a set of order weights and define the multipoint discrete Lagrangian as

$$L_d(q_0^0, q_0^1, \ldots, q_0^s, h) = \mathfrak{G}^s(q_d(t; q_0^\nu, h)), \tag{4.27}$$

and the appropriate discrete action sum over the entire trajectory to be

$$\mathfrak{G}_d(\{(q_k = q_k^0, q_k^1, \ldots, q_k^s = q_{k+1})\}_{k=0}^{N-1}) = \sum_{k=0}^{N-1} L_d(q_k^0, q_k^1, \ldots, q_k^s, h).$$

Similar to the action integral we approximate the virtual work for one time interval $\mathfrak{W}^s : \mathcal{C}([0,h], Q) \times \mathcal{D}([0,h], U) \to \mathbb{R}$ by

$$\mathfrak{W}^s(q_d(t; q_0^\nu, h), u_d(t; u_0^\eta, h)) = h \sum_{i=1}^{s} b_i f_{LC}(q_d(c_i h), \dot{q}_d(c_i h), u_d(c_i h)) \cdot \delta q_d(c_i h)$$

and define the appropriate discrete virtual work over the entire trajectory to be

$$\begin{aligned}\mathfrak{W}_d(\{(q_k = q_k^0, q_k^1, \ldots, q_k^s = q_{k+1})\}_{k=0}^{N-1}, \{(u_k^0, \ldots, u_k^m)\}_{k=0}^{N-1}) = \\ \sum_{k=0}^{N-1} h \sum_{i=1}^{s} b_i f_{LC}(q_d(t_k + c_i h), \dot{q}_d(t_k + c_i h), u_d(t_k + c_i h)) \cdot \delta q_d(t_k + c_i h).\end{aligned}$$

We define the multipoint discrete forces as follows

$$\begin{aligned} f_{C_d}^{\nu+}(q_k^0, \ldots, q_k^s, u_k^0, \ldots, u_k^m, h) &= h \sum_{i=1}^{s} b_i f_{LC}(t_k + c_i h) \frac{\partial q_d(t_k + c_i h)}{\partial q_k^\nu}, \\ f_{C_d}^{\nu-}(q_k^0, \ldots, q_k^s, u_k^0, \ldots, u_k^m, h) &= h \sum_{i=1}^{s} b_i f_{LC}(t_k + c_i h) \frac{\partial q_d(t_k + c_i h)}{\partial q_k^\nu}, \end{aligned}$$

with $f_{LC}(t_k + c_i h) = f_{LC}(q_d(t_k + c_i h), \dot{q}_d(t_k + c_i h), u_d(t_k + c_i h))$. To simplify the notation we denote the left and right discrete forces $f_{C_d}^{\nu\pm}(q_k^0, \ldots, q_k^s, u_k^0, \ldots, u_k^m, h)$ by $f_k^{\nu\pm}$.

With $\delta q_d(t_k + c_i h) = \sum_{\nu=0}^{s} \frac{\partial q_d(t_k + c_i h)}{\partial q_k^\nu} \delta q_k^\nu$ and requiring that the discrete Lagrange d'Alembert principle holds for $\mathfrak{G}_d$ and $\mathfrak{W}_d$, $\mathfrak{G}_d$ leads to the extended set of discrete Euler-Lagrange equations

$$D_{\nu+1} L_d(q_k^0, \ldots, q_k^s, h) + f_{C_d}^{\nu\pm}(q_k^0, \ldots, q_k^s, u_k^0, \ldots, u_k^m, h) = 0, \quad \nu = 1, \ldots, s-1 \tag{4.28a}$$

$$\begin{aligned} &D_{s+1} L_d(q_k^0, \ldots, q_k^s, h) + D_1 L_d(q_{k+1}^0, \ldots, q_{k+1}^s, h) + \\ &\quad f_{C_d}^{s+}(q_k^0, \ldots, q_k^s, u_k^0, \ldots, u_k^m, h) + f_{C_d}^{0-}(q_{k+1}^0, \ldots, q_{k+1}^s, u_{k+1}^0, \ldots, u_{k+1}^m, h) = 0. \end{aligned} \tag{4.28b}$$

Following [113] the $(s+1)$-point discrete Lagrangian (4.27) can be used to derive a standard two-point discrete Lagrangian by taking

$$L_d(q_k, q_{k+1}, h) = \mathrm{ext}_{(q_k^1,\ldots,q_k^{s-1})} L_d(q_k = q_k^0, q_k^1, \ldots, q_k^s = q_{k+1}, h),$$

where extL_d means that L_d should be evaluated at extreme or critical values of $q_k^1, \ldots, q_k^{s-1}$, that means evaluated on the trajectory within the step which solves (4.28a). We define the left and right discrete forces to be

$$f_{C_d}^+(q_k, q_{k+1}, u_k, h) = f_{C_d}^{s+}(q_k^0, \ldots, q_k^s, u_k^0, \ldots, u_k^m, h) + \sum_{\nu=1}^{s-1} f_{C_d}^{\nu+}(q_k^0, \ldots, q_k^s, u_k^0, \ldots, u_k^m, h) \cdot \frac{\partial q_k^\nu}{\partial q_{k+1}}, \tag{4.29a}$$

$$f_{C_d}^-(q_k, q_{k+1}, u_k, h) = f_{C_d}^{0-}(q_k^0, \ldots, q_k^s, u_k^0, \ldots, u_k^m, h) + \sum_{\nu=1}^{s-1} f_{C_d}^{\nu-}(q_k^0, \ldots, q_k^s, u_k^0, \ldots, u_k^m, h) \cdot \frac{\partial q_k^\nu}{\partial q_k}, \tag{4.29b}$$

and combine them to a single one-form as

$$f_{C_d}(q_k, q_{k+1}, u_k, h) \cdot (\delta q_k, \delta q_{k+1}) = f_{C_d}^+(q_k, q_{k+1}, u_k, h) \cdot \delta q_{k+1} + f_{C_d}^-(q_k, q_{k+1}, u_k, h) \cdot \delta q_k.$$

Note that the forced discrete Euler-Lagrange equations with these definitions satisfy

$$\begin{aligned}
&D_1 L_d(q_k, q_{k+1}, h) + D_2 L_d(q_{k-1}, q_k, h) + f_{C_d}^+(q_{k-1}, q_k, u_{k-1}, h) + f_{C_d}^-(q_k, q_{k+1}, u_k, h) = \\
&D_1 L_d(q_k, q_k^1, \ldots, q_k^{s-1}, q_{k+1}, h) + \sum_{\nu=1}^{s-1} D_{\nu+1} L_d(q_k, q_k^1, \ldots, q_k^{s-1}, q_{k+1}, h) \cdot \frac{\partial q_k^\nu}{\partial q_k} + \\
&D_{s+1} L_d(q_{k-1}, q_{k-1}^1, \ldots, q_{k-1}^{s-1}, q_k, h) + \sum_{\nu=1}^{s-1} D_{\nu+1} L_d(q_{k-1}, q_{k-1}^1, \ldots, q_{k-1}^{s-1}, q_k, h) \cdot \frac{\partial q_{k-1}^\nu}{\partial q_k} \\
&+ f_{C_d}^{s+}(q_{k-1}^0, \ldots, q_{k-1}^s, u_{k-1}^0, \ldots, u_{k-1}^m, h) \\
&+ \sum_{\nu=1}^{s-1} f_{C_d}^{\nu+}(q_{k-1}^0, \ldots, q_{k-1}^s, u_{k-1}^0, \ldots, u_{k-1}^m, h) \cdot \frac{\partial q_{k-1}^\nu}{\partial q_k} \\
&+ f_{C_d}^{0-}(q_k^0, \ldots, q_k^s, u_k^0, \ldots, u_k^m, h) + \sum_{\nu=1}^{s-1} f_{C_d}^{\nu-}(q_k^0, \ldots, q_k^s, u_k^0, \ldots, u_k^m, h) \cdot \frac{\partial q_k^\nu}{\partial q_k} =
\end{aligned}$$

$$
\begin{aligned}
&D_1 L_d(q_k, q_k^1, \ldots, q_k^{s-1}, q_{k+1}, h) + D_{s+1} L_d(q_{k-1}, q_{k-1}^1, \ldots, q_{k-1}^{s-1}, q_k, h) \\
&\quad + f_{C_d}^{s+}(q_{k-1}^0, \ldots, q_{k-1}^s, u_{k-1}^0, \ldots, u_{k-1}^m, h) + f_{C_d}^{0-}(q_k^0, \ldots, q_k^s, u_k^0, \ldots, u_k^m, h) \\
&\quad + \sum_{\nu=1}^{s-1} \left(D_{\nu+1} L_d(q_k, q_k^1, \ldots, q_k^{s-1}, q_{k+1}, h) + f_{C_d}^{\nu-}(q_k^0, \ldots, q_k^s, u_k^0, \ldots, u_k^m, h) \right) \cdot \frac{\partial q_k^\nu}{\partial q_k} \\
&\quad + \sum_{\nu=1}^{s-1} \Big(D_{\nu+1} L_d(q_{k-1}, q_{k-1}^1, \ldots, q_{k-1}^{s-1}, q_k, h) \\
&\qquad + f_{C_d}^{\nu+}(q_{k-1}^0, \ldots, q_{k-1}^s, u_{k-1}^0, \ldots, u_{k-1}^m, h) \Big) \cdot \frac{\partial q_{k-1}^\nu}{\partial q_k} =
\end{aligned}
$$

$$
\begin{aligned}
&D_1 L_d(q_k, q_k^1, \ldots, q_k^{s-1}, q_{k+1}, h) + D_{s+1} L_d(q_{k-1}, q_{k-1}^1, \ldots, q_{k-1}^{s-1}, q_k, h) \\
&\quad + f_{C_d}^{s+}(q_{k-1}^0, \ldots, q_{k-1}^s, u_{k-1}^0, \ldots, u_{k-1}^m, h) + f_{C_d}^{0-}(q_k^0, \ldots, q_k^s, u_k^0, \ldots, u_k^m, h) = 0,
\end{aligned}
$$

and thus are equivalent to the Euler-Lagrange equations (4.28).

4.4.2 High-order discrete optimal control problem

We now formulate the optimal control problem of high-order discretizations obtained via the quadrature approximation described above.

In the previous section we have shown, how to discretize the Lagrange-d'Alembert principle via a quadrature approximation of the Lagrangian and the virtual work. However, we still have to find appropriate discrete high-order versions for the objective function, the boundary conditions, and the path constraints.

Boundary conditions In a straightforward manner compared to Section 4.2, we set up the boundary conditions on the configuration level as $q_0 = q^0$. For the constraint on the velocity level we use the discrete version of the corresponding continuous constraint on the conjugate momentum and define the discrete multipoint boundary condition as

$$
\bar{r}_d(q_{N-1}^0, \ldots, q_{N-1}^s, u_{N-1}^0, \ldots, u_{N-1}^m, q^T, \dot{q}^T) \quad = \quad \tilde{r}(q_N, p_N, \mathbb{F}L(q^T, \dot{q}^T)),
$$

where the final momentum p_N is given by the discrete Legendre transform as $p_N = D_{s+1} L_d(q_{N-1}^0, \ldots, q_{N-1}^s, h) + f_{C_d}^{s+}(q_{N-1}^0, \ldots, q_{N-1}^s, u_{N-1}^0, \ldots, u_{N-1}^m, h)$. To trace the discrete multipoint boundary condition back to the discrete boundary condition defined in Section 4.2 we define

$$
\begin{aligned}
&r_d(q_{N-1}, q_N, u_{N-1}, q^T, \dot{q}^T) = \\
&\qquad \bar{r}_d(q_{N-1}^0, \ldots, q_{N-1}^s, u_{N-1}^0, \ldots, u_{N-1}^m, q^T, \dot{q}^T),
\end{aligned}
$$

where $u_{N-1} = \{u_d(t_{N-1} + c_i h; u_{N-1}^0, \ldots, u_{N-1}^m, h)\}_{i=1}^s$ is the sequence of control parameters guiding the system from q_{N-1} to q_N as defined in Section 3.3.5.

Discrete path constraints As before, we replace the path constraints $h(q_d(t_k + c_i h; q_k^\nu, h), \dot{q}_d(t_k + c_i h; q_k^\nu, h), u_d(t_k + c_i h; u_k^\eta, h)) \geq 0$ on each substep of each time interval $[t_k + c_i h, t_k + c_{i+1} h], k = 0, \ldots, N-1$, $i = 1, \ldots, s-1$ by the discrete path constraint

$$\bar{h}_d(q_k^0, \ldots, q_k^s, u_k^0, \ldots, u_k^m) \geq 0,$$

$k = 0, \ldots, N-1,\ i = 1, \ldots, s$. With h_d defined as

$$h_d(q_k, q_{k+1}, u_k) = \bar{h}_d(q_k^0, \ldots, q_k^s, u_k^0, \ldots, u_k^m)$$

we obtain the original form of the discrete path constraints defined in Section 4.2.

Discrete objective function Analogous to the discrete Lagrangian we approximate the objective functional $\int_0^T C(q(t), \dot{q}(t), u(t))\,\mathrm{d}t$ with the same quadrature rule as

$$\bar{C}_d(q_0^0, \ldots, q_0^s, u_0^0, \ldots, u_0^m) = h \sum_{i=1}^{s} b_i C(q_d(c_i h), \dot{q}_d(c_i h), u_d(c_i h))$$

and the final condition analogous to the boundary condition as

$$\bar{\Phi}_d(q_{N-1}^0, \ldots, q_{N-1}^s, u_{N-1}^0, \ldots, u_{N-1}^s).$$

This results to the discrete objective function

$$J_d(q_d, u_d) = \sum_{k=0}^{N-1} \bar{C}_d(q_k^0, \ldots, q_k^s, u_k^0, \ldots, u_k^m) + \bar{\Phi}_d(q_{N-1}^0, \ldots, q_{N-1}^s, u_{N-1}^0, \ldots, u_{N-1}^s).$$

With C_d defined as

$$C_d(q_k, q_{k+1}, u_k) = \bar{C}_d(q_k^0, \ldots, q_k^s, u_k^0, \ldots, u_k^m),$$

and Φ_d being defined as

$$\Phi_d(q_{N-1}, q_N, u_{N-1}) = \bar{\Phi}_d(q_{N-1}^0, \ldots, q_{N-1}^s, u_{N-1}^0, \ldots, u_{N-1}^m),$$

we obtain the original expression for the discrete objective function

$$J_d(q_d, u_d) = \sum_{k=0}^{N-1} C_d(q_k, q_{k+1}, u_k) + \Phi_d(q_{N-1}, q_N, u_{N-1}).$$

Optimal control problem of high-order The optimal control problem of high-order discretizations obtained via quadrature approximation can now be formulated in the same way as Problem 4.2.2

$$\min_{q_d,u_d} J_d(q_d,u_d) = \sum_{k=0}^{N-1} C_d(q_k,q_{k+1},u_k) + \Phi_d(q_{N-1},q_N,u_N) \tag{4.30a}$$

subject to

$$q_0 = q^0, \tag{4.30b}$$
$$D_2L(q^0,\dot{q}^0) + D_1L_d(q_0,q_1) + f_0^- = 0, \tag{4.30c}$$
$$D_2L_d(q_{k-1},q_k) + D_1L_d(q_k,q_{k+1}) + f_{k-1}^+ + f_k^- = 0, \quad k=1,\dots,N-1, \tag{4.30d}$$
$$h_d(q_k,q_{k+1},u_k) \geq 0, \quad k=0,\dots,N-1, \tag{4.30e}$$
$$r_d(q_{N-1},q_N,u_N,q^T,\dot{q}^T) = 0. \tag{4.30f}$$

Within the formulation above, the extended Euler-Lagrange equations (4.28a) have to be satisfied and represent extra conditions for the resulting optimization problem.

Examples 4.4.1 (a) Let the configuration trajectory $q(t)$ be approximated by straight lines, that is a polynomial of order $s=1$ as $q_d(t) = q_k + \frac{t-t_k}{h}(q_{k+1}-q_k)$, for $t \in [t_k,t_{k+1}]$, and the control $u(t)$ by a polynomial of order $m=0$ as $u_d(t) = u((t_k+t_{k+1})/2)$ on $[t_k,t_{k+1}]$. Choose quadrature points $c=\frac{1}{2}$ and weights $b=1$ to obtain a midpoint quadrature approximation as $L_d = hL(\frac{q_k+q_{k+1}}{2}, \frac{q_{k+1}-q_k}{h}, u(t_k+h/2))$.

(b) By taking quadrature points c_i as done in the Gauss-Legendre quadrature, which is the highest-order quadrature for a given number of points, and by enforcing $c_0=0$ and $c_s=1$, we obtain the Lobatto quadrature.

4.4.3 Correspondence to Runge-Kutta discretizations

In the following we show, that the discrete optimal control problem derived via the discrete Lagrange-d'Alembert principle is equivalent to the optimization problem resulting from a symplectic partitioned Runge-Kutta discretization for the Hamiltonian dynamics.

First, we introduce symplectic partitioned Runge-Kutta methods. We propose corresponding expressions for the objective function, the boundary conditions, and the path constraints. Using these expressions we formulate the optimal control problem from the Hamiltonian point of view discretized via a Runge-Kutta map.

Symplectic partitioned Runge-Kutta methods

As shown in [113] (Theorem 2.6.1), the discrete Hamiltonian map generated by the discrete Lagrangian is a symplectic partitioned Runge-Kutta method. A similar statement is true for discrete Hamiltonian maps with forces. The resulting method is still a partitioned Runge-Kutta method, but no longer symplectic in the original sense since the symplectic form is not preserved anymore due to the presence of control forces. However, we still denote it as a symplectic method having in mind that the symplectic form is preserved only in absence of external control forces.

A partitioned Runge-Kutta method for the regular forced Lagrangian system L and f_{LC} is a map $T^*Q \times U^s \times \mathbb{R} \to T^*Q$ specified by the coefficients $b_i, a_{ij}, \tilde{b}_i, \tilde{a}_{ij}$ for $i = 1, \ldots, s$, and defined by $(q_0, p_0, u_0) \mapsto (q_1, p_1)$ for

$$q_1 = q_0 + h \sum_{j=1}^{s} b_j \dot{Q}_j, \qquad p_1 = p_0 + h \sum_{j=1}^{s} \tilde{b}_j \dot{P}_j, \tag{4.31a}$$

$$Q_i = q_0 + h \sum_{j=1}^{s} a_{ij} \dot{Q}_j, \qquad P_i = p_0 + h \sum_{j=1}^{s} \tilde{a}_{ij} \dot{P}_j, \tag{4.31b}$$

$$P_i = \frac{\partial L}{\partial \dot{q}}(Q_i, \dot{Q}_i), \qquad \dot{P}_i = \frac{\partial L}{\partial q}(Q_i, \dot{Q}_i) + f_{LC}(Q_i, \dot{Q}_i, U_i), \tag{4.31c}$$

$i = 1, \ldots, s$, where the points (Q_i, P_i) are known as the internal stages and U_i are the control samples given by $U_i = u_{0i} = u_d(t_0 + c_i h)$. For $a_{ij} = \tilde{a}_{ij}$ and $b_i = \tilde{b}_i$ the partitioned Runge-Kutta method is a Runge-Kutta method.

The method is symplectic (that is, it preserves the canonical symplectic form Ω on T^*Q in absence of external forces) if the coefficients satisfy

$$b_i \tilde{a}_{ij} + \tilde{b}_j a_{ji} = b_i \tilde{b}_j, \qquad i, j = 1, \ldots, s, \tag{4.32a}$$

$$b_i = \tilde{b}_i, \qquad i = 1, \ldots, s. \tag{4.32b}$$

Since discrete Lagrangian maps are symplectic, we can assume that we have conditions satisfying (4.32) and write a discrete Lagrangian and discrete Lagrangian control forces that generate the corresponding symplectic partitioned Runge-Kutta method. Given points $(q_0, q_1) \in Q \times Q$, we can regard (4.31) as implicitly defining $p_0, p_1, Q_i, P_i, \dot{Q}_i$ and $\dot{P}_i$ for $i = 1, \ldots, s$. Taking these to be defined as functions of (q_0, q_1), we construct a discrete Lagrangian

$$L_d(q_0, q_1, h) = h \sum_{i=1}^{s} b_i L(Q_i, \dot{Q}_i), \tag{4.33}$$

and left and right discrete forces as

$$f_{C_d}^{+}(q_0, q_1, u_0, h) = h \sum_{i=1}^{s} b_i f_{LC}(Q_i, \dot{Q}_i, U_i) \cdot \frac{\partial Q_i}{\partial q_1}, \tag{4.34a}$$

$$f_{C_d}^{-}(q_0, q_1, u_0, h) = h \sum_{i=1}^{s} b_i f_{LC}(Q_i, \dot{Q}_i, U_i) \cdot \frac{\partial Q_i}{\partial q_0}. \tag{4.34b}$$

Based on the lines of [113] (Theorem 2.6.1) we show, that the corresponding forced discrete Hamiltonian map is exactly the map $(q_0, p_0, u_0) \mapsto (q_1, p_1)$ which is the symplectic partitioned Runge-Kutta method for the forced Hamiltonian system (3.18).

Theorem 4.4.2 *The discrete Hamiltonian map generated by the discrete Lagrangian (4.33) together with the discrete forces (4.34) is a symplectic partitioned Runge-Kutta method.*

Proof: We need to check that the equations (3.26) are satisfied. It holds

$$\begin{aligned}
&\frac{\partial L_d}{\partial q_0}(q_0, q_1) + f_{C_d}^{-}(q_0, q_1, u_0) \\
&= h \sum_{i=1}^{s} b_i \left[\frac{\partial L}{\partial q} \cdot \frac{\partial Q_i}{\partial q_0} + \frac{\partial L}{\partial \dot{q}} \cdot \frac{\partial \dot{Q}_i}{\partial q_0} \right] + h \sum_{i=1}^{s} b_i f_{LC} \cdot \frac{\partial Q_i}{\partial q_0} \\
&= h \sum_{i=1}^{s} b_i \left[\left(\dot{P}_i - f_{LC} \right) \cdot \frac{\partial Q_i}{\partial q_0} + P_i \cdot \frac{\partial \dot{Q}_i}{\partial q_0} + f_{LC} \cdot \frac{\partial Q_i}{\partial q_0} \right] \\
&= h \sum_{i=1}^{s} b_i \left[\dot{P}_i \cdot \frac{\partial Q_i}{\partial q_0} + P_i \cdot \frac{\partial \dot{Q}_i}{\partial q_0} \right],
\end{aligned}$$

using the definitions for P_i and $\dot{P}_i$ in (4.31). Differentiating the definition for Q_i in (4.31b) with respect to q_0 and substituting the resultant expression and the definition of P_i in (4.31b) gives

$$\begin{aligned}
&\frac{\partial L_d}{\partial q_0}(q_0, q_1) + f_{C_d}^{-}(q_0, q_1, u_0) \\
&= h \sum_{i=1}^{s} b_i \left[\dot{P}_i \cdot \left(I + h \sum_{j=1}^{s} a_{ij} \frac{\partial \dot{Q}_j}{\partial q_0} \right) + \left(p_0 + h \sum_{j=1}^{s} \tilde{a}_{ij} \dot{P}_j \right) \cdot \frac{\partial \dot{Q}_i}{\partial q_0} \right] \\
&= h \sum_{i=1}^{s} b_i \left[\dot{P}_i + p_0 \cdot \frac{\partial \dot{Q}_i}{\partial q_0} \right] + h^2 \sum_{i=1}^{s} \sum_{j=1}^{s} (b_i \tilde{a}_{ij} + b_j a_{ij}) \dot{P}_j \cdot \frac{\partial \dot{Q}_i}{\partial q_0},
\end{aligned}$$

and with the symplecticity identities (4.32) we obtain

$$\begin{aligned}
&\frac{\partial L_d}{\partial q_0}(q_0, q_1) + f^-_{C_d}(q_0, q_1, u_0) \\
&\quad = \quad p_0 \cdot \left[h \sum_{i=1}^{s} b_i \frac{\partial \dot{Q}_i}{\partial q_0} \right] + h \sum_{i=1}^{s} b_i \dot{P}_i + h \sum_{j=1}^{s} b_j \dot{P}_j \left[h \sum_{i=1}^{s} b_i \frac{\partial \dot{Q}_i}{\partial q_0} \right] \\
&\quad = \quad -p_0,
\end{aligned}$$

where we have differentiated the expression for q_1 in (4.31a) with respect to q_0 to obtain the identity

$$h \sum_{i=1}^{s} b_i \frac{\partial \dot{Q}_i}{\partial q_0} = -I.$$

This establishes the satisfaction of (3.26a). Analogously, we can show that (3.26b) holds, and therefore the discrete Hamiltonian map $\tilde{F}L_d$ generated by the discrete Lagrangian (4.33) together with the discrete forces (4.34) is indeed the symplectic partitioned Runge-Kutta method for the forced Hamiltonian system (3.18). □

Optimal control and Runge-Kutta discretizations

In this section, we carry forward the results of the previous section into the context of optimal control problems. To formulate the optimal control problem for the discrete system in terms of Runge-Kutta discretizations, we have to give appropriate expressions for the boundary conditions, the path constraints, and the objective functional.

Concerning the dynamics of the mechanical system, we have already seen that the discretization obtained via the discrete Lagrange-d'Alembert principle can be rewritten as a Runge-Kutta scheme for the corresponding mechanical system in terms of (p, q) as in (4.31). Since we consider regular Lagrangians and regular Hamiltonians, we reformulate (4.31c) with the help of the Hamiltonian as

$$\begin{aligned}
\dot{Q}_{ki} &= \frac{\partial H}{\partial p}(Q_{ki}, P_{ki}), \\
\dot{P}_{ki} &= -\frac{\partial H}{\partial q}(Q_{ki}, P_{ki}) + f_{HC}(Q_{ki}, P_{ki}, U_{ki}),
\end{aligned}$$

where the additional index k denotes the dependence of the intermediate state and control variables on the time interval $[t_k, t_{k+1}]$.

Boundary conditions Due to a formulation of the optimal control problem within the Hamiltonian framework, we use the same formulation for the boundary constraint as the one for the continuous Hamiltonian optimal control problem 4.1.3 evaluated at (q_N, p_N), which reads

$$\tilde{r}(q_N, p_N, q^T, p^T) = 0.$$

Discrete path constraints Again we use the formulation of the Hamiltonian optimal control problem 4.1.3 and enforce the path constraints to hold in each time step (Q_i, P_i, U_i) as

$$\tilde{h}(Q_{ki}, P_{ki}, U_{ki}) \geq 0, \quad k = 0, \ldots, N-1, \quad i = 1, \ldots, s.$$

Discrete objective function We construct the discrete objective function in the same way as the discrete Lagrangian (4.33). However, corresponding to the Hamiltonian formulation evaluated in each substep (Q_i, P_i, U_i), it now reads

$$J_d(q_d, p_d, u_d) = \sum_{k=0}^{N-1} h \sum_{i=1}^{s} b_i \tilde{C}(Q_{ki}, P_{ki}, U_{ki}) + \tilde{\Phi}(q_N, p_N),$$

where the final constraint holds for the node corresponding to the final time T.

Combining all terms, the discrete optimal control problem from the Hamiltonian point of view reads

$$\min_{q_d, p_d, u_d} J(q_d, p_d, u_d) = \sum_{k=0}^{N-1} h \sum_{i=1}^{s} b_i \tilde{C}(Q_{ki}, P_{ki}, U_{ki}) + \tilde{\Phi}(q_N, p_N) \tag{4.35a}$$

subject to

$$q_{k+1} = q_k + h \sum_{j=1}^{s} b_j \dot{Q}_{kj}, \quad Q_{ki} = q_k + h \sum_{j=1}^{s} a_{ij} \dot{Q}_{kj}, \quad q_0 = q^0, \tag{4.35b}$$

$$p_{k+1} = p_k + h \sum_{j=1}^{s} \tilde{b}_j \dot{P}_{kj}, \quad P_{ki} = p_k + h \sum_{j=1}^{s} \tilde{a}_{ij} \dot{P}_{kj}, \quad p_0 = p^0, \tag{4.35c}$$

$$\dot{Q}_{ki} = \frac{\partial H}{\partial p}(Q_{ki}, P_{ki}), \quad \dot{P}_{ki} = -\frac{\partial H}{\partial q}(Q_{ki}, P_{ki}) + f_{HC}(Q_{ki}, P_{ki}, U_{ki}), \tag{4.35d}$$

$$0 \leq \tilde{h}(Q_{ki}, P_{ki}, U_{ki}), \quad k = 0, \ldots, N-1, \ i = 1, \ldots, s, \tag{4.35e}$$

$$0 = \tilde{r}(q_N, p_N, q^T, p^T). \tag{4.35f}$$

Problem (4.35) is the finite dimensional optimization problem resulting from the Hamiltonian optimal control problem 4.1.3 that is discretized via a symplectic partitioned Runge-Kutta scheme.

Equivalence With $Q_{ki} = q_d(t_k + c_i h; q_k^\nu, h)$ and $\dot{Q}_{ki} = \dot{q}_d(t_k + c_i h; q_k^\nu, h)$ and since with (4.31c) $(Q_{ki}, P_{ki}) = \mathbb{F}L(Q_{ki}, \dot{Q}_{ki})$ holds the equivalence of problem (4.30) and problem (4.35) can be shown: each discrete optimal control problem derived via the discrete Lagrange-d'Alembert principle (4.30) can be reformulated as an optimal control problem derived via a Runge-Kutta discretization for the Hamiltonian dynamics (4.35). In particular, according to Theorem 4.4.2, for a given discrete Lagrangian (4.26) and discrete forces defined in (4.29) we always find a symplectic partitioned Runge-Kutta map describing the discrete Hamiltonian mechanical system. On the other hand, for each symplectic partitioned Runge-Kutta map there exist a discrete Lagrangian and discrete forces generating this map. Additionally, with the results of Section 4.1.2, the feasible sets of the intermediate points $(Q_{ki}, \dot{Q}_{ki})$ and (Q_{ki}, P_{ki}) defined by the boundary conditions and path constraints in tangent and cotangent space, respectively, are equal under the Legendre transform.

Mayer formulation Similar as for the discrete Lagrangian optimal control problem, (4.35) can be transformed into an optimal control problem of Mayer type as follows: Analogous to Section 4.2.2, we introduce extra variables $y_d = \{y_l\}_{l=0}^N$ as

$$\begin{aligned} y_0 &= 0, \\ y_l &= \sum_{k=0}^{l-1} h \sum_{i=1}^{s} b_i \tilde{C}(Q_{ki}, P_{ki}, U_{ki}), \quad l = 1, \dots, N, \end{aligned}$$

yielding the discrete optimal control problem of Mayer type as

$$\min_{q_d, p_d, u_d, y_d} \bar{\Phi}(q_N, p_N, y_N) = y_N + \tilde{\Phi}(q_N, p_N) \tag{4.36a}$$

subject to

$$q_{k+1} = q_k + h \sum_{j=1}^{s} b_j \dot{Q}_{kj}, \quad Q_{ki} = q_k + h \sum_{j=1}^{s} a_{ij} \dot{Q}_{kj}, \quad q_0 = q^0, \tag{4.36b}$$

$$p_{k+1} = p_k + h \sum_{j=1}^{s} \tilde{b}_j \dot{P}_{kj}, \quad P_{ki} = p_k + h \sum_{j=1}^{s} \tilde{a}_{ij} \dot{P}_{kj}, \quad p_0 = p^0, \tag{4.36c}$$

$$y_{k+1} = y_k + h \sum_{i=1}^{s} b_i \tilde{C}(Q_{ki}, P_{ki}, U_{ki}), \quad y_0 = 0, \tag{4.36d}$$

$$\dot{Q}_i = \frac{\partial H}{\partial p}(Q_{ki}, P_{ki}), \quad \dot{P}_{ki} = -\frac{\partial H}{\partial q}(Q_{ki}, P_{ki}) + f_{HC}(Q_{ki}, P_{ki}, U_{ki}), \tag{4.36e}$$

$$0 \leq \tilde{h}(Q_{ki}, P_{ki}, U_{ki}), \quad k = 0, \ldots, N-1, \quad i = 1, \ldots, s, \tag{4.36f}$$

$$0 = \tilde{r}(q_N, p_N, q^T, p^T). \tag{4.36g}$$

We obtain exactly the same problem by discretizing the continuous Hamiltonian optimal control problem of Mayer type (as introduced in Section 4.1.3) with the same partitioned Runge-Kutta discretization for the extended system of differential equations

$$\dot{\tilde{q}}(t) = \nu(\tilde{q}(t), \tilde{p}(t), u(t)), \quad \tilde{q}(0) = \tilde{q}^0,$$
$$\dot{\tilde{p}}(t) = \eta(\tilde{q}(t), \tilde{p}(t), u(t)), \quad \tilde{p}(0) = \tilde{p}^0,$$

with $\tilde{q} = (q, y)$, $\tilde{p} = p$, $\nu(\tilde{q}(t), \tilde{p}(t), u(t)) = (\nabla_p H(q(t), p(t)), \tilde{C}(q(t), p(t), u(t)))$, $\eta(\tilde{q}(t), \tilde{p}(t), u(t)) = -\nabla_p H(q(t), p(t)) + f_{HC}(q(t), p(t), u(t))$, $\tilde{q}^0 = (q^0, 0)$ and $\tilde{p}^0 = p^0$.

Examples 4.4.3 (a) With $b = 1$ and $a = \frac{1}{2}$ we obtain the implicit midpoint rule as a symplectic Runge-Kutta scheme, that is the partitioned scheme reduces to a standard one-stage Runge-Kutta scheme. The resulting discretization is equivalent to the discretization derived via the Lagrangian approach with midpoint quadrature as introduced in Example 4.4.1(a).

(b) The standard Lobatto IIIA-IIIB partitioned Runge-Kutta method is obtained by using the Lobatto quadrature for the discrete Lagrangian as explained in Example 4.4.1(b).

Remark 4.4.4 The formulations of the discrete optimal control problem on the one hand based on the discrete Lagrange-d'Alembert principle and on the other hand based on a Runge-Kutta discretization of the Hamiltonian dynamics are equivalent, in the sense that the same discrete solution set is described. Note however, that the Lagrangian formulation needs less discrete variables and less constraints for the optimization problem, as it is formulated on the configuration space only, rather than on the space consisting of configurations and momenta: For $q \in \mathbb{R}^n$ and N intervals of discretization we obtain with the Lagrangian approach $(Ns+1)n$ unknown configurations q_k^ν, $k = 0, \ldots, N-1$, $\nu = 0, \ldots, s$ with $q_k^s = q_{k+1}^0$, $k = 1, \ldots, N-1$ and $nN(s-1) + n(N-1)$ extended discrete Euler-Lagrange equations, so altogether, $(Ns-1)n$ constraints for the optimization problem excluding boundary conditions. The Runge-Kutta approach for the Hamiltonian system yields $2(Ns+1)n$ unknown configurations and momenta and $2nN + 2nN(s-1) = 2nNs$ equality constraints. Thus, via the Runge-Kutta

approach we obtain twice as many state variables and $(Ns+1)n$ more equality constraints such that the resulting optimization problem is numerically more expensive. Comparisons concerning the computational effort are presented in Section 5.2.2.

4.5 Adjoint system

The adjoint system provides necessary optimality conditions for the optimal control problem. In the continuous case the adjoint system is derived by the Pontryagin maximum principle. The KKT equations provide the adjoint system for the discrete optimal control problem. In this section we derive a transformed adjoint system of the discrete optimal control problem. This adjoint system is then compared to the continuous one and we determine the corresponding order of approximation.

All derivations are based on an analysis by Hager. In [53] he derives a transformed adjoint system using standard Runge-Kutta discretizations of the optimal control problem. He identifies constraints on the Runge-Kutta coefficients to determine the order of approximation of the adjoint scheme. In this way, the resulting optimality system, after some change of variables, is a partitioned Runge-Kutta scheme and Hager computes the order conditions for order up to 4. In [23] Bonnans et al. extend this approach to the order conditions for order up to 7.

By using the same strategy as Hager in [53], we show, that the DMOC discretization leads to a discretization of the same order for the adjoint system as for the state system. Therefore no additional order conditions on the coefficients determining the corresponding discretization scheme are necessary.

In the following we ignore path and control constraints and restrict ourselves to the case of unconstrained optimal control problems.

4.5.1 Continuous setting

First of all, instead of considering the Lagrangian optimal control problem 4.1.1, we analyze the Hamiltonian optimal control problem that is formulated in an equivalent way. For simplicity, we restrict ourselves to the case without final constraint and without path constraints.

Problem 4.5.1

$$\min_{q,p,u} \Phi(q(T), p(T)) \tag{4.37a}$$

subject to

$$\dot{q}(t) = \nu(q(t), p(t)), \quad \text{for all } t \in [0, T], \tag{4.37b}$$
$$\dot{p}(t) = \eta(q(t), p(t), u(t)), \quad \text{for all } t \in [0, T], \tag{4.37c}$$
$$q(0) = q^0,\ p(0) = p^0, \tag{4.37d}$$
$$u(t) \in U,\ q, p \in W^{1,\infty},\ u \in L^\infty, \tag{4.37e}$$

with $\nu : \mathbb{R}^n \times \mathbb{R}^n \to \mathbb{R}^n, \nu(q(t), p(t)) = \nabla_p H(q(t), p(t))$, $\eta : \mathbb{R}^n \times \mathbb{R}^n \times \mathbb{R}^m \to \mathbb{R}^n, \eta(q(t), p(t), u(t)) = -\nabla_q H(q(t), p(t)) + f_{HC}(q(t), p(t), u(t))$ and $U \subset \mathbb{R}^m$ is closed and convex. Since we want to neglect constraints on the control function, we assume $U = \mathbb{R}^m$ for the following analysis.

$W^{m,p}(\mathbb{R}^n)$ is the Sobolev space consisting of vector-valued measurable functions $q : [0, T] \to \mathbb{R}^n$ whose j-th derivative lies in L^p for all $0 \leq j \leq m$ with the norm

$$\|q\|_{W^{m,p}} = \sum_{j=0}^{m} \|q^{(j)}\|_{L^p}.$$

$B_a(x)$ is the closed ball centered at x with radius a.

Remark 4.5.2 In the case of objective functionals of Bolza type, we transform the optimal control problem into the Mayer form and consider an extended system $\dot{\tilde{q}}(t) = \tilde{\nu}(\tilde{q}(t), p(t), u(t))$ with $\tilde{q} = (q, y)$ and $\tilde{\nu} : \mathbb{R}^n \times \mathbb{R}^n \times \mathbb{R}^m \to \mathbb{R}^{n+1}$, $\tilde{\nu}(\tilde{q}(t), p(t), u(t)) = (\nabla_p H(q(t), p(t)), \tilde{C}(q(t), p(t), u(t)))$. However, within this section we restrict ourselves to the formulation of Problem 4.5.1, having in mind, that a Bolza problem can be analyzed in a straightforward way.

For brevity, we introduce the notation $x(t) = (q(t), p(t))$, $x^0 = (q^0, p^0)$ and define

$$\tilde{f}(x(t), u(t)) = \begin{pmatrix} \nu(q(t), p(t)) \\ \eta(q(t), p(t), u(t)) \end{pmatrix}, \quad \Phi(x(T)) = \Phi(q(T), p(T)),$$

such that (4.37b) - (4.37d) reads as

$$\dot{x}(t) = \tilde{f}(x(t), u(t)) \quad \text{for all } t \in [0, T], \quad x(0) = x^0.$$

In the following we will need both kinds of notation.

Along the lines of [53], we now present the assumptions that are employed in the analysis of DMOC discretizations of Problem 4.5.1. First, a smoothness assumptions is required to ensure regularity of the solution and the problem functions. Second, we enforce a growth condition that allows for having a unique solution for the control function of the optimal control problem.

Assumption 4.5.3 (Smoothness) For some integer $\kappa \geq 2$, Problem 4.5.1 has a local solution (x^*, u^*) which lies in $W^{\kappa,\infty} \times W^{\kappa-1,\infty}$. There exists an open set $\Omega \subset \mathbb{R}^{2n} \times \mathbb{R}^m$ and $\rho > 0$ such that $B_\rho(x^*(t), u^*(t)) \subset \Omega$ for every $t \in [0, T]$. The first κ derivatives of ν and η are Lipschitz continuous in Ω, and the first κ derivatives of Φ are Lipschitz continuous in $B_\rho(x^*(T))$.

Under this assumption there exits an associated Lagrange multiplier $\psi^* = (\psi^{q,*}, \psi^{p,*}) \in W^{\kappa,\infty}$ for which the following form of the first-order optimality conditions derived via the Pontryagin maximum principle is satisfied at (x^*, ψ^*, u^*):

$$\dot{q}(t) = \nu(q(t), p(t)) \quad \text{for all } t \in [0, T], \quad q(0) = q^0, \tag{4.38a}$$
$$\dot{p}(t) = \eta(q(t), p(t), u(t)) \quad \text{for all } t \in [0, T], \quad p(0) = p^0, \tag{4.38b}$$
$$\dot{\psi}^q(t) = -\nabla_q \mathcal{H}(q(t), p(t), \psi^q(t), \psi^p(t), u(t)) \quad \text{for all } t \in [0, T], \tag{4.38c}$$
$$\psi^q(T) = \nabla_q \Phi(q(T), p(T)), \tag{4.38d}$$
$$\dot{\psi}^p(t) = -\nabla_p \mathcal{H}(q(t), p(t), \psi^q(t), \psi^p(t), u(t)) \quad \text{for all } t \in [0, T], \tag{4.38e}$$
$$\psi^p(T) = \nabla_p \Phi(q(T), p(T)), \tag{4.38f}$$
$$u(t) \in U, \ \nabla_u \mathcal{H}(q(t), p(t), \psi^q(t), \psi^p(t), u(t)) = 0 \text{ for all } t \in [0, T], \tag{4.38g}$$

with $\mathcal{H}$ the Hamiltonian defined by

$$\mathcal{H}(q(t), p(t), \psi^q(t), \psi^p(t), u(t)) = \psi^q \nu(q, p) + \psi^p \eta(q, p, u), \tag{4.39}$$

where ψ^q and ψ^p are row vectors in $\mathbb{R}^n$. For brevity, we define

$$\mathcal{H}(x(t), \psi(t), u(t)) := \psi \tilde{f}(x, u), \tag{4.40}$$

such that (4.38c) - (4.38f) reads as

$$\dot{\psi}(t) = -\nabla_x \mathcal{H}(x(t), \psi(t), u(t)) \quad \text{for all } t \in [0, T],$$
$$\psi(T) = \nabla_x \Phi(x(T)).$$

To formulate the second-order sufficient optimality conditions along the lines of [53], we define the following matrices:

$$A(t) = \nabla_x \tilde{f}(x^*(t), u^*(t)), \ B(t) = \nabla_u \tilde{f}(x^*(t), u^*(t)), \ V = \nabla^2 \Phi(x^*(T)),$$
$$P(t) = \nabla_{xx} \mathcal{H}(x^*(t), \psi^*(t), u^*(t)), \ R(t) = \nabla_{uu} \mathcal{H}(x^*(t), \psi^*(t), u^*(t)),$$
$$S(t) = \nabla_{xu} \mathcal{H}(x^*(t), \psi^*(t), u^*(t)).$$

Let $\mathcal{B}$ be the quadratic form defined by

$$\mathcal{B}(x, u) = \frac{1}{2} \left(x(T)^T V x(T) + \langle x, Px \rangle + \langle u, Ru \rangle + 2\langle x, Su \rangle \right),$$

where $\langle \cdot, \cdot \rangle$ denotes the usual L^2 inner product.

Assumption 4.5.4 (Coercivity) There exists a constant $\alpha > 0$ such that

$$\mathcal{B}(x,u) \geq \alpha \|u\|_{L_2}^2 \text{ for all } (x,u) \in \mathcal{M},$$

where

$$\mathcal{M} = \{(x,u) \,:\, x \in W^{1,2}, u \in L^2, \dot{x} = Ax + Bu,$$
$$x(0) = 0,\ u(t) \in \mathbb{R}^m \text{ a. e. } t \in [0,T]\}.$$

Coercivity is a strong form of a second-order sufficient optimality condition in the sense that it implies not only strict local optimality, but also Lipschitzian dependence of the solution and multipliers on parameters (see for example [38]).

By coercivity and smoothness the *control uniqueness property* holds (as shown in [40] and [52]). That means the Hamiltonian has a locally unique minimizer in the control, such that there exists a locally unique solution denoted by $u(x,\psi)$ depending Lipschitz continuously on x and ψ.

In the case where the control is uniquely determined by (x,ψ) through minimization of the Hamiltonian, let $\phi = (\phi^q, \phi^p)$ denote the function defined by

$$\phi^q(q,p,\psi^q,\psi^p) = -\nabla_q \mathcal{H}(q,p,u,\psi^q,\psi^p)|_{u=u(q,p,\psi^q,\psi^p)},$$
$$\phi^p(q,p,\psi^q,\psi^p) = -\nabla_p \mathcal{H}(q,p,u,\psi^q,\psi^p)|_{u=u(q,p,\psi^q,\psi^p)}.$$

Additionally, let $\eta(q,p,\psi^q,\psi^p)$ denote the function $\eta(q,p,u(\psi^q,\psi^p))$. By substituting in (4.38) the control obtained by solving (4.38g) for $u(t)$ in terms of $(x(t),\psi(t))$, we obtain the following two-point boundary-value problem:

$$\dot{q}(t) = \nu(q(t),p(t)), \quad q(0) = q^0, \tag{4.41a}$$
$$\dot{p}(t) = \eta(q(t),p(t),\psi^q(t),\psi^p(t)), \quad p(0) = p^0, \tag{4.41b}$$
$$\dot{\psi}^q(t) = \phi^q(q(t),p(t),\psi^q(t),\psi^p(t)), \quad \psi^q(T) = \nabla_q \Phi(q(T),p(T)), \tag{4.41c}$$
$$\dot{\psi}^p(t) = \phi^p(q(t),p(t),\psi^q(t),\psi^p(t)), \quad \psi^p(T) = \nabla_p \Phi(q(T),p(T)), \tag{4.41d}$$

or, equivalently,

$$\dot{x}(t) = \tilde{f}(x(t),\psi(t)), \quad x(0) = x^0,$$
$$\dot{\psi}(t) = \phi(x(t),\psi(t)), \quad \psi(T) = \nabla_x \Phi(x(T)).$$

4.5.2 Discrete setting

In Section 4.4.3 it has been shown that the discretization of the mechanical system obtained by using the discrete Lagrange d'Alembert principle is equivalent to a discretization obtained by using a s-stage symplectic partitioned Runge-Kutta time-stepping scheme, that is

$$
\begin{aligned}
q'_k &= \sum_{i=1}^{s} b_i \dot{Q}_{ki}, \quad q_0 = q^0, \\
Q_{ki} &= q_k + h \sum_{j=1}^{s} a^q_{ij} \dot{Q}_{kj}, \\
p'_k &= \sum_{i=1}^{s} b_i \dot{P}_{ki}, \quad p_0 = p^0, \\
P_{ki} &= p_k + h \sum_{j=1}^{s} a^p_{ij} \dot{P}_{kj},
\end{aligned}
$$

$1 \leq i \leq s$, $0 \leq k \leq N-1$, with $b_i a^p_{ij} + b_j a^q_{ji} = b_i b_j$ to ensure the symplecticity of the Runge-Kutta scheme. Prime denotes, in this discrete context, the forward divided differences:

$$
q'_k = \frac{q_{k+1} - q_k}{h}.
$$

Q_{kj}, $\dot{Q}_{kj}$, P_{kj} and $\dot{P}_{kj}$ are the intermediate state variables on the interval $[t_k, t_{k+1}]$. With

$$
\begin{aligned}
\dot{Q}_{ki} &= \nabla_p H(Q_{ki}, P_{ki}), \\
\dot{P}_{ki} &= -\nabla_q H(Q_{ki}, P_{ki}) + f_{HC}(Q_{ki}, P_{ki}, U_{ki}),
\end{aligned}
$$

where U_{ki} are the intermediate control variables on $[t_k, t_{k+1}]$, we can reformulate the discrete Lagrangian optimal control problem 4.2.2 and obtain an equivalent problem formulation as follows:

$$
\min_{q_d, p_d, u_d} C(q_N, p_N) \tag{4.43a}
$$

subject to

$$
q'_k = \sum_{i=1}^{s} b_i \nu(Q_{ki}, P_{ki}), \quad q_0 = q^0, \tag{4.43b}
$$

$$
Q_{ki} = q_k + h \sum_{j=1}^{s} a^q_{ij} \nu(Q_{kj}, P_{kj}), \tag{4.43c}
$$

$$
p'_k = \sum_{i=1}^{s} b_i \eta(Q_{ki}, P_{ki}, U_{ki}), \quad p_0 = p^0, \tag{4.43d}
$$

$$
P_{ki} = p_k + h \sum_{j=1}^{s} a^p_{ij} \eta(Q_{kj}, P_{kj}, U_{kj}), \tag{4.43e}
$$

$$
1 \leq i \leq s, \quad 0 \leq k \leq N-1.
$$

For small enough h, and for $x_k = (q_k, p_k)$ near $x^*(t_k) = (q^*(t_k), p^*(t_k))$ and U_{kj}, $1 \leq j \leq s$, near $u^*(t_k)$, the intermediate variables Q_{ki} and P_{ki} in (4.43c) and (4.43e) are uniquely determined. This follows from smoothness and the implicit function theorem as for standard Runge-Kutta discretization as stated in [53] (see for example [46]).

Let $\nu^h : \mathbb{R}^{2n} \times \mathbb{R}^{sm} \to \mathbb{R}^n$, $\eta^h : \mathbb{R}^{2n} \times \mathbb{R}^{sm} \to \mathbb{R}^n$ and $\tilde{f}^h : \mathbb{R}^{2n} \times \mathbb{R}^{sm} \to \mathbb{R}^{2n}$ be defined by

$$\begin{aligned}
\nu^h(q,p,u) &= \sum_{i=1}^{s} b_i \nu(Q_i(q,p,u), P_i(q,p,u)), \\
\eta^h(q,p,u) &= \sum_{i=1}^{s} b_i \eta(Q_i(q,p,u), P_i(q,p,u), U_i) \quad \text{and} \\
\tilde{f}^h(x,u) &= \begin{pmatrix} \nu^h(q,p,u) \\ \eta^h(q,p,u) \end{pmatrix}.
\end{aligned}$$

In other words,

$$\begin{aligned}
\nu^h(q,p,u) &= \sum_{i=1}^{s} b_i \nu(Q_i, P_i), \\
\eta^h(q,p,u) &= \sum_{i=1}^{s} b_i \eta(Q_i, P_i, U_i),
\end{aligned}$$

where $y = (Q, P)$ is the solution of (4.43c) and (4.43e) given by the state uniqueness property and $u = (U_1, U_2, \ldots, U_s) \in \mathbb{R}^{sm}$. The corresponding discrete Hamiltonian $H^h : \mathbb{R}^{2n} \times \mathbb{R}^{2n} \times \mathbb{R}^{sm} \to \mathbb{R}$ is defined to be

$$\mathcal{H}^h(p, q, \psi^q, \psi^p, u) = \psi^q \nu^h(q,p,u) + \psi^p \eta^h(q,p,u).$$

For brevity, we also use the notation

$$\mathcal{H}^h(x, \psi, u) = \psi \tilde{f}^h(q,p,u).$$

We consider the following version of the first-order necessary optimality conditions associated with (4.43) (Karush-Kuhn-Tucker conditions):

$$q_k' = \nu^h(q_k, p_k, u_k), \quad q_0 = q^0, \tag{4.44a}$$

$$p_k' = \eta^h(q_k, p_k, u_k), \quad p_0 = p^0, \tag{4.44b}$$

$$(\psi_k^q)' = -\nabla_q \mathcal{H}^h(q_k, p_k, \psi_{k+1}^q, \psi_{k+1}^p, u_k), \quad \psi_N^q = \nabla_q \Phi(q_N, p_N), \tag{4.44c}$$

$$(\psi_k^p)' = -\nabla_p \mathcal{H}^h(q_k, p_k, \psi_{k+1}^q, \psi_{k+1}^p, u_k), \quad \psi_N^p = \nabla_p \Phi(q_N, p_N), \tag{4.44d}$$

$$U_{ki} \in U, \quad \nabla_{U_i} \mathcal{H}^h(q_k, p_k, \psi_{k+1}^q, \psi_{k+1}^p, u_k) = 0, \quad 1 \leq i \leq s, \tag{4.44e}$$

where $\psi_k^q, \psi_k^p \in \mathbb{R}^n$, $0 \leq k \leq N-1$. Here, $u_k \in \mathbb{R}^{ms}$ is the entire discrete control vector at time level k:

$$u_k = (U_{k1}, U_{k2}, \ldots, U_{ks}) \in \mathbb{R}^{ms}.$$

For $\psi_k = (\psi_k^q, \psi_k^p) \in \mathbb{R}^{2n}$, (4.44) reads

$$x_k' = \tilde{f}^h(x_k, u_k), \quad x_0 = x^0, \tag{4.45a}$$
$$\psi_k' = -\nabla_x \mathcal{H}^h(x_k, \psi_{k+1}, u_k), \quad \psi_N = \nabla\Phi(x_N), \tag{4.45b}$$
$$U_{ki} \in U, \quad \nabla_{U_i} \mathcal{H}^h(x_k, \psi_{k+1}, u_k) = 0, \quad 1 \leq i \leq s. \tag{4.45c}$$

4.5.3 The transformed adjoint system

To rewrite the first order conditions (4.44) in a way that is better suited for the analysis and computation, we now use the same strategy as Hager in [53]. We just describe the essential steps in this section. A detailed explanation of the transformation steps is presented in Appendix B. In contrast to Hager's formulation, we already start with a partitioned Runge-Kutta scheme for the state equations. However, we can use the same transformation as in [53] applied to the scheme for both state variables q and p, respectively, leading to two symplectic partitioned Runge-Kutta schemes for two state-costate equations. Due to the symplecticity of the discretization, we obtain altogether one extended symplectic partitioned scheme for the state-adjoint system. This scheme is of the same order as the state scheme that discretizes the Hamiltonian system.

To reformulate the adjoint system, Hager's and therefore our transformation strategy can be summarized as follows: First of all we introduce multipliers for the intermediate equations (4.43c) and (4.43e) in addition to the multipliers for equations (4.43b) and (4.43d) and formulate the corresponding KKT equations. After some transformation and change of variables (see Appendix B) we obtain

$$\psi_k^q = \psi_{k+1}^q + h \sum_{i=1}^{s} b_i \left(\chi_{ki}^q \nabla_q \nu(Q_{ki}, P_{ki}) + \chi_{ki}^p \nabla_q \eta(Q_{ki}, P_{ki}, U_{ki}) \right),$$

$$\psi_N^q = \nabla_q \Phi(q_N, p_N), \tag{4.46a}$$

$$\psi_k^p = \psi_{k+1}^p + h \sum_{i=1}^{s} b_i \left(\chi_{ki}^q \nabla_p \nu(Q_{ki}, P_{ki}) + \chi_{ki}^p \nabla_p \eta(Q_{ki}, P_{ki}, U_{ki}) \right),$$

$$\psi_N^p = \nabla_p \Phi(q_N, p_N), \tag{4.46b}$$

$$\chi_{ki}^q = \psi_{k+1}^q + h \sum_{j=1}^{s} \frac{b_j a_{ji}^q}{b_i} \left(\chi_{kj}^q \nabla_q \nu(Q_{kj}, P_{kj}) + \chi_{kj}^p \nabla_q \eta(Q_{kj}, P_{kj}, U_{kj}) \right), \tag{4.46c}$$

$$\chi_{ki}^p = \psi_{k+1}^p + h \sum_{j=1}^{s} \frac{b_j a_{ji}^p}{b_i} \left(\chi_{kj}^q \nabla_p \nu(Q_{kj}, P_{kj}) + \chi_{kj}^p \nabla_p \eta(Q_{kj}, P_{kj}, U_{kj}) \right), \tag{4.46d}$$

$$U_{ki} \in U, \quad -\chi_{ki}^p \nabla_u \eta(Q_{ki}, P_{ki}, U_{ki}) = 0, \tag{4.46e}$$

$1 \leq i \leq s$ and $0 \leq k \leq N-1$.

The conditions (4.46a) - (4.46d) are in essence a partitioned Runge-Kutta scheme applied to the continuous adjoint equations (4.38c) - (4.38f).

Along the lines of [53] it holds, that the transformed first-order system (4.46) (for h sufficiently small and $(x_k, U_{kj}) \in B_\beta(x^*(t_k), u^*(t_k))$ for each j and k) and the Karush-Kuhn-Tucker equations (4.44) are equivalent if $b_j > 0$ for each j (see Appendix B). So far, the costate equations (4.46a) - (4.46d) march backwards in time. Therefore, we reverse the order of time. Furthermore, we apply again the control uniqueness property to get rid of the control variables from the state multiplier equations. The transformed adjoint system now reads as

$$q_{k+1} = q_k + h \sum_{i=1}^{s} b_i \nu(Q_{ki}, P_{ki}), \quad q_0 = q^0, \tag{4.47a}$$

$$p_{k+1} = p_k + h \sum_{i=1}^{s} b_i \eta(Q_{ki}, P_{ki}, \chi_{ki}^q, \chi_{ki}^p), \quad p_0 = p^0, \tag{4.47b}$$

$$\psi_{k+1}^q = \psi_k^q + h \sum_{i=1}^{s} b_i \phi^q(Q_{ki}, P_{ki}, \chi_{ki}^q, \chi_{ki}^p), \quad \psi_N^q = \nabla_q \Phi(q_N, p_N), \tag{4.47c}$$

$$\psi_{k+1}^p = \psi_k^p + h \sum_{i=1}^{s} b_i \phi^p(Q_{ki}, P_{ki}, \chi_{ki}^q, \chi_{ki}^p), \quad \psi_N^p = \nabla_p \Phi(q_N, p_N), \tag{4.47d}$$

$$Q_{ki} = q_k + h \sum_{j=1}^{s} a_{ij}^q \nu(Q_{kj}, P_{kj}), \tag{4.47e}$$

$$P_{ki} = p_k + h \sum_{j=1}^{s} a_{ij}^p \eta(Q_{kj}, P_{kj}, \chi_{kj}^q, \chi_{kj}^p), \tag{4.47f}$$

$$\chi_{ki}^q = \psi_k^q + h \sum_{j=1}^{s} \bar{a}_{ij}^q \phi^q(Q_{kj}, P_{kj}, \chi_{kj}^q, \chi_{kj}^p), \tag{4.47g}$$

$$\chi_{ki}^p = \psi_k^p + h \sum_{j=1}^{s} \bar{a}_{ij}^p \phi^p(Q_{kj}, P_{kj}, \chi_{kj}^q, \chi_{kj}^p), \tag{4.47h}$$

$$\bar{a}_{ij}^q = \frac{b_i b_j - b_j a_{ji}^q}{b_i}, \quad \bar{a}_{ij}^p = \frac{b_i b_j - b_j a_{ji}^p}{b_i}. \tag{4.47i}$$

Since $u(x, \psi)$ depends Lipschitz continuously on x near $x^*(t)$ and ψ near $\psi^*(t)$ for any $t \in [0, T]$, we have, analogous to the state uniqueness property, uniquely determined intermediate costates, such that there exists a locally unique solution $(Q_{ki}, P_{ki}, \chi_{ki}^q, \chi_{ki}^p)$, $1 \leq i \leq s$ of (4.47e) - (4.47h).

The scheme (4.47) can be viewed as a discretization of the two-point boundary-value problem (4.41). To ensure a desired order of approximation for this two-point boundary-value problem, Hager derives in [53] constraints on the coefficients of the Runge-Kutta scheme via Taylor expansion. However, in case of the DMOC discretizations, we obtain the following result concerning the order of consistency.

Theorem 4.5.5 (Order of consistency) *If the symplectic partitioned Runge-Kutta discretization of the state system is of order κ and $b_i > 0$ for each i, then the scheme for the adjoint system is again a symplectic partitioned Runge-Kutta scheme of the same order (in particular we obtain the same schemes for (q, p) and (ψ^p, ψ^q)).*

Proof: With the symplecticity condition $a_{ij}^p = \frac{b_i b_j - b_j a_{ji}^q}{b_i}$ it holds

$$\bar{a}_{ij}^q = a_{ij}^p,$$
$$\bar{a}_{ij}^p = a_{ij}^q.$$

□

With Theorem 4.3.3 and 4.4.2 it follows immediately:

Lemma 4.5.6 *Let a Lagrangian optimal control problem with regular Lagrangian L and Lagrangian control force f_{LC} be given. If the discrete Lagrangian L_d (4.33) and the discrete control force $f_{C_d}^{\pm}$ (4.34) with $b_i > 0$ for each i are both of order κ, then the corresponding adjoint scheme is also of order κ.*

Remark 4.5.7 From the equations (4.47) we see that the discretization of the dynamics by a Runge-Kutta map always leads to a symplectic partitioned Runge-Kutta scheme for the state-adjoint system. In general, a direct solution method can be viewed as taking discrete variations of the objective functional that is augmented by the system's differential equation of motion. This procedure yields a variational integration of the neccessary optimality conditions. This makes the resulting scheme symplectic. Direct and indirect methods are therefore linked by the symplectic integration of the state-adjoint system as illustrated in Figure 4.3.

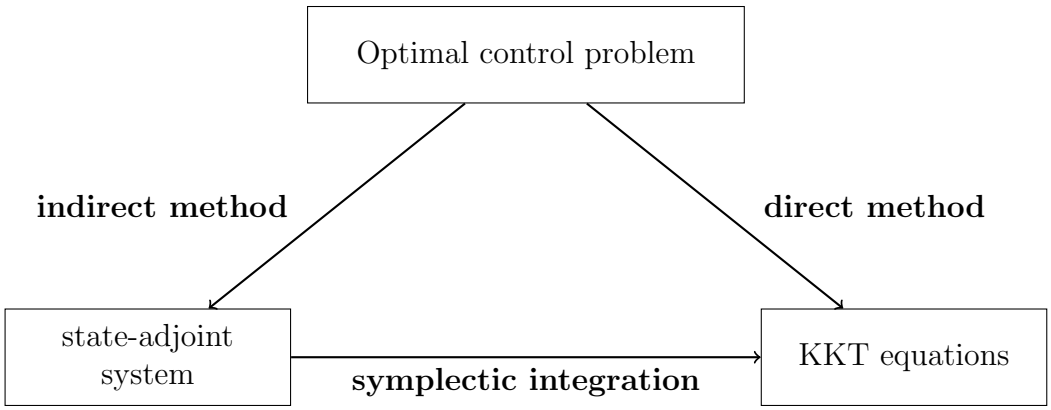

Figure 4.3: Correspondence of indirect and direct methods in optimal control theory.

4.6 Convergence

In this chapter we show convergence of DMOC, that is solutions of the discrete optimal control problem (4.9a) - (4.9d) converge to solutions of the Lagrangian optimal control problem (4.3a) - (4.3c). For example, approximating the optimal control problem by a discrete Lagrangian and discrete forces of second order we show that if the functions defining the control problem are smooth enough and a coercivity condition holds, the error in the discrete approximation is $\mathcal{O}(h)$ if the optimal control is Lipschitz continuous, $o(h)$ if the derivative of the optimal control is Riemann integrable, and $\mathcal{O}(h^2)$ if the derivative of the optimal control has bounded variation.

In recent years, it has become clear that standard convergence theorems frequently employed in the analysis of differential equations are not applicable to discretizations of optimal control problems. For example, Hager [53] has shown

that Runge-Kutta methods converging in a purely differential equation setting can diverge in an optimal control setting. On the other hand Betts et al. [13] demonstrate that Runge-Kutta methods that do not converge for the simulation of differential equations can converge if applied to optimal control problems.

Therefore, during the last years, convergence of optimal control problems has been investigated for a variety of different transcription methods and modifications. Schwartz and Polak [137] consider a nonlinear optimal control problem with control and endpoint constraints and analyze consistency of explicit Runge-Kutta approximations. Convergence is proved for the global solution of the discrete problem to the global solution of the continuous problem. Malanowski, Büskens and Maurer [107] analyze Euler discretizations of a nonlinear problem with mixed control and state constraints. Reddien [131] discusses collocation at Gauss points and derives convergence rates for unconstrained optimal control problems, assuming positive definiteness of the Hamiltonian for all points (functions) in a bounded neighborhood of the true solution. Kameswaran and Biegler [70] present convergence results along with an adjoint estimation procedure for direct transcription of unconstrained optimal control problems using collocation at Radau points. In [71] they prove convergence and convergence rates in the presence of final-time equality constraints.

As in Section 4.5, we restrict ourselves to the case without path and control constraints and without final point constraint. Our convergence statement is based on that of Hager in [41] and [53], who proved convergence for standard Runge-Kutta discretizations. Therefore, in this section, we give only a brief summary the proof strategy. In Appendix C a more detailed explanation of the single steps is presented.

The proof strategy is as follows: First, the necessary optimality conditions for the continuous and the discrete optimal control problem are derived. Secondly, we have to show convergence of solutions of the resulting discrete scheme to solutions of the corresponding boundary value problem. Preparatory work for this step was already done in the previous section. There we derived the adjoint system and determined the order of consistency. A standard strategy to show convergence of a discrete scheme is to prove consistency and stability. This is abstractly stated within a result by Hager (see for example [39]), which Hager's and our convergence proof are based on:

Proposition 4.6.1 *Let $\mathcal{X}$ be a Banach space and let $\mathcal{Y}$ be a linear normed space with the norm in both spaces denoted by $\|\cdot\|$. Let $\mathcal{F} : \mathcal{X} \mapsto 2^{\mathcal{Y}}$ be a set-valued map, let $\mathcal{L} : \mathcal{X} \mapsto \mathcal{Y}$ be a bounded, linear operator, and let $\mathcal{T} : \mathcal{X} \mapsto \mathcal{Y}$ with $\mathcal{T}$ continuously Frechét differentiable in $B_r(w^*)$ for some $w^* \in \mathcal{X}$ and $r > 0$. Suppose that the following conditions hold for some $\delta \in \mathcal{Y}$ and scalars ϵ, λ and $\sigma > 0$:*

(P1) $\mathcal{T}(w^*) + \delta \in \mathcal{F}(w^*)$.

(P2) $\|\nabla\mathcal{T}(w) - \mathcal{L}\| \leq \epsilon$ *for all* $w \in B_r(w^*)$.

(P3) The map $(\mathcal{F} - \mathcal{L})^{-1}$ *is single-valued and Lipschitz continuous in* $B_\sigma(\pi), \pi = (\mathcal{T} - \mathcal{L})(w^*)$, *with Lipschitz constant* λ.

If $\epsilon\lambda < 1$, $\epsilon r \leq \sigma$, *and* $\|\delta\| \leq (1 - \lambda\epsilon)r/\lambda$, *then there exists a unique* $w \in B_r(w^*)$ *such that* $\mathcal{T}(w) \in \mathcal{F}(w)$. *Moreover, we have the estimate*

$$\|w - w^*\| \leq \frac{\lambda}{1 - \lambda\epsilon}\|\delta\|. \tag{4.48}$$

Proof: See for example [54]. □

Proposition 4.6.1 says roughly

Consistency + Stability ⇒ Convergence,

where consistency corresponds to assumption (P1) and the bounds on the norm of δ, stability corresponds to assumption (P3) and the bound on the Lipschitz constant λ for the linearization, and convergence is stated in (4.48).

The main result is formulated in terms of the averaged modulus of smoothness of the optimal control (see [53]). If $J \subset \mathbb{R}$ is an interval and $v : J \to \mathbb{R}^n$, let $\omega(v, J; t, h)$ denote the modulus of continuity:

$$\omega(v, J; t, h) = \sup\{|v(s_1) - v(s_2)| \ : \ s_1, s_2 \in [t - h/2, t + h/2] \cap J\}. \tag{4.49}$$

The averaged modulus of smoothness τ of v over $[0, T]$ is the integral of the modulus of continuity:

$$\tau(v; h) = \int_0^T \omega(v, [0, T]; t, h)\, \mathrm{d}t.$$

It is shown in [139] that $\lim_{h\to\infty} \tau(v; h) = 0$ if and only if v is Riemann integrable, and $\tau(v; h) \leq ch$ with constant c if v has bounded variation. Our main result based on the convergence theorem in [53] (Theorem 2.1) is stated below in the context of unconstrained Lagrangian optimal control problems.

Theorem 4.6.2 (Convergence) *If smoothness and coercivity hold, the discrete Lagrangian* L_d *(4.33) and the discrete control force* $f_{Cd}^{\pm}$ *(4.34) are of order* κ *with* $b_i > 0$ *for each* i, *and* $U = \mathbb{R}^m$, *then for all sufficiently small* h, *there exists a strict local minimizer* (x^h, u^h) *of the discrete optimal control problem (4.9a) -*

(4.9d) and an associated adjoint variable ψ^h satisfying (4.45a) and (4.45b) such that

$$\begin{aligned}\max_{0\le k\le N} \left|x_k^h - x^*(t_k)\right| + \left|\psi_k^h - \psi^*(t_k)\right| + \left|u(x_k^h,\psi_k^h) - u^*(t_k)\right| \\ \le c h^{\kappa-1}\left(h + \tau\left(\tfrac{d^{\kappa-1}}{dt^{\kappa-1}}u^*; h\right)\right),\end{aligned} \tag{4.50}$$

where $u(x_k^h,\psi_k^h)$ is a local minimizer of the Hamiltonian (4.40) corresponding to $x = x_k$ and $\psi = \psi_k$. Furthermore, $(x^*(t), u^*(t)) = (q^*(t), p^*(t), u^*(t))$ is the optimal solution of the Lagrangian optimal control problem (4.3a) - (4.3c).

Remark 4.6.3 Note that the estimate for the error in the discrete control in (4.50) is expressed in terms of $u(x_k^h,\psi_k^h)$ not u_k. This is due to the fact, that we derive the estimate via the transformed adjoint system with removed control due to the control uniqueness property. In [41] the estimate is proved in terms of u_k for Runge-Kutta discretization of second order.

Proof of Theorem 4.6.2 With Theorem 4.3.3 and 4.4.2 we know that a discrete Langrangian and discrete forces both of order κ lead to a symplectic partitioned Runge-Kutta discretization of order κ for the optimal control system. Because of smoothness and coercivity we can build up a discrete adjoint scheme for the optimal control problem with eliminated control that approximates the continuous adjoint scheme with order κ (see Lemma 4.5.6). This leads in Hager's notation to a *Runge-Kutta scheme of order κ for optimal control*, and therefore Hager's convergence result for standard Runge-Kutta schemes in [53] (Theorem 2.1) is directly applicable (see Appendix C). □

Remark 4.6.4 Theorem 4.6.2 can be extended to optimal control problems with constraints on the control function $u(t)$ as it was done in [53] for Runge-Kutta discretizations of order 2.

Chapter 5

Implementation, applications and extension

In this chapter, we first explain in Section 5.1 how to implement DMOC efficiently using existing routines for the optimization and differentiation of the problem. Additionally, we demonstrate the capability of DMOC to solve optimal control problems resulting from real applications. In Section 5.2 we start with simple systems to numerically verify the preservation and convergence properties of DMOC. We demonstrate the benefits of using DMOC compared to other standard methods for the solution of optimal control problems. In Sections 5.3 and 5.4 we consider more challenging problems from trajectory planning and multibody systems. Here, we use a variety of different formulations for the objective functionals, the boundary conditions, and the path constraints. In Section 5.5 we present an application from space mission design to introduce a spatial decentralized approach to the solution of the corresponding optimal control problem.

5.1 Implementation

As a balance between accuracy and efficiency we employ the midpoint rule for approximating the relevant integrals for the example computations in the following section, that is we set

$$C_d(q_k, q_{k+1}, u_k) = hC\left(\frac{q_{k+1}+q_k}{2}, \frac{q_{k+1}-q_k}{h}, u_{k+1/2}\right),$$

$$L_d(q_k, q_{k+1}) = hL\left(\frac{q_{k+1}+q_k}{2}, \frac{q_{k+1}-q_k}{h}\right),$$

$k = 0, \ldots, N-1$, as well as

$$\int_{kh}^{(k+1)h} f_{LC}(q(t), \dot{q}(t), u(t)) \cdot \delta q(t)\, \mathrm{d}t \approx$$
$$h f_{LC}\left(\frac{q_{k+1}+q_k}{2}, \frac{q_{k+1}-q_k}{h}, u_{k+1/2}\right) \cdot \frac{\delta q_{k+1}+\delta q_k}{2} =$$
$$\frac{h}{2} f_{LC}\left(\frac{q_{k+1}+q_k}{2}, \frac{q_{k+1}-q_k}{h}, u_{k+1/2}\right) \cdot \delta q_k$$
$$+\frac{h}{2} f_{LC}\left(\frac{q_{k+1}+q_k}{2}, \frac{q_{k+1}-q_k}{h}, u_{k+1/2}\right) \cdot \delta q_{k+1}.$$

Here, $f_k^- = f_k^+ = \frac{h}{2} f_{LC}\left(\frac{q_{k+1}+q_k}{2}, \frac{q_{k+1}-q_k}{h}, u_{k+1/2}\right)$ are used as the left and right discrete forces with $q_k = q(t_k)$ and $u_{k+1/2} = u\left(\frac{t_k+t_{k+1}}{2}\right)$.

SQP Method We solve the resulting finite dimensional constrained optimization problem by a standard SQP method (see Section 2.3.2) as implemented for example in the routine `fmincon` of MATLAB. For more complex problems with higher dimensions we use the routine `nag_opt_nlp_sparse` of the NAG library[1]. SQP is a local optimization method. That means if the problem has more than one local optimum, different guesses for initializing the algorithm can lead to different optimal solutions. This can be observed for almost all our example computations.

Automatic Differentiation To compute an optimal solution of the optimization problem the SQP method makes use of the first and second derivatives of the constraints and the objective function. In the case where no derivatives are provided, the used algorithms approximate those by finite differences. This approximation is time-consuming and round-off errors in the discretization process occur leading to worse convergence behavior of the algorithm.

To avoid these drawbacks we make use of the concept of *Automatic Differentiation (AD)* (see [51, 130, 160] for a basic introduction), a method to numerically evaluate the derivative of a function specified by a computer program. AD exploits the fact that any computer program that implements a vector function $y = F(x)$ (generally) can be decomposed into a sequence of elementary assignments, any one of which may be trivially differentiated by a simple table lookup. These elemental partial derivatives, evaluated at a particular argument, are combined in accordance with the chain rule from differential calculus to yield information on the derivative of F (such as gradients, tangents, and the Jacobian matrix).

[1] `www.nag.com`

This process yields (to numerical accuracy) exact derivatives. Because symbolic transformations occur only at the most basic level, AD avoids the computational problems inherent to complex symbolic computation.

In particular, for some of our optimal control problems, we implemented the package ADOL-C (**A**utomatic **D**ifferentiation by **O**ver**L**oading in **C**++, [157]) that has been written primarily for the evaluation of gradient vectors (rows or columns of Jacobians). It turns out that the optimization process performs in a faster and more robust way when providing the derivatives by automatic differentiation rather than via finite differences.

5.2 Comparison to existing methods

In this section, we apply DMOC and other standard methods to the solution of two optimal control problems: the low thrust orbital transfer and the optimal control of a two-link manipulator. In this way, we compare different numerical properties and results indicating the quality of performance of the different algorithms.

5.2.1 Low thrust orbital transfer

In this application we investigate the problem of optimally transferring a satellite with a continuously acting propulsion system from one circular orbit around the Earth to another one.

Consider a satellite with mass m which moves in the gravitational field of the Earth (mass M). The satellite is to be transferred from one circular orbit to one in the same plane with a larger radius, while the number of revolutions around the Earth during the transfer process is fixed. In 2d-polar coordinates $q = (r, \varphi)$, the Lagrangian of the system has the form

$$L(q, \dot{q}) = \frac{1}{2} m(\dot{r}^2 + r^2 \dot{\varphi}^2) + \gamma \frac{Mm}{r},$$

where γ denotes the gravitational constant. Assume that the propulsion system continuously exhibits a force u in the direction of motion of the satellite, such that the corresponding Lagrangian control force is given by

$$f_{LC} = \begin{pmatrix} 0 \\ r\,u \end{pmatrix}.$$

Boundary conditions Assume further that the satellite initially moves on a circular orbit of radius r^0. Let $(r(0), \varphi(0)) = (r^0, 0)$ be its position at $t = 0$, then

its initial velocity is given by $\dot{r}(0) = 0$ and $\dot{\varphi}(0) = \sqrt{\gamma M/(r^0)^3}$. Using its thruster, the satellite is required to reach the point $(r^T, 0)$ at time $T = d(T^0 + T^T)/2$ and, without any further control input, to continue to move on the circle with radius r^T. Here, d is a prescribed number of revolutions around the Earth and T^0 and T^T are the orbital periods of the initial and the final circle, respectively. Thus, the boundary values at $t = T$ are given by $(r(T), \varphi(T)) = (r^T, 0)$ and $(\dot{r}(T), \dot{\varphi}(T)) = (0, \sqrt{\gamma M/(r^T)^3})$.

Objective functional During this transfer, our goal is to minimize the control effort, correspondingly the objective functional is given by

$$J(q, \dot{q}, u) = \int_0^T u(t)^2 \, \mathrm{d}t.$$

Results The computations are performed with the following parameter values:

$$\begin{gathered} m = 100, \ M = 6 \cdot 10^{24}, \\ \gamma = 6.673 \cdot 10^{-26}, \ r^0 = 5, \ r^T = 6, \\ T^0 = 2\pi\sqrt{(r^0)^3/(\gamma M)}, \ T^T = 2\pi\sqrt{(r^T)^3/(\gamma M)}. \end{gathered}$$

We compare DMOC to a simple finite difference approach, where the dynamical constraints are discretized by applying a one-step method to the associated ordinary differential equations of the system (the forced Euler-Lagrange equations). For demonstration purposes, the forward Euler scheme is used, in which case the constraints read

$$x_{k+1} - x_k - h\, F(x_k, u_k) = 0, \quad k = 0, \ldots, N-1,$$

(where $x_k = (q_k, \dot{q}_k)$ and F denotes the vector field of the forced Euler-Lagrange equations), as well as the midpoint rule, yielding the constraints

$$x_{k+1} - x_k - h\, F\left(\frac{x_{k+1} + x_k}{2}, \frac{u_{k+1} + u_k}{2}\right) = 0,$$

$k = 0, \ldots, N-1$.

We consider $d = 1$ and $d = 2$ revolutions around the Earth and solve the problem for various N. In Figure 5.1 the dependence of the resulting cost on N for all methods as well as for $d = 1$ (top) and $d = 2$ (bottom) is shown. It is intriguing to see that the cost is almost constant for the variational approach (DMOC), even for very large step sizes, whereas the cost of the Euler-based method seems to converge towards this "benchmark value" for larger N. The midpoint rule performs, as one might have expected, almost equally well as the

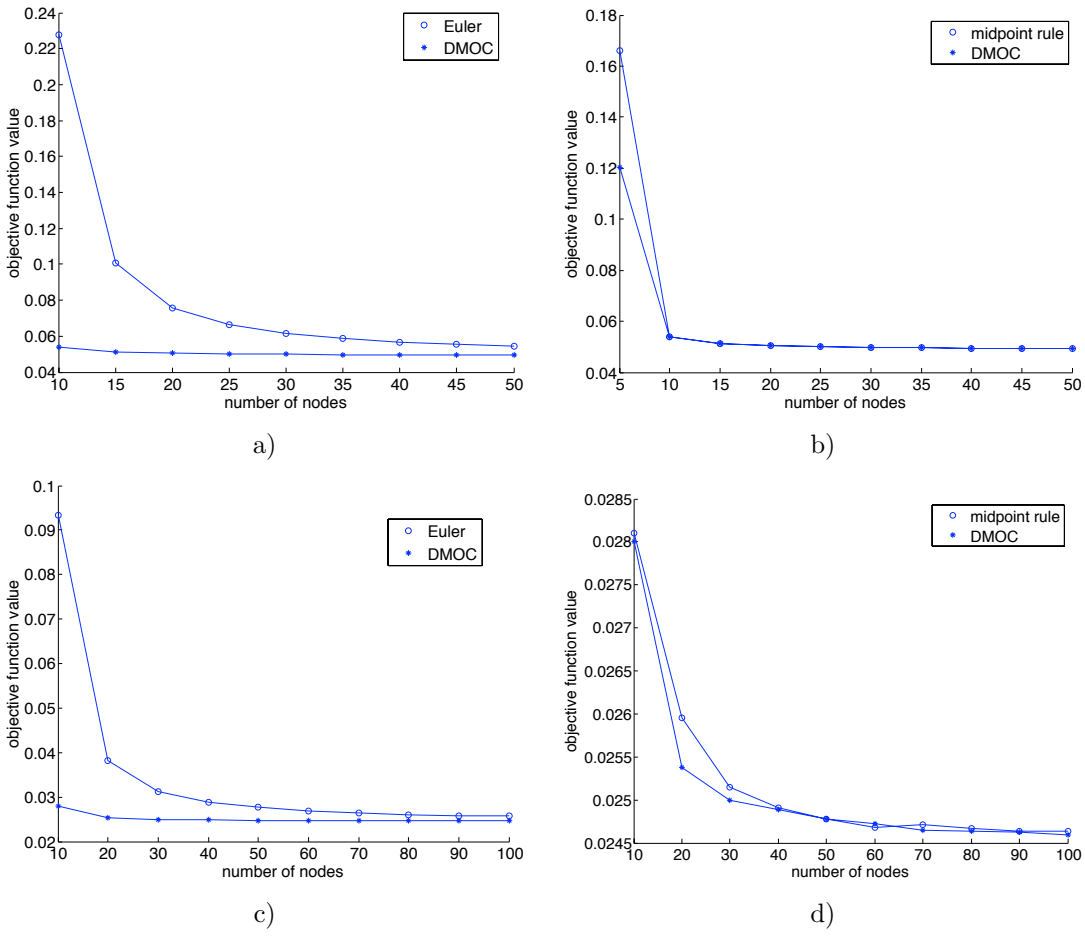

Figure 5.1: Variational approach (DMOC) vs. a finite difference based discretization (Euler's scheme and midpoint rule): approximated cost of the orbital transfer in dependence of the number N of discretization points for one [a) and b)] and two [c) and d)] revolutions around the Earth.

DMOC discretization. As a second numerical test we investigate how well the balance between the change in angular momentum and the amount of the control force is preserved. Due to the invariance of the Lagrangian under the rotation φ, the angular momentum of the satellite is preserved in the absence of external forces (as stated in Noether's theorem). However, in the presence of control forces, equation (3.19) gives a relation between the forces and the evolution of the angular momentum. In Figure 5.2, we compare the amount of the acting force with the change in angular momentum in each time interval. For the solution resulting from DMOC, the change in angular momentum equals exactly the sum of the applied control force (to numerical accuracy). The Euler scheme and the midpoint rule fail to capture the change in angular momentum accurately. These results are consistent with the well-known conservation properties of variational integrators. However, note that for the DMOC discretization, the resulting optimization problem is only half as large as for the finite difference schemes. As a third numerical test, we investigate how well the computed open loop control performs for "the real solution". To this end, the forced Euler-Lagrange equations are integrated using the classical fourth order Runge-Kutta scheme with very small constant step size $h = 10^{-3}$, where the computed control values are interpolated by a cubic spline. In Figure 5.3 the deviation of the resulting final state (at $t = T$) from the requested one is shown. Again, DMOC and the midpoint rule perform similar in the order of accuracy, as they are schemes of the same order. As accepted the Euler scheme lacks accuracy, especially for larger step sizes.

5.2.2 Two-link manipulator

As a second numerical example we consider the optimal control of a two-link manipulator. We compare solutions obtained by applying DMOC to those resulting from a collocation method of the same order. To this end, we apply the collocation method to the Hamiltonian system, expressed in the coordinates q and p and to the system formulated in state space with the coordinates q and $\dot{q}$, denoted by v.

Model The two-link manipulator (see Figure 5.4) consists of two coupled planar rigid bodies with mass m_i, length l_i and moment of inertia J_i, $i = 1, 2$, respectively. For $i \in 1, 2$, we let θ_i denote the orientation of the ith link measured counterclockwise from the positive horizontal axis. If we suppose one end of the first link to be fixed in an inertial reference frame, the configuration of the system is specified by $q = (\theta_1, \theta_2)$.

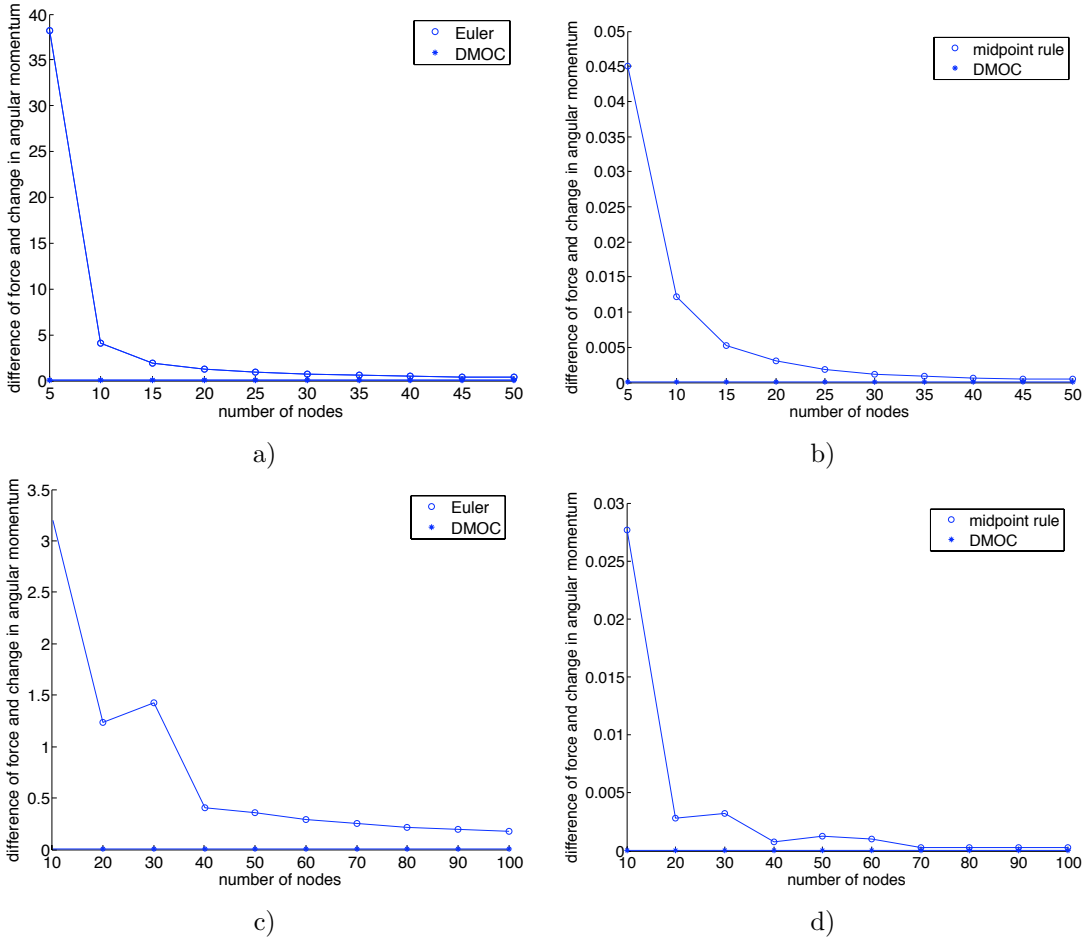

Figure 5.2: Variational approach (DMOC) vs. a finite difference based discretization (Euler's scheme and midpoint rule): difference of force and change in angular momentum of the orbital transfer in dependence on the number N of discretization points for one [a) and b)] and two [c) and d)] revolutions around the Earth.

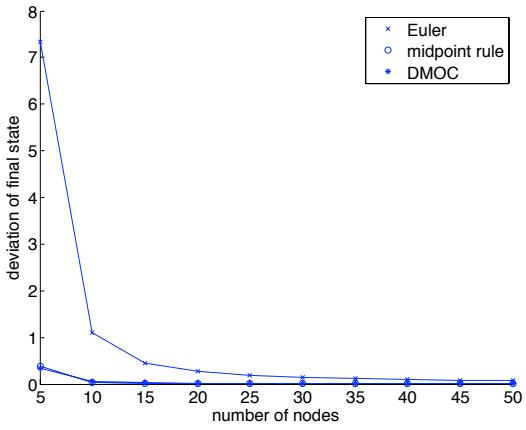

Figure 5.3: Comparison of the accuracy of the computed open loop control for DMOC, the Euler-based approach, and the midpoint rule: Deviation of the actual final state of the satellite from the requested one in dependence of the number of discretization points.

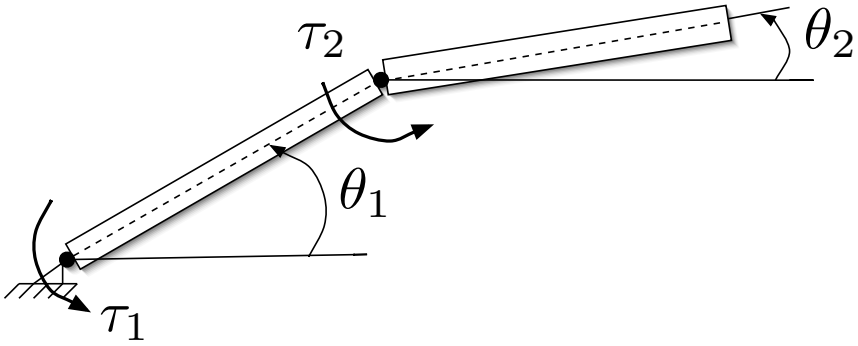

Figure 5.4: Model of a two-link manipulator.

The Lagrangian is given via the kinetic and potential energy

$$K(q,\dot{q}) = \frac{1}{8}(m_1 + 4m_2)l_1^2\dot{\theta}_1^2 + \frac{1}{8}m_2 l_2^2\dot{\theta}_2^2 + \frac{1}{2}m_2 l_1 l_2 \cos(\theta_1 - \theta_2)\dot{\theta}_1\dot{\theta}_2 + \frac{1}{2}J_1\dot{\theta}_1^2 + \frac{1}{2}J_2\dot{\theta}_2^2$$

and

$$V(q) = \frac{1}{2}m_1 g l_1 \sin\theta_1 + m_2 g l_1 \sin\theta_1 + \frac{1}{2}m_2 g l_2 \theta_2,$$

with the gravitational acceleration g. Control torques τ_1, τ_2 are applied at the base of the first link and at the joint between the two links. This leads to the Lagrangian control force

$$f_{LC}(\tau_1,\tau_2) = \begin{pmatrix} \tau_1 - \tau_2 \\ \tau_2 \end{pmatrix}.$$

Boundary conditions The two-link manipulator is to be steered from the stable equilibrium point $q^0 = (-\frac{\pi}{2}, -\frac{\pi}{2})$ with zero angular velocity $\dot{q}^0 = (0,0)$ to the instable equilibrium point $q^T = (\frac{\pi}{2}, \frac{\pi}{2})$ with velocity $\dot{q}^T = (0,0)$.

Objective functional For the motion of the manipulator the control effort is to be minimized as

$$J(\tau_1,\tau_2) = \int_0^T \frac{1}{2}(\tau_1^2(t) + \tau_2^2(t))\,\mathrm{d}t$$

with a final time $T = 1$.

Results As for the orbital transfer in Section 5.2.1 we solve the problem for various N. In Figure 5.5 the dependence on N of a) the resulting cost and b) the difference of the amount of force (including the control and the gravitational force) and the change in angular momentum for all methods is shown. The collocation method of order 2 corresponds to a discretization via the implicit midpoint rule. Thus, the optimization problem resulting from DMOC is equivalent to that obtained by applying collocation to the Hamiltonian formulation of the system as demonstrated in Example 4.4.3 a). Obviously, we obtain exactly equal solutions by applying both methods. The midpoint rule applied to the system formulated on tangent space performs, as one might have expected, equally well with respect to the objective value evolution depending on the step size. However, it does not reflect the momentum-force consistency as good as the other methods as shown in Figure 5.5. In Figure 5.6 the convergence rates are depicted.

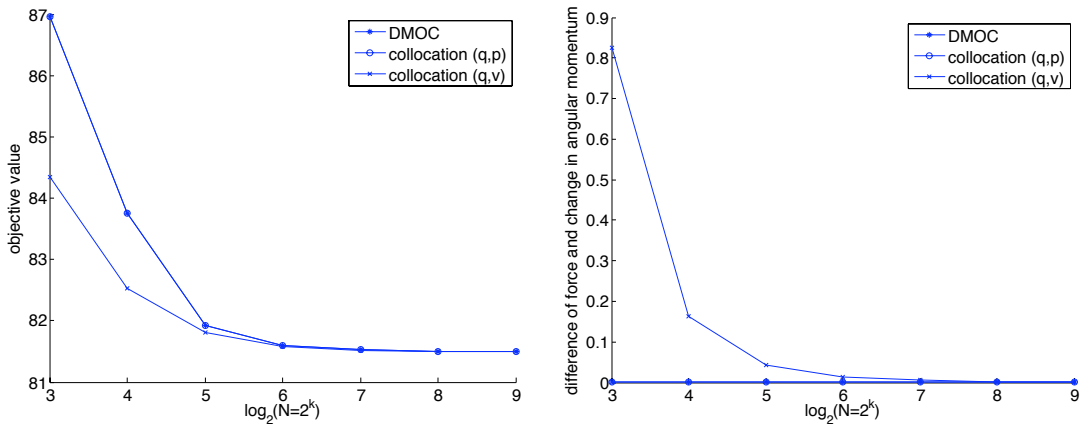

a) b)

Figure 5.5: Comparison of the accuracy of the computed open loop control for DMOC and a collocation approach: a) approximated cost b) difference of force and change in angular momentum in dependence on the number of discretization points.

Table 5.1: Comparison of CPU times in seconds

number of nodes	8	16	32	64	128	256	512
CPU time (DMOC)	0.02	0.05	0.1	0.18	0.71	4.26	45.22
CPU time (collocation (q,p))	0.03	0.08	0.22	0.82	2.64	7.69	67.71
CPU time (collocation (q,v))	0.04	0.18	0.24	2.01	2.31	16.34	89.29

Here, a reference trajectory is computed with $N = 512$ discretizations points and time step $h = 1.9 \cdot 10^{-3}$. The error in the configuration and control parameter of the discrete solution with respect to the reference solution is computed as $\max_{k=0,\dots,N} |q(t_k) - q_{\text{ref}}(t_k)|$ and $\max_{k=0,\dots,N} |u(t_k) - u_{\text{ref}}(t_k)|$, respectively, where $|\cdot|$ is the Euclidean norm. For all three methods the convergence rate for the configuration and control trajectory is $\mathcal{O}(h^2)$, as expected for a scheme of second order accuracy.

However, DMOC performs much faster than the collocation method (compare the CPU times in Table 5.1). This is due to the formulation on the discrete tangent space $Q \times Q$ that yields an optimization problem with less variables and less constraints as stated in Remark 4.4.4.

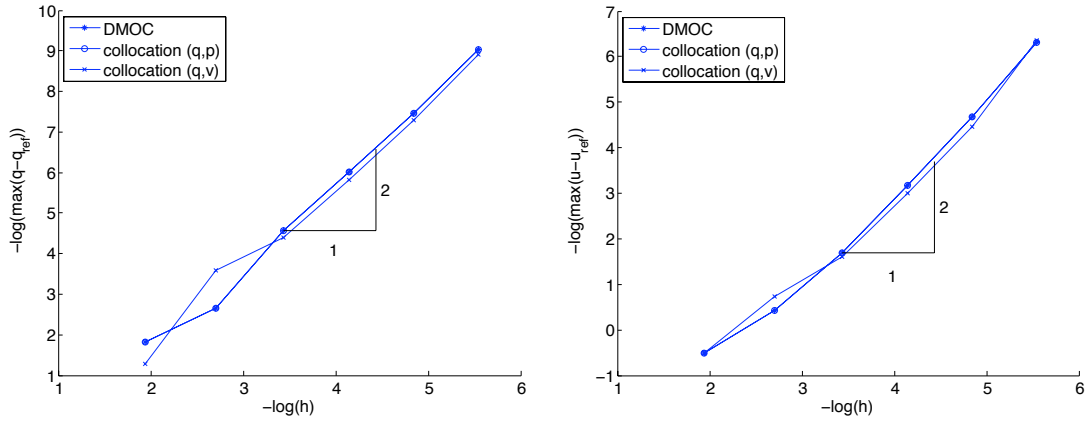

a) b)

Figure 5.6: Comparison of the convergence rates in dependence of the time step h for DMOC and a collocation approach. a) Error of configuration trajectory. b) Error of control trajectory.

5.3 Application: Trajectory planning

Trajectory planning represents a huge application area for optimal control theory. In this section, we apply DMOC to two typical problems from this field. We consider for both applications an additional specific feature concerning the problem formulation. Rather than fixing the final state via a final point constraint, we formulate a target manifold for a group of hovercraft that allows the system to adopt a final state with certain degrees of freedom. As a second example we consider the motion of a perfect underwater glider. Here, we treat the maneuver time (the final time of the movement) as an additional free variable that has to be optimized. In addition, we formulate an objective functional consisting of the weighted sum of two different objectives and investigate the problem in dependence on the weighting of both objectives.

5.3.1 A group of hovercraft

We consider a group of (identical) hovercraft which, starting from an arbitrary initial state, are required to attain a given final formation with minimal control effort. The final formation is defined by a set of equality constraints on the final configurations of the individual hovercraft and a fixed final velocity.

Model The configuration of a hovercraft is described by three degrees of freedom: its position $(x, y) \in \mathbb{R}^2$ and its orientation $\theta \in S^1$, that is, its configuration

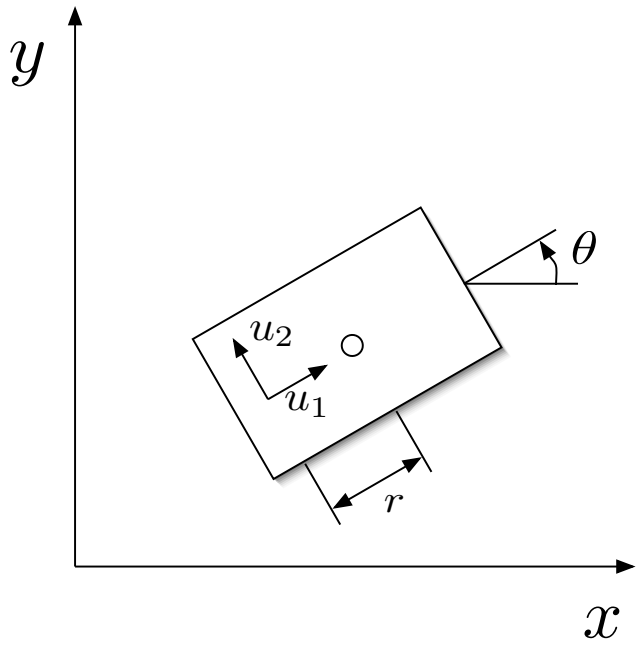

Figure 5.7: Hovercraft model.

manifold is $Q = \mathbb{R}^2 \times S^1$. It is actuated by a control force $u = (u_1, u_2)$, applied at a distance r from the center of mass (see Figure 5.7). The force u_1 acts in the direction of motion of the body, while u_2 acts orthogonally to it. The system is underactuated, but still configuration controllable [123], that means each point in configuration space can be reached by applying suitably chosen forces $u_1(t)$ and $u_2(t)$.

The Lagrangian of the system consists only of its kinetic energy,

$$L(q, \dot{q}) = \frac{1}{2}(m\dot{x}^2 + m\dot{y}^2 + J\dot{\theta}^2),$$

where $q = (x, y, \theta)$, m is the mass of the hovercraft and J its moment of inertia. The Lagrangian control forces acting in x-, y- and θ-direction resulting from u_1 and u_2 are

$$f_{LC}(\theta(t), u(t)) = \begin{pmatrix} \cos\theta(t)u_1(t) - \sin\theta(t)u_2(t) \\ \sin\theta(t)u_1(t) + \cos\theta(t)u_2(t) \\ -ru_2(t) \end{pmatrix}.$$

We denote by $q^i = (x^i, y^i, \theta^i)$ the configuration of the i-th hovercraft and by $u^i = (u_1^i, u_2^i)$ the corresponding forces.

Objective functional and boundary conditions The goal is to minimize the control effort while, at the same time, attaining the desired final formation. As a suitable objective functional for each hovercraft we choose a measure of the control effort

$$J(q^i, u^i) = \int_0^T \left(u_1^i(t)\right)^2 + \left(u_2^i(t)\right)^2 \, \mathrm{d}t, \tag{5.1}$$

while the objective functional for the entire group is given by the sum of these.

The final configuration of the group has certain degrees of freedom: In the case of three hovercraft the final formation has an overall rotational degree of freedom; it is determined by the following conditions:

(a) a fixed final orientation φ^i of each hovercraft:

$$\theta^i(T) = \varphi^i, \quad i = 1, 2, 3,$$

(b) equal distances d between the final positions:

$$(x^i(T) - x^j(T))^2 + (y^i(T) - y^j(T))^2 = d^2, \quad 1 \leq i, j \leq 3, i \neq j;$$

(c) the center $M = (M_x, M_y)$ of the formation is prescribed:

$$\begin{aligned} (x^1(T) + x^2(T) + x^3(T))/3 &= M_x, \\ (y^1(T) + y^2(T) + y^3(T))/3 &= M_y, \end{aligned}$$

(d) fixed final velocities:

$$\dot{x}^i = v_x^i, \ \dot{y}^i = v_y^i, \ \dot{\theta}^i = v_\theta^i, \quad i = 1, 2, 3,$$

where v_x^i, v_y^i and v_θ^i are given.

The boundary conditions for the case of a group of six hovercraft are determined analogously, that is, the craft are required to form a regular hexagon.

Results The group of three hovercraft starts from an initial configuration along a line, the group of six craft from a random initial configuration and with zero initial velocity for each craft, respectively. The group has to optimally arrange into an equilateral triangle, or into a hexagon, respectively. Using different initial guesses different orders of arrangement on the target manifold are adopted by the group. To obtain the solution with the lowest costs we perform several runs of the optimization with a variety of different initial guesses. In Figure 5.8 the configuration trajectories for a formation of three and six hovercraft, respectively, are illustrated. As the rotational and the translational motion is coupled via the influence of the control force u, the hovercraft have to perform on large curves to reach the desired final orientation φ^i.

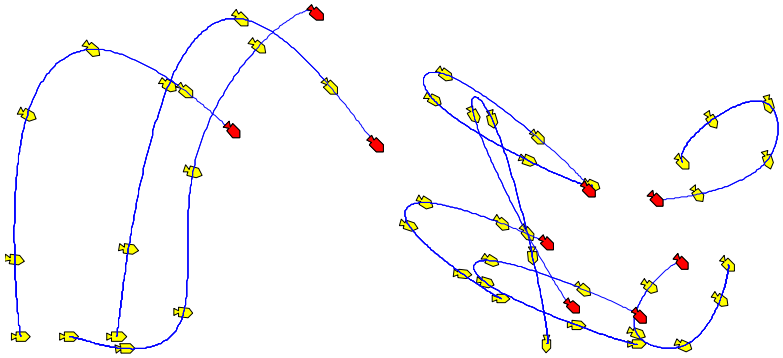

Figure 5.8: Left: Optimal rearrangement of a group of three hovercraft from an initial configuration along a line into an equilateral triangle. Right: Optimal rearrangement of a group of six hovercraft from a random initial configuration into a hexagon.

5.3.2 Perfect underwater glider

As an application with free final time we consider a class of Autonomous Underwater Vehicles (AUVs) known as gliders. AUVs are becoming increasingly popular for collecting scientific data in the ocean because they are low cost and highly sustainable (see for example [4, 45, 135]). However, it is desirable to minimize the amount of energy the gliders use for transport in order to keep the gliders autonomously operational for the greatest amount of time. Therefore, it is advantageous to make use of ocean currents to help propel the gliders around the ocean for sustainable missions (see for example [62]).

The problem considered here is to find an optimal trajectory of a glider that needs to move from one location to another within a prescribed current. Here, the glider is assumed to be actuated by a gyroscopic force which implies that the relative forward speed of the glider is constant. However, the orientation of the glider cannot change instantly and the control force induces the change in the orientation of the glider. In addition to the minimization of the amount of control effort, our goal is to identify trajectories that are also time-optimal, such that the glider needs as little time as possible to reach the final destination.

Dynamic model As in [161] the glider is modeled as a pointmass in $\mathbb{R}^2$ and actuated by a gyroscopic force acting orthogonal to the relative velocity between fluid and body given by

$$F_{gyr}(q(t), \dot{q}(t), u(t), t) = \begin{pmatrix} -mu(t)\left(\dot{y}(t) - V_y(t)\right) \\ mu(t)\left(\dot{x}(t) - V_x(t)\right) \end{pmatrix} \tag{5.2}$$

with the glider mass m, the configuration $q(t) = (x(t), y(t))$, the absolute glider velocity $\dot{q}(t) = (\dot{x}(t), \dot{y}(t))$, the current velocity field $V(t) = (V_x(t), V_y(t))$, and the control input $u(t) \in \mathbb{R}$ representing the change in the orientation.

By introducing $\dot{q}_{rel}(t) = (\dot{q}(t) - V(t))$ as relative velocity, the Lagrangian in the body fixed frame consists of the kinetic energy of the relative motion of the glider, therefore

$$L(q_{rel}(t), \dot{q}_{rel}(t)) = \frac{1}{2}\dot{q}_{rel}(t)' M \dot{q}_{rel}(t) \tag{5.3}$$

with constant Mass matrix $M = \begin{pmatrix} m & 0 \\ 0 & m \end{pmatrix}$ and $q_{rel}(t) = q(t)$. The corresponding gyroscopic force acting on the system is then given by

$$f_{LC}(q_{rel}(t), \dot{q}_{rel}(t), u(t)) = \begin{pmatrix} -mu(t)\,\dot{q}_{rel,y}(t) \\ mu(t)\,\dot{q}_{rel,x}(t) \end{pmatrix}.$$

The resulting Euler-Lagrange equations read as

$$\begin{aligned} \ddot{x}(t) &= -u(t)(\dot{y}(t) - V_y(t)) + \dot{V}_x(t), \\ \ddot{y}(t) &= u(t)(\dot{x}(t) - V_x(t)) + \dot{V}_y(t). \end{aligned}$$

Objective functional The perfect glider has to be steered within the time span $[0, T]$ with free final time T from an initial configuration $q(0) = q^0$ to a final one $q(T) = q^T$, optimally with respect to the objective function

$$J = w_1 \int_0^T \|f(q_{rel}(t), \dot{q}_{rel}(t), u(t))\|^2 \,\mathrm{d}t + w_2\, T.$$

So, the aim is to minimize the control effort and duration time at once by using a weighted objective function of both goals with weights $w_1 > 0$ and $w_2 > 0$. In the discrete setting we model the free final time by a variable step size h that acts as an additional optimization variable bounded as $0 < h \leq h_{max}$ to ensure positive step size and solutions of desired accuracy. For a fixed number of discretization points the final time is then given by $T = (N-1)h$.

Boundary conditions As initial constraint we assume a prescribed initial configuration $q_{rel}(0) = (10, 0)$ and an initial relative velocity as $\dot{q}_{rel}(0) = (-10, -10)$. The final configuration is given by $q_{rel}(T) = (15, 2)$, while the final relative velocity is free with same magnitude as the initial one, as the control force only influences the orientation, rather than the magnitude of the relative velocity.

Results For weights $w_1, w_2 \in (0,1)$ with $w_1 + w_2 = 1$ we compute the corresponding optimal solutions. As a first example, the current velocity of the fluid is assumed to be zero. In a second computation, we impose a current velocity with configuration dependent x- and zero y-component as $V = (x, 0)$. Figure 5.9 shows the trajectories of the configuration and the controls for both problems. For both cases the initial velocity is directed away from the destination. Therefore, for the case of zero fluid velocity, the gyroscopic control force enforces the glider performing a circular motion starting in direction of the initial velocity towards the destination as depicted in Figure 5.9. For increasing weight of the final time objective and decreasing weight of the control effort objective, the circular motion becomes smaller and the corresponding control parameter adopts higher values as shown in Figure 5.9 b). Concerning the behavior dependent on the weights, we observe the same behavior for nonzero fluid velocity (see Figure 5.9 c) and d)). However, due to the fluid velocity in x-direction, the gilder moves along different trajectories to reach the desired final location as depicted in Figure 5.9 c). Since the gyroscopic force is acting orthogonal to the relative velocity of the glider, that means the work resulting from the control force is zero, the energy of the system should be constant. Figure 5.10 shows that DMOC nicely captures the preservation of constant energy a) and zero work b). In Figure 5.10 c) the solutions for different weights are shown. As expected, the control effort increases for decreasing maneuver time. However, the fluid velocity under consideration does not help propel the glider towards the desired final location: For the same maneuver time the control effort for a glider moving in zero current velocity is lower compared to the solutions for a glider moving in a current with velocity $V = (x, 0)$.

5.4 Application: Optimal control of multi-body systems

In this section, we apply DMOC to simple multi-body systems. To this end, we use a formulation in generalized coordinates as opposed to the constrained formulation of a multi-body system introduced in Chapter 6.

5.4.1 The falling cat

A nice example to demonstrate the structure-preserving properties of DMOC is the falling cat that performs from an inverted orientation an overall rotation of π, landing back on its feet in an optimal way. For this the cat flips itself side up, even though its angular momentum is zero. It does this by changing its shape.

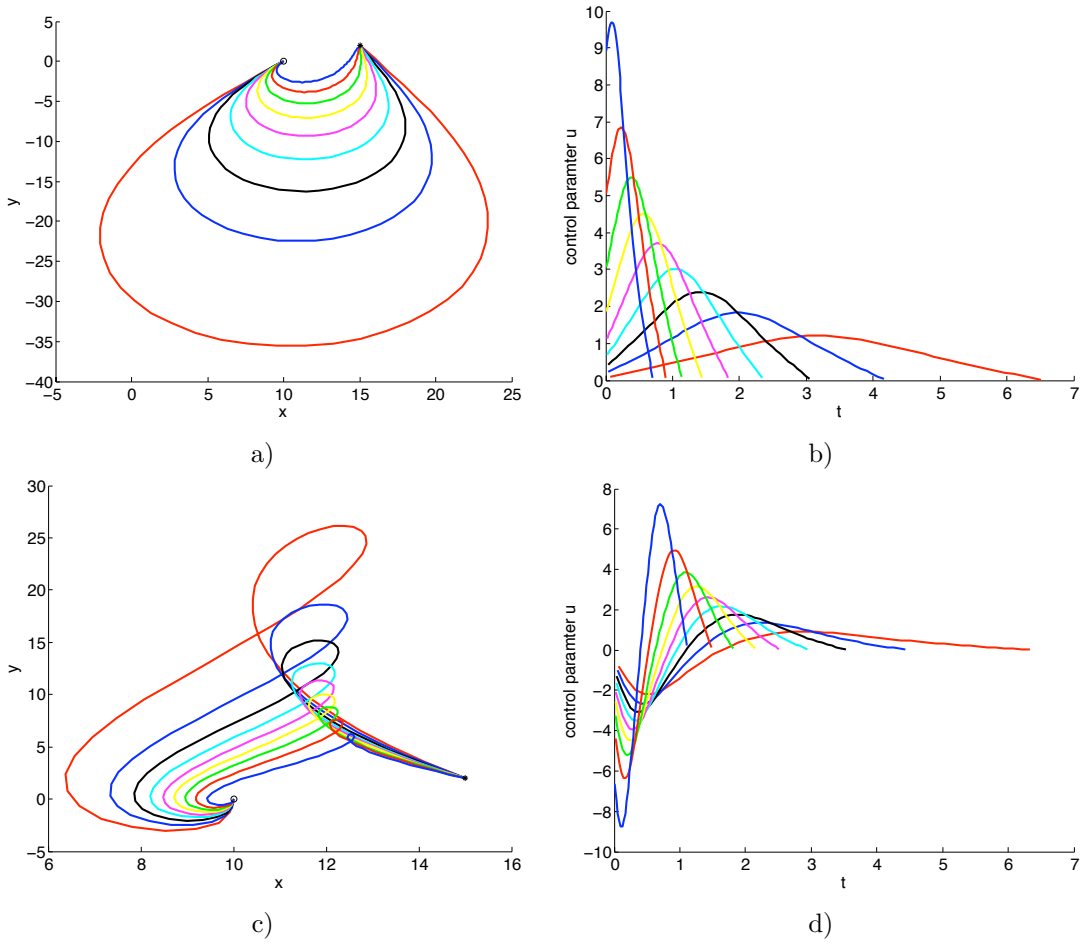

Figure 5.9: Optimal trajectories of the motion of an underwater glider in dependence of the weights w_1 and w_2 for the maneuver time and the control effort in the objective function. Top: The glider moves in zero current velocity $V = (0, 0)$. a) Optimal trajectories in configuration space, b) optimal control parameter. Bottom: The glider moves in current velocity $V = (x, 0)$. c) Optimal trajectories in configuration space, d) optimal control parameter. Red: $w_1 = 0.9, w_2 = 0.1$. Blue: $w_1 = 0.8, w_2 = 0.2$. Black: $w_1 = 0.7, w_2 = 0.3$. Cyan: $w_1 = 0.6, w_2 = 0.4$. Mangenta: $w_1 = 0.5, w_2 = 0.5$. Yellow: $w_1 = 0.4, w_2 = 0.6$. Green: $w_1 = 0.3, w_2 = 0.7$. Red: $w_1 = 0.2, w_2 = 0.8$. Blue: $w_1 = 0.1, w_2 = 0.9$.

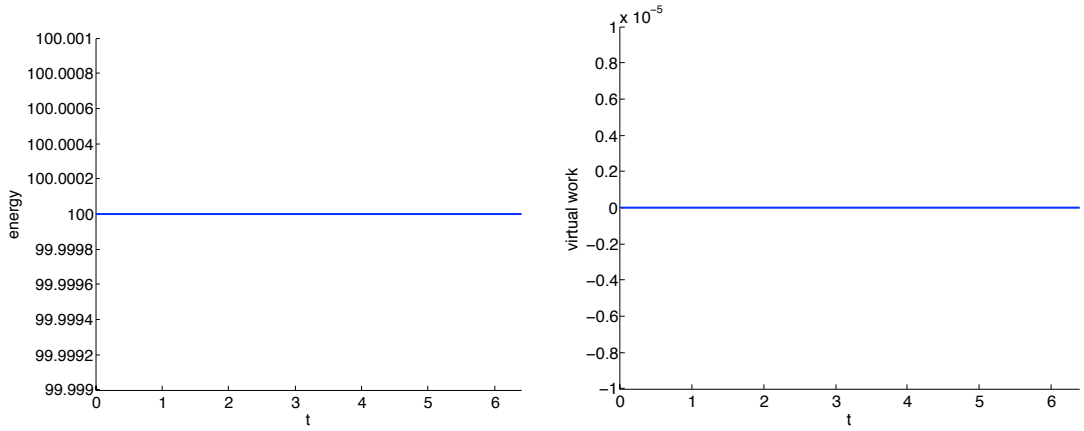

Figure 5.10: a) The total energy of the underwater glider is constant. This corresponds to the b) zero work that is done by the control force since the gyroscopic force is acting orthogonal to the relative velocity of the glider. c) Objective values (maneuver time and control effort) in dependence on the weights in the objective function.

Remark 5.4.1 In 1991, Montgomery investigated the associated optimal control problem, which resulted in Montgomery's falling cat theorem [118, 119, 120, 121] that relates the optimal reorientation of the falling cat to the dynamics of particles in a Yang-Mills field.

Model As in [120], the falling cat is modeled as two identical cylinders (which can be thought of as the upper torso and the lower torso), which are attached at a joint in the center of the cat's body. The reference configuration for this system is shown in Figure 5.11.

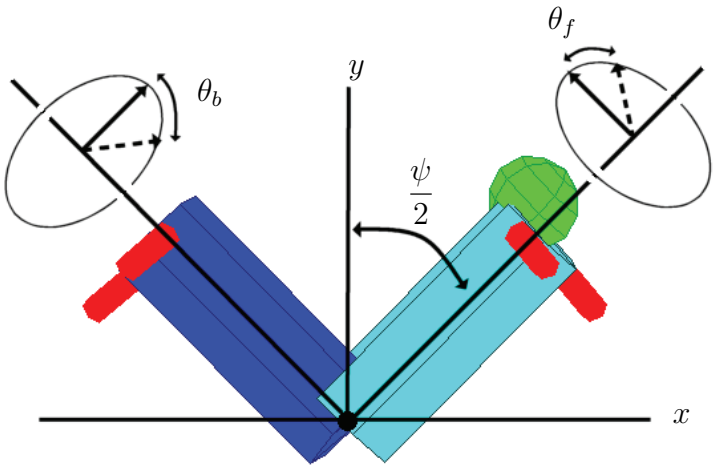

Figure 5.11: Falling cat model.

Each cylinder is allowed to rotate around its symmetric axis by an angle θ_f for the front body half, and θ_b for the back body half. When $\theta_b = \theta_f = 0$, the cat is oriented upright and facing along the x-axis. The cat is also allowed to bend at its center joint. The parameter ψ describes the angle between the symmetric axes of the two cylinders. The cat is completely straight when $\psi = \pi$, and the cat is completely folded onto itself when $\psi = 0$. Additionally, the system as a whole is given an orientation $g \in SO(3)$, which represents the orientation about the center of mass between the line containing the system's center of mass and the hinge point, and the y-axis in the reference configuration shown in Figure 5.11.

Each cylinder has mass m and radius a. The distance from the joint to each of the individual cylinder's center of mass is denoted by r. The cylinders' moment of inertia tensors have the form $I = \text{diag}(J_1, J_1, J_3)$. Finally, torques are applied independently to the internal variables θ_f, θ_b and ψ to affect the dynamics of the

cat and ultimately enable the desired flipping motion.[2]

We restrict ourselves to the *no-twist* model, in which the cat is allowed to bend in the direction ψ, and twist the front and back halves of its body in equal proportions; that is, $\theta = \theta_f = \theta_b$. This assumption reduces the global orientation of the system to a subset $g \in S^1 \subset SO(3)$.

Assuming that the cat is in free fall, we can treat the system as an articulated body rotating about its center of mass, with the Lagrangian equalling the total system kinetic energy consisting of linear and rotational kinetic energy (for a derivation of the Lagrangian we refer to [115]):

$$\begin{aligned} L(q,\dot{q}) &= K_{\text{lin}}(q,\dot{q}) + K_{\text{rot}}(q,\dot{q}) \\ &= J_3\dot{\theta}^2 + \frac{1}{2}(J_1+J_3)\dot{g}^2 + \frac{1}{8}(2J_1+mr^2)\dot{\psi}^2 \\ &\quad + \frac{1}{8}\Big(4(J_1-J_3)\dot{g}^2 + mr^2\dot{\psi}^2\Big)\cos\psi - 2\dot{g}\dot{\theta}J_3\sin\frac{\psi}{2}, \end{aligned}$$

with $q = (\theta, \psi, g)$. The control force as described above reads

$$f_{LC}(\tau_1,\tau_2) = \begin{pmatrix} \tau_1 \\ \tau_2 \\ 0 \end{pmatrix}.$$

Since the Lagrangian is invariant under rotations around its center of mass (that is $\phi(g,q) = g \cdot q$ represents the group action that is a symmetry of the Lagrangian) and the control force is orthogonal to that group action (there is no torque influencing directly this degree of freedom), we know from the forced Noether's theorem that the angular momentum

$$\frac{\partial L}{\partial \dot{g}} = \dot{g}(J_1 + J_3 + (J_1 - J_3)\cos\psi) - 2\dot{\theta}J_3\sin\frac{\psi}{2}$$

should be zero during the entire motion of the cat.

Boundary conditions We must specify boundary conditions consistent with the motion of a falling cat. The simplest choice of these parameters is to specify conditions which correspond to a perfectly straight inverted and correctly oriented cat

$$(\theta^0,\psi^0,g^0) = (0,\pi,\pi) \qquad \text{and} \qquad (\theta^T,\psi^T,g^T) = (0,\pi,0).$$

Additionally, the cat is assumed to start and end with zero angular velocities, that is

$$(\dot{\theta}^0,\dot{\psi}^0,\dot{g}^0) = (0,0,0) \qquad \text{and} \qquad (\dot{\theta}^T,\dot{\psi}^T,\dot{g}^T) = (0,0,0).$$

[2]This dynamical model stands in contrast to Montgomery's kinematic model, in which the angular rates of the internal variables are directly controlled.

Objective functional We attempt to minimize the control effort required by the cat to perform the flip, using

$$J(\tau) = \frac{1}{2} \int_0^T \left(\tau_1(t)^2 + \tau_2(t)^2 \right) \, \mathrm{d}t,$$

where $\tau = (\tau_1, \tau_2)$ is the control torque associated with $\dot{\theta}$ and $\dot{\psi}$.

Results One fascinating result that we can demonstrate immediately with this simple no-twist system is that the DMOC solution actually mimics the behavior of real cats. Figure 5.12 a) contains image captures of our model at different time intervals, and these images have a striking resemblance to the image captures of real live falling cats. In Figure 5.12 b) and c) the orientation angles and the corresponding control torques are shown, respectively. In Figure 5.13 a) the energy behavior with zero initial and final kinetic energy is depicted. As stated above, the cat's total angular momentum is supposed to be zero, since the cat can just adjust its orientation due to shape changes. The momentum preservation is nicely captured by DMOC to numerical accuracy of the algorithm as shown in Figure 5.13 b).

5.4.2 A gymnast (three-link mechanism)

A further application of the optimal control of a mechanical system is the determination of optimal motion sequences in sports. As a simple example we consider a gymnast performing a giant swing around a bar. After one giant we want the gymnast to have maximal energy to perform the next giant, that means the aim is to maximize the kinetic energy in the handstand position.

Model description The gymnast is modeled as a multi-body system consisting of three rigid bodies, the arms, the torso, and the legs, coupled by revolute joints. Since the gymnast is assumed to stay in one plane during his performance, we consider a planar model with mass m_i and length l_i of body i (see Figure 5.14). The bar is located at the coordinate origin, θ_1 is the angle between the vertical and the arms, θ_2 determines the angle between arms and torso, and θ_3 describes the bending in the hip. Here, we assume that arms and legs are outstretched during the whole motion. Furthermore, we assume that the gymnast is able to control the shoulder and the hip muscles to create a desired motion. We model the influence of the muscle forces by two external control torques acting on the system: τ_1 influences the motion of the torso relative to the arms. The second torque, τ_2, enables the gymnast to move his legs relative to the torso.

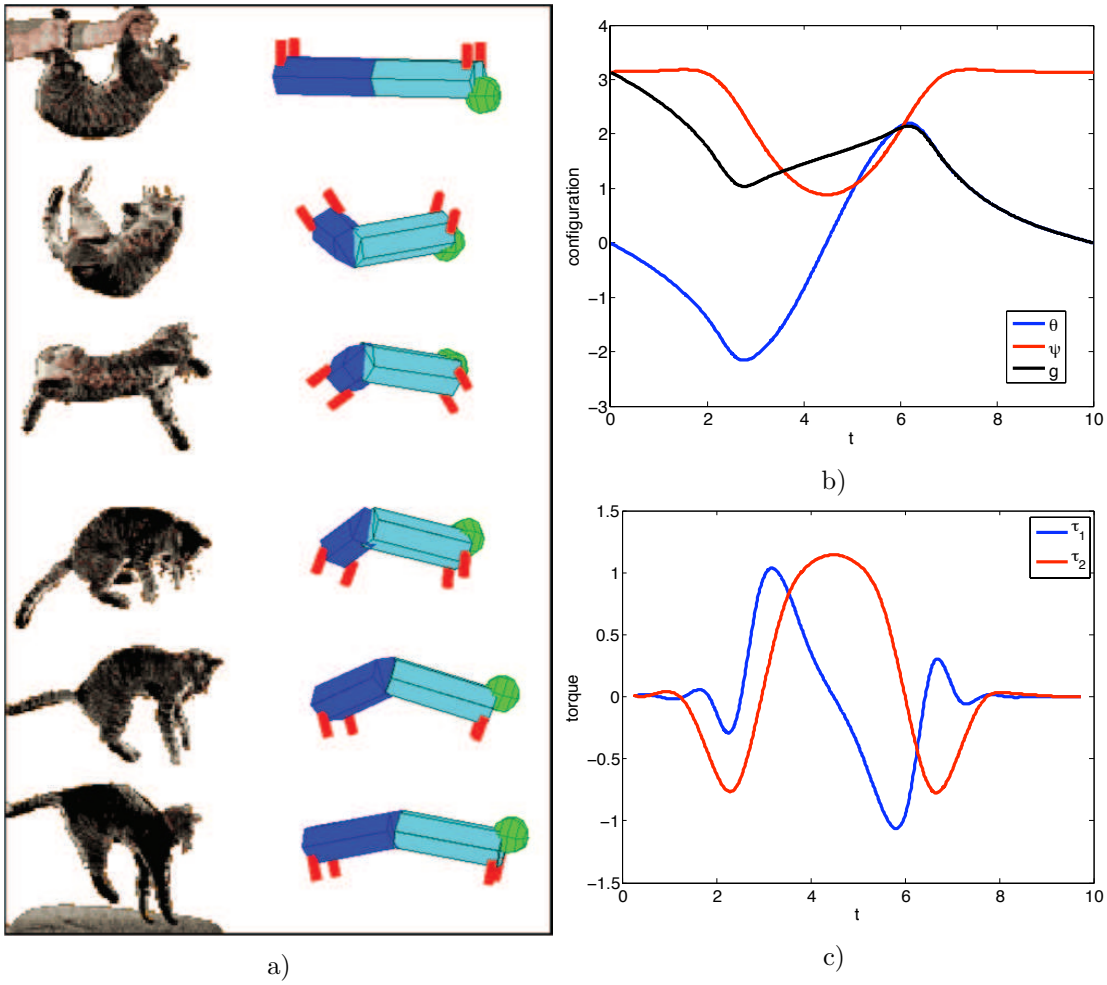

Figure 5.12: Optimal solution trajectory of the falling cat. a) Image captures of the falling cat: comparison of a real cat with the computed solution. b) Configuration (rotation θ around its body half's symmetric axis, bending angle ψ, overall orientation g) over time. c) Control torques over time.

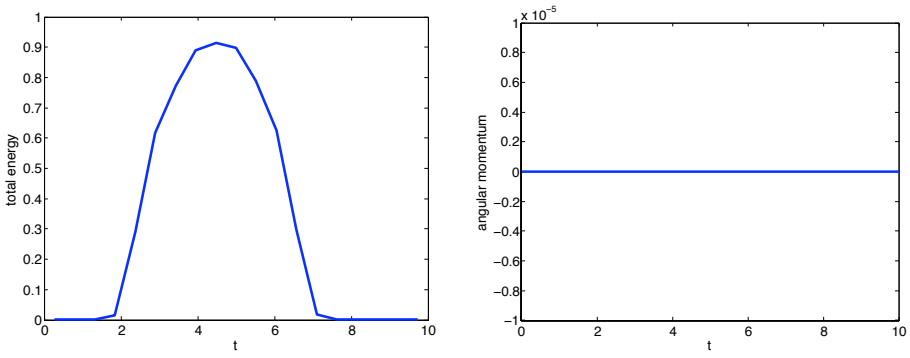

a) b)

Figure 5.13: a) Energy behavior of the falling cat. b) The total angular momentum of the cat is zero since it adjusts its orientation due to shape changes.

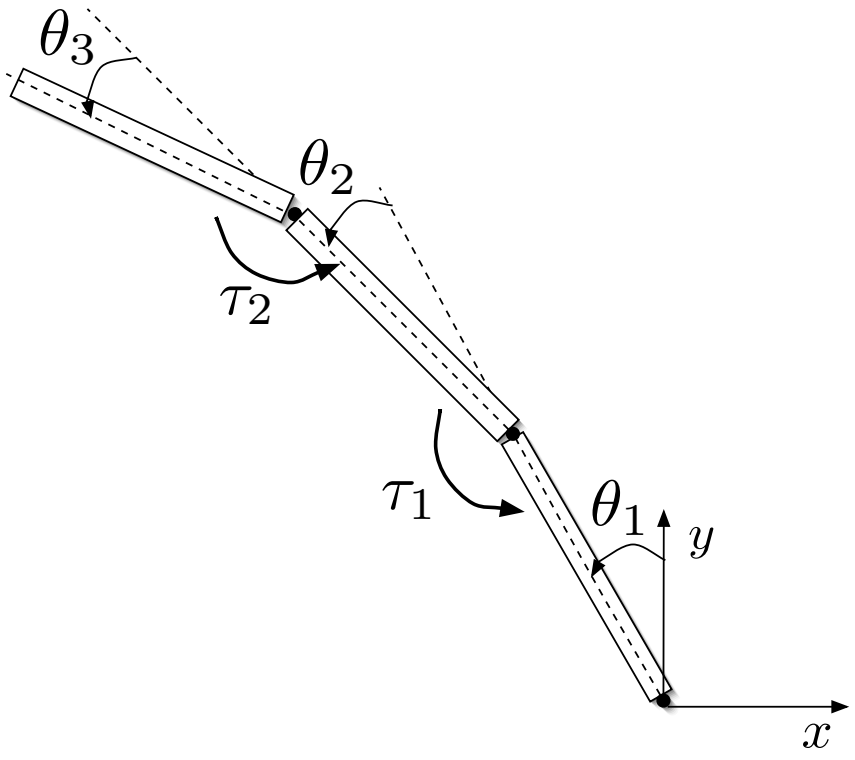

Figure 5.14: A gymnast performing a swing giant modeled as three-link mechanism.

The Lagrangian consisting of kinetic and potential energy of each single rigid body with g the gravitational acceleration reads as

$$
\begin{aligned}
L(\theta,\dot{\theta}) = \quad & K(\theta,\dot{\theta}) - V(\theta) = \\
& \left[\frac{1}{2}m_2 l_1^2 + \frac{1}{6}m_1 l_1^2 + \frac{1}{6}m_2 l_2^2 + \frac{1}{2}m_2 l_1 l_2 \cos\theta_2 + \frac{1}{3}m_3 l_1^2 + \frac{1}{2}m_3 l_2^2 \right. \\
& \left. + \frac{1}{6}m_3 l_3^2 + m_3 l_1 l_2 \cos\theta_2 + \frac{1}{2}m_3 l_1 l_3 \cos(\theta_1+\theta_2) + \frac{1}{2}m_3 l_2 l_3 \cos\theta_3 \right] \dot{\theta}_1^2 \\
& + \left[\frac{1}{6}m_2 l_2^2 + m_3 l_2^2 + \frac{1}{3}m_3 l_3^2 + m_3 l_1 l_2 \cos\theta_2 \right. \\
& \left. + \frac{1}{2}m_3 l_1 l_3 \cos(\theta_1+\theta_2) + m_3 l_2 l_3 \cos\theta_3 \right] \dot{\theta}_1\dot{\theta}_2 \\
& + \left[\frac{1}{3}m_3 l_3^2 + \frac{1}{2}m_3 l_1 l_3 \cos(\theta_1+\theta_2) + \frac{1}{2}m_3 l_2 l_3 \cos\theta 3\right] \dot{\theta}_1\dot{\theta}_3 \\
& + \left[\frac{1}{6}m_2 l_2^2 + \frac{1}{2}m_3 l_2^2 + \frac{1}{2}m_3 l_2 l_3 \cos\theta_3\right] \dot{\theta}_2^2 \\
& + \left[\frac{1}{3}m_3 l_3^2 + \frac{1}{2}m_3 l_2 l_3 \cos\theta_3\right] \dot{\theta}_2\dot{\theta}_3 + \left[\frac{1}{6}m_3 l_3^2\right] \dot{\theta}_3^2 \\
& + \left(\frac{1}{2}m_1 + m_2 + m_3\right) l_1 g \cos\theta_1 + \left(\frac{1}{2}m_2 + m_3\right) l_2 g \cos(\theta_1+\theta_2) \\
& + \frac{1}{2}m_3 l_3 g \cos(\theta_1+\theta_2+\theta_3).
\end{aligned}
$$

The control torques τ_1 and τ_2 yield the virtual work

$$W(\tau,\theta) = \int_0^T \tau(t)\cdot\delta\theta(t)\,\mathrm{d}t,$$

with $\theta = (\theta_1,\theta_2,\theta_3)$ and $\tau = (0,\tau_1,\tau_2)$.

Boundary conditions, objective function, and path constraints The gymnast starts in the handstand position, $\theta^0 = (\pi,0,0)$ with initial angular velocity ω^0. We now determine the optimal trajectories $(\theta,\dot{\theta})$, the optimal control force τ and the optimal duration time T for one rotation around the bar, such that the kinetic energy in the final configuration $\theta(T) = \theta^T = \theta^0$ is maximized, so the objective function reads as

$$J(\theta,\dot{\theta}) = K(\theta(T),\dot{\theta}(T)).$$

To restrict to realistic motions we need to incorporate bounds on the configuration variables as $\theta_i^l \leq \theta_i \leq \theta_i^u,\ i = 1, 2, 3$ that are in accordance with the human body's anatomy. In addition, we have bounds on the torques $\tau_i^l \leq \tau_i \leq \tau_i^u,\ i = 1, 2$, representing the possible amount of torque that a muscle force can generate in a specific joint.

Results The computations are performed with an initial angular velocity $\omega^0 = (1, 1, -2)$ and with bounds on the joint angles and the control torques as $\theta^l = (-\infty, -\frac{\pi}{12}, -\frac{\pi}{12})$, $\theta^u = (\infty, \frac{11}{12}\pi, \frac{5}{6}\pi)$ and $\tau^l = (-60, -70)$, $\tau^u = (60, 70)$. In Figure 5.15 and 5.16 one particular locally optimal solution is shown. Although we use a simple model without taking into account the effect of the muscles the results nicely approximate the motion of a real giant swing:

In general, two phases in performing a motion exist: the hyperextension and the contraction phase. A posture is called hyperextended if the extension of a bodily joint is beyond its normal range of motion. This condition effects an initial tension and allows to build up more muscle strength. The creation of the necessary muscle strength is the preparation for the contraction phase, also known as active phase: Here, the muscles are contracted and therefore the angles in shoulder and hip decrease. This changes the moment of inertia of the system and allows the gymnast to move his body to the desired position.

Figure 5.16 shows snapshots of the optimal solution for different time points. The yellow and purple sticks demonstrate orientation and the amount of the applied control torques in shoulder and hip joint, respectively.

The pictures 1 to 7 show the swing down while the pictures 8 to 11 correspond to the swing up of the giant. During the swing down we observe in the pictures 2 to 5 a hyperextension of the gymnast's body, that is followed by a contraction phase (picture 6) to move the body from a horizontal aligned position (picture 5) to the vertical position. Then, again a hyperextened posture (picture 7) allows a real gymnast to build up the necessary muscle strength in continuing his motion to the desired handstand position (last picture) during another contraction phase.

In Figure 5.15 the evolution of joint angles, applied torques, angular velocities and energy over time are shown. The angle θ_1 between arms and bar increases smoothly, that means the gymnast's body rotates uniformly around the bar. The small oscillations of the shoulder θ_2 and hip angle θ_3 indicate permanent changes between a hyperextension and contraction phase that is also observed in Figure 5.16 as well as for real giant swing motions. Since the kinetic energy in the final configuration is maximized ($K(\theta(T), \dot{\theta}(T)) = 504.6485$), the control torques reach the value of the prescribed bounds τ^l and τ^u, respectively. Here, the time of the giant swing duration is $T = 2.0338$ seconds.

Remark 5.4.2 As observed for the previous two applications of multi-body sys-

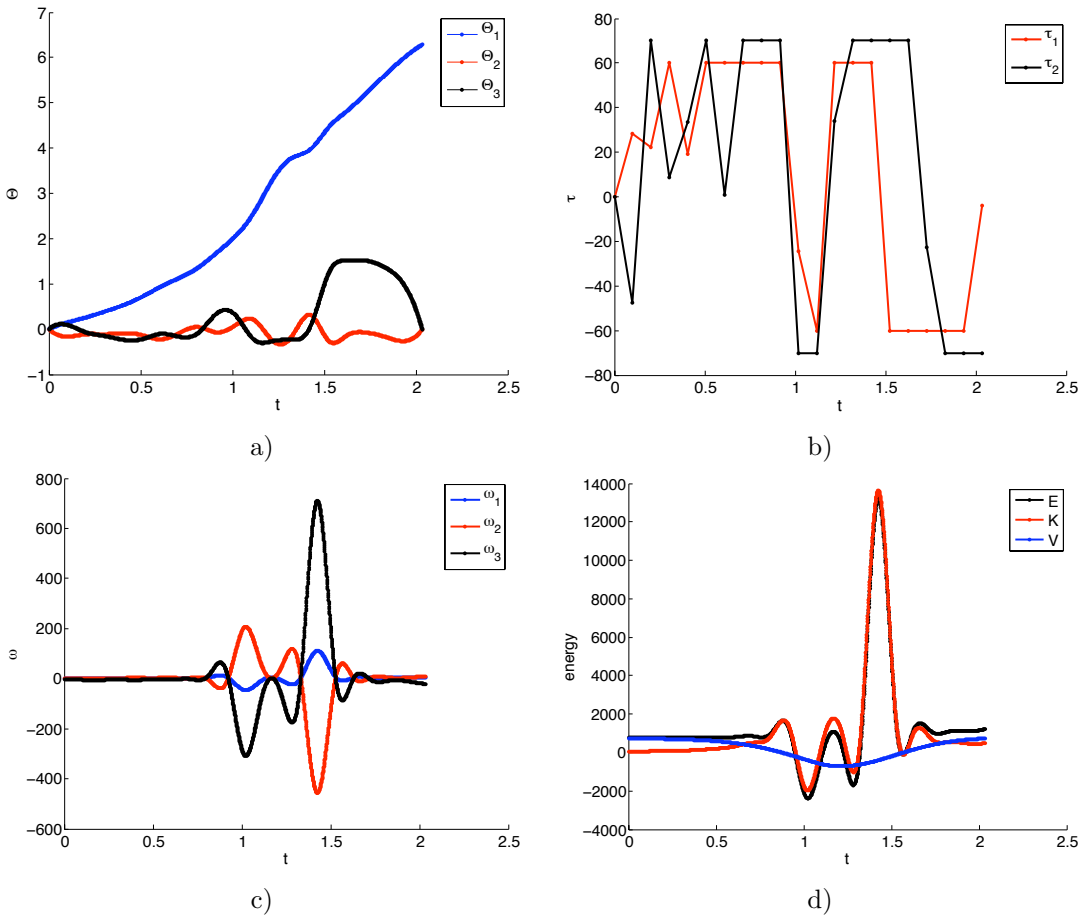

Figure 5.15: A gymnast performing a swing giant with initial angular velocity $\omega^0 = (1, 1, -2)$, configuration bounds $\theta^l = (-\infty, -\frac{\pi}{12}, -\frac{\pi}{12})$, $\theta^u = (\infty, \frac{11}{12}\pi, \frac{5}{6}\pi)$, torque bounds $\tau^l = (-60, -70)$, $\tau^u = (60, 70)$, final time $T = 2.0338$ seconds, and final kinetic energy $K(\theta(T), \dot{\theta}(T)) = 504.6485$. a) Angle between hand and bar θ_1, shoulder angle θ_2 and hip angle θ_3 over time t. b) Control torque τ_1 in the shoulder and torque τ_2 in the hip joint over time t. c) Angular velocity ω over time t. d) Total energy over time t.

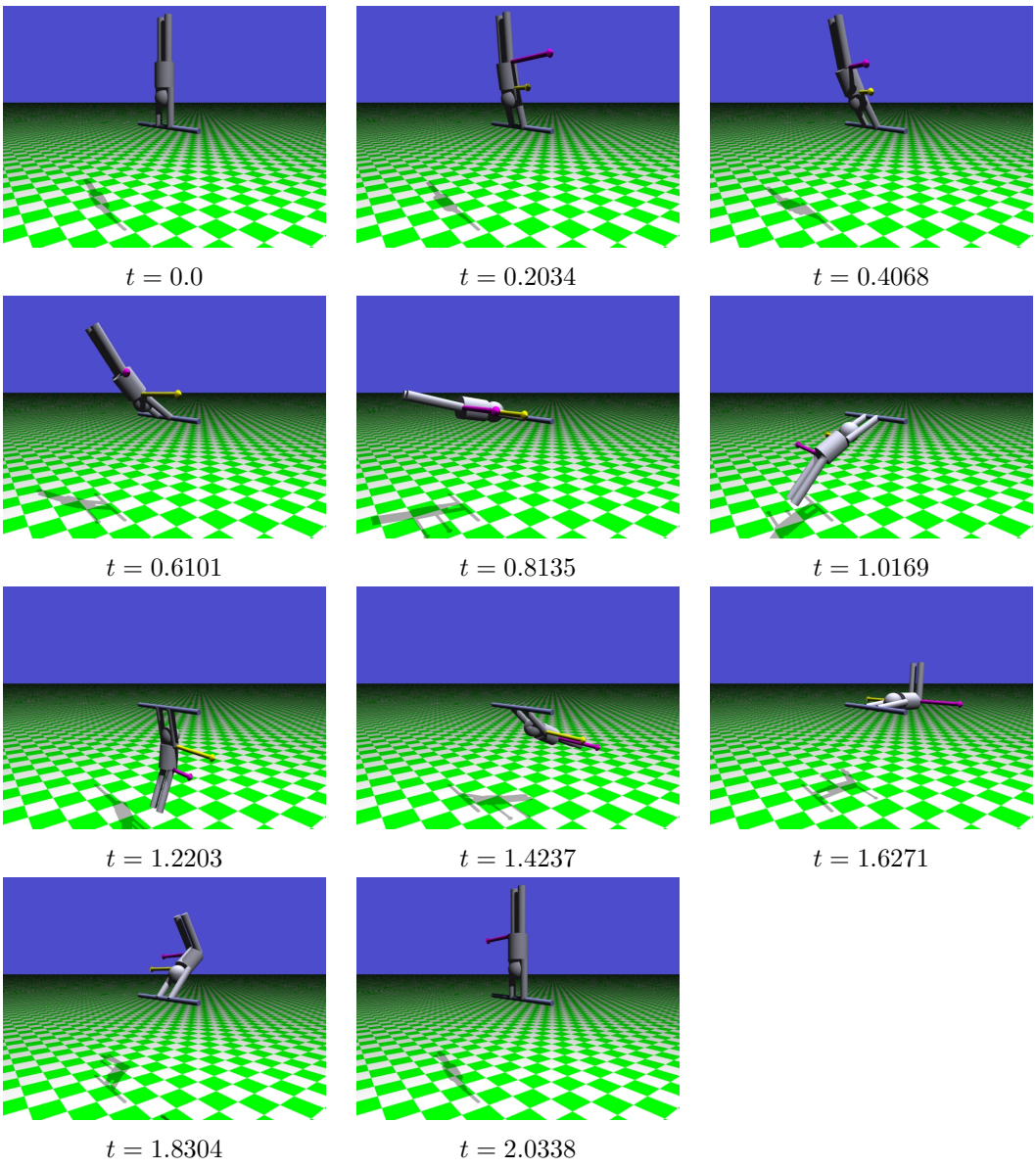

Figure 5.16: Snapshots of the motion sequence of a gymnast's swing giant: The swing down and the swing up motion goes along with changes between hyperextension and contraction phases as for real gymnasts that perform a giant.

tems, the expressions for the Lagrangians in generalized coordinates typically become long and complicated for complex multi-body models. In Chapter 6 we therefore propose an alternative approach to the optimal control of multi-body systems formulated within a mechanical framework with holonomic constraints. This novel approach has several advantages, in particular, it simplifies the mathematical expressions for the Lagragian functions substantially.

5.5 Reconfiguration of formation flying spacecraft – a decentralized approach

The following application presents a decentralized approach to the optimal reconfiguration of formation flying spacecraft based on a hierarchical framework of DMOC developed in [68]. For upcoming space missions like *Darwin*[3], control strategies have to be devised that enable precise formation flying of a group of spacecraft. In light of the tight mass budget of these missions it is of great interest to minimize the propellant consumption in performing the associated maneuvers (see [35]).

A group of n spacecraft, viewed as one large mechanical system, is placed in the vicinity of an L_2-Halo orbit and is required to adopt a certain configuration of the spacecraft relative to each other.

To exploit the structure of the given system, which is in fact composed of many identical subsystems, we develop a decentralized approach for solving the given (large) optimal control problem. We derive a hierarchical formulation of the optimal control problem by exploiting this structure. The hierarchical formulation is naturally suited for a solution of the associated subproblems in parallel.

Model Each spacecraft is modeled as a rigid body with six degrees of freedom (position and orientation), so its configuration manifold is $SE(3)$. We assume that each spacecraft can be controlled in this configuration space by a force-torque pair (F, τ), acting on its center of mass.

For several reasons (consistent solar illumination characteristics, lack of disturbing perturbations, relative ease of sending and retrieving spacecraft), an attractive region in space for missions like Darwin is in the vicinity of a Libration orbit around the Earth-Sun L_2 Lagrange point. Correspondingly, for each spacecraft the dynamical model for the motion of its center of mass is given by the *circular restricted three body problem (CRTBP)* [149, 150]: Two large bodies (the *primaries*, Sun and Earth in our case) with masses m_1 and m_2 rotate on circles with common angular velocity ω around their common center of mass. A third

[3] `http://www.esa.int/science/darwin`

body, the spacecraft, moves within their gravitational potential without affecting the motion of the primaries. We neglect gravitational forces between the spacecraft. Figure 5.17 a) shows the position of the primaries and the equilibria (the *Lagrange points*) $L_1, \ldots, L_5$ in the x-y-plane of a rotating coordinate system. In Figure 5.17 b) we plot a family of periodic orbits (*Halo orbits*) in the vicinity of the L_2 Lagrange point. This family has been computed by a predictor corrector method on an initial orbit found by a shooting technique (see [66]). In a normal-

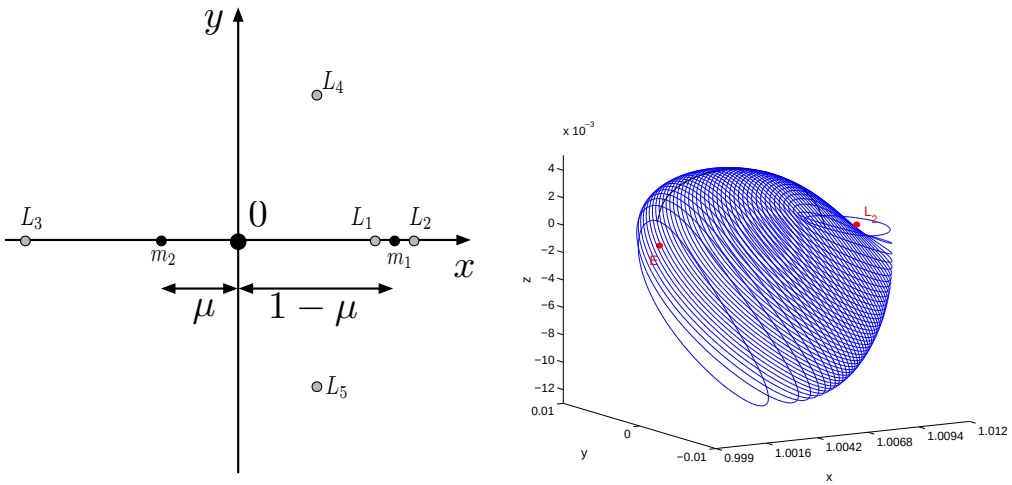

a) b)

Figure 5.17: a) Rotating coordinate system: location of the primaries and the Lagrange points [138]. b) Family of periodic orbits in the circular restricted three body problem in the vicinity of the L_2-Lagrange point [66].

ized, rotating coordinate system (see Figure 5.17 a)), the potential energy of the spacecraft at position $x = (x_1, x_2, x_3) \in \mathbb{R}^3$ is given by

$$V(x) = -\frac{1-\mu}{|x-(1-\mu,0,0)|} - \frac{\mu}{|x-(-\mu,0,0)|}, \tag{5.4}$$

where $\mu = m_1/(m_1+m_2)$ is the normalized mass. Its kinetic energy is the sum of

$$K_{\text{trans}}(x,\dot{x}) = \frac{1}{2}((\dot{x}_1 - \omega x_2)^2 + (\dot{x}_2 + \omega x_1)^2 + \dot{x}_3^2) \quad \text{and} \quad K_{\text{rot}}(\Omega) = \frac{1}{2}\Omega^T J \Omega,$$

where $\Omega \in \mathbb{R}^3$ is the angular velocity and J the inertia tensor of the spacecraft.

The control problem

Our goal is to compute control laws $(F^{(i)}(t), \tau^{(i)}(t))$, $i = 1, \dots, n$, for each spacecraft, such that the group of spacecraft moves from a given initial state $(x^{(i)}, p^{(i)}, \dot{x}^{(i)}, \dot{p}^{(i)})_{i=1}^n$ into a prescribed target manifold within a prescribed time interval. Here, the unit quaternion $p^{(i)} \in \mathbb{R}^4$ represents the orientation of the i-th spacecraft, and the unity constraint is incorporated as additional optimization constraint. In our application context, the target manifold is defined by prescribing the relative positioning of the spacecraft, their common velocity, as well as a common orientation.

Boundary conditions For their target state, we require the spacecraft to be located in a planar regular polygonal configuration with center on a Halo orbit. Let $\nu \in \mathbb{R}^3$ be a given unit vector representing the "line of sight" of the spacecraft. The target manifold $M \subset TSE(3)^n$ is the set of all states $(x^{(i)}, p^{(i)}, \dot{x}^{(i)}, \dot{p}^{(i)})_{i=1}^n$ such that

1. all spacecraft are located in a plane with normal ν, that is

$$\langle x^{(i)} - x^{(j)}, \nu \rangle = 0, \quad i, j = 1, \dots, n; \tag{5.5}$$

2. within that plane, the spacecraft are located at equal distances on a circle with prescribed radius and prescribed center on a Halo orbit. Let $r_0 \in \mathbb{R}$ be a given radius and $\bar{x} \in \mathbb{R}^3$ a certain point on a Halo orbit and let $\nu_1^\perp \perp \nu_2^\perp \in \mathbb{R}^3$ be two perpendicular unit vectors that are perpendicular to ν. For $i = 1, \dots, n$ we consider the vector

$$z^{(i)} = [\nu_1^\perp \ \nu_2^\perp]^T (x^{(i)} - \bar{x}) \in \mathbb{R}^2 \tag{5.6}$$

and require that

$$h(z^{(i)}) = \|z^{(i)}\| - r_0 = 0, \ i = 1, \dots, n \tag{5.7}$$

and

$$k(z) = 0, \quad z = (z^{(1)}, \dots, z^{(n)}), \tag{5.8}$$

with functions $h : \mathbb{R}^2 \to \mathbb{R}$ and $k : \mathbb{R}^{2n} \to \mathbb{R}^n$, where the constraint (5.7) forces each spacecraft to be at a distance r_0 from the center and the constraint (5.8) guarantees an equidistant arrangement.

The idea of this formulation is not to prescribe a particular point on the circle for each spacecraft but rather to let the optimization process determine the best possible arrangement.

3. all spacecraft have their "line of sight" aligned with ν. For simplicity we impose a more restrictive condition, namely that each spacecraft is rotated according to a prescribed unit quaternion $p^{T,(i)}$, that is we require that

$$p^{(i)} = p^T, \quad i = 1, \dots, n; \tag{5.9}$$

4. all spacecraft have the same prescribed translational velocity,

$$\dot{x}^{(i)} = \dot{x}^T, \quad i = 1, \dots, n,$$

where $\dot{x}_N$ will typically be determined on basis of the Halo orbit under consideration, and they have zero angular velocity, that is

$$\Omega^{(i)} = 2\dot{p}^{(i)}\bar{p}^{(i)} = 0, \quad i = 1, \dots, n,$$

where $\bar{p}^{(i)}$ is the conjugate quaternion to $p^{(i)}$.

Objective functional While controlling the formation to reach the target manifold, we would like to minimize the fuel consumption of the spacecraft. Here, we consider the objective functional

$$\begin{aligned} J(F, \tau) &= \sum_{i=1}^{n} J_i(F^{(i)}, \tau^{(i)}) \\ &= \sum_{i=1}^{n} \int_0^T |F^{(i)}(t)|^2 + |\tau^{(i)}(t)|^2 \, \mathrm{d}t, \end{aligned} \tag{5.10}$$

where J_i is the objective functional for spacecraft i and $F(t) = (F^{(1)}(t), \dots, F^{(n)}(t))$ and $\tau(t) = (\tau^{(1)}(t), \dots, \tau^{(n)}(t))$ denote the force and torque functions for the system.

Remark 5.5.1 A major numerical challenge for a direct application of DMOC are the scales of interest. These differ by a factor of around 10^{17}: the distance between the Sun and the Earth is of the order of 10^{11} m, while the distances between the spacecraft are of the order of several 100 m and have to be kept constant up to an error of 10^{-6} m. When using standard double-precision floating point arithmetic, rounding errors will notably influence any corresponding computation. On the other hand, we are only interested in the relative positions of the spacecraft with respect to each other. We therefore perform our computations in a local coordinate system by linearizing the system around a Halo-orbit. The discrete forced Euler-Lagrange equations linearized around the points $(q_k^H, \dot{q}_k^H)$, $k = 1, \dots, N$, on a given Halo-orbit then provide constraints for the discrete optimization problem (see [69] for a detailed description).

Decentralization

When collision avoidance concerns[4] are neglected, the optimal control problem described in the previous section is "almost" decoupled in the sense that the coupling only enters through the constraints (5.8) on the final configuration. In this section, we show how one can exploit this fact in order to carry out the associated computations in parallel.

Hierarchical optimal control problem The basic observation is that the problem can be formulated as a hierarchical optimization problem, where the *outer problem* relates to the correct arrangement of the final configuration and the n *inner problems* determine the optimal trajectory for one spacecraft with fixed initial and final configuration, respectively.

We parametrize the final positions of the spacecraft projected onto the prescribed plane by the vector $\varphi = (\varphi^{(1)}, \ldots, \varphi^{(n)})$ via

$$z^{(i)} = \begin{pmatrix} r_0 \cos \varphi^{(i)} \\ r_0 \sin \varphi^{(i)} \end{pmatrix}, \tag{5.11}$$

where $\varphi^{(i)}$ is the angle of spacecraft i, determining the final position on a given circle with prescribed center (see Figure 5.18). First, we want to derive the final

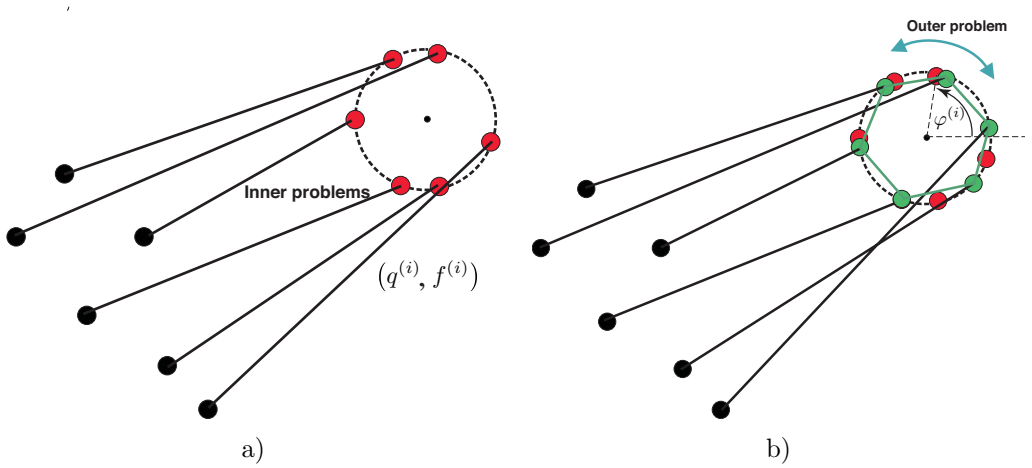

Figure 5.18: Hierarchical formulation of the optimal control of formation flying spacecraft. a) The n inner problems determine the optimal trajectory for one spacecraft with fixed initial and final configuration, respectively. b) The outer problem relates to the correct arrangement of the final configuration.

[4]See [69] for incorporating collision avoidance strategies.

constraint (5.8) with the help of this parametrization. We define the artificial potential $G : S^n \to \mathbb{R}$ by

$$G(\varphi) = \sum_{i,j=1, i\neq j}^{n} \frac{1}{\|z^{(i)} - z^{(j)}\|^2}.$$

This artificial potential is comparable to a gravitational potential that affects attraction or repulsion, respectively, between bodies. For an equidistant arrangement on the circle the resulting forces $dG/d\varphi$ acting on each spacecraft have to be zero. Therefore, we obtain as final constraint

$$g(\varphi) = \frac{dG}{d\varphi}(\varphi) = 0,$$

with a function $g : S^n \to \mathbb{R}^n$. With the parametrization (5.11) it holds by defining a function $\tilde{G} : \mathbb{R}^{2n} \to \mathbb{R}, \tilde{G}(z) := G(\varphi)$

$$0 = g(\varphi) = \frac{dG}{d\varphi}(\varphi) = \frac{d\tilde{G}}{dz}(z) \cdot \frac{dz}{d\varphi} =: k(z), \tag{5.12}$$

which results in the final constraint (5.8).

With parametrization (5.11) the problem has the following hierarchical form: Let $q^{(i)} = \begin{pmatrix} x^{(i)} \\ p^{(i)} \end{pmatrix} \in Q = SE(3)$ denote the configuration and $f^{(i)} = \begin{pmatrix} F^{(i)} \\ \tau^{(i)} \end{pmatrix}$ the control force of spacecraft i. By optimizing within a fixed time interval $I = [0, T]$ we obtain the optimal control problem

$$\min_{\varphi} J(\varphi) = \min_{\varphi} \sum_{i=1}^{n} \min J_i(q^{(i)}, f^{(i)}),$$

where the first minimization is constrained by $g(\varphi) = 0$ and the second minimization is constrained by $q^{(i)} : [0, T] \to Q, f^{(i)} : [0, T] \to T^*Q, q^{(i)}(0) = q^{0,(i)}$, $\dot{q}^{(i)}(0) = \dot{q}^{0,(i)}, A\, q^{(i)}(T) = b(\varphi^{(i)})$, $\dot{q}^{(i)}(T) = \dot{q}^{T,(i)}$. Furthermore, $(q^{(i)}, f^{(i)})$ have to fulfill the dynamics of spacecraft i. Here, the matrix is $A = \begin{pmatrix} [\nu_1^\perp\ \nu_2^\perp]^T & 0 \\ 0 & I_4 \end{pmatrix} \in \mathbb{R}^{6\times 7}$, where I_4 is the unit 4×4 matrix and the vector $b(\varphi^{(i)}) = \begin{pmatrix} z^{(i)} + [\nu_1^\perp\ \nu_2^\perp]^T \bar{x} \\ p^T \end{pmatrix} \in \mathbb{R}^6$ is defined by equations (5.6) and (5.9). Due to the parametrization (5.11), we do not have to incorporate the constraint (5.7).

The inner problems are uncoupled since for each spacecraft its costs have to be minimized separately subject to fixed initial and final states and its dynamics.

The outer problem includes the constraint for the final configuration, that is the coupling of the system. We use SQP for the solution of both, the inner and the outer problems. In each step of the solution of the outer problem all n inner problems have to be solved anew with the new boundary constraints.

Remark 5.5.2 Constraint (5.12) provides a discrete solution set of the final configurations $\varphi^{(i)}$. Due to the local optimality of SQP, the sequence of spacecraft on the circle depends on the initial guess for the optimization problem.

Equivalence of both optimal control problems In order to show the equivalence of the "monolithic" formulation of the optimal control problem to the hierarchical one, we consider the following abstract optimization problem:

$$\min_{(x,\varphi)\in X\times\Phi} J(x,\varphi) \quad \text{s.t. } A(x,\varphi)=0,\ g(\varphi)=0, \tag{5.13}$$

where $X\subset\mathbb{R}^{d_x}, \Phi\subset\mathbb{R}^{d_y}$ are compact and $J: X\times\Phi\to\mathbb{R}$, $A: X\times\Phi\to\mathbb{R}^a$ and $g:\Phi\to\mathbb{R}^g$ are continuous. Defining $X(\varphi)=\{x\in X \mid A(x,\varphi)=0\}$, we see that

$$\bigcup_{\varphi\in g^{-1}(0)} X(\varphi)\times\{\varphi\} = \{(x,\varphi)\mid A(x,\varphi)=0, g(\varphi)=0\}.$$

Thus,

$$\begin{aligned}
&\min\{J(x,\varphi)\mid A(x,\varphi)=0, g(\varphi)=0\}\\
&=\min\left\{J(x,\varphi)\mid (x,\varphi)\in\bigcup_{\varphi\in g^{-1}(0)} X(\varphi)\times\{\varphi\}\right\}\\
&=\min\bigcup_{\varphi\in g^{-1}(0)}\{J(x,\varphi)\mid (x,\varphi)\in X(\varphi)\times\{\varphi\}\}\\
&=\min\left\{\min\{J(x,\varphi)\mid x\in X(\varphi)\}\mid\varphi\in g^{-1}(0)\right\}\\
&=\min\{\min\{J(x,\varphi)\mid A(x,\varphi)=0\}\mid g(\varphi)=0\},
\end{aligned}$$

that means we finally obtain a hierarchical formulation of the problem. The "inner problem" is given by minimizing $J(x,\varphi)$ subject to $A(x,\varphi)=0$ (for a fixed $\varphi\in\Phi$), while the "outer problem" is given by minimizing

$$\hat{J}(\varphi)=\min\{J(x,\varphi)\mid A(x,\varphi)=0\}\quad\text{s.t. } g(\varphi)=0.$$

Since in our specific application, the inner objective function, $J(x,\varphi)$ is given by the sum

$$\sum_{i=1}^{n}\min J_i(q^{(i)},f^{(i)})$$

and since all J_i are nonnegative, the inner problem decouples into n independent subproblems which can be solved independently.

Parallelization The hierarchical structure of the problem enables a computational solution in parallel, as we are faced with n uncoupled inner problems in each step of the solution of the outer problem. These n subproblems are solved in n different tasks. Our implementation uses the software package PUB (**P**aderborn **U**niversity **B**SP-Library, [24]) developed within the DFG research project CRC 376 "Massively Parallel Computation" at the University of Paderborn. In the terminology of PUB, each step of the iteration scheme for the solution of the outer problem represents one *superstep*. After each superstep, the tasks have to communicate during the *synchronization* phase.

Example computations In all following computations we use $N = 10$ time intervals in the time discretization of the trajectories and solve the resulting finite-dimensional (nonlinear) optimization problem by the SQP method as implemented in the routine `E04UEF` of the NAG-library. We use numerical derivatives both for the cost and for the constraint functions.

First, we consider a group of six spacecraft in the vicinity of a Halo-orbit and require the spacecraft to adopt a planar hexagonal formation with center on the orbit. Figure 5.19 a) shows the Halo orbit (in normalized coordinates) that we have chosen for this computation and the part of the orbit that we use for the linearization of the problem.

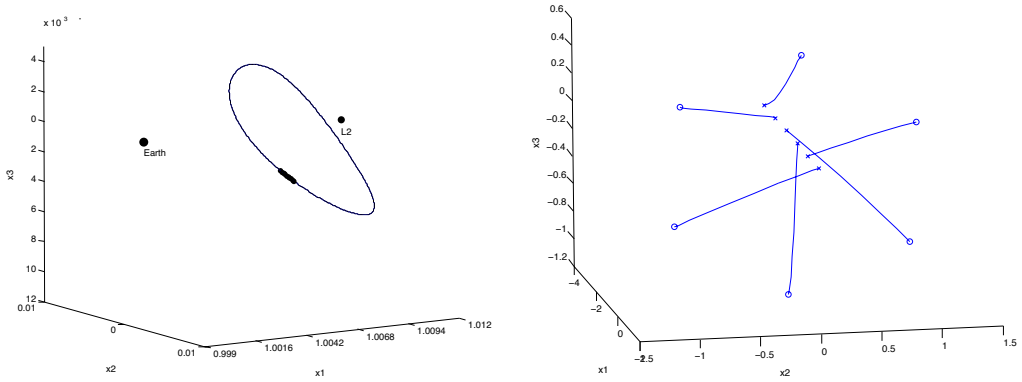

a) b)

Figure 5.19: a) L_2 Halo-orbit chosen for the example computations (thin line) and the part used for the linearization (thick line). b) Initial positions ($\times$), optimal trajectories and final positions ($\circ$) for a reconfiguration of six spacecraft in the CRTBP.

Figure 5.19 b) shows (in normalized coordinates) the initial positions ($\times$), the optimal trajectories, as well as the final positions ($\circ$). Initially, the group

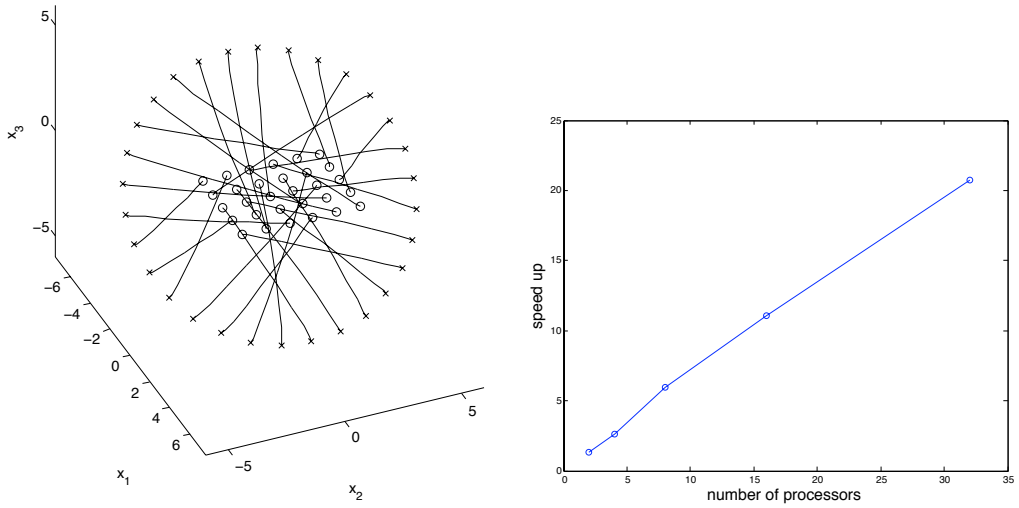

a) b)

Figure 5.20: a) Initial positions ($\circ$), optimal trajectories and final positions ($\times$) for a reconfiguration of 30 spacecraft in the CRTBP in x_1-x_2-x_3-space. b) Speed up diagram in dependence on the number of processors for the reconfiguration of 30 spacecraft in the CRTBP.

Table 5.2: Speed up diagram.

number of processors	2	4	8	16	32
speed up	1.33	2.65	5.98	11.09	20.76
CPU time [10^4 sec]	9.55	4.8	2.13	1.15	0.62

is located along a line with initial orientation $p^{0,(i)} = (\cos\frac{\pi}{2}, \sin\frac{\pi}{2} \cdot (1,0,0))$ for each spacecraft i (that is a rotation of $\theta = \pi$ around the x_1-axis). The final configuration is a hexagonal formation in the plane with normal $n = (1,0,1)$ and final orientation $p^{T,(i)} = (\cos\pi, \sin\pi \cdot (0,1,0))$ for each spacecraft i (that is a rotation of $\theta = 2\pi$ around the x_2-axis).

As a second example we consider a group of 30 spacecraft modeled as rigid bodies in 3-space, with the circular restricted three body problem governing their dynamics. Figure 5.20 a) shows the initial positions ($\circ$), the optimal trajectories, as well as the final positions ($\times$) in normalized coordinates. Initially, the group is located on a grid in the x_1-x_2-plane with initial orientation $p^{0,(i)} = (\cos\frac{\pi}{2}, \sin\frac{\pi}{2} \cdot (1,0,0))$ for each spacecraft i (that is a rotation of $\theta = \pi$ around the x_1-axis). The final configuration is a circle formation in the plane with normal $n = (1,0,1)$ and final orientation $p^{T,(i)} = (\cos\pi, \sin\pi \cdot (0,1,0))$ for each spacecraft i (that is a rotation of $\theta = 2\pi$ around the x_2-axis).

Figure 5.20 b) and Table 5.2 show the dependence of the computation time on the number of processors (for only one processor the computation time is $12.75 \cdot 10^4$ seconds). The almost linear speed up indicates the effectiveness of our decentralized approach.

Chapter 6

Optimal control of constrained mechanical systems in multi-body dynamics

In this chapter, we formulate a framework for the optimal control of constrained mechanical systems. Such systems occur in multi-body dynamics.[1] For the applications in Section 5.4 we searched for generalized coordinates for the underlying multi-body system. These are often not easy to determine. In contrast, in this chapter the multi-body system is formulated as a constrained system, that is each body is viewed as a constrained continuum, described in terms of redundant coordinates subject to holonomic constraints. The couplings between the bodies are characterized via external holonomic constraints which describe the kinematic conditions that arise from the specific joint connections.

To optimally control these kinds of systems, in Sections 6.1 and 6.2 we extend the variational formulation of DMOC to a constrained version: In the first place, configuration constraints are enforced using Lagrange multipliers. Then, to reduce the number of unknowns (configurations and torques at the time nodes) and the dynamic constraints to the minimal possible number, the discrete null space method method ([7]) is used, which is suitable for the accurate, robust and efficient time integration of constrained dynamical systems (in particular for multi-body dynamics). This procedure does not only lead to lower computational costs for the optimization algorithm, but it also inherits the conservation properties from the constrained scheme. Furthermore, it has the advantage of circumventing the difficulties associated with rotational parameters ([8]). The benefit of exact constraint fulfillment, correct computation of the change in momentum maps and good energy behavior is guaranteed by the optimization algorithm.

[1] See for example [25, 154] for other methods to the optimal control of multi-body dynamics.

The combination of DMOC and the nullspace method has first been presented in [99] and is currently investigated in [98].

In particular, in Section 6.3 we develop an optimal control framework for a rigid body and for multi-body dynamics. The constrained formulation as well as the actuation via control forces are described in more detail. Finally, in Section 6.4, we apply the developed method to the optimal control of two multi-body systems arising in robotics and biomechanics.

Remark 6.0.3 Compared to the previous chapters, we use a slightly different notation to be consistent with the notation in [98, 99] (see the nomenclature). Therefore, the control parameters denoted by $u(t) \in U$ are represented by the generalized independent control forces $\tau(t) \in W$, whereas u represents the generalized independent coordinates of the system. C denotes the manifold determined via the holonomic constraints. We denote the cost function of the objective functional J by B. Furthermore, we restrict ourselves to fixed boundary conditions on the configuration and the velocity level $(q(0), \dot{q}(0)) = (q^0, \dot{q}^0)$ and $(q(T), \dot{q}(T)) = (q^T, \dot{q}^T)$.

6.1 Constrained dynamics and optimal control

This section presents the derivation of the equations of motion for forced constrained systems which have to be fulfilled as constraints in the optimization problem. The transformation of the differential algebraic equations by the null space method and reparametrization, and in particular the equivalence of the resulting equations of motion, is described in detail in [97] for unforced systems.

Consider an n-dimensional mechanical system with the time-dependent configuration vector $q(t) \in Q$ and velocity vector $\dot{q}(t) \in T_{q(t)}Q$, where $t \in [0, T] \subset \mathbb{R}$ denotes the time and $T \in \mathbb{N}$. Let the configuration be constrained by the function $g(q) = 0 \in \mathbb{R}^m$ and influenced by the force field $f : W \times TQ \to T^*Q$. Due to the presence of constraints, the forces f are not independent. They can be calculated in terms of the time dependent generalized control forces $\tau(t) \in W \subseteq \mathbb{R}^{n-m}$.

6.1.1 Optimization problem

The goal is to determine the optimal force field, such that the system is moved from the initial state $(q^0, \dot{q}^0)$ to the final state $(q^T, \dot{q}^T)$ while the objective functional

$$J(q, \dot{q}, f) = \int_0^T B(q, \dot{q}, f(q, \dot{q}, \tau)) \, \mathrm{d}t \tag{6.1}$$

is minimized. Note that J denotes a function $J : TQ \times T^*Q \to \mathbb{R}$ rather than $J : TQ \times U \to \mathbb{R}$ as in Chapter 4.

6.1.2 Constrained Lagrange-d'Alembert principle

Contemporaneously, the motion $(q, \dot{q})$ has to be in accordance with an equation of motion which in the present case is based on a constrained version of the Lagrange-d'Alembert principle (see for example [113]) requiring

$$\delta \int_0^T L(q, \dot{q}) - g^T(q) \cdot \lambda \, \mathrm{d}t + \int_0^T f(q, \dot{q}, \tau) \cdot \delta q \, \mathrm{d}t = 0 \tag{6.2}$$

for all variations $\delta q \in TQ$ and $\delta\lambda \in \mathbb{R}^m$ vanishing at the endpoints. The Lagrangian $L : TQ \to \mathbb{R}$ comprises the kinetic energy $\frac{1}{2}\dot{q}^T \cdot M \cdot \dot{q}$ including the consistent mass matrix $M \in \mathbb{R}^{n\times n}$ and a potential function $V : Q \to \mathbb{R}$. Furthermore, $\lambda(t) \in \mathbb{R}^m$ represents the vector of time dependent Lagrange multipliers. The constrained Lagrange-d'Alembert principle (6.2) leads to the differential-algebraic system of equations of motion

$$\frac{\partial L(q, \dot{q})}{\partial q} - \frac{\mathrm{d}}{\mathrm{d}t}\left(\frac{\partial L(q, \dot{q})}{\partial \dot{q}}\right) - G^T(q) \cdot \lambda + f(q, \dot{q}, \tau) = 0, \tag{6.3a}$$

$$g(q) = 0, \tag{6.3b}$$

where $G(q) = Dg(q)$ denotes the Jacobian of the constraints. The vector $-G^T(q) \cdot \lambda$ represents the constraint forces that prevent the system from deviations of the constraint manifold

$$C = \{q \in Q \,|\, g(q) = 0\}\,. \tag{6.4}$$

6.1.3 Null space method

Assuming that the constraints are independent, for every $q \in C$ the basis vectors of T_qC form an $n \times (n-m)$ matrix $P(q)$ with corresponding linear map $P(q) : \mathbb{R}^{n-m} \to T_qC$. This matrix is called null space matrix, since

$$\mathrm{range}\,(P(q)) = \mathrm{null}\,(G(q)) = T_qQ. \tag{6.5}$$

Thus a premultiplication of the differential equation (6.3a) by $P^T(q)$ eliminates the constraint forces including the Lagrange multipliers from the system. The resulting equations of motion read

$$\begin{aligned} P^T(q) \cdot \left(\frac{\partial L(q, \dot{q})}{\partial q} - \frac{\mathrm{d}}{\mathrm{d}t}\left(\frac{\partial L(q, \dot{q})}{\partial \dot{q}}\right) + f(q, \dot{q}, \tau)\right) &= 0, \\ g(q) &= 0. \end{aligned} \tag{6.6}$$

6.1.4 Reparametrization

For many applications it is possible to find a reparametrization of the constraint manifold $F : U \subseteq \mathbb{R}^{n-m} \to C$ in terms of independent generalized coordinates $u \in U$. Then the Jacobian $DF(u)$ of the coordinate transformation plays the role of a null space matrix. Since the constraints (6.3b) are fulfilled automatically by the reparametrized configuration variable $q = F(u)$, the system is reduced to $n-m$ second order differential equations. This is the minimal possible dimension for the present mechanical system which consists of precisely $n-m$ configurational degrees of freedom. Consequently, there are $n-m$ independent generalized forces $\tau \in W \subseteq \mathbb{R}^{n-m}$ acting on the degrees of freedom. These can be calculated as $\tau = \left(\frac{\partial F}{\partial u}\right)^T \cdot f$, see for example [50].

6.2 Constrained discrete dynamics and optimal control

Analogous steps are performed in the temporal discrete variational setting to derive the forced constrained discrete Euler-Lagrange equations and their reduction to minimal dimension. Again, these steps have been investigated in detail in [97] for unforced systems.

As in Section 3.1.2, corresponding to the configuration manifold Q, the discrete phase space is defined by $Q \times Q$ which is locally isomorphic to TQ. For a constant time step $h \in \mathbb{R}$, a path $q : [0, T] \to Q$ is replaced by a discrete path $q_d : \{0 = t_0, t_0 + h, , \ldots, t_0 + Nh = T\} \to Q$, $N \in \mathbb{N}$, where $q_k = q_d(t_0 + kh)$ is viewed as an approximation of $q(t_0 + kh)$. Similarly, $\lambda_k = \lambda_d(t_k)$ approximates the Lagrange multiplier at $t_k = t_0 + kh$, while the force field f is approximated by the two discrete forces $f_k^-, f_k^+ : W \times Q \to T^*C$ defined in (6.17).

6.2.1 Discrete constrained Lagrange-d'Alembert principle

According to the derivation of variational integrators for constrained dynamics in [97], the action integral in (6.2) is approximated in a time interval $[t_k, t_{k+1}]$ using the discrete Lagrangian $L_d : Q \times Q \to \mathbb{R}$ and the discrete constraint function $g_d : Q \to \mathbb{R}^m$ via

$$L_d(q_k, q_{k+1}) - \frac{1}{2} g_d^T(q_k) \cdot \lambda_k - \frac{1}{2} g_d^T(q_{k+1}) \cdot \lambda_{k+1} \approx \int_{t_k}^{t_{k+1}} L(q, \dot{q}) - g^T(q) \cdot \lambda \, \mathrm{d}t. \quad (6.7)$$

Among various possible choices to approximate this integral, the midpoint rule is used for the Lagrangian, that is

$$L_d(q_k, q_{k+1}) = hL\left(\frac{q_{k+1}+q_k}{2}, \frac{q_{k+1}-q_k}{h}\right) \tag{6.8}$$

and

$$g_d^T(q_k) = hg^T(q_k) \tag{6.9}$$

for the constraints. Likewise, the virtual work is approximated by

$$f_k^- \cdot \delta q_k + f_k^+ \cdot \delta q_{k+1} \approx \int_{t_k}^{t_{k+1}} f(q, \dot{q}, \tau) \cdot \delta q \, \mathrm{d}t, \tag{6.10}$$

where f_k^+, f_k^- are the left and right discrete forces, respectively. They are specified in (6.17).

The discrete version of the constrained Lagrange-d'Alembert principle (6.2) requires the discrete path $\{q_k\}_{k=0}^N$ and multipliers $\{\lambda_k\}_{k=0}^N$ to fulfill

$$\delta \sum_{k=0}^{N-1} L_d(q_k, q_{k+1}) - \frac{1}{2} g_d^T(q_k) \cdot \lambda_k - \frac{1}{2} g_d^T(q_{k+1}) \cdot \lambda_{k+1} + \sum_{k=0}^{N-1} \left[f_k^- \cdot \delta q_k + f_k^+ \cdot \delta q_{k+1} \right] = 0 \tag{6.11}$$

for all variations $\{\delta q_k\}_{k=0}^N$ and $\{\delta \lambda_k\}_{k=0}^N$ with $\delta q_0 = \delta q_N = 0$, which is equivalent to the constrained forced discrete Euler-Lagrange equations

$$D_2 L_d(q_{k-1}, q_k) + D_1 L_d(q_k, q_{k+1}) - G_d^T(q_k) \cdot \lambda_k + f_{k-1}^+ + f_k^- = 0, \tag{6.12a}$$

$$g(q_{k+1}) = 0, \tag{6.12b}$$

for $k = 1, \ldots, N-1$, where $G_d(q_k)$ denotes the Jacobian of $g_d(q_k)$. As in Section 3.1.2 the time-stepping scheme (6.12) has not been deduced discretizing (6.3) but via a discrete variational principle.

6.2.2 Discrete null space method

A reduction of the time-stepping scheme (6.12) can be accomplished in analogy to the continuous case according to the discrete null space method. In order to eliminate the discrete constraint forces from the equations, a discrete null space matrix fulfilling

$$\operatorname{range}(P(q_k)) = \operatorname{null}(G_d(q_k)) \tag{6.13}$$

is employed. Analogous to (6.6), the premultiplication of (6.12) by the transposed discrete null space matrix cancels the constraint forces from the system, that is the

Lagrange multipliers are eliminated from the set of unknowns and the dimension of the system is reduced to n as

$$P^T(q_k) \cdot \left(D_2 L_d(q_{k-1}, q_k) + D_1 L_d(q_k, q_{k+1}) + f_{k-1}^+ + f_k^-\right) = 0, \quad (6.14a)$$

$$g(q_{k+1}) = 0. \quad (6.14b)$$

6.2.3 Nodal reparametrization

Similar to the continuous case, a reduction of the system to the minimal possible dimension can be accomplished by a local reparametrization of the constraint manifold in the neighborhood of the discrete configuration variable $q_k \in C$. At the time nodes, q_k is expressed in terms of the discrete generalized coordinates $u_k \in U \subseteq \mathbb{R}^{n-m}$ by the map $F : U \subseteq \mathbb{R}^{n-m} \times Q \to C$, such that the constraints are fulfilled:

$$q_k = F(u_k, q_{k-1}) \quad \text{with} \quad g(q_k) = g(F(u_k, q_{k-1})) = 0, \quad k = 1, \ldots, N. \quad (6.15)$$

The discrete generalized control forces are assumed to be constant in each time interval (see Figure 6.1). First of all, the effect of the generalized forces acting in $[t_{k-1}, t_k]$ and in $[t_k, t_{k+1}]$ is transformed to the time node t_k via

$$\tau_{k-1}^+ = \frac{h}{2}\tau_{k-1}, \ (k = 1, \ldots, N), \qquad \tau_k^- = \frac{h}{2}\tau_k, \ (k = 0, \ldots, N-1). \quad (6.16)$$

Secondly, the components of the discrete force vectors f_k^+ and f_k^- can be calculated as

$$\begin{aligned} f_{k-1}^+ &= f\left(q_k, \tau_{k-1}^+\right), \qquad f_k^- = f\left(q_k, \tau_k^-\right) \qquad \in T_{q_k}^* C, \\ f_k &= f_k^+ + f_k^-, \\ f_d &= \{f_k\}_{k=0}^{N-1}. \end{aligned} \quad (6.17)$$

Thus f_{k-1}^+ denotes the effect of the generalized force τ_{k-1} acting in $[t_{k-1}, t_k]$ on q_k while f_k^- denotes the effect on q_k of τ_k acting in $[t_k, t_{k+1}]$. f_k is the total discrete force in $[t_k, t_{k+1}]$ resulting from the generalized force τ_k.

Insertion of the nodal reparametrizations for the configuration (6.15) and the force (6.17) into the scheme redundantizes (6.14b). The resulting scheme

$$P^T(q_k) \cdot \left(D_2 L_d(q_{k-1}, q_k) + D_1 L_d(q_k, F(u_{k+1}, q_k)) + f_{k-1}^+ + f_k^-\right) = 0 \quad (6.18)$$

has to be solved for u_{k+1} whereupon q_{k+1} is obtained from (6.15). (6.18) is equivalent to the constrained scheme (6.12), thus it also has the key properties of exact constraint fulfilment, symplecticity and momentum consistency, that is any change in the value of a momentum map reflects exactly the applied forces. When no load is present, momentum maps are conserved exactly.

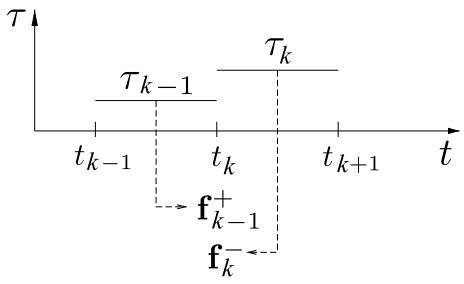

Figure 6.1: Relation of redundant forces at t_k to piecewise constant discrete generalized forces.

6.2.4 Boundary conditions

In the next step, the boundary conditions $q(0) = q^0, \dot{q}(0) = \dot{q}^0$ and $q(T) = q^T, \dot{q}(T) = \dot{q}^T$ have to be specified. Those on the configuration level can be used as constraints for the optimization algorithm in a straightforward way. At $t = 0$ we can request $u_0 = u^0$. Within this work, we use an absolute reparametrization, that is (6.15) is changed to $q_k = F(u_k, q_0)$, then $u_N = u^T$ is prescribed (see [98] for the formulation with relative reparametrization). Along the lines of Section 4.2 the velocity conditions have to be transformed to conditions on the conjugate momentum, which is defined at each and every time node using the discrete Legendre transform. The presence of forces as well as constraint forces at the time nodes has to be incorporated into that transformation leading to constrained forced discrete Legendre transforms $\mathbb{F}^{cf^-}L_d : Q \times Q \to T^*Q$ and $\mathbb{F}^{cf^+}L_d : Q \times Q \to T^*Q$ reading

$$\begin{aligned} \mathbb{F}^{cf^-}L_d &: (q_k, q_{k+1}) \mapsto (q_k, p_k^-) \\ p_k^- &= -D_1 L_d(q_k, q_{k+1}) + \frac{1}{2} G_d^T(q_k) \cdot \lambda_k - f_k^-, \end{aligned} \tag{6.19a}$$

$$\begin{aligned} \mathbb{F}^{cf^+}L_d &: (q_{k-1}, q_k) \mapsto (q_k, p_k^+) \\ p_k^+ &= D_2 L_d(q_{k-1}, q_k) - \frac{1}{2} G_d^T(q_k) \cdot \lambda_k + f_{k-1}^+. \end{aligned} \tag{6.19b}$$

As in the unforced case, the time-stepping scheme (6.12a) can be interpreted as a matching of momenta $p_k^+ - p_k^- = 0$ such that along the discrete trajectory, there is a unique momentum at each time node k which can be denoted by p_k. However, just as the appearance of Lagrange multipliers is avoided in the dynamic constraints for the optimization problem (6.18), their presence in the initial and final momentum conditions complicates matters unnecessarily. Even though they can be related to the discrete trajectory via

$$\lambda_k = R_d^T(q_k) \cdot \left(D_1 L_d(q_k, q_{k+1}) + D_2 L_d(q_{k-1}, q_k) + f_{k-1}^+ + f_k^- \right), \tag{6.20}$$

where

$$R_d(q_k) = G_d^T(q_k) \cdot \left(G_d(q_k) \cdot G_d^T(q_k)\right)^{-1}, \tag{6.21}$$

the following versions of the discrete Legendre transforms do not need the Lagrange multipliers. The projected discrete Legendre transforms ${}^{Q}\mathbb{F}^{cf^-}L_d : Q \times Q \to \eta\left(T^*_{q_k}C\right)$ and ${}^{Q}\mathbb{F}^{cf^+}L_d : Q \times Q \to \eta\left(T^*_{q_k}C\right)$ read

$$\begin{aligned} {}^{Q}p_k^- &= Q(q_k) \cdot \left(-D_1 L_d(q_k, q_{k+1}) - f_k^-\right), & (6.22a)\\ {}^{Q}p_k^+ &= Q(q_k) \cdot \left(D_2 L_d(q_{k-1}, q_k) + f_{k-1}^+\right), & (6.22b) \end{aligned}$$

where $Q(q_k)$ is given by (see [113])

$$Q = I_{n\times n} - G_d^T \cdot \left(G_d \cdot M^{-1} \cdot G_d^T\right)^{-1} G_d \cdot M^{-1}, \tag{6.23}$$

and fulfills $Q(q_k) \cdot G_d^T(q_k) = 0_{n\times m}$. Note that for the constrained discrete Legendre transforms and for the projected discrete Legendre transforms the output is an n-dimensional momentum vector. In the projected case, it lies in the $(n-m)$-dimensional submanifold $\eta\left(T^*_{q_k}C\right)$ being the embedding of $T^*_{q_k}C$ into $T^*_{q_k}Q$. Yet another possibility is to compute an $(n-m)$-dimensional momentum vector by projecting with the discrete null space matrix. The reduced discrete Legendre transforms ${}^{P}\mathbb{F}^{cf^-}L_d : Q \times Q \to T^*U$ and ${}^{P}\mathbb{F}^{cf^+}L_d : Q \times Q \to T^*U$ are given by

$$\begin{aligned} {}^{P}p_k^- &= P^T(q_k) \cdot \left(-D_1 L_d(q_k, q_{k+1}) - f_k^-\right), & (6.24a)\\ {}^{P}p_k^+ &= P^T(q_k) \cdot \left(D_2 L_d(q_{k-1}, q_k) + f_{k-1}^+\right). & (6.24b) \end{aligned}$$

This version is most appropriate to be used as a constraint in the optimization problem, since it yields the minimal number of independent conditions, while conditions formulated using (6.22) are redundant and (6.19) involves the Lagrange multipliers. Note that according to the range of the projection (6.23), ${}^{Q}p_k$ fulfills the constraints on the momentum level h_d, that is

$$h_d(q_k, {}^{Q}p_k) = G(q_k) \cdot M^{-1} \cdot {}^{Q}p_k = 0, \tag{6.25}$$

while this is not in general the case for p_k. This question is superfluous for ${}^{P}p_k$.

Prescribed initial and final velocities of course should be consistent with the constraints on the velocity level. Using the standard continuous Legendre transform $\mathbb{F}L : TC \to T^*C$

$$\mathbb{F}L : (q, \dot{q}) \mapsto (q, p) = (q, D_2 L(q, \dot{q})) \tag{6.26}$$

yields momenta which are consistent with the constraints on the momentum level as well. With these preliminaries, the velocity boundary conditions are transformed to the following conditions on the momentum level $p_0 = p^0, p_N = p^T$, which read in detail

$$\begin{aligned} P^T(q_0) \cdot \left(D_2 L(q^0, \dot{q}^0) + D_1 L_d(q_0, q_1) + f_0^-\right) &= 0,\\ P^T(q_N) \cdot \left(-D_2 L(q^T, \dot{q}^T) + D_2 L_d(q_{N-1}, q_N) + f_{N-1}^+\right) &= 0. \end{aligned} \tag{6.27}$$

6.2.5 Discrete constrained optimization problem

Now the discrete optimal control problem for the constrained discrete dynamical problem can be formulated. To begin with, we define an approximation

$$B_d(q_k, q_{k+1}, f_k) \approx \int_{t_k}^{t_{k+1}} B(q, \dot{q}, f(\tau, q, \dot{q}))\,\mathrm{d}t \tag{6.28}$$

of the continuous objective functional (6.1). Similar to the approximations in (6.8) the midpoint rule is applied, that is

$$B_d(q_k, q_{k+1}, f_k) = hB\left(\frac{q_{k+1}+q_k}{2}, \frac{q_{k+1}-q_k}{h}, f_k\right) \tag{6.29}$$

with the discrete forces given in (6.17). This yields the discrete objective function

$$J_d(q_d, f_d) = \sum_{k=0}^{N-1} B_d(q_k, q_{k+1}, f_k), \tag{6.30}$$

where the discrete configurations and forces are expressed in terms of their corresponding independent generalized quantities. Alternatively a new objective function can be formulated directly in the generalized quantities

$$\bar{J}_d(u_d, \tau_d) = \sum_{k=0}^{N-1} \bar{B}_d(u_k, u_{k+1}, \tau_k) \tag{6.31}$$

depending on the desired interpretation of the optimization problem. In any case, (6.30) or (6.31) has to be minimized with respect to u_d, τ_d subject to the constraints

$$\begin{aligned}
u_0 - u^0 &= 0, \\
u_N - u^T &= 0, \\
P^T(q_0)\cdot\left(D_2L(q^0,\dot{q}^0) + D_1L_d(q_0,q_1) + f_0^-\right) &= 0, \\
P^T(q_N)\cdot\left(-D_2L(q^T,\dot{q}^T) + D_2L_d(q_{N-1},q_N) + f_{N-1}^+\right) &= 0, \\
P^T(q_k)\cdot\left(D_2L_d(q_{k-1},q_k) + D_1L_d(q_k,q_{k+1}) + f_{k-1}^+ + f_k^-\right) &= 0,
\end{aligned} \tag{6.32}$$

for $k = 1, \ldots, N-1$.

6.3 Optimal control for rigid body dynamics

6.3.1 Constrained formulation of rigid body dynamics

The treatment of rigid bodies as structural elements relies on the kinematic assumptions (see [10]) that the placement of a material point in the body's configuration $X = X_I d_I \in \mathcal{B} \subset \mathbb{R}^3$ relative to an orthonormal basis $\{e_I\}$ fixed in space

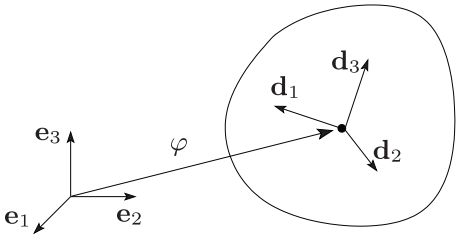

Figure 6.2: Configuration of a rigid body with respect to an orthonormal frame $\{e_I\}$ fixed in space.

can be described as

$$x(X,t) = \varphi(t) + X_I d_I(t), \tag{6.33}$$

see Figure 6.2 for an illustration. Here $X_I \in \mathbb{R}$, $I = 1,2,3$ represent coordinates in the body-fixed director triad $\{d_I\}$. The time-dependent configuration variable of a rigid body

$$q(t) = \begin{pmatrix} \varphi(t) \\ d_1(t) \\ d_2(t) \\ d_3(t) \end{pmatrix} \in \mathbb{R}^{12} \tag{6.34}$$

consists of the placement of the center of mass $\varphi \in \mathbb{R}^3$ and the directors $d_I \in \mathbb{R}^3, I = 1,2,3$ which are constrained to stay orthonormal during the motion, representing the rigidity of the body and its orientation. Thus we work with the embedding of the constraint manifold $C = \mathbb{R}^3 \times SO(3)$ into the configuration manifold $Q = \mathbb{R}^{12}$. These orthonormality conditions pertaining to the kinematic assumptions of the underlying theory are termed *internal constraints*. There are $m_{int} = 6$ independent internal constraints for the rigid body with associated constraint functions

$$g_{int}(q) = \begin{pmatrix} \frac{1}{2}[d_1^T \cdot d_1 - 1] \\ \frac{1}{2}[d_2^T \cdot d_2 - 1] \\ \frac{1}{2}[d_3^T \cdot d_3 - 1] \\ d_1^T \cdot d_2 \\ d_1^T \cdot d_3 \\ d_2^T \cdot d_3 \end{pmatrix}. \tag{6.35}$$

For simplicity, it is assumed that the axes of the body frame coincide with the principal axes of inertia of the rigid body. Then the body's Euler tensor with respect to the center of mass can be related to the inertia tensor J via

$$E = \frac{1}{2}(\mathrm{tr}J)I - J, \tag{6.36}$$

where I denotes the 3×3 identity matrix. The principal values of the Euler tensor E_i together with the body's total mass M_φ build the rigid body's constant symmetric positive definite mass matrix

$$M = \begin{pmatrix} M_\varphi I & 0 & 0 & 0 \\ 0 & E_1 I & 0 & 0 \\ 0 & 0 & E_2 I & 0 \\ 0 & 0 & 0 & E_3 I \end{pmatrix}, \tag{6.37}$$

where 0 denotes the 3×3 zero matrix. The angular momentum of the rigid body can be computed as

$$L = \varphi \times p_\varphi + d_I \times p_I, \tag{6.38}$$

where Einstein's summation convention is used to sum over the repeated index I.

Null space matrix This description of rigid body dynamics has been discussed in [7, 96] where also the null space matrix

$$P_{int}(q) = \begin{pmatrix} I & 0 \\ 0 & -\widehat{d_1} \\ 0 & -\widehat{d_2} \\ 0 & -\widehat{d_3} \end{pmatrix} \tag{6.39}$$

corresponding to the constraints (6.35) has been derived. Here $\widehat{a}$ denotes the skew-symmetric 3×3 matrix with corresponding axial vector $a \in \mathbb{R}^3$. With the null space matrix, the independent generalized velocities of the rigid body, namely the translational velocity $\dot{\varphi} \in \mathbb{R}^3$ and the angular velocity $\omega \in \mathbb{R}^3$ being comprised in the twist of the rigid body

$$t = \begin{pmatrix} \dot{\varphi} \\ \omega \end{pmatrix} \tag{6.40}$$

can be mapped to the redundant velocities $\dot{q} = P(q) \cdot t$.

Nodal reparametrization When the nodal reparametrization of unknowns is applied, the configuration of the free rigid body is specified by six unknowns $u_{k+1} = (u_{\varphi_{k+1}}, \theta_{k+1}) \in U \subset \mathbb{R}^3 \times \mathbb{R}^3$, characterizing the incremental displacement and incremental rotation, respectively. Accordingly, in the present case the nodal reparametrization $F : U \to C$ introduced in (6.15) assumes the form

$$q_{k+1} = F_d(u_{k+1}, q_k) = \begin{pmatrix} \varphi_k + u_{\varphi_{k+1}} \\ \exp(\widehat{\theta_{k+1}}) \cdot (d_1)_k \\ \exp(\widehat{\theta_{k+1}}) \cdot (d_2)_k \\ \exp(\widehat{\theta_{k+1}}) \cdot (d_3)_k \end{pmatrix}, \tag{6.41}$$

where Rodrigues' formula is used to obtain a closed form expression of the exponential map, see for example [111].

6.3.2 Actuation of the rigid body

The single rigid body can be actuated by generalized forces consisting of a translational force $\tau_\varphi \in \mathbb{R}^3$ and a torque $\tau_\theta \in \mathbb{R}^3$. Assume that the force is not applied in the center of mass, but in material points of the rigid body located at

$$\varrho = \varrho_I d_I \tag{6.42}$$

away from the center of mass. This results in the force τ_φ^1 to be applied in the center of mass and a torque τ_θ^1 as

$$\tau_\varphi^1 = \tau_\varphi \quad \text{and} \quad \tau_\theta^1 = \tau_\theta + \varrho \times \tau_\varphi. \tag{6.43}$$

Then the redundant forces can be computed as

$$f_\varphi = \tau_\varphi^1 \quad \text{and} \quad f_I = \frac{1}{2}\tau_\theta^1 \times d_I. \tag{6.44}$$

For the rigid body, the transformation (6.16) of the generalized forces acting in $[t_{k-1}, t_k]$ and in $[t_k, t_{k+1}]$ to the time node t_k reads

$$\begin{aligned} \tau_{\varphi k-1}^{1+} &= \frac{h}{2}\tau_{\varphi k-1} \quad \text{and} \quad \tau_{\theta\, k-1}^{1+} = \frac{h}{2}\left(\tau_{\theta k-1} + \varrho_k \times \tau_{\varphi k-1}\right), \\ \tau_{\varphi k}^{1-} &= \frac{h}{2}\tau_{\varphi k} \quad \text{and} \quad \tau_{\theta\, k}^{1-} = \frac{h}{2}\left(\tau_{\theta k} + \varrho_k \times \tau_{\varphi k}\right). \end{aligned} \tag{6.45}$$

Insertion into (6.17) and taking into account (6.44) yields the 12-dimensional left and right discrete forces f_{k-1}^+, f_k^- for the rigid body. A straightforward calculation shows

$$P^T(q_k) \cdot (f_{k-1}^+ + f_k^-) = \begin{pmatrix} \tau_{\varphi k-1}^{1+} + \tau_{\varphi k}^{1-} \\ \\ \tau_{\theta\, k-1}^{1+} + \tau_{\theta\, k}^{1-} \end{pmatrix}. \tag{6.46}$$

Thus the resulting reduced forces in (6.18) are correct and meaningful.

Proposition 6.3.1 *The definition of the redundant left and right discrete forces guarantees that the change in angular momentum along the solution trajectory q_d of (6.18) is induced only by the discrete generalized forces.*

Proof: Computation of p^+_{k+1} and via p^-_k the discrete Legendre transforms (6.19a) and (6.19b), respectively, and insertion into the definition of angular momentum (6.38) yields

$$\begin{aligned}
&L_{k+1} - L_k = \\
&\varphi_{k+1} \times p^+_{\varphi k+1} + d_{Ik+1} \times p^+_{I\,k+1} - \varphi_k \times p^-_{\varphi k} - d_{Ik} \times p^-_{I\,k} = \\
&\varphi_{k+1} \times \left(f^+_{\varphi k}\right) + d_{Ik+1} \times \left(f^+_{I\,k}\right) - \varphi_k \times \left(-f^-_{\varphi k}\right) - d_{Ik} \times \left(-f^-_{I\,k}\right) = \\
&\varphi_{k+1} \times \tau^{1+}_{\varphi k} + \varphi_k \times \tau^{1-}_{\varphi k} + d_{Ik+1} \times \left(\frac{1}{2}\tau^{1+}_{\theta\,k} \times d_{Ik+1}\right) + d_{Ik} \times \left(\frac{1}{2}\tau^{1-}_{\theta\,k} \times d_{Ik}\right) = \\
&\varphi_{k+1} \times \tau^{1+}_{\varphi k} + \varphi_k \times \tau^{1-}_{\varphi k} + \tau^{1+}_{\theta\,k} + \tau^{1-}_{\theta\,k}.
\end{aligned} \tag{6.47}$$

□

Remark 6.3.2 (Gravitation) The computation in (6.47) is performed for the case in which no potential is present. In the presence of gravity of value $g \in \mathbb{R}$ in the negative e_3-direction, the corresponding potential reads

$$V(q) = \begin{pmatrix} 0 \\ 0 \\ -M_\varphi g \\ 0 \\ \vdots \\ 0 \end{pmatrix}^T \cdot q. \tag{6.48}$$

In this case, (6.47) yields

$$L_{k+1} - L_k = \varphi_{k+1} \times \tau^{1+}_{\varphi k} + \varphi_k \times \tau^{1-}_{\varphi k} + \tau^{1+}_{\theta\,k} + \tau^{1-}_{\theta\,k} - (\varphi_{k+1} + \varphi_k) \times \begin{pmatrix} 0 \\ 0 \\ -M_\varphi g \end{pmatrix}, \tag{6.49}$$

meaning that the third component of the angular momentum changes only according to the applied forces. In particular in the absence of any external forces, this shows that the third component of the angular momentum is exactly conserved.

6.3.3 Kinematic pairs

In this chapter, we present the constrained formulation of the dynamics of kinematic pairs and the subsequent reduction of the equations of motion via the

discrete null space method with nodal reparametrization. Furthermore, we show how the generalized forces of a kinematic pair act on the respective bodies.

The coupling of two neighboring links (body 1 and body 2) by a specific joint J yields $m_{ext}^{(J)}$ *external constraints* $g_{ext}(q) \in \mathbb{R}^{m_{ext}^{(J)}}$ where

$$q = \begin{pmatrix} q^1 \\ q^2 \end{pmatrix}. \tag{6.50}$$

Depending on the number of external constraints $m_{ext}^{(J)}$, the degrees of freedom of the relative motion of one body with respect to the other is decreased from 6 to $r^{(J)} = 6 - m_{ext}^{(J)}$.

Altogether, $m = m_{int} + m_{ext}$ constraints describing the multi-body system and the corresponding constraint Jacobians can be combined to

$$g(q) = \begin{pmatrix} g_{int}(q) \\ g_{ext}(q) \end{pmatrix} \in \mathbb{R}^m, \qquad G(q) = \begin{pmatrix} G_{int}(q) \\ G_{ext}(q) \end{pmatrix} \in \mathbb{R}^{m \times n}. \tag{6.51}$$

In [96, 98] details of the external constraints caused by lower kinematic pairs and their treatment in the framework of the discrete null space method are discussed. With the null space matrices for kinematic pairs at hand, a generalization to multi-body systems being composed by pairs can be performed easily, see [7, 96, 97].

Null space matrix In a kinematic pair, the motion of the second body with respect to an axis fixed in the first body can be accounted for by introducing $r^{(J)}$ joint velocities $\tau^{(J)}$. Thus the motion of the kinematic pair can be characterized by the independent generalized velocities $\nu^{(J)} \in \mathbb{R}^{6+r^{(J)}}$ with

$$\nu^{(J)} = \begin{pmatrix} t^1 \\ \tau^{(J)} \end{pmatrix}. \tag{6.52}$$

In particular, introducing the $6 \times (6 + r^{(J)})$ matrix $P_{ext}^{2,(J)}(q)$, the twist of the second body $t^2 \in \mathbb{R}^6$ can be expressed as

$$t^{2,(J)} = P_{ext}^{2,(J)}(q) \cdot \nu^{(J)}. \tag{6.53}$$

Accordingly, the twist of the kinematic pair J can be written in the form

$$t^{(J)} = P_{ext}^{(J)}(q) \cdot \nu^{(J)} \tag{6.54}$$

with the $12 \times (6 + r^{(J)})$ matrix $P_{ext}^{(J)}(q)$, which may be partitioned according to

$$P_{ext}^{(J)}(q) = \begin{pmatrix} I_{6\times 6} & 0_{6\times r^{(J)}} \\ P_{ext}^{2,(J)}(q) \end{pmatrix}. \tag{6.55}$$

Once $P_{ext}^{(J)}(q)$ has been established, the total null space matrix pertaining to the kinematic pair under consideration can be calculated from

$$P^{(J)}(q) = P_{int}(q) \cdot P_{ext}^{(J)}(q) = \begin{pmatrix} P_{int}^{1}(q^1) & 0_{12\times r^{(J)}} \\ P_{int}^{2}(q^2) \cdot P_{ext}^{2,(J)}(q) \end{pmatrix}. \tag{6.56}$$

Finally, the 24-dimensional redundant velocity vector of the kinematic pair can be expressed in terms of the independent generalized velocities $\nu^{(J)} \in \mathbb{R}^{6+r^{(J)}}$ via

$$\dot{q} = P^{(J)}(q) \cdot \nu^{(J)}. \tag{6.57}$$

Provided that $P_{ext}^{2,(J)}(q)$ has been properly deduced from (6.53),

$$\dot{q} \in \text{null } (G^{(J)}(q)), \tag{6.58}$$

and the above procedure warrants the design of viable null space matrices which automatically satisfy the relationship

$$G^{(J)}(q) \cdot P^{(J)}(q) = 0. \tag{6.59}$$

To summarize, in order to construct a null space matrix pertaining to a specific kinematic pair, essentially relationship (6.53) is applied to deduce the matrix $P_{ext}^{2,(J)}(q)$. Once $P_{ext}^{2,(J)}(q)$ has been determined, the complete null space matrix pertaining to a specific pair follows directly from (6.56).

Nodal reparametrization Corresponding to the independent generalized velocities $\nu^{(J)} \in \mathbb{R}^{6+r^{(J)}}$ introduced in (6.52), the redundant coordinates $q \in \mathbb{R}^{24}$ of each kinematic pair J may be expressed in terms of $6 + r^{(J)}$ independent generalized coordinates. Concerning the reparametrization of unknowns in the discrete null space method, relationships of the form

$$q_{k+1} = F^{(J)}(\mu_{k+1}^{(J)}, q_k) \tag{6.60}$$

are required, where

$$\mu_{k+1}^{(J)} = (u_{\varphi_{k+1}}^{1}, \theta_{k+1}^{1}, \vartheta_{k+1}^{(J)}) \in \mathbb{R}^{6+r^{(J)}} \tag{6.61}$$

consists of a minimal number of incremental unknowns in $[t_k, t_{k+1}]$ for a specific kinematic pair. In (6.61), $(u_{\varphi_{k+1}}^{1}, \theta_{k+1}^{1}) \in \mathbb{R}^3 \times \mathbb{R}^3$ are incremental displacements and rotations, respectively, associated with the first body (see Section 6.3.1). Furthermore, $\vartheta_{k+1}^{(J)} \in \mathbb{R}^{r^{(J)}}$ denote incremental unknowns which characterize the configuration of the second body relative to the axis of relative motion fixed in the

first body. In view of (6.50), the mapping in (6.60) may be partitioned according to

$$\begin{aligned} q^1_{k+1} &= F^1(u^1_{\varphi_{k+1}}, \theta^1_{k+1}, q^1_k), \\ q^2_{k+1} &= F^{2,(J)}(\mu^{(J)}_{k+1}, q_k). \end{aligned} \tag{6.62}$$

Here, $F^1(u^1_{\varphi_{k+1}}, \theta^1_{k+1}, q^1_k)$ is given by (6.41). It thus remains to specify the mapping $F^{2,(J)}(\mu^{(J)}_{k+1}, q_k)$ for each kinematic pair under consideration. Of course, the mapping $F^{(J)}(\mu^{(J)}_{k+1}, q_k)$ is required to satisfy the constraints specified by (6.51), that is $g^{(J)}_{ext}(F^{(J)}(\mu^{(J)}_{k+1}, q_k)) = 0$, for arbitrary $\mu^{(J)}_{k+1}$.

In [7, 96] details of the treatment of specific kinematic pairs J are provided. In essence, the present approach requires the specification of (i) the external constraint function $g^{(J)}_{ext}(q)$, along with the corresponding constraint Jacobian $G^{(J)}_{ext}(q)$, and (ii) the null space matrix $P^{2,(J)}_{ext}(q)$, which is needed to set up the complete null space matrix (6.56). Finally, (iii) the mapping $F^{2,(J)}(\mu^{(J)}_{k+1}, q_k)$ is specified, which is needed to perform the reparametrization of unknowns according to (6.60), and allows the reduction of the discrete system of equations of motion to the minimal possible dimension.

Actuation of a kinematic pair The actuation of kinematic pairs is twofold. First of all, the overall motion of the pair can be influenced by applying translational forces $\tau_\varphi \in \mathbb{R}^3$ and torques $\tau_\theta \in \mathbb{R}^3$ to one of the bodies, say body 1. Any resulting change in the first bodies velocities will be transferred to the second body via the constrained equations of motion. Secondly, the relative motion of the pair can be influenced. Actuation of the joint connection itself affects both bodies, where according to actio equals reactio, the resulting generalized forces on the bodies are equal, but opposite in sign. The dimension of the joint force $\tau^{(J)}$ is determined by the number of relative degrees of freedom $r^{(J)}$ permitted by the specific joint.

The forces τ^α_φ and torques τ^α_θ on the α-th body depend on $\tau_\varphi, \tau_\theta$ and $\tau^{(J)} \in \mathbb{R}^{r(J)}$ according to the specific joint used. The redundant forces f^α on each body can then be computed analogous to (6.44) by

$$f^\alpha_\varphi = \tau^\alpha_\varphi \quad \text{and} \quad f^\alpha_I = \frac{1}{2}\tau^\alpha_\theta \times d^\alpha_I, \tag{6.63}$$

and the total redundant force vector reads

$$f = \begin{pmatrix} f^1 \\ f^2 \end{pmatrix}. \tag{6.64}$$

Besides depending on the translational forces $\tau_{\varphi_{k-1}}, \tau_{\varphi_k}$ and torques $\tau_{\theta_{k-1}}, \tau_{\theta_k}$, the resulting forces and torques on body 1 in (6.45) now include the effect of the joint actuation ${\tau^{(J)}_{k-1}}^+ = \frac{h}{2}\tau^{(J)}_{k-1}$ and ${\tau^{(J)}_k}^- = \frac{h}{2}\tau^{(J)}_k$.

Similar to (6.46), the product of the null space matrix and the redundant forces of the kinematic pair yields

$$P^T(q_k) \cdot (f_{k-1}^+ + f_k^-) = \begin{pmatrix} \tau_{\varphi\,k-1}^{1\,+} + \tau_{\varphi\,k}^{1\,-} \\ \\ \tau_{\theta\,k-1}^{1\,+} + \tau_{\theta\,k}^{1\,-} \\ \\ \tau_{k-1}^{(J)\,+} + \tau_k^{(J)\,-} \end{pmatrix}. \tag{6.65}$$

In [98] an overview of various lower kinematic pairs, their representation and their actuation are given in detail. Additionally, it is proved for various specific joints that the change in angular momentum along the solution trajectory q_d of (6.18) is induced only by the discrete generalized forces.

6.4 Applications

In this section, we demonstrate the optimal control method for two multi-body systems arising in applications from robotics and biomechanics. Besides demonstrating the suitability of the methodology to optimally control the motion of real systems with high complexity, the preservation properties of the algorithm are numerically shown.

6.4.1 Optimal control of a rigid body with rotors

Fully actuated case

Inspired by space telescopes such as the Hubble telescope, whose change in orientation is induced by external spinning rotors, we analyze a multi-body system consisting of a main body to which rotors are connected by revolute joints. The revolute joints allow each rotor to rotate relative to the main body around an axis through its center which is fixed in the main body. The goal is to determine optimal torques to guide the main body into the final position $u_\theta^T = \frac{\pi}{14}(1,2,3)$, where the absolute reparametrization $q_k = F(u_k, q_0)$ is used instead of (6.15) here. The motion starts and ends at rest. The duration is 5 seconds and the time step is $h = 0.1$, thus $N = 50$. The objective function $\bar{J}_d = h\sum_{k=0}^{N-1} ||\tau_k||^2$ represents the control effort to be minimized. Due to the presence of three rotors with non-planar axes of rotation, this problem is fully actuated.

Figure 6.3 shows the configuration of the system at $t = 0, \ldots, 5$ seconds. The static frame represents the required final orientation where the axes must coincide with the centers of the rotors as the motion ends (see last picture). The optimal torques, which are constant in each time interval, are depicted in Figure 6.4.

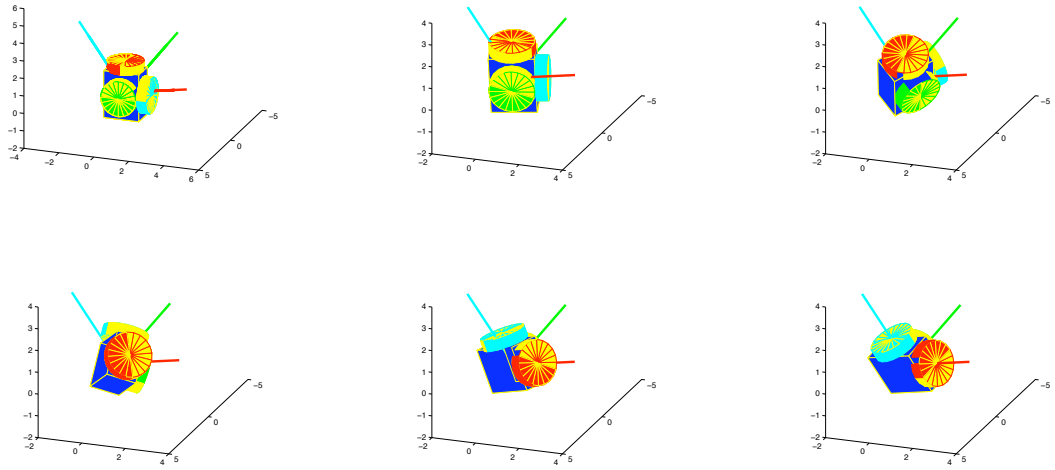

Figure 6.3: Rigid body with three rotors: configuration at $t = 0, \ldots, 5$ ($h = 0.1$).

They yield a control effort of $\bar{J}_d = 2.8242 \cdot 10^6$. Finally Figure 6.5 illustrates the evolution of the kinetic energy and a special attribute of the system under consideration. It has a geometric phase which means that the motion occurs although the total angular momentum remains zero at all times. As shown in Figure 6.5, the algorithm is able to represent this correctly.

Underactuated case

The same rest-to-rest maneuver is investigated for the underactuated system where one momentum wheel has been removed. Using the same time step and the same number of time steps as for the fully actuated case, the reorientation maneuver depicted in Figure 6.6 requires only slightly more control effort $\bar{J}_d = 2.9168 \cdot 10^6$.

Consistency of angular momentum is observable from Figure 6.8. It also shows that the energy does not evolve as symmetrically as for the fully actuated problem. That means that acceleration phase and breaking phase are not exactly inverse to each other. This becomes also obvious from Figure 6.7 which shows the evolution of the optimal generalized forces.

6.4.2 Biomechanics: The optimal pitch

Motivated by the determination of the optimal motion sequences of a gymnast in Section 5.4.2, in this section we aim at the investigation of the optimal pitch.

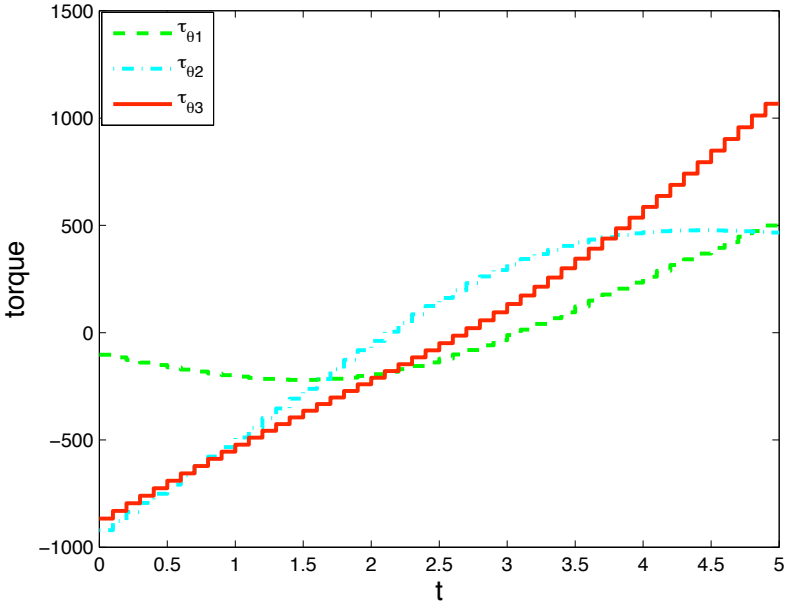

Figure 6.4: Rigid body with three rotors: torque over time ($h = 0.1$).

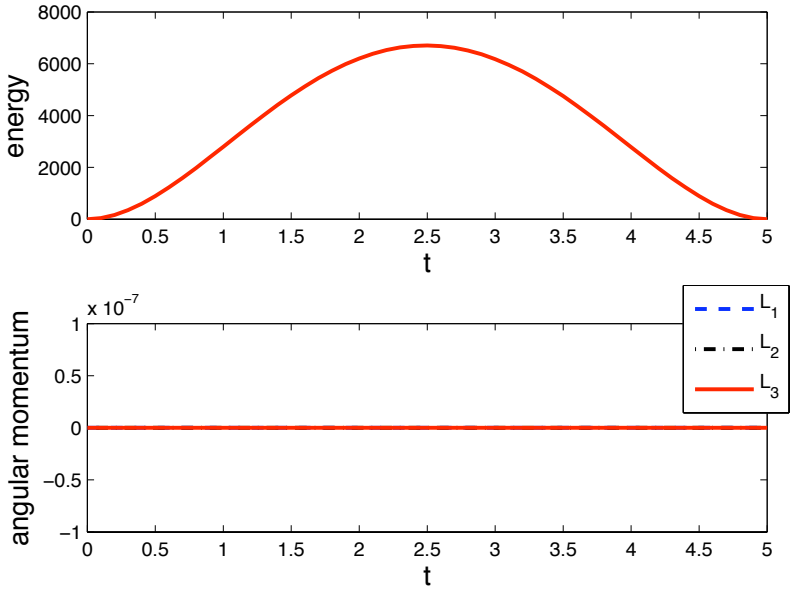

Figure 6.5: Rigid body with three rotors: energy and components of angular momentum vector $L = L_I e_I$ over time ($h = 0.1$).

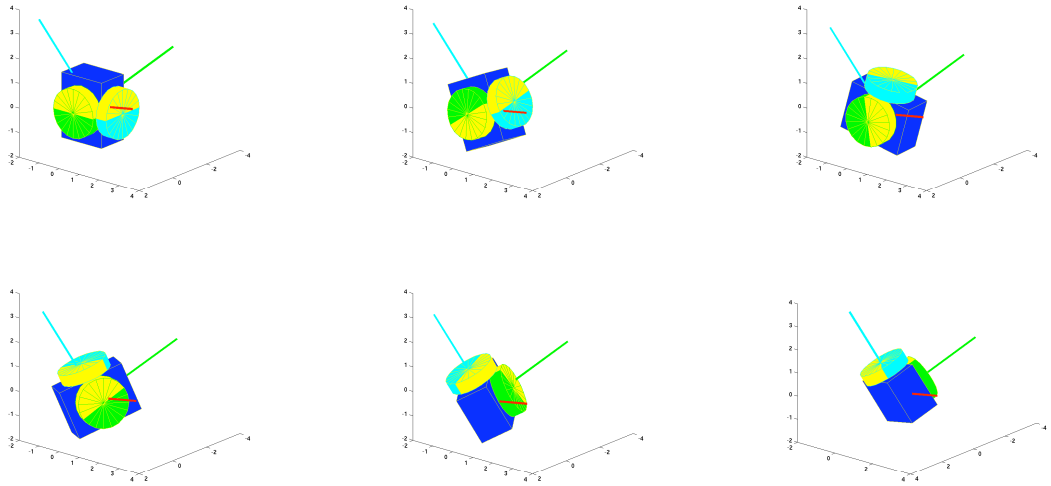

Figure 6.6: Rigid body with two rotors: configuration at $t = 0, \ldots, 5$ ($h = 0.1$).

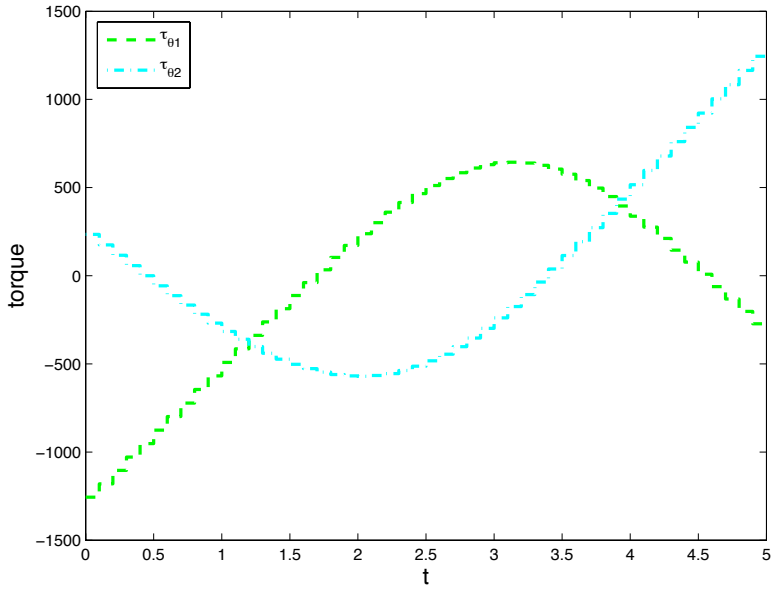

Figure 6.7: Rigid body with two rotors: torque over time ($h = 0.1$).

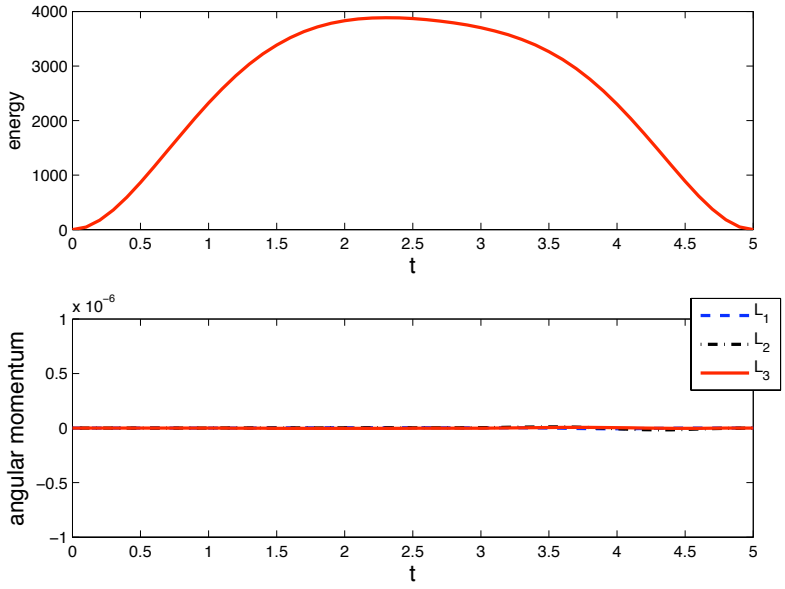

Figure 6.8: Rigid body with two rotors: energy and components of angular momentum vector $L = L_I e_I$ over time ($h = 0.1$).

We model the collarbone, the upper and the forearm as multi-body system (see Figure 6.9), where the single bodies are interconnected by joints and actuated via external control torques representing the muscle activation.

Model The first rigid body, representing the collarbone is assumed to be fixed in the inertial frame via a revolute joint modelling the rotation of the torso around the e_3-axes. Collarbone and upper arm are connected via a spherical joint, representing the three dimensional rotation of the shoulder. A revolute joint serves as the elbow between upper and forearm allowing the forearm to rotate around a prescribed axis fixed in the upper arm.

The actuations via the muscles are modeled as external torques $\tau_i,\ i = 1, 2, 3$, acting in the joints. Here, it is assumed that all degrees of freedom, that is the rotations of the collarbone, the shoulder and the elbow, are directly steerable. That means there is one rotational torque $\tau_s \in \mathbb{R}^3$ acting in the shoulder joint and two scalar torques τ_c and $\tau_e \in \mathbb{R}$ acting in the first revolute joint and the elbow joint, respectively. We describe the system by five generalized joint coordinates $\theta_1, \theta_5 \in S^1$, and $\theta_s = (\theta_2, \theta_3, \theta_4) \in SO(3)$ that constitute the degrees of freedom actuated by the torques.

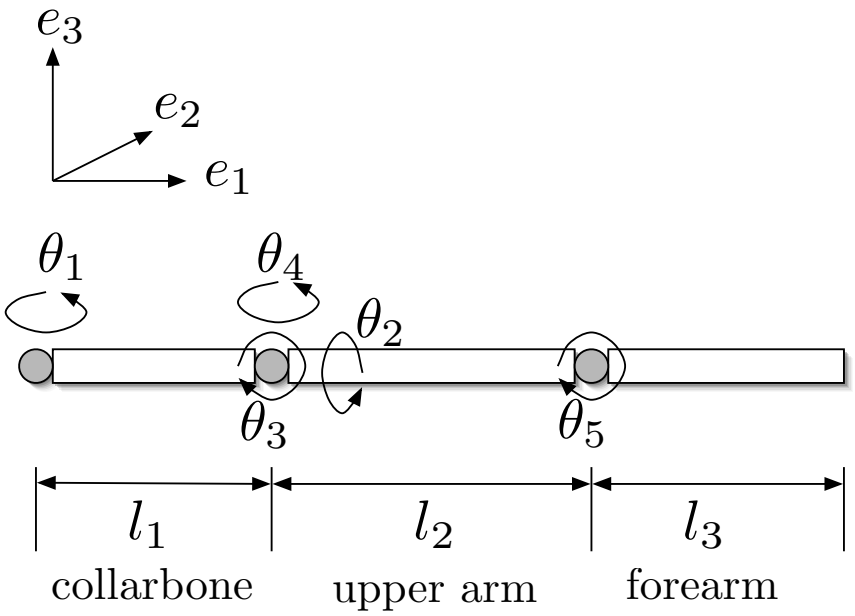

Figure 6.9: Model for a pitcher's arm consisting of collarbone, upper arm, and fore arm.

Boundary conditions, objective functional and path constraints The pitcher is assumed to begin his motion with prescribed initial configuration and zero velocity. Rather than prescribing final configurations for all present bodies, we formulate a limited, but not fixed final configuration of the hand position[2], for example positive e_2- and e_3-position. Due to the human body's anatomy each joint has only a limited degree of freedom. To obtain realistic motions, each generalized configuration variable is bounded as $\theta_i^l \leq \theta_i \leq \theta_i^u,\ i = 1, \ldots, 5$, for example the forearm is assumed to bend in only one direction. In addition we also need to incorporate bounds $\tau_i^l \leq \tau_i \leq \tau_i^u,\ i = 1, \ldots, 5$, on the control torques, since the muscles are not able to create an arbitrary amount of strength.

The goal is to maximize the velocity of the hand in e_2-direction. During the optimization the final time is free, that means we also determine the optimal duration of the pitch.

Numerical results Starting from an initial position of the joints as $\theta_1 = \theta_2 = \theta_3 = \theta_4 = 0$, $\theta_5 = -\frac{\pi}{4}$, we obtain, depending on the initial guesses for the optimization problem, different solutions for the optimal motion. In Figure 6.10

[2]Since the hand is not modeled as a separate rigid body within the system, we assume it to be located at the endpoint of the forearm.

snapshots of a particular locally optimal motion are depicted with the optimal final time $T = 0.306$. The final configuration and velocity of the hand is $q_{hand} = (0.009,\ -0.662,\ 0.363)$ and $\dot{q}_{hand} = (-3.359,\ -48.575,\ 21.070)$. Starting from the initial configuration shown in the first picture, the pitcher strikes out rearwards, pulls his arm above his head, before he finally moves his arm like a whip to obtain the necessary swing to maximize the final velocity.

This application demonstrates the capacity of the developed method for the optimal control of constrained multi-body dynamics in biomotion. Based on first results presented within this thesis, an analysis of different local optimal solutions varying in the values for the objective functional, the time duration and the applied control effort is investigated in [151].

To obtain more realistic motions, the next step is to consider more complex and thus more realistic models that behave more realistically. For example, instead of modeling the actuation of the limbs by external control torques, the interaction of the muscles and the resulting muscle force can be modeled as well (as also investigated in [151]). Due to the constrained formulation of multi-body dynamics, model extensions can easily be incorporated by coupling new bodies to the system via constraints.

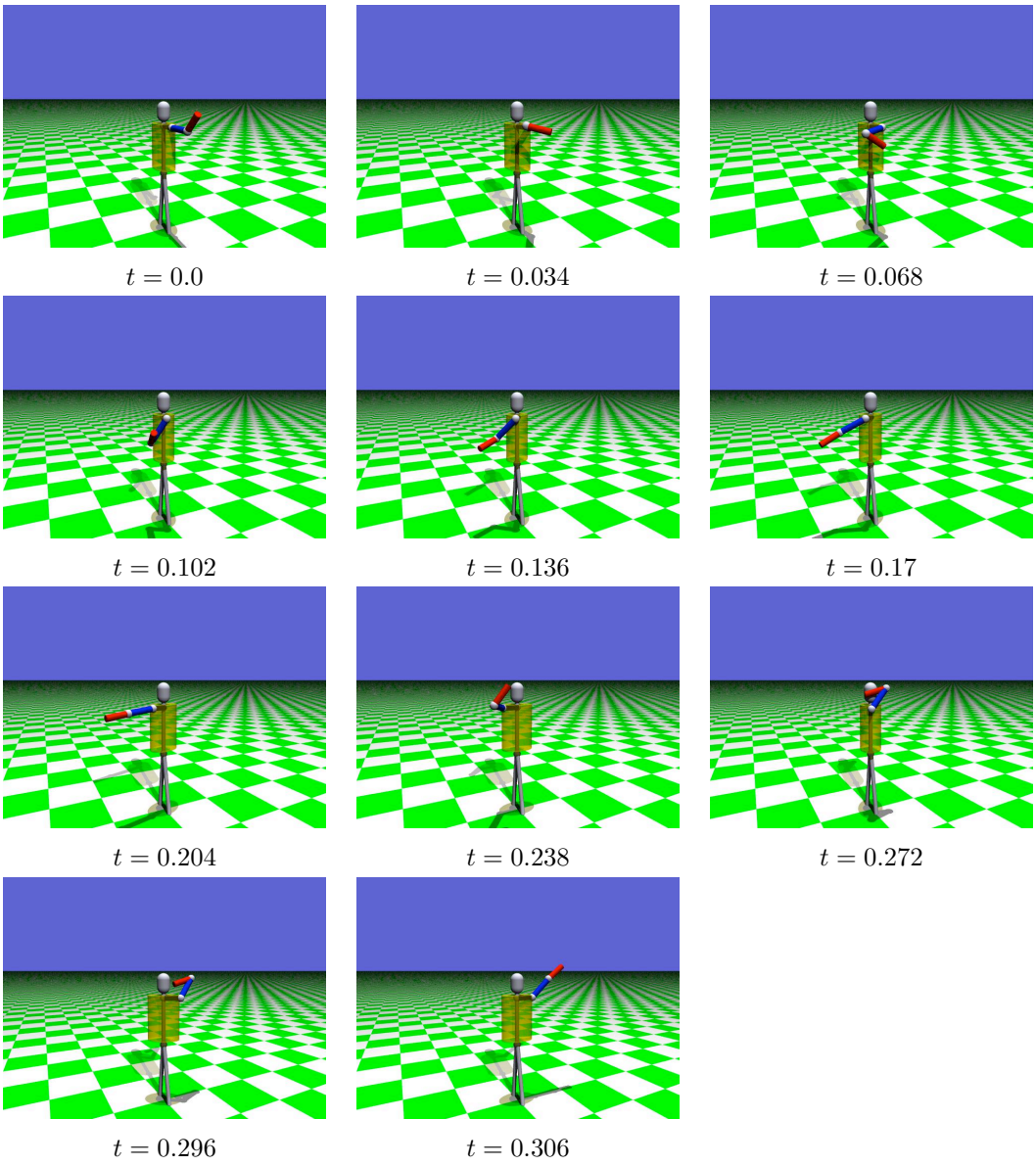

Figure 6.10: The optimal pitch: snapshots of the motion sequence.

Chapter 7

Conclusions and outlook

Analogous to the variational formulation of the continuous optimal control of mechanical systems, in this thesis a fully discrete formulation is developed. Based on discrete variational principles on all levels the discrete optimal control problem yields a strategy for the efficient solution of these kinds of problems. This optimal control methodology is denoted by DMOC.

In contrast to other methods that rely on a direct integration of the associated ordinary differential equations or on its fulfillment at certain grid points (for example shooting, multiple shooting, or collocation methods), DMOC is based on the discretization of the variational structure of the mechanical system. In the context of variational integrators, the discretization of the Lagrange-d'Alembert principle leads to structure-preserving time-stepping equations which serve as equality constraints for the resulting finite dimensional nonlinear optimization problem. This can be solved by standard nonlinear optimization techniques like sequential quadratic programming.

The benefits of variational integrators are passed on to the optimal control context. For example in the presence of symmetry groups in the continuous dynamical system, also along the discrete trajectory the change in momentum maps is consistent with the control forces (as also numerically shown for specific examples). Choosing the objective functional to represent the control effort to be minimized is only meaningful if the system responds exactly according to the control forces.

To discretize the optimal control problem, we approximate the tangent space via two copies of the configuration space itself, that means, the algorithm works on the configuration level rather than on the configuration-momentum or configuration-velocity level. This yields computational savings as we just determine the optimal trajectory for the configuration and the control forces and reconstruct the corresponding momenta and velocities via the forced discrete Legendre transform. The computational savings are numerically verified via a CPU time comparison

between DMOC and a collocation approach of the same order.

Due to the symplecticity of variational integrators, the order of approximation of the discrete adjoint dynamics is the same as for the state dynamics. This is in contrast to other standard non-symplectic discretizations. This fact guarantees a convergence rate of the algorithm depending on the order of discretization of the underlying mechanical system and is numerically confirmed via the convergence rate computation in a simple standard example.

Besides theoretical and numerical investigations of the proposed optimal control method, we developed efficient decentralized computational approaches to exploit system structures based on a hierarchical decomposition of the problem under consideration. This approach reduces the discrete optimal control system to a set of several smaller identical subproblems. In this way, the computational effort of the optimization algorithm can be decreased significantly by parallel computations as numerically demonstrated.

Finally, we developed an efficient approach to solving problems in mechanics with holonomic constraints occurring in multi-body dynamics. The presented strategy enables us to treat interesting and exciting applications in robotics and biomechanics in an accurate and computationally efficient way.

Outlook

Open problems

Although the developed method works very successfully in the examples considered within this thesis, there are still some open problems and challenges.

Evolution of conserved quantities for controlled systems When applying symplectic integration to a conservative system, a certain modified energy of the original system is conserved (see for example [55]). This is an important property if the long-term behavior of dynamical systems is considered. When forcing or dissipation is added to a Lagrangian or a Hamiltonian system, then the symplectic form, the momentum maps and the energy are no longer preserved by the flow. However, it is often important to be able to correctly simulate the amount by which these quantities change over time. For the case of the optimal control of systems with a long maneuver time, such as low thrust space missions, it would be interesting to investigate the balance between modified energy and virtual work. The variational framework for discrete systems with forcing given in Section 3 offers a way in which this evolution can be studied, both for the discrete system and for the true Lagrangian system. Concepts and ideas of variational

backward error analysis and variational integrators with forcing might be helpful for theoretical investigations.

Convergence for state constraint problems From an optimal control point of view a convergence result in the presence of state constraints would be important and interesting. In particular, for applications from biomechanics involving the human body, the incorporation of appropriate bounds on the joints is crucial to guarantee realistic motions that are in accordance with the body's anatomy. These state constraints complicate the dynamics of the system and pose theoretical questions about the convergence of the used control method. On the other hand, the application of homotopy or continuation techniques might be helpful to improve and speed up the convergence of the optimization algorithm. The solution of a simplified problem with relaxed or even no state constraints can be useful to find a solution for a less simplified problem.

Future directions

Having built the appropriate variational framework for the optimal control of mechanical systems, there are many directions one could focus on for future investigations.

The framework could be extended to the optimal control of mechanical systems with **stochastic influence** or **contact problems** making use of the theory of stochastic ([26]) and nonsmooth variational integrators ([44]), respectively. Due to the variational formulation of DMOC, an extension towards the optimal control of **partial differential equations** for the treatment of fluid and continuum mechanics might be interesting as well (see [112, 108] for basic extensions of variational integrators to the context of PDEs).

From a computational point of view, the savings in CPU time using hierarchical decentralized approaches indicate worthwhile extensions of a **spatial and time hierarchical decomposition** of complex networked systems.

Appropriate areas of application comprising the proposed extensions are hybrid optimal control systems and the optimal control of complex multi-body systems in biomechanics:

Hybrid systems Approaches from variational collision integrators might be helpful to find a variational formulation for hybrid optimal control systems, in particular, for systems whose discrete behavior is determined via contact conditions describing instantaneous changes in velocity, acceleration, and forces. In the second place, an efficient computational approach has to be developed to treat the discontinuities within the optimal control problem. In general, both

the collision point and the collision time are a priori unknown. In principle, a multi-phase optimal control problem with unknown phase transition times and states is associated with each of the discrete state sequence candidates. Akin to the decentralized method applied for the control of formation flying satellites in Section 5.5, a decomposition approach is possible: in an inner loop multi-phase optimal control problems are numerically solved for a given sequence of phases in parallel whereas the order and type of phases is varied during the outer iteration. A simplified version of this approach was already applied to the optimal control of a compass gait biped ([124]).

Relevant applications are the actuation of systems with contact, for example collisions of vehicle formations or walking robots. In addition, the developed concepts and methods for the control of hybrid systems find an ideal application in the control of biomechanical systems, such as the contact of club and ball in optimizing a golf swing.

Complex multi-body systems in biomechanics It is of great interest to understand the muscle activation and coordination of the human body for several reasons, for example to construct prostheses and implants in modern medical surgery. Another area of growing interest is the optimization of movements in sports. The knowledge gained from optimal control simulations might help to improve individual techniques or might even suggest the development of new techniques (as it has been observed during the last decades, for example for high and ski jumping). In order to optimize the human body's movements, the development of robust models, structure exploiting control methods, and efficient computational techniques are in demand.

Due to the high complexity of the dynamics for an increasing number of connected rigid bodies, it is important to identify those limbs and those parts of the body that are important for the underlying task. The activation of muscles depending on the configuration and velocity of the corresponding joint angle has to be included in the model. The initial steps in that direction are presented in [151]. Here, the motion of a pitcher's arm is optimized, with the muscles modeled by the Hill model; ([148]) the activation levels are treated as control parameters. Besides the incorporation of appropriate bounds on the joints due to the human body's anatomy, the choice of an objective functional is important for the quality of the optimal solution. Depending on the specific task, one or multiple objectives have to be determined. The development of a hierarchical decomposition of the overall system is applicable for these kinds of applications. Here, optimal solutions for a system consisting of only the most relevant parts of the human body are used to create solutions for more complex models including additional limbs. Due to the constrained formulation of multi-body dynamics, model extensions

can easily be incorporated by coupling new bodies to the system via constraints. This procedure is assumed to improve and speed up the convergence properties of the optimization algorithm of the complex dynamical multi-body systems. Convergence and optimality of solutions resulting from the hierarchical approach should be compared to a non-hierarchical one. In addition, different models and different objectives for different phases of the motion sequence are logical (see for example the different phases of a long jump motion).

Furthermore, to account for the uncertainties arising from the discrepancy between the model and reality and the difficulty of measuring model parameters as for the muscles, a stochastic component can be included in the model.

In summary, this thesis gives initial impulses in the direction of a complete discrete variational point of view of the optimal control in mechanics. As indicated by the long list of possible future directions, it is an exciting and worthwhile area of research where there is still a large potential for the development of new and efficient techniques for relevant applications.

Appendix A

Definitions

The following standard definitions are mainly based on the representations in [111].

Definition A.1 (Differentiable manifold) Given a set M, a *chart* on M is an open set U in Euclidean space $\mathbb{R}^n$ with coordinates $(x^1, \ldots, x^n)$ (more generally U can be open in a Banach space) together with a one-to-one map φ of U onto some subset of M,

$$\varphi : U \to \varphi(U) \subset M.$$

We call M a *differentiable manifold* if the following holds:

(M1) It is covered by a collection of charts, that is, every point is represented in at least one chart.

(M2) If two charts U, U' have an overlapping image in M, then $V = \varphi^{-1}(\varphi(U) \cap \varphi'(U'))$ and $V' = (\varphi')^{-1}(\varphi(U) \cap \varphi'(U'))$ are open sets in $\mathbb{R}^n$. Hence the mapping $\varphi'^{-1} \circ \varphi : V \to V'$ from an open subset of $\mathbb{R}^n$ to a subset of $\mathbb{R}^n$ is defined. The charts U, U' are called *compatible* if these n functions of n variables $\varphi'^{-1} \circ \varphi$ are C^∞.

(M3) M has an *atlas*, that is, M can be written as a union of compatible charts.

Two atlases are called *equivalent* if their union is also an atlas. One often rephrases the definition by saying that a differentiable structure on a manifold is an equivalence class of atlases.

A *neighborhood* of a point x in a manifold M is the image under a map $\varphi : U \to M$ of a neighborhood of the representation of x in a chart U. Neighborhoods define open sets and the open sets in M define a topology, that is assumed to be Hausdorff. A differentiable manifold M is called an n-manifold if every chart has domain in an n-dimensional vector space.

Definition A.2 (Differentiable submanifold) A subset S of a differentiable manifold M is a *differentiable submanifold* if, for each point $x \in S$, there is an admissible chart (U, φ) for M with $x \in U$, and such that

(i) φ takes its value in a product $\mathbb{R}^k \times \mathbb{R}^{n-k}$, and

(ii) $\varphi(U \cap S) = \varphi(U) \cap (\mathbb{R}^k \times \{0\})$.

A chart with these properties is a *submanifold chart* for S.

Definition A.3 (Tangent vector, tangent space, tangent bundle) Two curves $t \mapsto c_1$ and $t \mapsto c_2$ in an n-manifold M are called *equivalent at* x if

$$c_1(0) = c_2(0) = x \quad \text{and} \quad (\varphi^{-1} \circ c_1)'(0) = (\varphi^{-1} \circ c_2)'(0)$$

in some chart φ. This definition is chart independent. A *tangent vector* v to a manifold M at a point $x \in M$ is an equivalence class of curves at x. Let U be a chart of an atlas for M with coordinates $(x^1, \ldots, x^n)$. The *components* of the tangent vector v to the curve $t \mapsto (\varphi^{-1} \circ c)(t)$ are defined by

$$v^i = \frac{d}{dt}(\varphi^{-1} \circ c)^i \bigg|_{t=0}, \quad i = 1, \ldots, n.$$

The set of tangent vectors to M at x forms a vector space, called the *tangent space* to M at x, denoted by T_xM. The *tangent bundle* of M, denoted by TM, is the differentiable manifold whose underlying set is the disjoint union of the tangent spaces to M at the points $x \in M$, that is,

$$TM = \bigcup_{x \in M} T_xM.$$

Let $x^1, \ldots, x^n$ be local coordinates on M and let $v^1, \ldots, v^n$ be components of a tangent vector in this coordinate system. Then the $2n$ numbers $x^1, \ldots, x^n, v^1, \ldots, v^n$ give a local coordinate system on TM.

Definition A.4 (Natural projection, fiber) The *natural projection* is the map $\tau_M : TM \to M$ that takes a tangent vector v to the point $x \in M$ at which the vector is attached. The inverse image $\tau_M^{-1}(x)$ of a point $x \in M$ under the natural projection τ_M is the tangent space T_xM. This space is called the *fiber* of the tangent bundle over the point $x \in M$.

Definition A.5 (Derivative) Let $f : M \to N$ be a map of a manifold M to a manifold N. f is called *differentiable* (or C^k) if in local coordinates on M and N

it is given by differentiable (or C^k) functions. The *derivative* (or *tangent lift*) of a differentiable map $f : M \to N$ at a point $x \in M$ is defined to be the linear map

$$T_x f : T_x M \to T_{f(x)} N$$

constructed in the following way: For $v \in T_x M$, choose a curve $c :]-\epsilon, \epsilon[\to M$ with $c(0) = x$, and velocity vector $dc/dt|_{t=0} = v$. Then $T_x f \cdot v$ is the velocity vector at $t = 0$ of the curve $f \circ c : \mathbb{R} \to N$, that is

$$T_x f \cdot v = \frac{d}{dt} f(c(t))\bigg|_{t=0}.$$

The vector $T_x f \cdot v$ does not depend on the curve c but only on the vector v. If M and N are manifolds and $f : M \to N$ is of class C^{r+1}, then $Tf : TM \to TN$ is a mapping of class C^r.

Definition A.6 (Vector field, integral curve, flow) A *vector field* X on a manifold M is a map $X : M \to TM$ that assigns a vector $X(x)$ at the point $x \in M$, that is, $\tau_M \circ X = id$. An *integral curve* of X with initial condition x_0 at $t = 0$ is a (differentiable) map $c :]a, b[\to M$ such that $]a, b[$ is an open interval containing 0, $c(0) = x_0$ and

$$c'(t) = X(c(t))$$

for all $t \in]a, b[$. The *flow* of X is the collection of maps

$$\varphi_t : M \to M$$

such that $t \mapsto \varphi_t(x)$ is the integral curve of X with initial condition x.

Definition A.7 (Differential, cotangent bundle) Let M be a manifold and $f : M \to \mathbb{R}$ be a smooth function, we can differentiate it at any point $x \in M$ to obtain a map $T_x f : T_x M \to T_{f(x)}\mathbb{R}$. Identifying the tangent space of $\mathbb{R}$ at any point with itself, we get the linear map $\mathbf{d}f(x) : T_x M \to \mathbb{R}$. That is $\mathbf{d}f(x) \in T_x^* M$, the dual of the vector space $T_x M$, and reads in coordinates

$$\mathbf{d}f(x) \cdot v = \sum_{i=1}^{n} \frac{\partial f}{\partial x^i} v^i,$$

with $v \in T_x M$. (We will employ the summation convention and drop the summation sign when there are repeated indices.) $\mathbf{d}f$ is called the *differential* of f.

We can identify a basis of $T_x M$ using the operators $\partial/\partial x^i$ and write

$$(e_1, \ldots, e_n) = \left(\frac{\partial}{\partial x^1}, \ldots, \frac{\partial}{\partial x^n} \right)$$

for this basis so that $v = v^i \partial/\partial x^i$.

If we replace each vector space T_xM with its dual T_x^*M, we obtain a new $2n$-manifold called the *cotangent bundle* and denoted T^*M. The dual basis to $\partial/\partial x^i$ is denoted dx^i. Thus, relative to a choice of local coordinates we get the basic formula

$$\mathbf{d}f(x) = \frac{\partial f}{\partial x^i} dx^i$$

for any smooth function $f : M \to \mathbb{R}$.

Definition A.8 (Differential form) A *two-form* Ω on M is a function $\Omega(x) : T_xM \times T_xM \to \mathbb{R}$ that assigns to each point $x \in M$ a skew-symmetric bilinear form on the tangent space T_xM to M at x. More generally, a *k-form* α (also called *differentiable form of degree k*) on a manifold M is a function $\alpha(x) : T_xM \times \cdots \times T_xM$ (k factors) $\to \mathbb{R}$ that assigns to each point $x \in M$ a skew-symmetric k-multilinear map on the tangent space T_xM to M at x.

Let $x^1, \ldots, x^n$ denote coordinates on M, let

$$\{e_1, \ldots, e_n\} = \{\partial/\partial x^1, \ldots, \partial/\partial x^n\}$$

be the corresponding basis for T_xM, and let $\{e^1, \ldots, e^n\} = \{dx^1, \ldots, dx^n\}$ be the dual basis for T_x^*M. Then at each $x \in M$, we can write a two-form as

$$\Omega_x(v, w) = \Omega_{ij}(x) v^i w^j, \quad \text{where} \quad \Omega_{ij}(x) = \Omega_x\left(\frac{\partial}{\partial x^i}, \frac{\partial}{\partial x^j}\right),$$

and more generally a k-form can be written

$$\alpha_x(v_1, \ldots, v_k) = \alpha_{i_1 \ldots i_k}(x) v_1^{i_1} \ldots v_k^{i_k},$$

summed on $i_1, \ldots, i_k$, with

$$\alpha_{i_1 \ldots i_k}(x) = \alpha_x\left(\frac{\partial}{\partial x^{i_1}}, \ldots, \frac{\partial}{\partial x^{i_k}}\right),$$

and where $v_i = v_i^j \partial/\partial x^j$, with a sum on j.

Definition A.9 (Pullback, pushforward) Let $\varphi : M \to N$ be a C^∞ map from the manifold M to the manifold N and α be a k-form on N. The *pullback* $\varphi^*\alpha$ of α by φ is the k-form on M given by

$$(\varphi^*\alpha)_x(v_1, \ldots, v_k) = \alpha_{\varphi(x)}(T_x\varphi \cdot v_1, \ldots, T_x\varphi \cdot v_k).$$

If Y is a vector field on the manifold N and φ is a diffeomorphism, the pullback φ^*Y is a vector field on M defined by

$$(\varphi^*Y)(x) = T_x\varphi^{-1} \circ Y \circ \varphi.$$

If φ is a diffeomorphism, the *pushforward* φ_* is defined by $\varphi_* = (\varphi^{-1})^*$.

Definition A.10 (Interior product) Let α be a k-form on a manifold M and X a vector field. The *interior product* $\mathbf{i}_X\alpha$ (also called the contraction of X and α, and written $\mathbf{i}(X)\alpha$) is the $(k-1)$-form

$$(\mathbf{i}_X\alpha)_x(v_2,\ldots,v_k) = \alpha_x(X(x),v_2,\ldots,v_k)$$

for $x \in M$ and $(v_2,\ldots,v_k) \in T_xM$.

Definition A.11 (Exterior derivative) The *exterior derivative* $\mathbf{d}\alpha$ of a k-form α on M is the $(k+1)$-form on M, which is uniquely determined by the following properties:

(i) If α is a 0-form, that is, $\alpha = f \in C^\infty(M)$, then $\mathbf{d}f$ is the one-form which is the differential of f.

(ii) $\mathbf{d}\alpha$ is linear in α.

(iii) $\mathbf{d}\alpha$ satisfies the product rule, that is,

$$\mathbf{d}(\alpha\wedge\beta) = \mathbf{d}\alpha\wedge\beta + (-1)^k\alpha\wedge\mathbf{d}\beta,$$

where α is a k-form and β is an l-form.

(iv) $\mathbf{d}^2 = 0$, that is, $\mathbf{d}(\mathbf{d}\alpha) = 0$ for any k-form α.

(v) $\mathbf{d}$ is a local operator, that is, $\mathbf{d}\alpha(x)$ only depends on α restricted to any open neighborhood of x. If U is open in M, then

$$\mathbf{d}(\alpha|U) = (\mathbf{d}\alpha)|U.$$

Definition A.12 (Jacobi-Lie bracket) Let M be a smooth C^∞ manifold, $f \in \mathcal{F}(M)$ (with $\mathcal{F}(M)$ the set of continuously differentiable real-valued functions on M) and $X, Y : M \to TM$ two vector fields on M. Then the derivation

$$f \mapsto X[Y[f]] - Y[X[f]],$$

where $X[f] = \mathbf{d}f\cdot X$, determines a unique vector field denoted by $[X,Y]$ and called the *Jacobi-Lie bracket* of X and Y.

Definition A.13 (Cotangent lift) Given two manifolds M and N and a diffeomorphism $f : M \to N$, the *cotangent lift* $T^*f : T^*N \to T^*M$ of f is defined by

$$\langle T^*f(\alpha_s), v\rangle = \langle \alpha_s, (Tf\cdot v)\rangle,$$

where

$$\alpha_s \in T_s^*N, \quad v \in T_qM, \quad \text{and} \quad s = f(q).$$

Definition A.14 (Lie group) A *Lie group* is a differentiable manifold G that has a group structure consistent with its manifold structure in the sense that the group operations

$$\begin{aligned} \mu : G \times G \to G; &\quad (g,h) \mapsto gh \\ I : G \to G; &\quad g \mapsto g^{-1} \end{aligned}$$

are C^∞ maps. The maps $L_g : G \to G; h \mapsto gh$, and $R_h : G \to G; g \mapsto gh$ are called the *left and right translation maps*.

Definition A.15 (Left invariant vector field) A vector field X on G is called *left invariant* if for every $g \in G$, $L_g^* X = X$, that is, if

$$(T_h L_g) X(h) = X(gh)$$

for every $h \in G$.

Definition A.16 (Lie bracket, Lie algebra) Let V be a vector space and $[\cdot,\cdot] : V \times V \to V$ a *Lie bracket*, i. e. it is a bilinear, skew-symmetric map which fulfills the Jacobi-identity

$$[A,[B,C]] + [B,[C,A]] + [C,[A,B]] = 0 \quad \text{for all } A,B,C \in V.$$

Then the pair $(V,[\cdot,\cdot])$ is called *Lie algebra*.

More specific, every Lie group G induces a Lie algebra: the vector space $\mathfrak{X}_L(G)$ of left invariant vector fields on G is isomorphic to the tangential space T_eG to G at the neutral element e. Define the Lie bracket for $\xi, \eta \in T_eG$ by

$$[\xi,\eta] := [X_\xi, X_\eta](e),$$

where X_ξ, X_η are the vector fields induced by ξ and η, respectively, and $[X_\xi, X_\eta]$ is the Jacobi-Lie bracket of vector fields. This makes T_eG into a Lie algebra. It is denoted by $\mathfrak{g} = \mathrm{Lie}(G)$ and is called *Lie algebra of* G.

Definition A.17 (Exponential map) Let G be a Lie group. For all $\xi \in \mathfrak{g} = Lie(G)$ let $\gamma_\xi : \mathbb{R} \to G$ denote the integral curve of the left-invariant vector field X_ξ on G induced by ξ, which is defined uniquely by claiming

$$X_\xi(e) = \xi, \quad \gamma_\xi(0) = e, \quad \gamma_\xi'(t) = X_\xi(\gamma_\xi(t)) \quad \text{for all } t \in \mathbb{R}.$$

The map

$$\exp : \mathfrak{g} \to G, \quad \exp(\xi) = \gamma_\xi(1)$$

is called *exponential map* of the Lie algebra $\mathfrak{g}$ in G.

Definition A.18 (Action of Lie groups) Let M be a manifold and let G be a Lie group. A (*left*) *action* of a Lie group G on M is a smooth mapping $\phi : G \times M \to M$ such that:

(i) $\phi(e, x) = x$ for all $x \in M$, and

(ii) $\phi(g, \phi(h, x)) = \phi(gh, x)$ for all $g, h \in G$ and $x \in M$.

A *right action* is a map $\Psi : M \times G \to M$ that satisfies $\Psi(x, e) = x$ and $\Psi(\Psi(x, g), h) = \Psi(x, gh)$.

Definition A.19 (Infinitesimal generator) Suppose $\phi : G \times M \to M$ is an action. For $\xi \in \mathfrak{g}$, the map $\phi^\xi : \mathbb{R} \times M \to M$, defined by $\phi^\xi(t, x) = \phi(\exp t\xi, x)$, is an $\mathbb{R}$-action on M. In other words, $\phi_{\exp t\xi} : M \to M$ is a flow on M. The corresponding vector field on M, given by

$$\xi_M(x) := \left.\frac{d}{dt}\right|_{t=0} \phi_{\exp t\xi}(x),$$

is called the *infinitesimal generator* of the action corresponding to ξ.

Definition A.20 (Symplectic manifold) A *symplectic manifold* is a pair (P, Ω) where P is a manifold and Ω is a closed (weakly) nondegenerated two-form on P.

Ω is called *closed* if $\mathbf{d}\Omega = 0$, where $\mathbf{d}$ is the exterior derivative, and it is called *weakly nondegenerated* if for $z \in P$ the induced map $\Omega_z^\flat : T_zP \to T_z^*P$ with $\Omega_z^\flat(x)(y) = \Omega_z(x, y)$ is injective, i. e. let $x \in T_zP$, if $\Omega_z(x, y) = 0$ for all $y \in T_zP$ then $x = 0$. In the case of strong nondegeneracy $\Omega_z^\flat$ is an isomorphism.

If P is finite dimensional, weak nondegeneracy and strong degeneracy are equivalent.

Definition A.21 (Symplectic / canonical transformation) A differentiable map $f : P_1 \to P_2$ between symplectic manifolds (P_1, Ω_1) and (P_2, Ω_2) is called *symplectic* (or *canonical transformation*) if

$$f^*\Omega_2 = \Omega_1.$$

That is, by definition of the pullback of a two-form

$$(f^*\Omega_2)_z(x, y) = \Omega_{2_{f(z)}}(T_zf(x), T_zf(y)) = \Omega_{1_z}(x, y)$$

for each $z \in P_1$ and all $x, y \in T_zP_1$, with the derivative $T_zf : T_zP_1 \to T_{f(z)}P_2$.

Definition A.22 (Momentum map) Let a Lie algebra $\mathfrak{g}$ act canonically (on the left) on the symplectic manifold P. Suppose there is a linear map $J : \mathfrak{g} \to \mathcal{F}(P)$ such that

$$X_{J(\xi)} = \xi_P$$

for all $\xi \in \mathfrak{g}$. The map $\mathbf{J} : P \to \mathfrak{g}^*$ defined by

$$\langle \mathbf{J}(z), \xi \rangle = J(\xi)(z)$$

for all $\xi \in \mathfrak{g}$ and $z \in P$ is called a *momentum mapping* of the action.

Definition A.23 (Hamiltonian momentum map) Let the Lie algebra $\mathfrak{g}$ act on the left on the manifold M, such that $\mathfrak{g}$ acts on $P = T^*M$ on the left by the canonical action $\xi_P = \xi'_M$, where ξ'_M is the cotangent lift of ξ_M to P and $\xi \in \mathfrak{g}$. Then, the *Hamiltonian momentum map* $\mathbf{J}_H : P \to \mathfrak{g}^*$ is given by

$$\langle \mathbf{J}_H(\alpha_q), \xi \rangle = \langle \alpha_q, \xi_M(q) \rangle.$$

Definition A.24 (Lagrangian momentum map) Let the Lie algebra $\mathfrak{g}$ act on the left on the manifold M and assume that $L : TM \to \mathbb{R}$ is a regular Lagrangian. Endow TM with the Lagrangian symplectic form $\Omega_L = (\mathbb{F}L)^*\Omega$, where $\Omega = -\mathbf{d}\Theta$ is the canonical symplectic form on T^*M. Then $\mathfrak{g}$ acts canonically on $P = TM$ by

$$\xi_P(v_q) = \left.\frac{d}{dt}\right|_{t=0} T_q\varphi_t(v_q),$$

where φ_t is the flow of ξ_M and the *Lagrangian momentum map* $\mathbf{J}_L : TM \to \mathfrak{g}^*$ is given by

$$\langle \mathbf{J}_L(v_q), \xi \rangle = \langle \mathbb{F}L(v_q), \xi_M(q) \rangle.$$

Definition A.25 (Fiber-preserving map) A diffeomorphism $\varphi : T^*S \to T^*Q$ is a *fiber-preserving map* iff

$$f \circ \pi_Q = \pi_S \circ \varphi^{-1},$$

with $\pi_Q : T^*Q \to Q$ and $\pi_S : T^*S \to S$ the canonical projections and where $f : Q \to S$ is defined by $f = \varphi^{-1}|Q$. For $\varphi : T^*Q \to T^*Q$ being a *fiber-preserving map over the identity* it holds

$$id \circ \pi_Q = \pi_Q \circ \varphi^{-1},$$

and therefore, we have $\pi_Q \circ \varphi = \pi_Q$.

Definition A.26 (Vertical vector field, horizontal one-form) A vector field Y on TQ is *vertical* if $T\tau_Q \circ Y = 0$, with $\tau_Q : TQ \to Q$ the canonical projection. Such a vector field Y defines a *horizontal one-form* on TQ by

$$\Delta^Y = -\mathbf{i}_Y \Omega_L,$$

i. e. , $\Delta^Y(U) = 0$ for any vertical vector field U on TQ.

Proposition A.1 *Any fiber-preserving map $F : TQ \to T^*Q$ over the identity induces a horizontal one-form $\tilde{F}$ on TQ by*

$$\tilde{F}(v) \cdot V_v = \langle F(v), T_v\tau(V_v) \rangle, \tag{A.1}$$

where $v \in TQ$ and $V_v \in T_v(TQ)$. Conversely, equation (A.1) defines, for any horizontal one-form $\tilde{F}$ a fiber-preserving map F over the identity.

Proof: A proof can be found in [111].

Definition A.27 (Variation) Let $\gamma : [a, b] \to M$ be a C^2-curve. A *variation* of γ is a C^2-map $\vartheta : J \times [a, b] \to M$ with the properties

(i) $J \subset \mathbb{R}$ is an interval for which $0 \in \mathrm{int}(J)$,

(ii) $\vartheta(0, t) = \gamma(t)$ for all $t \in [a, b]$,

(iii) $\vartheta(s, a) = \gamma(a)$ for all $s \in J$, and

(iv) $\vartheta(s, b) = \gamma(b)$ for all $s \in J$.

The *infinitesimal variation* associated with a variation ϑ is the vector field along γ given by

$$\delta\vartheta(t) = \left.\frac{\mathrm{d}}{\mathrm{d}s}\right|_{s=0} \vartheta(s, t) \in T_{\gamma(t)}M.$$

Appendix B

Adjoint system

This section presents in detail how to derive the transformed adjoint system (4.46) from the discrete optimal control problem (4.43). Furthermore, its equivalence to the adjoint system (4.44) is shown.

Suppose that a multiplier $\lambda_{ki} = (\lambda^q_{ki}, \lambda^p_{ki})$ is introduced for the i-th intermediate equations (4.43c) and (4.43e) on $[t_k, t_{k+1}]$ in addition to the multiplier ψ_{k+1} for equations (4.43b) and (4.43d). Taking into account these additional multipliers, the Karush-Kuhn-Tucker equations are the following:

$$\psi^q_k - \psi^q_{k+1} = \sum_{i=1}^{s} \lambda^q_{ki}, \quad \psi^q_N = \nabla_q \Phi(q_N, p_N), \tag{B.1a}$$

$$\psi^p_k - \psi^p_{k+1} = \sum_{i=1}^{s} \lambda^p_{ki}, \quad \psi^p_N = \nabla_p \Phi(q_N, p_N), \tag{B.1b}$$

$$\begin{aligned} &h\left(b_j \psi^q_{k+1} + \sum_{i=1}^{s} \lambda^q_{ki} a^q_{ij}\right) \nabla_q \nu(Q_{kj}, P_{kj}) \\ &\quad + h\left(b_j \psi^p_{k+1} + \sum_{i=1}^{s} \lambda^p_{ki} a^p_{ij}\right) \nabla_q \eta(Q_{kj}, P_{kj}, U_{kj}) = \lambda^q_{kj}, \end{aligned} \tag{B.1c}$$

$$\begin{aligned} &h\left(b_j \psi^q_{k+1} + \sum_{i=1}^{s} \lambda^q_{ki} a^q_{ij}\right) \nabla_p \nu(Q_{kj}, P_{kj}) \\ &\quad + h\left(b_j \psi^p_{k+1} + \sum_{i=1}^{s} \lambda^p_{ki} a^p_{ij}\right) \nabla_p \eta(Q_{kj}, P_{kj}, U_{kj}) = \lambda^p_{kj}, \end{aligned} \tag{B.1d}$$

$$U_{kj} \in U, \quad -\left(b_j \psi^p_{k+1} + \sum_{i=1}^{s} a^p_{ij} \lambda^p_{ki}\right) \nabla_u \eta(Q_{kj}, P_{kj}, U_{kj}) = 0, \tag{B.1e}$$

$1 \le j \le s$ and $0 \le k \le N-1$. Here and elsewhere, the dual multipliers are

treated as row vectors. In the case $b_j > 0$ for each j, we reformulate the first-order conditions in terms of the variables $\chi_{kj} = (\chi^q_{kj}, \chi^p_{kj})$ defined by

$$\chi^q_{kj} = \psi^q_{k+1} + \sum_{i=1}^{s} \frac{a^q_{ij}}{b_j} \lambda^q_{ki}, \quad 1 \le j \le s, \tag{B.2a}$$

$$\chi^p_{kj} = \psi^p_{k+1} + \sum_{i=1}^{s} \frac{a^p_{ij}}{b_j} \lambda^p_{ki}, \quad 1 \le j \le s. \tag{B.2b}$$

With this definition, (B.1c) and (B.1d) reduce to

$$hb_j \left(\chi^q_{kj} \nabla_q \nu(Q_{kj}, P_{kj}) + \chi^p_{kj} \nabla_q \eta(Q_{kj}, P_{kj}, U_{kj}) \right) = \lambda^q_{kj}, \tag{B.3a}$$

$$hb_j \left(\chi^q_{kj} \nabla_p \nu(Q_{kj}, P_{kj}) + \chi^p_{kj} \nabla_p \eta(Q_{kj}, P_{kj}, U_{kj}) \right) = \lambda^p_{kj}. \tag{B.3b}$$

Multiplying (B.3a) by a^q_{ij}/b_i, and (B.3b) by a^p_{ij}/b_i, summing over j, and substituting from (B.2a) and (B.2b), respectively, we have

$$h \sum_{j=1}^{s} \frac{b_j a^q_{ji}}{b_i} \left(\chi^q_{kj} \nabla_q \nu(Q_{kj}, P_{kj}) + \chi^p_{kj} \nabla_q \eta(Q_{kj}, P_{kj}, U_{kj}) \right) = \sum_{j=1}^{s} \frac{a^q_{ji}}{b_i} \lambda^q_{kj} = \chi^q_{ki} - \psi^q_{k+1}, \tag{B.4a}$$

$$h \sum_{j=1}^{s} \frac{b_j a^p_{ji}}{b_i} \left(\chi^q_{kj} \nabla_p \nu(Q_{kj}, P_{kj}) + \chi^p_{j} \nabla_p \eta(Q_{kj}, P_{kj}, U_{kj}) \right) = \sum_{j=1}^{s} \frac{a^p_{ji}}{b_i} \lambda^p_{kj} = \chi^p_{ki} - \psi^p_{k+1}. \tag{B.4b}$$

Summing in (B.3) over j and utilizing (B.1a) and (B.1b) gives

$$h \sum_{i=1}^{s} b_j \left(\chi^q_{kj} \nabla_q \nu(Q_{kj}, P_{kj}) + \chi^p_{kj} \nabla_q \eta(Q_k j, P_{kj}, U_{kj}) \right) = \sum_{i=1}^{s} \lambda^q_{kj} = \psi^q_k - \psi^q_{k+1}, \tag{B.5a}$$

$$h \sum_{i=1}^{s} b_j \left(\chi^q_{kj} \nabla_p \nu(Q_{kj}, P_{kj}) + \chi^p_{kj} \nabla_p \eta(Q_{kj}, P_k j, U_{kj}) \right) = \sum_{i=1}^{s} \lambda^p_{kj} = \psi^p_k - \psi^p_{k+1}. \tag{B.5b}$$

Finally, substituting (B.2b) in (B.1e) yields

$$U_{kj} \in U, \quad -b^p_j \chi^p_{kj} \nabla_u \eta(Q_{kj}, P_{kj}, U_{kj}) = 0, \quad 1 \le j \le s. \tag{B.6}$$

The positive factor b_j in (B.6) can be removed and equations (B.4) - (B.6) yield the transformed first-order system (4.46).

The remainder of this section shows the equivalence of the two transformed adjoint systems (B.1) and (4.46), and consequently the equivalence of the adjoint systems (4.44) and (4.46).

Proposition B.1 *If $b_j > 0$ for each j, then the first-order system (B.1) and the transformed first-oder system (4.46) are equivalent. That is, if $\lambda_1^q, \ldots, \lambda_s^q$, $\lambda_1^p, \ldots, \lambda_s^p$ satisfy (B.1), then (4.46) holds for χ_j^q and χ_j^p defined in (B.2). Conversely, if $\chi_1^q, \ldots \chi_s^q$, $\chi_1^p, \ldots \chi_s^p$ satisfy (4.46), then (B.1) holds for λ_j^q and λ_j^p defined in (B.3).*

Proof: We already derived the transformed first-order conditions starting from the original first-order conditions. Now suppose that $\chi_1^q, \ldots \chi_s^q$, $\chi_1^p, \ldots \chi_s^p$ satisfy the transformed conditions (4.46). Summing over j in (B.3), and utilizing (4.46a) and (4.46b) yields (B.1a) and (B.1b). To verify (B.1c) - (B.1e), we substitute for λ_i^q and λ_i^p using (B.3), respectively, to obtain

$$\begin{aligned} b_j\psi_{k+1}^q + \sum_{i=1}^s a_{ij}^q \lambda_i^q &= b_j\psi_{k+1}^q + h\sum_{i=1}^s b_i a_{ij}^q \left(\chi_i^q \nabla_q \nu(w_i, z_i) + \chi_i^p \nabla_q \eta(w_i, z_i, u_{ki})\right) \\ &= b_j\psi_{k+1}^q + hb_j \sum_{i=1}^s \tfrac{a_{ij}^q b_i}{b_j} \left(\chi_i^q \nabla_q \nu(w_i, z_i) + \chi_i^p \nabla_q \eta(w_i, z_i, u_{ki})\right) \\ &= b_j \chi_j^q \end{aligned} \tag{B.7}$$

and

$$\begin{aligned} b_j\psi_{k+1}^p + \sum_{i=1}^s a_{ij}^p \lambda_i^p &= b_j\psi_{k+1}^p + h\sum_{i=1}^s b_i a_{ij}^p \left(\chi_i^q \nabla_p \nu(w_i, z_i) + \chi_i^p \nabla_p \eta(w_i, z_i, u_{ki})\right) \\ &= b_j\psi_{k+1}^p + hb_j \sum_{i=1}^s \tfrac{a_{ij}^p b_i}{b_j} \left(\chi_i^q \nabla_p \nu(w_i, z_i) + \chi_i^p \nabla_p \eta(w_i, z_i, u_{ki})\right) \\ &= b_j \chi_j^p, \end{aligned} \tag{B.8}$$

respectively, where the last lines come from (4.46c) and (4.46d). Multiplying (B.7) on the right by $\nabla_q \nu(w_j, z_j)$, multiplying (B.8) on the right by $\nabla_q \eta(w_j, z_j, u_{kj})$, adding these terms and substituting from (B.3a) gives (B.1c). Equivalently, we obtain (B.1d). Multiplying (B.8) on the right by $\nabla_u \eta(w_j, z_j, u_{kj})$ and utilizing (4.46e) yields (B.1e). ∎

With the $s \times s$ block matrix M whose (i, j) block is the $2n \times 2n$ matrix

$$\begin{pmatrix} a_{ij}^q \nabla_q \nu(w_j, z_j) & a_{ij}^p \nabla_p \nu(w_j, z_j) \\ a_{ij}^q \nabla_q \eta(w_j, z_j, u_{kj}) & a_{ij}^p \nabla_p \eta(w_j, z_j, u_{kj}) \end{pmatrix},$$

it follows from [53] (Prop. 3.3), that the multipliers ψ_k^q and ψ_k^p obtained by solving (4.46c) - (4.46d) and substituting into (4.46a) - (4.46b) are identical to the multipliers obtained from (4.44c) - (4.44d). Moreover, the condition (4.46e) involving χ_j^p satisfying (4.46c) - (4.46d) is equivalent to the condition (4.44e).

Appendix C

Convergence proof

This section presents the proof arguments of our convergence result 4.6.2 stated in Section 4.6.

By applying Proposition 4.6.1 we follow the same arguments as in [53]: We utilize discrete analogues of various continuous spaces and norms. In particular, for a sequence $z_0, z_1, \ldots, z_N$ whose i-th element is a vector $z_i \in \mathbb{R}^n$, the discrete analogues of the L^p and L^∞ norms are the following:

$$\|z\|_{L^p} = \left(\sum_{i=0}^{N} h|z_i|^p \right)^{\frac{1}{p}} \quad \text{and} \quad \|z\|_{L^\infty} = \sup_{0 \le i \le N} |z_i|.$$

With this notation, the space $\mathcal{X}$ in the discrete control problem is the discrete L^∞ space consisting of 3-tuples $w = (x, \psi, u)$ where

$$\begin{aligned} x &= (x^0, x_1, x_2, \ldots, x_N), \quad x_k \in \mathbb{R}^{2n}, \\ \psi &= (\psi_0, \psi_1, \psi_2, \ldots, \psi_N), \quad \psi_k \in \mathbb{R}^{2n}, \\ u &= (u_0, u_1, u_2, \ldots, u_{N-1}), \quad u_k \in \mathbb{R}^{sm}. \end{aligned}$$

The mappings $\mathcal{T}$ and $\mathcal{F}$ of Proposition 4.6.1 are selected in the following way (according to [53]):

$$\mathcal{T}(x, \psi, u) = \begin{pmatrix} x'_k - f^h(x_k, u_k), \quad 0 \le k \le N-1 \\ \psi'_k + \nabla_x H^h(x_k, \psi_{k+1}, u_k), \quad 0 \le k \le N-1 \\ \nabla_{u_j} H^h(x_k, \psi_{k+1}, u_k), \quad 1 \le j \le s, 0 \le k \le N-1 \\ \psi_N - \nabla C(x_N) \end{pmatrix}$$

and $\mathcal{F}(x, \psi, u) = 0$.

The space $\mathcal{Y}$, associated with the four components of $\mathcal{T}$, is a space of 4-tuples of finite sequences in $L^1 \times L^1 \times L^\infty \times \mathbb{R}^{2n}$. The reference point w^* is the sequence

with elements

$$w_k^* = (x_k^*, \psi_k^*, u_k^*),$$

where $x_k^* = x^*(t_k), \psi_k^* = \psi^*(t_k)$, and $u_{ki}^* = u(y_{ki}^*, \chi_{ki}^*)$. Here y_{ki}^* and χ_{ki}^* are the solutions to (4.47e) - (4.47h) corresponding to $x = x(t_k)$ and $\psi = \psi(t_k)$. The operator $\mathcal{L}$ is obtained by linearizing around w^*, evaluating all variables on each interval at the grid point to the left, and dropping terms that vanish at $h = 0$. In particular, we choose

$$\mathcal{L}(w) = \begin{pmatrix} x_k' - A_k x_k - B_k u_k b, \quad 0 \le k \le N-1 \\ \psi_k' + \psi_{k+1} A_k + (q_k x_k + S_k u_k b)^T, \quad 0 \le k \le N-1 \\ b_j(u_{kj}^T R_k + x_k^T S_k + \psi_{k+1} B_k), \quad 1 \le j \le N-2, 0 \le k \le N-1 \\ \psi_n + V x_N \end{pmatrix}.$$

In [41] and [53] Hager examines each of the hypotheses of Proposition 4.6.1 for this choice of spaces and functions. In [41] (Lemma 5.1) he shows that by smoothness,

$$\|\nabla \mathcal{T}(w) - \mathcal{L}\| \le \|\nabla \mathcal{T}(w) - \mathcal{L}\|_{L^\infty} \le c(\|w - w^*\| + h) \tag{C.1}$$

for every $w \in B_\beta(w^*)$, where β appears in the state uniqueness property. Moreover, by smoothness, coercivity, and [41] (Lemma 6.1), the map $(\mathcal{F} - \mathcal{L})^{-1}$ is Lipschitz continuous with a Lipschitz constant λ independent of h for h sufficiently small. Thus we can take $\sigma = \infty$ in Proposition 4.6.1.

Since we focus on the case where $U = \mathbb{R}^m$ and $\mathcal{F} = 0$, obtaining an estimate for $\|\mathcal{T}(w^*)\|$ is equivalent to estimating the distance from $\mathcal{T}(w)$ to $\mathcal{F}(w)$ to examine (P1) of Proposition 4.6.1. In [53] Hager shows that the estimation is given by

$$\|\mathcal{T}(w^*)\| \le c h^{\kappa - 1} \left(h + \tau(u^{*(\kappa-1)}; h)\right). \tag{C.2}$$

To complete the proof of Theorem 4.6.2, by using Proposition 4.6.1, let λ be large enough and let $\bar{h}$ be small enough such that the Lipschitz constant of $\mathcal{L}^{-1}$ is less than λ for all $h \le \bar{h}$. Choose ϵ small enough such that $\epsilon\lambda < 1$. Choose a small r and choose $\bar{h}$ smaller if necessary such that $c(r + \bar{h}) \le \epsilon$ where c is the constant appearing (C.1). Finally, choose $\bar{h}$ smaller if necessary such that for the residual bound in (C.2), we have

$$c\bar{h}^{\kappa-1}\left(\bar{h} + \tau(u^{*(\kappa-1)}; \bar{h})\right) \le (1 - \lambda\epsilon) r/\lambda.$$

Since the hypotheses of Proposition 4.6.1 are satisfied, we conclude that for each $h \le \bar{h}$, there exists $w^h = (x^h, \psi^h, u^h) \in B_r(w^*)$ such that $\mathcal{T}(w^h) = 0$ and the estimate (4.48) holds, which establishes the bounds for the state and costate variables in (4.50). The estimate in (4.50) for the error in the control follows from the control uniqueness property and the fact that $\nabla_u \mathcal{H}(x^*(t_k), \psi^*(t_k), u^*(t_k)) = 0$. Finally, by [41] (Lemma 7.2), (x^h, u^h) is a strict local minimizer in (4.43) for h sufficiently small. ∎

Bibliography

[1] O. Abel, A. Helbig, and W. Marquadt. *DYNOPT User Manual (Release 2.4)*. Lehrstuhl für Prozesstechnik, RWTH Aachen, 1999.

[2] U. Ascher, J. Christiansen, and R. D. Russell. A collocation solver for mixed order systems of boundary value problems. *Mathematics of Computation*, 33:659–679, 1979.

[3] U. Ascher, R. Mattheij, and R. D. Russell. *Numerical solution of Boundary Value Problems for Differential Equations*. SIAM, 1988.

[4] R. Bachmayer, N. E. Leonard, J. Graver, E. Fiorelli, P. Bhatta, and D. Paley. Underwater gliders: Recent developments and future applications. In *International Symposium on Underwater Technology*, Taipei, Taiwan, China, 2004.

[5] V. Bär. Ein Kollokationsverfahren zur numerischen Lösung allgemeiner Mehrpunktrandwertaufgaben mit Schalt- und Sprungbedingungen mit Anwendungen in der Optimalen Steuerung und der Parameteridentifizierung. Diploma thesis, Bonn, 1983.

[6] A. Barclay, P. E. Gill, and J. B. Rosen. SQP methods and their application to numerical optimal control. In W. H. Schmidt, K. Heier, L. Bittner, and R. Bulirsch, editors, *Variational Calculus. Optimal Control and Application*, 1998.

[7] B. Betsch and S. Leyendecker. The discrete null space method for the energy consistent integration of constrained mechanical systems. Part II: Multibody dynamics. *International Journal for Numerical Methods in Engineering*, 4:499–552, 2006.

[8] P. Betsch, A. Menzel, and E. Stein. On the parametrization of finite rotations in computational mechanics; A classification of concepts with application to smooth shells. *Computer Methods in Applied Mechanics and Engineering*, 155:273–305, 1998.

[9] P. Betsch and P. Steinmann. Inherently energy conserving time finite elements for classical mechanics. *Computational Physics*, 160:88–116, 2000.

[10] P. Betsch and P. Steinmann. Constrained integration of rigid body dynamics. *Computer Methods in Applied Mechanics and Engineering*, 191:467–488, 2001.

[11] J. T. Betts. Survey of numerical methods for trajectory optimization. *AIAA J. Guidance, Control, and Dynamics*, 21(2):193–207, 1998.

[12] J. T. Betts. Practical methods for optimal control using nonlinear programming. *SIAM, Philadelphia, PA*, 2001.

[13] J. T. Betts, N. Biehn, and S. L. Campbell. Convergence of nonconvergent IRK discretizations of optimal control problems with state inequality constraints. *SIAM J. Scientific Computing*, 23(6):1981–2007, 2002.

[14] J. T. Betts and P. D. Frank. A sparse nonlinear optimization algorithm. *Optimization Theory and Applications*, 82(3):519–541, 1994.

[15] J. T. Betts and W. P. Huffmann. Mesh refinement in direct transcription methods for optimal control. *Optimal Control, Applications and Methods*, 19:1–21, 1998.

[16] L. T. Biegler. Solution of dynamic optimization problems by successive quadratic programming and orthogonal collocation. *Computers and Chemical Engineering*, 8(3/4):243–248, 1984.

[17] T. Binder, L. Blank, H. G. Bock, R. Bulirsch, W. Dahmen, M. Diehl, T. Kronseder, W. Marquardt, J. P. Schlöder, and O. von Stryk. Introduction to model based optimization of chemical processes on moving horizons. In M. Grötschel, S. O. Krumke, and J. Rambau, editors, *Online Optimization of Large Scale Systems: State of the Art*, pages 295–340. Springer, 2001.

[18] A. I. Bobenko and Y. B. Suris. Discrete Lagrangian reduction, discrete Euler-Poincaré equations, and semidirect products. *Letters in Mathematical Physics*, 49:79–93, 1999.

[19] A. I. Bobenko and Y. B. Suris. Discrete time Lagrangian mechanics on Lie groups, with an application to the Lagrange top. *Communication in Mathematical Physics*, 204:147–188, 1999.

[20] H. G. Bock. Numerical solutions of nonlinear multipoint boundary value problems with applications to optimal control. *ZAMM*, 58(T407), 1978.

[21] H. G. Bock and K. J. Plitt. A multiple shooting algorithm for direct solution of optimal control problems. In *9th IFAC World Congress*, pages 242–247, Budapest, Hungary, 1984. Pergamon Press.

[22] P. T. Boggs and J. W. Tolle. Sequential quadratic programming. *Acta Numerica*, 4:1–50, 1995.

[23] J. F. Bonnans and J. Laurent-Varin. Computation of order conditions for symplectic partitioned Runge-Kutta schemes with application to optimal control. *Numerische Mathematik*, 103(1):1–10, 2006.

[24] O. Bonorden, M. Dynia, J. Gehweiler, and R. Wanka. Pub-library - user guide and function reference. *Release 8.1-pre*, 2003.

[25] C. L. Bottasso and A. Croce. Optimal control of multibody systems using an energy preserving direct transcription method. *Multibody System Dynamics*, 12(1), 2004.

[26] N. Bou-Rabee and H. Owhadi. Stochastic variational integrators. Submitted, 2007.

[27] A. E. Bryson and Y. C. Ho. *Applied Optimal Control*. Hemisphere, 1975.

[28] R. Bulirsch. Die Mehrzielmethode zur numerischen Lösung von nichtlinearen Randwertproblemen und Aufgaben der optimalen Steuerung. Report of the Carl-Cranz-Gesellschaft e.V., DLR, Oberpfaffenhofen, 1971.

[29] J. A. Cadzow. Discrete calculus of variations. *International Journal of Control*, 11:393–407, 1970.

[30] J. A. Cadzow. *Discrete-Time Systems: an introduction with interdisciplinary applications*. Prentice-Hall, 1973.

[31] A. L. Cauchy. Méthode générale pour la résolution systèmes d'équations simultanées. *Comptes rendus de l'Académie des scinces*, 25:536–538, 1847.

[32] A. Cervantes and L. T. Biegler. Large-scale DAE optimization using a simultaneous NLP formulation. *AIChE Journal*, 44(5):1038–1050, 1998.

[33] F. L. Chernousko and A. A. Luybushin. Method of successive approximations for optimal control problems (survey paper). *Optimal Control, Applications and Methods*, 3:101–114, 1982.

[34] M. Crisfield and J. Shi. An energy conserving co-rotational procedure for nonlinear dynamics with finite elements. *Nonlinear Dynamics*, 9:37–52, 1996.

[35] M. Dellnitz, O. Junge, A. Krishnamurthy, S. Ober-Blöbaum, K. Padberg, and R. Preis. Efficient control of formation flying spacecraft. In Friedhelm Meyer auf der Heide and Burkhard Monien, editors, *New Trends in Parallel & Distributed Computing*, volume 181, pages 235–247. Heinz Nixdorf Institut Verlagsschriftreihe, 2006.

[36] P. Deuflhard. A modified newton method for the solution of ill-conditioned systems of nonlinear equations with application to multiple shooting. *Numerische Mathematik*, 22:289–315, 1974.

[37] E. D. Dickmanns and K. H. Well. Approximate solution of optimal control problems using third order hermite polynomial functions. *Lecture Notes in Computer Science*, 27:158–166, 1975.

[38] A. L. Dontchev and W. W. Hager. Lipschitzian stability in nonlinear control and optimization. *SIAM J. Control and Optimization*, 31:569–603, 1993.

[39] A. L. Dontchev and W. W. Hager. The Euler approximation in state constrained optimal control. *Mathematics of Computation*, 70:173–203, 2001.

[40] A. L. Dontchev, W. W. Hager, A. B. Poore, and B. Yang. Optimality, stability and convergence in nonlinear control. *Applied Mathematics and Optimization*, 31:297–326, 1995.

[41] A. L. Dontchev, W. W. Hager, and V. M. Veliov. Second order Runge-Kutta approximations in control constrained optimal control. *SIAM J. Numerical Analysis*, 38:202–226, 2000.

[42] G. Engl, A. Kröner, T. Kronseder, and O. von Stryk. Numerical simulation and optimal control of air separation plants. In H.-J. Bungartz, F. Durst, and Chr. Zenger, editors, *High Performance Scientific and Engineering Computing*, volume 8 of *Lecture Notes in Computational Science and Engineering*, pages 221–231. Springer, 1999.

[43] A. Fedorova and M. Zeitlin. Wavelets in dynamics, optimal control and Galerkin approximations. In *IEEE Digital Signal Processing Workshop*, pages 409–412, Norway, 1996.

[44] R. C. Fetecau, J. E. Marsden, M. Ortiz, and M. West. Nonsmooth Lagrangian mechanics and variational collision integrators. *SIAM J. Applied Dynamical Systems*, 2(3):381–416, 2003.

[45] E. Fiorelli, N. E. Leonard, P. Bhatta, D. Paley, R. Bachmayer, and D.M. Fratantoni. Multi-AUV control and adaptive sampling in Monterey Bay. In *IEEE Autonomous Underwater Vehicles 2004: Workshop on Multiple AUV Operations (AUV04)*, Sebasco, ME, 2004.

[46] L. Flatto. *Advanced Calculus.* Williams & Wilkins, 1976.

[47] L. Fox. Some numerical experiments with eigenvalue problems in ordinary differential equations. In R. E. Langer, editor, *Boundary Value Problems in Differential Equations*, 1960.

[48] P. E. Gill, W. Murray, and M. A. Saunders. SNOPT: An SQP algorithm for large-scale constrained optimization. Report NA 97-2, Department of Mathematics, University of California, San Diego, CA, USA, 1997.

[49] P. E. Gill, W. Murray, M. A. Saunders, and M. H. Wright. User's guide for NPSOL (version 5.0): a Fortran package for nonlinear programming. Numerical Analysis Report 98-2, Department of Mathematics, University of California, San Diego, CA, USA, 1998.

[50] H. Goldstein, C. Poole, and J. Safko. *Classical Mechanics*. Addison Wesley, 2002.

[51] A. Griewank. *Evaluating Derivatives: Principles and Techniques of Algorithmic Differentiation*. SIAM, 2000.

[52] W. W. Hager. Convex control and dual approximations. In *Constructive Approaches to Mathematical Models*, pages 189–202. Academic Press, New York, 1979.

[53] W. W. Hager. Runge-Kutta methods in optimal control and the transformed adjoint system. *Numerische Mathematik*, 87:247–282, 2000.

[54] W. W. Hager. Numerical analysis in optimal control. In *International Series of Numerical Mathematics*, volume 139, pages 83–93. Birkhäuser Verlag, Basel, Switzerland, 2001.

[55] E. Hairer, C. Lubich, and G. Wanner. *Geometric numerical integration*, volume 31 of *Springer Series in Computational Mathematics*. Springer, 2002.

[56] E. Hairer, G. Wanner, and C. Lubich. *Geometric Numerical Integration: Structure- Preserving Algorithms for Ordinary Differential Equations*. Springer, 2004.

[57] S. P. Han. Superlinearly convergent variable-metric algorithms for general nonlinear programming problems. *Mathematical Programming*, 11:263–282, 1976.

[58] R. F. Hartl, S.P. Sethi, and R.G. Vickson. A survey of the maximum principle for optimal control problems with state constraints. *SIAM Review*, 37(2):181–218, 1995.

[59] M. R. Hestenes. *Calculus of Variations and Optimal Control Theory*. John Wiley & Sons, 1966.

[60] P. Hiltmann. *Numerische Lösung von Mehrpunkt-Randwertproblemen und Aufgaben der optimalen Steuerung über endlichdimensionalen Räumen*. PhD thesis, Fakultät für Mathematik und Informatik, Technische Universität München, 1990.

[61] C. L. Hwang and L. T. Fan. A discrete version of Pontryagin's maximum principle. *Operations Research*, 15:139–146, 1967.

[62] T. Inanc, S. C. Shadden, and J. E. Marsden. Optimal trajectory generation in ocean flows. In *American Control Conference*, Portland, OR, USA, 2005.

[63] R. Isaacs. *Differential Games: A Mathematical Theory with Applications to Warfare and Pursuit, Control and Optimization*. John Wiley & Sons, 1965.

[64] F. Jarre and J. Stoer. *Optimierung*. Springer, 2004.

[65] B. W. Jordan and E. Polak. Theroy of a class of discrete optimal control systems. *Journal of Electronics and Control*, 17:697–711, 1964.

[66] O. Junge, J. Levenhagen, A. Seifried, and M. Dellnitz. Identification of halo orbits for energy efficient formation flying. In *International Symposium Formation Flying*, Toulouse, France, 2002.

[67] O. Junge, J. E. Marsden, and S. Ober-Blöbaum. Discrete mechanics and optimal control. In *16th IFAC World Congress*, Prague, Czech Republic, 2005.

[68] O. Junge, J. E. Marsden, and S. Ober-Blöbaum. Optimal reconfiguration of formation flying spacecraft - a decentralized approach. In *IEEE Conference on Decision and Control and European Control Conference ECC*, pages 5210–5215, San Diego, CA, USA, 2006.

[69] O. Junge and S. Ober-Blöbaum. Optimal reconfiguration of formation flying satellites. In *IEEE Conference on Decision and Control and European Control Conference ECC*, Seville, Spain, 2005.

[70] S. Kameswaran and L. T. Biegler. Convergence rates for direct transcription of optimal control problems using collocation at Radau points. Preprint.

[71] S. Kameswaran and L. T. Biegler. Convergence rates for direct transcription of optimal control problems with final-time equality constraints using collocation at Radau points. In *American Control Conference*, pages 165–171, Minneapolis, Minnesota, USA, 2006.

[72] C. Kane, J. E. Marsden, and M. Ortiz. Symplectic energy-momentum integrators. *Mathematical Physics*, 40:3353–3371, 1999.

[73] C. Kane, J. E. Marsden, M. Ortiz, and M. West. Variational integrators and the Newmark algorithm for conservative and dissipative mechanical systems. *International Journal for Numerical Methods in Engineering*, 49(10):1295–1325, 2000.

[74] E. Kanso and J. E. Marsden. Optimal motion of an articulated body in a perfect fluid. In *IEEE Conference on Decision and Control and European Control Conference ECC*, Seville, Spain, 2005.

[75] W. Karush. Minima of functions of several variables with inequalities as side constraints. Master's thesis, Department of Mathematics, University of Chicago, 1939.

[76] H. J. B. Keller. *Numerical Methods for Two-Point Boundary Value problems*. Waltham: Blaisdell, 1968.

[77] H. J. Kelley. Gradient theory of optimal flight paths. *Journal of the American Rocket Society*, 30:947–953, 1960.

[78] M. Kobilarov, M. Desbrun, J. E. Marsden, and G. S. Sukhatme. A discrete geometric optimal control framework for systems with symmetries. In *Robotics: Science and Systems (R:SS)*, Zurich, Switzerland, 2007.

[79] M. Kobilarov and G. S. Sukhatme. Optimal control using nonholonomic integrators. In *IEEE International Conference on Robotics and Automation (ICRA)*, pages 1832–1837, Rome, Italy, 2007.

[80] D. Kraft. On converting optimal control problems into nonlinear programming problems. In K. Schittkowsky, editor, *Compuational Mathematical Programming*, volume F15 of *NATO ASI series*, pages 261–280. Springer, 1985.

[81] H. W. Kuhn and A. W. Tucker. Nonlinear programming. In J. Neyman, editor, *Proceedings of the Second Berkeley Symposium on Mathematical Statisics and Probability*. University of California Press, Berkeley, 1951.

[82] R. A. LaBudde and D. Greenspan. Energy and momentum conserving methods of arbitrary order for the numerical integration of equations of motion, I. Motion of a single particle. *Numerische Mathematik*, 25:323–346, 1976.

[83] R. A. LaBudde and D. Greenspan. Energy and momentum conserving methods of arbitrary order for the numerical integration of equations of motion, II. Motion of a system of particles. *Numerische Mathematik*, 26:1–16, 1976.

[84] J.-L. Lagrange. Applications de la methode exposée dans le mémoire précédent a la solution de différents problèmes de dynamique. *Oeuvres*, 1:365–468, 1760.

[85] J.-L. Lagrange. Méchanique analitique. Paris, 1788.

[86] S. Lall and M. West. Discrete variational Hamiltonian mechanics. *Journal of Physics A: Mathematical and General*, 39(19):5509–5519, 2006.

[87] T. Lee, N. H. McClamroch, and M. Leok. Attitude maneuvers of a rigid spacecraft in a circular orbit. In *American Control Conference*, pages 1742–1747, Minneapolis, Minnesota, USA, 2006.

[88] T. Lee, N. H. McClamroch, and M. Leok. Optimal control of a rigid body using geometrically exact computations on SE(3). In *IEEE Conference on Decision and Control and European Control Conference ECC*, pages 2710–2715, San Diego, CA, USA, 2006.

[89] T. D. Lee. Can time be a discrete dynamical variable? *Physical Letters B*, 121:217–220, 1983.

[90] T. D. Lee. Difference equations and conservation laws. *Journal of Statistical Physics*, 46:843–860, 1987.

[91] B. Leimkuhler and G. Patrick. A sympletic integrator for Riemannian manifolds. *Nonlinear Science*, pages 1–19, 1996.

[92] D. B. Leineweber. Efficient reduced SQP methods for the optimization of chemical processes described by large sparse DAE models. In *Fortschr.-Bericht VDI Reihe 3, Verfahrenstechnik*, volume 613. VDI-Verlag, 1999.

[93] A. Lew, J. E. Marsden, M. Ortiz, and M. West. Asynchronous variational integrators. *Archive for Rational Mechanics and Analysis*, 167:85–146, 2003.

[94] A. Lew, J. E. Marsden, M. Ortiz, and M. West. An overview of variational integrators. In L. P. Franca, T. E. Tezduyar, and A. Masud, editors, *Finite Element Methods: 1970's and Beyond*, pages 98–115. CIMNE, 2004.

[95] A. Lew, J. E. Marsden, M. Ortiz, and M. West. Variational time integrators. *International Journal for Numerical Methods in Engineering*, 60(1):153–212, 2004.

[96] S. Leyendecker. *Mechanical Integrators for constrained dynamical systems in flexible multibody dynamics*. PhD thesis, University of Kaiserslautern, 2006.

[97] S. Leyendecker, J. E. Marsden, and M. Ortiz. Variational integrators for constrained dynamical systems. In preparation.

[98] S. Leyendecker, S. Ober-Blöbaum, and J. E. Marsden. Discrete mechanics and optimal control for constrained systems (DMOCC). In preparation.

[99] S. Leyendecker, S. Ober-Blöbaum, J. E. Marsden, and M. Ortiz. Discrete mechanics and optimal control for constrained multibody dynamics. In *6th International Conference on Multibody Systems, Nonlinear Dynamics, and Control, ASME International Design Engineering Technical Conferences*, Las Vegas, Nevada, USA, 2007.

[100] J. D. Logan. First integrals in the discrete calculus of variation. *Aequationes Mathematicae*, 9:210–220, 1973.

[101] Process Systems Enterprise Ltd. *gPROMS Advanced User Guide (Release 1.8)*. London, 2000.

[102] R. MacKay. Some aspects of the dynamics of Hamiltonian systems. In D. S. Broomhead and A. Iserles, editors, *The dynamics of numerics and the numerics of dynamics*, pages 137–193. Clarendon Press, Oxford, 1992.

[103] S. Maeda. Canonical structure and symmetries for discrete systems. *Mathematica Japonica*, 25:405–420, 1980.

[104] S. Maeda. Extension of discrete Noether theorem. *Mathematica Japonica*, 26:85–90, 1981.

[105] S. Maeda. Lagrangian formulation of discrete systems and concept of difference space. *Mathematica Japonica*, 27:345–356, 1981.

[106] K. Malanowski. Finite difference approximations to constrained optimal control problems. In *Optimization and Optimal Control*, Lecture Notes in Control and Information Sciences, pages 243–254. Springer, 1981.

[107] K. Malanowski, C. Büskens, and H. Maurer. Convergence of approximations to nonlinear optimal control problems. In A. V. Fiacco, editor, *Mathematical Programming with Data Perturbations*, volume 195 of *Lecture Notes in Pure and Applied Mathematics*, pages 253–284. Marcel Dekker, New York, 1979.

[108] J. E. Marsden, G. W. Patrick, and S. Shkoller. Multisymplectic geometry, variational integrators, and nonlinear PDEs. *Communication in Mathematical Physics*, 199:351–395, 1998.

[109] J. E. Marsden, S. Pekarsky, and S. Shkoller. Discrete Euler-Poincaré and Lie Poisson equations. *Nonlinearity*, 12:1647–1662, 1999.

[110] J. E. Marsden, S. Pekarsky, and S. Shkoller. Symmetry reduction of discrete Lagrangian mechanics on Lie groups. *Geometry and Physics*, 36:140–151, 1999.

[111] J. E. Marsden and T. Ratiu. *Introduction to Mechanics and Symmetry*, volume 17 of *Texts in Applied Mathematics*. Springer, 1994.

[112] J. E. Marsden and S. Shkoller. Multisymplectic geometry, covariant Hamiltonians, and water waves. *Mathematical Proceedings of the Cambridge Philosophical Society*, 125:553–575, 1999.

[113] J. E. Marsden and M. West. Discrete mechanics and variational integrators. *Acta Numerica*, 10:357–514, 2001.

[114] J. Martin. Discrete mechanics and optimal control. Master's thesis, Department of Control and Dynamical Systems, California Institute of Technology, 2006.

[115] J. Martin, S. Ober-Blöbaum, S. Leyendecker, and J. E. Marsden. Applications of DMOC: The falling cat. In preparation.

[116] R. I. McLachlan and S. Marsland. Discrete mechanics and optimal control for image registration. In *Computational Techniques and Applications Conference (CTAC)*, 2006.

[117] A. Miele. Gradient algorithms for the optimization of dynamic systems. In C. T. Leondes, editor, *Control and Dynamic Systems*, volume 60, pages 1–52, 1980.

[118] R. Montgomery. Isoholonomic problems and some applications. *Communication in Mathematical Physics*, 128:565–592, 1990.

[119] R. Montgomery. Optimal control of deformable bodies and its relation to gauge theory. In T. Ratiu, editor, *The Geometry of Hamiltonian Systems*, pages 403–438. Springer-Verlag, 1991.

[120] R. Montgomery. Gauge theory of the falling cat. *Fields Institute Communications*, 1:193–218, 1993.

[121] R. Montgomery. A tour of subriemannian geometries, their geodesics and applications. *American Mathematical Society, Mathematical Surveys and Monographs*, 91, 2002.

[122] I. Newton. Philosophiae naturalis principia mathematica. Londini anno MDCLXXXVII, 1687.

[123] S. Ober-Blöbaum. Zur optimalen Kontrolle von Verbunden starrer Körper. Diploma thesis, University of Paderborn, 2004.

[124] D. Pekarek, A. D. Ames, and J. E. Marsden. Discrete mechanics and optimal control applied to the compass gait biped. In *IEEE Conference on Decision and Control and European Control Conference ECC*, New Orleans, USA, 2007.

[125] L. Petzold, J. B. Rosen, P. E. Gill, L. O. Jay, and K. Park. Numerical optimal control of parabolic PDEs using DASOPT. In Biegler, Coleman, Conn, and Santosa, editors, *Large Scale Optimization with Applications, Part II*, Lecture Notes in Computational Science and Engineering, pages 271–299. Springer, 1997.

[126] E. Polak. *Optimization: Algorithms and consistent Approximations*. Springer, New York, 1997.

[127] L. S. Pontryagin, V. G. Boltyanski, R. V. Gamkrelidze, and E. F. Miscenko. *The Mathematical Theory of Optimal Processes*. John Wiley & Sons, 1962.

[128] M. J. D. Powell. A fast algorithm for nonlinearly constrained optimization calculations. In G. A. Watson, editor, *Numerical Analysis*, volume 630 of *Lecture Notes in Mathematics*, pages 261–280. Springer, 1978.

[129] R. Pytlak. *Numerical Methods for optimal Control Problems with State Constraints*. Springer, 1999.

[130] L. B. Rall. *Automatic Differentiation: Techniques and Applications*, volume 120 of *Lecture Notes in Computer Science*. Springer Verlag, Berlin, 1981.

[131] G. W. Reddien. Collocation at Gauss points as a discretization in optimal control. *SIAM J. Control and Optimization*, 17(2):298–306, 1979.

[132] S. Reich. Momentum conserving symplectic integrations. *Physica D*, 76(4):375–383, 1994.

[133] S. Reich. Enhancing energy conserving methods. *BIT*, 36:122–134, 1995.

[134] S. D. Ross. Optimal flapping strokes for self-propulsion in a perfect fluid. In *American Control Conference*, pages 4118–4122, Minneapolis, Minnesota, USA, 2006.

[135] D. L. Rudnick, R. E. Davis, C. C. Eriksen, D. M. Fratantoni, and M. J. Perry. Underwater gliders for ocean research. *Marine Technology Society Journal*, 38(1), 2004.

[136] V. H. Schulz. Solving discretized optimization problems by partially reduced SQP methods. *Computing and Visualization in Science*, 1:83–96, 1998.

[137] A. L. Schwartz and E. Polak. Consistent approximation for optimal control problems based on Runge-Kutta integration. *SIAM J. Control and Optimization*, 34(4):1235–1269, 1996.

[138] A. Seifried. Formationsflug von Raumfahrzeugen. Diploma thesis, University of Paderborn, 2003.

[139] B. Sendov and V. A. Popov. *The averaged moduli of smoothness.* John Wiley, 1988.

[140] J. Simo and O. Gonzalez. Assessment of energy-momentum and symplectic schemes for stiff dynamical systems. In *American Society of Mechanical Engineers, ASME Winter Annual Meeting*, New Orleans, Louisiana, USA, 1993.

[141] J. Simo, D. Lewis, and J. E. Marsden. Stability of relative equilibria. Part I: The reduced energy-momentum method. *Archive for Rational Mechanics and Analysis*, 115:15–59, 1991.

[142] J. Simo and N. Tarnow. A new energy and momentum conserving algorithm for the non-linear dynamics of shells. *International Journal for Numerical Methods in Engineering*, 37:2527–2549, 1994.

[143] J. Simo, N. Tarnow, and M. Doblare. Non-linear dynamics of three-dimensional rods: Exact energy and momentum conserving algorithms. *International Journal for Numerical Methods in Engineering*, 38:1431–1473, 1995.

[144] J. Simo, N. Tarnow, and K. Wong. Exact energy-momentum conserving algorithms and symplectic schemes for nonlinear dynamics. *Computer Methods in Applied Mechanics and Engineering*, 100:63–116, 1992.

[145] J. Simo and K. Wong. Unconditionally stable algorithms for rigid body dynamics that exactly preserve energy and momentum. *International Journal for Numerical Methods in Engineering*, 31:19–52,1321–1323, 1991.

[146] J. Stoer and R. Bulirsch. *Introduction into numerical analysis.* 2nd ed., Springer, 1993.

[147] Y. B. Suris. Hamiltonian methods of Runge-Kutta type and their variational interpretation. *Mathematical Modelling*, 2:78–87, 1990.

[148] M. Sust. Modular aufgebaute deterministische Modelle zur Beschreibung menschlicher Bewegungen. In R. Ballreich and W. Baumann, editors, *Grundlagen der Biomechanik des Sports.* Ferdinand-Enke-Verlag, Stuttgart, 1996.

[149] V. Szebehely. *Theory of orbits – The Restricted Problem of Three Bodies.* Academic Press, 1967.

[150] R. Thurman and A. Worfolk. The geometry of halo orbits in the circular restricted three-body problem. Technical Report GCG95, University of Minnesota, 1996.

[151] J. Timmermann. Die Nullraum-Methode in Kombination mit DMOC zur optimalen Steuerung mechanischer Systeme mit holonomen Zwangsbedingungen. Diploma thesis, University of Paderborn, 2008.

[152] H. Tolle. *Optimization Methods.* Springer, 1975.

[153] O. von Stryk. Numerical solution of optimal control problems by direct collocation. In R. Bulirsch, A. Miele, J. Stoer, and K. H. Well, editors, *Optimal Control - Calculus of Variation, Optimal Control Theory and Numerical Methods*, volume 111 of *International Series of Numerical Mathematics*, pages 129–143. Birkhäuser, 1993.

[154] O. von Stryk. Optimal control of multibody systems in minimal coordinates. *ZAMM*, 78(3):1117–1120, 1998.

[155] O. von Stryk. Numerical hybrid optimal control and related topics. Habilitation, Department of Mathematics, Technische Universität München, 2000.

[156] O. von Stryk and R. Bulirsch. Direct and indirect methods for trajectory optimization. *Annals of Operations Research*, 37:357–373, 1992.

[157] A. Walther, A. Kowarz, and A. Griewank. ADOL-C: A package for the automatic differentiation of algorithms written in C/C++. *ACM TOMS*, 22(2):131–167, 1996.

[158] J. M. Wendlandt and J. E. Marsden. Mechanical integrators derived from a discrete variational principle. *Physica D*, 106:223–246, 1997.

[159] J. M. Wendlandt and J. E. Marsden. Mechanical systems with symmetry, variational principles and integration algorithms. In M. Alber, B. Hu, and J. Rosenthal, editors, *Current and Future Directions in Applied Mathematics*, pages 219–261. Birkhäuser, 1997.

[160] R. E. Wengert. A simple automatic derivative evaluation program. *Communications of the ACM*, 7(8):463–464, 1964.

[161] W. Zhang, T. Inanc, S. Ober-Blöbaum, and J. E. Marsden. Optimal trajectory generation for a dynamic glider in ocean flows modeled by 3D B-Spline functions. In *IEEE International Conference on Robotics and Automation (ICRA)*, Pasadena, CA, USA, 2008.